


# COUPLING OF $InCl_3$-BAILs FOR CATALYTIC CONVERSION OF OIL PALM BIOMASS TO LEVULINIC ACID AND UPGRADING TO ETHYL LEVULINATE BIOFUEL

**TIONG YONG WEI**

**THESIS SUBMITTED TO**
**THE UNIVERSITY OF NOTTINGHAM FOR THE DEGREE OF DOCTOR OF PHILOSOPHY**

**SEPTEMBER 2018**

**Abstract**

Biomass has emerged as an abundant and relatively low cost carbon resource alternative to fossil fuels in the sustainable production of specialty chemicals and biofuel. Levulinic acid is an attractive platform chemical which can be obtained from biomass. Upgrading of levulinic acid produces ethyl levulinate biofuel, which serve as a transportation fuel and a fuel additive. Herein, this study reports a new environmentally friendly coupling mixed acids ionic liquids catalytic system, i.e. indium trichloride-1-methylimidazolium hydrogen sulphate ($InCl_3$-[HMIM][$HSO_4$]), for the catalytic conversions of oil palm empty fruit bunch and mesocarp fibre biomass to levulinic acid and upgrading to ethyl levulinate. In this two-step sequential reaction, i.e. the depolymerisation to levulinic acid, followed by the upgrading esterification to ethyl levulinate, the optimum depolymerisation occurred at 177°C in 4.8 h with 0.15 mmol indium trichloride in ionic liquids-to-biomass ratio of 6.6:1 (w/w) and 22.7% (w/w) of water, whilst esterification was at 105°C in 12.2 h with ethanol to substrate ratio of 7.2:1 (v/v). The maximum levulinic acid yields were 17.7% and 18.4%, followed by subsequent upgrading ethyl levulinate yields of 18.7% and 20.1% from the conversions of oil palm empty fruit bunch and mesocarp fibre biomass, respectively. Levulinic acid and ethyl levulinate efficiencies were >63% for both biomass conversions. These results further suggested that $InCl_3$-[HMIM][$HSO_4$] catalytic system offers a better or comparable catalytic activity than other ionic liquids catalytic system for the biomass conversion to levulinic acid and upgrading to ethyl levulinate. Additionally, through kinetic and thermodynamic studies for the oil palm mesocarp fibre cellulose conversion to levulinic acid and

upgrading to ethyl levulinate via $InCl_3$-[HMIM][$HSO_4$] catalytic system, relatively low activation energies of 56.5 kJ $mol^{-1}$ and 28.1 kJ $mol^{-1}$ were achieved for cellulose depolymerisation and the subsequent upgrading esterification, respectively. Meanwhile, the Gibbs free energy of activation for cellulose depolymerisation and the subsequent upgrading esterification were +115.5 kJ $mol^{-1}$ and +90.3 kJ $mol^{-1}$, respectively. These results were relatively lower than other catalytic systems, indicating that the present catalytic system was relatively more energetically and kinetically feasible. Finally, $InCl_3$-[HMIM][$HSO_4$] could be recycled up to three consecutive runs with a minimal loss of <25% ethyl levulinate yield. Hence, this would directly benefit the process development in terms of catalytic studies at pilot and industrial scales. Overall, this study highlighted the potential of novel coupling mixed acids $InCl_3$-[HMIM][$HSO_4$] catalytic system for biorefinery processing of oil palm empty fruit bunch and mesocarp fibre biomass to levulinic acid and upgrading to ethyl levulinate from a greener and more sustainable perspective.

**Keywords:** Levulinic acid; ethyl levulinate; ionic liquids; indium trichloride; oil palm biomass

## List of Publications

### Journal Papers

1. **Tiong, Y.W.**, Yap, C.L., Gan, S., Yap, W.S.P. 2017. Conversion of oil palm biomass to ethyl levulinate via ionic liquids. *Chemical Engineering Transactions*, 56, 1021-1026. DOI: 10.3303/CET1756171

2. **Tiong, Y.W.**, Yap, C.L., Gan, S., Yap, W.S.P. 2017. One-pot conversion of oil palm empty fruit bunch and mesocarp fiber biomass to levulinic acid and upgrading to ethyl levulinate via indium trichloride-ionic liquids. *Journal of Cleaner Production*, 168, 1251-1261. DOI: 10.1016/j.jclepro.2017.09.050

3. **Tiong, Y.W.**, Yap, C.L., Gan, S., Yap, W.S.P. 2018. Conversion of biomass and its derivatives to levulinic acid and levulinate esters via ionic liquids. *Industrial & Engineering Chemistry Research*, 57, 4749-4766. DOI: 10.1021/acs.iecr.8b00273

4. **Tiong, Y.W.**, Yap, C.L., Gan, S., Yap, W.S.P. 2019. Optimisation studies on the conversion of oil palm biomass to levulinic acid and ethyl levulinate via indium trichloride-ionic liquids: A response surface methodology approach. *Industrial Crops and Products*, 128, 221-234. DOI: 10.1016/j.indcrop.2018.10.087

5. **Tiong, Y.W.**, Yap, C.L., Gan, S., Yap, W.S.P. 2019. Kinetic and thermodynamic studies of oil palm mesocarp fiber cellulose conversion to levulinic acid and upgrading to ethyl levulinate via indium trichloride-ionic liquids. *Renewable Energy*. (Submitted, under review)

**Conference Proceedings**

6. **Tiong, Y.W.**, Yap, C.L., Gan, S., Yap, W.S.P. 2017. Optimisation of levulinic acid production from oil palm biomass via mono-alkylated ionic liquids. *In:* Proceedings of World Renewable Energy Congress XVI, Murdoch University, Perth, Western Australia; 5-9 February 2017.

7. **Tiong, Y.W.**, Yap, C.L., Gan, S., Yap, W.S.P. 2017. Ethyl levulinate production from oil palm biomass conversion in $InCl_3$-ionic liquids catalytic system. *In:* Proceedings of the 17$^{th}$ Congress, Asian Pacific Confederation of Chemical Engineering, Hong Kong; 23-27 August 2017.

8. **Tiong, Y.W.**, Yap, C.L., Gan, S., Yap, W.S.P. 2018. Kinetic study on oil palm biomass conversion to levulinic acid via indium trichloride-ionic liquids. *In:* 2nd International Conference on Energy and Environmental Science, University of Malaya, Kuala Lumpur; 16-18 January 2018. *IOP Conference Series: Earth and Environmental Science*, 164, 012007. DOI: 10.1088/1755-1315/164/1/012007

9. **Tiong, Y.W.**, Yap, C.L., Gan, S., Yap, W.S.P. 2018. Physical properties of noncorrosive $[HSO_4]^-$ based ionic liquids and its catalysis for ethyl levulinate biofuel production. *In:* Proceedings of the 14th International Symposium on Biocatalysis and Agricultural Biotechnology, Kuala Lumpur; 22-24 October 2018.

**Acknowledgements**

First of all, I would like to express my sincere gratitude to my principal supervisor, Dr. Yap Chiew Lin, for her continuous support for my PhD study and related research, as well as for her patience, motivation and immense knowledge. Her guidance helped me at all times of research and writing of papers for publication and this thesis. I am also deeply grateful to my co-supervisor, Prof. Dr. Gan Suyin, for her insightful comments and advice, as well as allowing me to access the laboratory and research facilities in the Engineering Research Building (Block N) conveniently. My sincere thanks also goes to my second co-supervisor, Dr. Winnie Yap Soo Ping, for her words of motivation and encouragement. In addition, I am grateful to the laboratory technicians from the Faculty of Engineering, especially Filzah, Fareez, Andrew, Fatihah, Khairani and Asyraf, for all their laboratory assistance and technical support. I am also grateful to the research officers at the Centre for Research and Instrumentation Management (CRIM), Universiti Kebangsaan Malaysia (UKM) for providing assistance in operating the nuclear magnetic resonance (NMR). Furthermore, my special thanks should go to my friends, who willingly shared their knowledge and experience with me, and thus have been my pillars during my difficult times. Their efforts and supports are priceless and much appreciated. I would also like to thank my family, especially my mother, for supporting me spiritually throughout my PhD study. Finally, I would like to acknowledge the financial support from the MyBrain15 scholarship and the Fundamental Research Grant Scheme (FRGS), both from the Ministry of Higher Education (MOHE), Malaysia. Last but not least, multiple thanks and glory to God, who made all things possible.

**Table of Contents**

**Abstract** ..... **II**

**List of Publications** ..... **IV**

**Acknowledgements** ..... **VI**

**Table of Contents** ..... **VII**

**List of Tables** ..... **XIV**

**List of Figures** ..... **XVI**

**List of Abbreviations** ..... **XX**

**List of Ionic Liquids** ..... **XXVI**

**List of Units** ..... **XXX**

**Chapter 1** ..... **1**

**Introduction** ..... **1**

1.1 Research Background ..... 1

1.2 Problem Statement ..... 7

1.3 Significance of Study ..... 10

1.4 Objectives ..... 13

1.5 Research Approach and Scope ..... 13

1.6 Limitations of Study ..... 16

**Chapter 2** ..... **18**

**Literature Review** ..... **18**

2.1 Oil palm ..... 18

2.1.1 Availability of oil palm biomass ..... 19

2.1.2 Oil palm biomass for energy ..... 21

2.2 Approaches for conversion of biomass to biofuels: Thermochemical and depolymerisation pathway ..... 23

2.3 Bio-based Chemicals: Levulinic acid (LA) and Levulinate esters (LE) .. 25

2.3.1 Levulinic acid (LA) ..... 25

2.3.1.1 LA in the production of biofuel or fuel additive ..... 27

2.3.2 Levulinate esters (LE) ..... 28

2.3.2.1 LE as potential biofuel or fuel additive ..... 29

2.4 Synthesis route of LA and LE from biomass ..... 30

2.5 Ionic Liquids (ILs) ..... 36

2.5.1 Task specific ionic liquids (TSILs) ..... 38

2.5.2 Acidic ionic liquids (AILs) ..... 39

2.5.3 Comparison of ILs with other catalysts ..... 42

2.6 Biomass pretreatment with ILs ..... 44

2.7 Conversions from biomass and its derivatives to LA and LE ..... 52

2.7.1 Sugars to LA and LE ..... 53

2.7.2 Cellulose to LA and LE ..... 60

2.7.3 Lignocellulosic biomass to LA and LE ..... 68

2.7.4 Furfuryl alcohol to LE ..... 76

2.7.5 LA to LE ..... 78

2.8 Overview of the current ILs catalytic status and associated factors ..... 81

2.9 Challenges ..... 84

2.10 Concluding Remarks ..... 86

**Chapter 3 ..... 88**

**Characterisation studies of oil palm biomass and ionic liquids ..... 88**

3.1 Introduction ..... 88

3.2 Methodology ..... 88

3.2.1 Materials ..... 88

3.2.2 Biomass composition study ..... 89

3.2.3 Physical properties of ILs ..... 89

3.3 Results and Discussion ..... 91

3.3.1 Biomass composition study ..... 91

3.3.2 Physical properties of ILs ..... 95

3.3.2.1 Density and viscosity ..... 95

3.3.2.2 Thermal stability ..... 99

3.3.2.3 Hammett acidity function ..... 100

3.4 Concluding Remarks ..... 102

**Chapter 4 ..... 104**

**Screening of ionic liquids for the catalytic conversion ..... 104**

4.1 Introduction ..... 104

4.2 Methodology ..... 104

4.2.1 Materials ..... 104

4.2.2 Two-step sequential reaction system in one-pot: Depolymerisation and esterification reactions ..... 105

4.2.3 Products isolation ..... 105

4.2.4 Products analysis ..... 106

4.3 Results and Discussion ..... 106

4.3.1 Conversion of oil palm biomass to EL via ILs ..... 106

4.3.1.1 Chloride $[Cl]^-$ imidazolium based ILs ..... 107

4.3.1.2 Hydrogen sulphate $[HSO_4]^-$ imidazolium based ILs ..... 108

4.4 Concluding Remarks ..... 110

**Chapter 5 ..... 111**

**Optimisation studies on the biomass conversion to levulinic acid ..... 111**

5.1 Introduction ..... 111

5.2 Methodology ..... 112

5.2.1 Materials ..... 112

5.2.2 Biomass conversion reaction and products isolation ..... 112

5.2.3 Products analysis ..... 112

5.2.4 Statistical analysis ..... 113

5.2.5 Physical properties of $InCl_3$-[HMIM][$HSO_4$] ..... 115

5.3 Results and Discussion ..... 116

5.3.1 Statistical analysis ..... 116

5.3.1.1 RSM based on CCD method ..... 116

5.3.1.2 Effect and interaction of variables on LA yields ..... 124

5.3.1.3 Optimisation and validation ..... 135

5.3.2 Addition of Lewis acidic $InCl_3$ coupled with [HMIM][$HSO_4$] ..... 137

5.3.3 Physical properties of $InCl_3$-[HMIM][$HSO_4$] ..... 138

5.4 Concluding Remarks ..... 142

**Chapter 6 ..... 144**

**Optimisation studies on the upgrading to ethyl levulinate ..... 144**

6.1 Introduction ..... 144

6.2 Methodology ..... 144

6.2.1 Materials ..... 144

6.2.2 Biomass conversion reaction and products isolation ..... 145

6.2.3 Products analysis ..... 145

6.2.4 Statistical analysis ..... 146

6.3 Results and Discussion ..... 147

6.3.1 Statistical analysis ..... 147

6.3.1.1 RSM based on CCD method ..... 147

6.3.1.2 Effect and interaction of variables on EL yields ..... 154

6.3.1.3 Optimisation and validation ..... 159

6.3.2 LA and EL syntheses with other by-products formation ..... 160

6.3.3 Comparative studies ..... 166

6.4 Concluding Remarks ..... 171

**Chapter 7 ..... 172**

**Kinetic and thermodynamic studies on the biomass conversion and upgrading ..... 172**

7.1 Introduction ..... 172

7.2 Methodology ..... 173

7.2.1 Materials ..... 173

7.2.2 Biomass conversion reaction and products isolation ..... 173

7.2.3 Products analysis ..... 173

7.2.4 Determination of kinetic and thermodynamic parameters ..... 174

7.3 Results and Discussion ..... 178

7.3.1 Effect of reaction temperature and time of the biomass conversion to LA and upgrading to EL ..... 178

7.3.2 Kinetic studies ..... 181

7.3.3 Thermodynamic studies ..... 195

7.4 Concluding Remarks ..... 201

**Chapter 8 ..... 202**

**Recyclability studies of $InCl_3$-[HMIM][$HSO_4$] ..... 202**

8.1 Introduction ..... 202

8.2 Methodology ..... 202

8.2.1 Materials ..... 202

8.2.2 Biomass conversion reaction, products isolation and analysis, and ILs recovery ..... 202

8.2.3 Products analysis ..... 203

8.3 Results and Discussion ..... 203

8.3.1 Recyclability test runs on the efficiency of EL production ..... 203

8.4 Concluding Remarks ..... 211

**Chapter 9 ..... 213**

**Conclusions and Recommendations ..... 213**

9.1 Conclusions ..... 213

9.2 Recommendations ..... 215

**References ..... 218**

**Appendices ..... 247**

Appendix 1 ..... 247

Appendix 2 ..... 248

Appendix 3 ..... 249

Appendix 4 ..... 252

Appendix 5 ..... 257

**List of Tables**

**Table 2.1** Main cations and anions of ILs. 37

**Table 2.2** Comparison of ILs with mineral acid and heterogeneous catalysts. 43

**Table 2.3** Studies on the conversion of sugars to (a) LA and (b) LE via ILs at various reaction conditions. 55

**Table 2.4** Studies on conversion of cellulose to (a) LA and (b) LE via ILs at various reaction conditions. 60

**Table 2.5** Studies on the direct conversion of various biomass to (a) LA and (b) LE via ILs at various reaction conditions. 69

**Table 2.6** Studies on the direct conversion of furfuryl alcohol to LE via ILs at various reaction conditions. 76

**Table 3.1** Composition of oil palm biomass. 93

**Table 3.2** Density and viscosity of ILs measured at various temperatures. 95

**Table 3.3** Hammett acidity function ($H_0$) data for the ILs studied. 101

**Table 5.1** Range of independent variables and experimental levels (LA yields). 114

**Table 5.2** CCD experimental design matrix and responses (LA yields). 117

**Table 5.3** ANOVA results for response parameters of LA yields. 119

**Table 5.4** F-values and associated p-values for the responses of $Y_1$ (conversion from OPEFB) and $Y_2$ (conversion from OPMF). 124

**Table 5.5** Optimisation and validation for LA yields. 136

**Table 5.6** Density and viscosity of $InCl_3$-[HMIM][$HSO_4$] compared to other ILs without Lewis acid analogues at various temperatures. 140

**Table 5.7** Hammett acidity function ($H_0$) data for $InCl_3$-[HMIM][$HSO_4$] compared to other ILs without Lewis acid analogues. 142

**Table 6.1** Range of independent variables and experimental levels (EL yields). 146

**Table 6.2** CCD experimental design matrix and responses (EL yields). 148

**Table 6.3** ANOVA results for response parameters of EL yields. 150

**Table 6.4** F-values and associated p-values for the responses of $Y_3$ (conversion from OPEFB) and $Y_4$ (conversion from OPMF). 154

**Table 6.5** Optimisation and validation for EL yields. 160

**Table 6.6** Typical components identified from the GC-MS analysis for the reaction mixture of LA syntheses. 161

**Table 6.7** Typical components identified from the GC-MS analysis for the reaction mixture of EL syntheses. 163

**Table 6.8** Comparison of the present LA and EL productions with other studies involving different biomass and ILs. 169

**Table 7.1** Kinetic parameters of LA and EL efficiencies. 185

**Table 7.2** An overview of kinetic studies on LA synthesis. 190

**Table 7.3** Thermodynamic parameters of cellulose depolymerisation and the subsequent upgrading esterification. 197

**Table 7.4** A comparison of present study with other studies for the thermodynamics of LA and EL syntheses. 200

**Table 8.1** Infrared spectra and band assignments for fresh ILs and reused ILs for the fifth cycle. 209

**List of Figures**

**Figure 2.1** Strategies for conversion of lignocellulosic biomass to liquid biofuels via thermochemical and depolymerisation routes. Adapted from Alonso et al. [107]. 24

**Figure 2.2** Chemical structure of LA. 25

**Figure 2.3** Derivatives of LA from the lignocellulosic biomass as a platform for liquid fuels and additives. Modified from Démolis et al. [15] and Mariscal Lopez et al. [120]. 28

**Figure 2.4** Chemical structure of EL. 29

**Figure 2.5** Conversion of lignocellulosic biomass components to LA and LE. Adapted from Girisuta et al. [130]. 32

**Figure 2.6** Reaction pathways of hexose and pentose route for production of LA and LE. Adapted from Neves et al [134]. 35

**Figure 2.7** Main evolution of TSIL generations. Modified from Yue et al. [61]. 39

**Figure 2.8** Main categories of AILs with examples given in each category. 41

**Figure 2.9** Schematic representation of pretreatment effect on lignocellulosic biomass. Adapted from Tadesse and Luque [158]. 45

**Figure 2.10** Proposed dissolution mechanisms of cellulose by imidazolium based ILs: (A) interactions between the basic anion and the cellulose hydroxyl groups break up the hydrogen bond network between the cellulose chains. (B) Hydrophobic interactions take place between the hydrophobic face of cellulose and the imidazolium ring. (C) The acidic proton at the C-2 position on the imidazolium ring interacts with the cellulose hydroxyl groups. Adapted from Wahlstrom and Suurnakki [159]. 45

**Figure 2.11** Comparison of conventional strategy and recently developed one-pot strategy, for the production of LA and LE from biomass feedstock. Adapted from Xu et al. [37]. 51

**Figure 2.12** Conversion of sugars to LA and LE. 54

**Figure 2.13** Esterification of alcohols and carboxylic acid catalysed by BAILs. Adapted from Yue et al. [61]. 81

**Figure 3.1** TGA analysis of oil palm biomass (a) OPEFB and (b) OPMF. 92

**Figure 3.2** Temperature effect on the density of ILs. 97

**Figure 3.3** Temperature effect on the viscosity of ILs. 98

**Figure 3.4** Thermal analysis of the ILs. 99

**Figure 4.1** EL yields from conversions of OPEFB and OPMF biomass via (a) [BMIM][$HSO_4$] and (b) [HMIM][$HSO_4$] at various ILs-to-biomass ratio (w/w). (Reaction conditions: Depolymerisation: 160$^oC$, 3 h; Esterification: 90$^oC$, 6 h, in 20% (w/w) water). 109

**Figure 5.1** Diagnostic of models (a) Relationship between predicted and actual values, (b) Normal % probability versus studentized residuals, and (c) Outliers T versus run number of LA yields from the conversions of (i) OPEFB ($Y_1$) and (ii) OPMF ($Y_2$). 123

**Figure 5.2** Corresponding response surface and contour plots for LA yield from OPEFB conversion ($Y_1$), based on (a) temperature and time; (b) temperature and ILs-to-biomass ratio; (c) temperature and water; (d) time and ILs-to-biomass ratio; (e) time and water; and (f) ILs-to-biomass ratio and water. 129

**Figure 5.3** Corresponding response surface and contour plots for LA yield from OPMF conversion ($Y_2$), based on (a) temperature and time; (b) temperature and

ILs-to-biomass ratio; (c) temperature and water; (d) time and ILs-to-biomass ratio; (e) time and water; and (f) ILs-to-biomass ratio and water. 132

**Figure 5.4** Effect of $InCl_3$ dosage on LA yields from conversions of (a) OPEFB and (b) OPMF biomass via [HMIM][$HSO_4$]. (Depolymerisation: ILs-to-biomass ratio of 6.6:1 (w/w), 177$^0$C, 4.8 h and 22.7% (w/w) water). 137

**Figure 5.5** Temperature effect of density of $InCl_3$-[HMIM][$HSO_4$] compared to other ILs without Lewis acid analogues. 139

**Figure 5.6** Temperature effect of viscosity of $InCl_3$-[HMIM][$HSO_4$] compared to other ILs without Lewis acid analogues. 140

**Figure 5.7** Thermal analysis of the $InCl_3$-[HMIM][$HSO_4$] compared to other ILs without Lewis acid analogues. 141

**Figure 6.1** Diagnostic of models (a) Relationship between predicted and actual values, (b) Normal % probability versus studentized residuals, and (c) Outliers T versus run number of EL yields for the conversions of (i) OPEFB ($Y_3$) and (ii) OPMF ($Y_4$). 153

**Figure 6.2** Corresponding response surface and contour plots for EL yield from OPEFB conversion ($Y_3$), based on (a) temperature and time; (b) temperature and ethanol-to-substrate ratio; and (c) time and ethanol-to-substrate ratio. 156

**Figure 6.3** Corresponding response surface and contour plots for EL yield from OPMF conversion ($Y_4$), based on (a) temperature and time; (b) temperature and ethanol-to-substrate ratio; and (c) time and ethanol-to-substrate ratio. 157

**Figure 6.4** Representative GC-MS chromatogram for the reaction mixture of LA syntheses. 161

**Figure 6.5** Representative GC-MS chromatogram for the reaction mixture of EL syntheses. 162

**Figure 7.1** Effect of reaction temperature and time on (a) LA efficiency and (b) EL efficiency. (ILs-to-biomass ratio of 6.6:1 (w/w) and water content of 22.7% (w/w), in excess ethanol medium for the subsequent esterification reaction) 181

**Figure 7.2** Plot of (a) pseudo-zero-order, (b) pseudo-first-order, and (c) pseudo-second-order kinetic model of LA efficiency. 183

**Figure 7.3** Plot of (a) pseudo-zero-order, (b) pseudo-first-order, and (c) pseudo-second-order kinetic model of EL efficiency. 184

**Figure 7.4** Arrhenius plot of ln k versus 1/T for (a) cellulose depolymerisation to LA, and the (b) subsequent upgrading esterification to EL. 187

**Figure 7.5** Eyring plots of ln (k/T) versus 1/T for (a) cellulose depolymerisation to LA, and the (b) subsequent upgrading esterification to EL. 196

**Figure 8.1** The performance of recycled $InCl_3$-[HMIM][$HSO_4$] on the EL yields from the conversions of OPEFB and OPMF biomass compared to the fresh ILs. (Depolymerisation: ILs-to-biomass ratio of 6.6:1 (w/w), 0.15 mmol $InCl_3$, 177$^{o}$C, 4.8h and 22.7% (w/w) water; Esterification: 105$^{o}$C, 12.2 h and ethanol to substrate ratio of 7.2:1 (v/v)). 204

**Figure 8.2** The colour change between the (a) fresh ILs (light yellow) and (b) reused ILs for the fifth cycle (dark brown). 205

**Figure 8.3** Temperature effect on the viscosities of fresh ILs and reuse ILs for the fifth cycle. 205

**Figure 8.4** $^{1}$H NMR spectra of $InCl_3$-[HMIM][$HSO_4$] in $D_2O$ (a) fresh ILs and (b) reuse ILs for the fifth cycle. 208

**Figure 8.5** FTIR/ATR spectroscopy for fresh ILs and reused ILs for the fifth cycle. 209

**Figure 8.6** Decomposition mechanisms of dialkylimidazolium cations. 211

## List of Abbreviations

| | |
|---|---|
| $(CF_3SO_2)3C$ | Tris((trifluoromethyl)sulphonyl) methanide |
| $[(CF_3SO_2)_2N]^-$ | Bistrifluoromethylsulphonyl imide ion |
| $[BF_4]^-$ | Tetrafluoroborate ion |
| $[Br]^-$ | Bromide ion |
| $[Cl]^-$ | Chloride ion |
| $[H_2PO_4]^-$ | Dihydrogen phosphate ion |
| $[HSO_4]^-$ | Hydrogen sulphate ion |
| [I] | Molar concentration of un-protonated form |
| $[I]^-$ | Iodide ion |
| $[IH^+]$ | Molar concentration of protonated form |
| $[InCl_m(SO_4)_n]^{2n-}$ | Indium sulphate complexes |
| $[NO_3]^-$ | Nitrate ion |
| $[PF_6]^-$ | Hexafluorophosphate ion |
| $[SO_4]^{2-}$ | Sulphate ion |
| $^{13}C$ NMR | Carbon-13 nuclear magnetic resonance |
| $^{1}H$ NMR | Proton nuclear magnetic resonance |
| 1-NS | Naphthalenesulphonate |
| 2D NMR | Two-dimensional nuclear magnetic resonance |
| 5-HMF | 5-hydroxymethylfurfural |
| *A* | Pre-exponential factor in Arrhenius equation |
| Adj. | Adjusted |
| AILs | Acidic ionic liquids |
| $Al_2Cl_7^-$ | Heptachlorodialuminate ion |
| ANOVA | Analysis of variance |
| AP | Adequate precision |
| aq. | Aqueous |
| ASTM | American Society for Testing and Materials |
| BAILs | Bronsted acidic ionic liquids |
| $BF_4$ | Tetrafluoroborate |
| BL | Butyl levulinate |
| BLAILs | Bronsted-Lewis acidic ionic liquids |

| | |
|---|---|
| C | Carbon |
| C2 | Second position of carbon branches |
| $C_5$ | Carbon-5 |
| $C_6$ | Carbon-6 |
| C=O | Carbonyl group |
| CCD | Central composite design |
| Cel | Cellulose |
| $CF_3COOH$ | Trifluoroacetic acid |
| $CF_3CO_2^-$ | Trifluoroacetate ion |
| $CF_3SO_3^-$ | Triflate ion |
| $CH_3$ | Methyl |
| $CH_3SO_3$ | Mesylate |
| $CH_4$ | Methane |
| $C_6H_5SO_3^-$ | Benzenesulphonate ion |
| ChCl | Choline chloride |
| Cl | Chlorine |
| conc | Concentration |
| -COOH | Carboxylic acid |
| Cor Total | Total corrected for the mean |
| $CO_2$ | Carbon dioxide |
| CPO | Crude palm oil |
| $Cr^{2+}$ | Chromium ion |
| $CrCl_2$ | Chromium(II) chloride |
| $CrCl_3$ | Chromium(III) chloride |
| $CuCl_2$ | Copper(II) chloride |
| $CuSO_4$ | Copper sulphate |
| $D_2O$ | Deuterium oxide |
| DFT | Density functional theory |
| DSC | Differential scanning calorimeter |
| $E_a$ | Activation energy |
| EL | Ethyl levulinate |
| $Et_2O$ | Diethyl ether |
| FAEEs | Fatty acid ethyl esters |

| | |
|---|---|
| FAMEs | Fatty acid methyl esters |
| $FeCl_3$ | Iron trichloride |
| $FeCl_4$ | Iron tetrachloride |
| FFB | Fresh fruit bunch |
| FTIR | Fourier transform infrared |
| FTIR/ATR | Fourier transform infrared/Attenuated total reflectance |
| F value | A ratio of the mean regression sum of squares divided by the mean error sum of squares |
| GC | Gas chromatography |
| GC-MS | Gas chromatography-mass spectrometry |
| Glc | Glucose |
| GVL | γ-valerolactone |
| H | Hydrogen |
| *h* | Plank's constant |
| –H | Hydroxyl acid |
| $H^+$ | Hydrogen ion |
| $H_0$ | Hammett acidity function |
| $H_2O$ | Water |
| $H_2SO_4$ | Sulfuric acid |
| $H_3PO_4$ | Phosphoric acid |
| HCl | Hydrochloric acid |
| $HNO_3$ | Nitric acid |
| HPA | Heteropolyacid |
| HR-ESI-MS | High-resolution electrospray ionisation mass spectrometry |
| IL-POMs | Ionic liquids-based polyoxometalate salts |
| ILs | Ionic liquids |
| $InCl_3$ | Indium trichloride |
| $InCl_3$-BAILs | Indium trichloride-Bronsted acidic ionic liquids |
| $InCl_3$-ILs | Indium trichloride-ionic liquids |
| $InCl_3$-SFILs | Indium trichloride-sulphonic acid funcationalised ionic liquids |

| | |
|---|---|
| IS | Internal standard |
| ISB | Interact System B |
| $k$ | Rate constant |
| $k_B$ | Boltzmann's constant |
| LA | Levulinic acid |
| LAILs | Lewis acid ionic liquids |
| LE | Levulinate esters |
| ln | Natural logarithm |
| log | Logarithm |
| $MeSO_4$ | Methyl sulphate |
| MIBK | Methyl isobutyl ketone |
| ML | Methyl levulinate |
| MS | Mass spectrometry |
| MTHF | 2-methyltetrahydrofuran |
| N / $N_2$ | Nitrogen |
| N.A. | Not available |
| $NaClO_2$ | Sodium chlorite |
| NaOH | Sodium hydroxide |
| $N_2O$ | Nitrous oxide |
| $N(CN)_2$ | Dicyanamide anion |
| $NH_3$ | Ammonia |
| $NiCl_2$ | Nickel(II) chloride |
| $NiSO_4$ | Nickel(II) sulphate |
| NIST | National Institute of Standards and Technology |
| NMR | Nuclear magnetic resonance |
| $NO_3^-$ | Nitrate ion |
| NREL | National Renewable Energy Laboratory |
| O | Oxygen |
| OH | Hydroxide |
| OPEFB | Oil palm empty fruit bunch |
| OPF | Oil palm frond |
| OPKS | Oil palm kernel shell |
| OPMF | Oil palm mesocarp fiber |

| | |
|---|---|
| OPS | Oil palm sludge |
| OPT | Oil palm trunk |
| $OSO_3^-$ | Osmium(VI) oxide |
| $PF_6$ | Hexafluorophophate |
| $pK_a$ | Acid dissociation constant at logarithmic scale |
| PKC | Palm kernel cake |
| PKO | Palm kernal oil |
| PLOF | Probability of lack of fit |
| $PO_4^{3-}$ | Phosphate ion |
| POME | Palm oil mill effluent |
| Pr | Propyl |
| Pred. | Predicted |
| PRESS | Predicted residual error sum of squares |
| P-value | Probability |
| Prob > F | Probability of observed F value if the null hypothesis is true |
| *R* | Universal gas constant |
| $R^2$ | Correlation coefficient of fitting |
| RSM | Response surface methodology |
| $SbF_6^-$ | Hexafluoroantimony(V) |
| SCILs | Solid catalysts with ionic liquids |
| SFILs | Sulphonic acid functionalised ionic liquids |
| $SiO_2$-$SO_3H$ | Silica functionalised sulphonic acid |
| SLIPCs | Supported ionic liquids phase catalysts |
| $SnCl_2$ | Tin(II) chloride |
| $SO_2$ | Sulphur dioxide |
| -$SO_3H$ | Sulphonic acid |
| Temp | Temperature |
| TGA | Thermal gravimetric analysis |
| TRS | Total reducing sugar |
| TSILs | Task specific ionic liquids |
| UK | United Kingdom |
| ULSD | Ultra-low sulfur diesel fuel |

| | |
|---|---|
| US / USA | United States |
| US-DOE | United States- Department of Energy |
| UV | Ultraviolet |
| VA | Valeric acid |
| $X_{EL}$ | Ethyl levulinate efficiency |
| $X_{LA}$ | Levulinic acid efficiency |
| $Y_1$ | LA yield from the conversion of OPEFB biomass |
| $Y_2$ | LA yield from the conversion of OPMF biomass |
| $Y_3$ | EL yield from the conversion of OPEFB biomass |
| $Y_4$ | EL yield from the conversion of OPMF biomass |
| $Zn^{2+}$ | Zinc ion |
| $ZnCl_2$ | Zinc chloride |
| α | Alpha |
| β | Beta |
| $\Delta G^{\ddagger}$ | Gibbs free energy of activation |
| $\Delta H^{\ddagger}$ | Activation enthalpy |
| $\Delta S^{\ddagger}$ | Activation entropy |
| η | Viscosity |
| ρ | Density |
| SD | Standard deviation |
| SE | Standard error |

**List of Ionic Liquids**

| | |
|---|---|
| $[(HSO_3\text{-}p)_2im]$ $[HSO_4]$ | 1,3-bis(3-sulfopropyl)-1H-imidazol-3-ium hydrogen sulphate |
| [BMIM][$BF_4$] | 1-butyl-3-methylimidazolium tetrafluoroborate |
| [BMIM][Br] | 1-butyl-3-methylimidazolium bromide |
| [BMIM][Cl] | 1-butyl-3-methylimidazolium chloride |
| [BMIM][$HSO_4$] | 1-butyl-3-methylimidazolium hydrogen sulphate |
| [BMIM][OAc] | 1-butyl-3-methylimidazolium acetate |
| [BMIM][$PF_6$] | 1-butyl-3-methylimidazolium hexafluorophophate |
| [BMIM][TFSI] | 1-butyl-3-methylimidazolium bis(trifluoromethylsulfonyl)imide |
| [BMIM-SH][$ClSO_3H$] | 1-butyl sulphonic acid, 3-methyl imidazolium chlorosulfuric acid |
| [BMIM-SH][$HSO_4$] | 1-butyl sulphonic acid, 3-methyl imidazolium hydrogen sulphate |
| [BMIM-SH][PTSA] | 1-butyl sulphonic acid, 3-methyl imidazolium p-toluenesulphonic acid |
| [BMIM-$SO_3H$][$HSO_4$] | 1-methyl-3-(4-sulfobutyl)imidazolium hydrogen sulphate |
| [BMIM-$SO_3H$][$NTf_2$] | 1-methyl-3-(4-sulfobutyl)imidazolium bis((trifluoromethyl)sulfonyl)amide |
| [BMIM-$SO_3H$][OMs] | 1-methyl-3-(4-sulfobutyl)imidazolium methanesulfonate |
| [BMIM-$SO_3H$][OTf] | 1-methyl-3-(4-sulfobutyl)imidazolium trifluoromethanesulfonate |
| [BmPy][Cl] | 3-methyl-N-butylpyridinium chloride |
| [BPyr-$SO_3H$][$HSO_4$] | 1-(4-sulfobutyl)pyridinium hydrogen sulphate |
| [BS$Et_3N$][$HSO_4$] | N-(4-sulfonic acid)butyl triethylammonium hydrogen sulphate |

| | |
|---|---|
| [BSMIM][Br] | 1-butylsulphonic-3-methylimidazolium bromide |
| [BSMIM][$HSO_4$] | 1-(4-sulphonic acid) butyl-3-methylimidazolium hydrogen sulphate |
| [$BSO_3$HMIM][Cl] | 1-butylsulfonate-3-methylimidazolium hydrogen sulphate |
| [BSPy][$HSO_4$] | 1-(4-sulfobutyl) pyridinium hydrogen sulphate |
| [BSTmG][$CF_3COO$] | N-(bis(dimethylamino)methylene)-4-sulfobutan-1-aminium trifluoromethanesulfonate |
| [BSTmG][$HSO_4$] | N-(bis(dimethylamino)methylene)-4-sulfobutan-1-aminium hydrogen sulphate |
| [$C_3N$][$SO_3CF_3$]-HCSs | Nitrogen-doped carbon-based BAILs hollow nanospheres |
| [$C_3SO_3$HMIM][1-NS] | 1-methyl- 3-(3-sulfopropyl)imidazolium 1-naphthalenesulfonate |
| [$C_3SO_3$HMIM][$CH_3SO_3$] | 1-methyl-3-(3-sulfopropyl)imidazolium methanesulfonate |
| [$C_3SO_3$HMIM][Cl] | 1-methyl-3-(3-sulfopropyl)imidazolium chloride |
| [$C_3SO_3$HMIM][$H_2PO_4$] | 1-methyl-3-(3-sulfopropyl)imidazolium dihydrogen phosphate |
| [$C_3SO_3$HMIM][$HSO_4$] | 1-methyl-3-(3-sulfopropyl)-imidazolium chloride |
| [$C_3SO_3$HMIM][$HSO_4$] | 1-methyl-3-(3-sulfopropyl)imidazolium hydrogen sulphate |
| [$C_3SO_3HMIM]^+$ | 1-methyl-3-(3-sulfopropyl)imidazolium |
| [$C_3SO_3HN_{111}$][$HSO_4$] | N,N,N-trimethyl-N-(3-sulfopropyl)ammonium hydrogen sulphate |
| [$C_3SO_3HN_{222}$][$HSO_4$] | N,N,N-triethyl-N-(3-sulfopropyl)ammonium hydrogen sulphate |
| [$C_3SO_3HPPh_3$][$HSO_4$] | Triphenyl(3-sulfopropyl)phosphonium hydrogen sulphate |

| | |
|---|---|
| $[C_3SO_3HPy][HSO_4]$ | N-(3-sulfopropyl)pyridinium hydrogen sulphate |
| $[C_4(MIM)_2][(2HSO_4)(H_2SO_4)_4]$ | 1,1-bis(3-methylimidazolium-1-yl) butylene bis-hydrogen sulphate |
| $[C_4(MIM)_2][2HSO_4]$ | 1,1-bis(3-methylimidazolium-1-yl) butylene dihydrogen sulphate |
| $[C_4(MIM)_2][CH_3SO_3]$ | 1,1-bis(3-methylimidazolium-1-yl) butylene methanesulfonate |
| $[C_4H_6N_2(CH_2)_3SO_3H][H_2PW_{12}O_{40}]$ | Heteropolyacid ionic liquids |
| $[C_4H_8SO_3HMIM][Cl]$ | 1-(4-sulfobutyl)-3-methylimidazolium chloride |
| $[C_4H_8SO_3HMIM][H_2PO_4]$ | 1-(4-sulfobutyl)-3-methylimidazolium dihydrogen phosphate |
| $[C_4H_8SO_3HMIM][HSO_4]$ | 1-(4-sulfobutyl)-3-methylimidazolium hydrogen sulphate |
| $[C_4SO_3HMIM][HSO_4]$ | 1-methyl-3-(4-sulfobutyl)imidazolium hydrogen sulphate |
| $[C_8MIM][NTf_2]$ | 1-methyl-3-octylimidazolium amide |
| $[CF_3COO]$ | Trifluoromethanesulfonate |
| [Ch][Arg] | Cholinium argininate |
| [Ch][OAc] | Cholinium acetate |
| [Ch][Tau] | Cholinium taurate |
| $[ClSO_3H]$ | Chlorosulfuric acid |
| [EMIM][ABS] | 1-butyl-3-methylimidazolium alkylbenzene sulfonate |
| [EMIM][Cl] | 1-ethyl-3-methylimidazolium chloride |
| [EMIM][Gly] | 1-ethyl-3-methylimidazolium glycinate |
| $[EMIM][MeSO_4]$ | 1-ethyl-3-methylimidazolium methyl sulphate |
| [EMIM][OAc] | 1-ethyl-3-methylimidazolium acetate |
| $[Et_3NH][H_2PO_4]$ | Triethylammonium dihydrogen phosphate |
| $[EtSO_4]$ | Ethyl sulphate |
| $[HCnim]^+$ | 1-alkylimidazolium |
| $[HeMIM][NTf_2]$ | 1-(2-Hydroxyethyl)-3-methylimidazolium bis(trifluoromethylsulfonyl)imide |

| | |
|---|---|
| [HMIM][Cl] | 1-methylimidazolium chloride |
| [HMIM][$HSO_4$] / [MIM][$HSO_4$] | 1-methylimidazolium hydrogen sulphate |
| [Hmpy][$HSO_4$] | 2-methylpyridine hydrogen sulphate |
| [$HNEt_3$][$HSO_4$] / [$Et_3NH$][$HSO_4$] | triethylammonium hydrogen sulphate |
| [Hpy][$HSO_4$] | Pyridinium hydrogen sulphate |
| [HPyrr][$HSO_4$] | N-methylpyrrolidinium hydrogen sulphate |
| [$HSO_3$-BMIM][$HSO_4$] | 1-methyl-3-(4-sulfobutyl) imidazole bisulphate |
| [$HSO_3S$-$(CH_2)_3$-MIM]Cl-$ZnCl_2$ | 1-(3-sulphonic acid)-propyl-3-methylimidazole chlorozincinate |
| [$HSO_4$] | Hydrogen sulphate |
| [$MeSO_4$] | Methyl sulphate |
| [MIM] | 1-methylimidazolium |
| [MIM] [$CF_3COO$] | 1-methylimidazolium trifluoroacetate |
| [$NEt_3B$-$SO_3H$][$HSO_4$] | N,N,N-triethyl-4-sulfobutan-ammonium hydrogen sulphate |
| [NMP] | N-methyl 2-pyrollidonium |
| [NMP] [$CF_3COO$] | N-methyl 2-pyrollidonium trifluoroacetate |
| [NMP][$HSO_4$] | N-methyl 2-pyrollidonium hydrogen sulphate |
| [OMIM][Cl] | 1-octyl-3-methylimidazolium chloride |
| [PTSA] | p-toluenesulphonic acid |
| [SMIM] | 1-sulphonic acid-3-methylimidazolium |
| [SMIM][Cl] | 1-sulphonic acid-3-methylimidazolium chloride |
| [SMIM][$FeCl_4$] | 1-sulphonic acid-3-methylimidazolium tetrachloroferrate |
| $H_3[PW_{12}O_{40}]$ | Keggin-type phosphotungstic acid |
| $InCl_3$-[HMIM][$HSO_4$] | Indium trichloride-1-methylimidazolium hydrogen sulphate |

**List of Units**

| | | | |
|---|---|---|---|
| $ | United States Dollar | kJ $mol^{-1}$ $K^{-1}$ | Kilojoule per mole per Kelvin |
| % | Percentage | | |
| ˚C | Degree Celsius | m | Metre |
| µl | Microlitre | $m^3$ | Cubic metre |
| atm | Atmosphere | mg | Milligram |
| $cm^{-1}$ | Per centimetre | mg $L^{-1}$ | Milligram per litre |
| g | Gram | min | Minute |
| g $cm^{-3}$ | Gram per cubic centimetre | $min^{-1}$ | Per minute |
| | | ml | Millilitre |
| g $mol^{-1}$ | Gram per mole | ml $min^{-1}$ | Millilitre per minute |
| Gha | Global hectare | mm | Millimetre |
| GJ | Gigajoules | mmol | Millimole |
| GJ/year | Gigajoules per year | mol % | Mole percentage |
| h | Hour | mol $L^{-1}$ | Mole per litre |
| ha | Hectare | mPa. s | Millipascal-second |
| J $mol^{-1}K^{-1}$ | Joule per mole per Kelvin | nm | Nanometre |
| | | $^oC$ $min^{-1}$ | Degree Celsius per minute |
| K | Kelvin | | |
| kg | Kilogram | rpm | Rotation per minute |
| $kg^{-1}$ | Per kilogram | t | Tonne |
| kJ $mol^{-1}$ | Kilojoule per mole | v/v | Volume/volume |
| | | w/w | Weight/weight |

# Chapter 1

# Introduction

## 1.1 Research Background

The rapid increase in global energy consumption of conventional fossil fuels has led to a swift decline in the fuel reserves alongside growing concerns over environmental pollution and carbon emissions [1]. Although a shift to shale gas has recently occurred, the adverse environmental impacts associated to the use of this energy source remain unresolved. Hence, international efforts have persisted in developing renewable energy such as biomass, solar, thermal, tidal, wind, hydro, etc. [2]. Among these, biomass has been recognised as the only carbon-based renewable resource, which affords an environmentally beneficial reduction in the carbon footprint of chemicals and liquid fuels production from a green and sustainable perspective [3].

Nature produces a vast amount of biomass annually estimated at 170 billion metric tonnes; 75% of which can be assigned to the category of carbohydrates, but only 3-4% of these compounds are consumed by humans for food and non-food purposes [4]. According to a report by the Imperial College Centre for Energy Policy and Technology, the available biologically productive land area is approximately 13 Gha (1 Gha = $10^9$ ha) whereby an estimated 1.5 Gha are used to grow arable crops and 4 Gha are occupied by forests [5]. Whilst, 3.5 Gha of land are covered by pasture and the rest are used for other applications [5]. Hence, this suggests that these biologically productive land has the potential of suppling biomass feedstock. This abundance and wide availability renders biomass as one of the most promising alternative energy source worldwide. In

the past 50 years, a substantial amount of research has been conducted to produce biodiesel and other biofuels to meet growing energy demands [6]. For instance, agricultural residues such as oil palm fronds [7], wheat straw [8], bamboo [9] as well as paper pulp, wood chips and switchgrass [10] were reportedly utilised to produce levulinate esters (LE), which is a high potential biofuel [11].

The palm oil industry is the major agricultural enterprise of South East Asia, whereby Malaysia and Indonesia are among the world's largest palm oil producers. Specifically, in Malaysia, palm oil industries generate an average of 53 million tonnes of residues annually [12]. The types of biomass residue generated by the palm oil industry include oil palm fronds (OPF), trunks (OPT), empty fruit bunches (OPEFB) and mesocarp fibre (OPMF), kernel shell (OPKS) and sludge (OPS). There is a growing concern with the huge quantities of palm residues, owing to unsuitable disposal methods which cause harm to the environment. The use of oil palm residues as a raw material for the production of biofuels can be both environmentally and economically viable means of tackling this problem. In addition, it also highly beneficial in enhancing oil security, reducing environmental pollution and developing the rural economy [13].

The strategy for biomass conversion into desired chemicals occurs through the formation of building blocks from biomass carbohydrates. The National Renewable Energy Laboratory (NREL), US has identified levulinic acid (LA) as one of the most promising building blocks for organic synthesis [14]. Levulinic is a member of gamma-keto acids which can be synthesised through deep hydrolysis of biomass [15]. The reactions include the breakdown of biomass into its sugars, i.e. glucose, which is the monomer of cellulose and

also the main constituents of biomass [7], followed by dehydration to 5-hydroxymethylfurfural (5-HMF) and finally rehydration to LA [8]. The importance of LA lies in its dual functional groups of ketone and carboxylic acid, which can undergo various type of reactions. It serves as an ideal platform chemical for the production of a wide range of value-added products such as textile dye, animal feed, coating material, resins, polymers, herbicides, pharmaceuticals, food flavouring agents, solvents, plasticisers and anti-freeze agents [16]–[18]. LA also acts as a precursor in the production of biofuels. For example, esterification of LA with alcohols produces LE [19], while hydrogenation of LA produces 2-methyltetrahydrofuran (MTHF) [20], γ-valerolactone (GVL) [21] and valeric acid (VA) [22]. VA can be further esterified to produce valerate esters [23]. Furthermore, dehydration of LA produces angelica lactone which can be further hydrodeoxygenated to form compounds with C7-C10 gasoline-like hydrocarbon branches [24].

As a high potential biofuel, LE are produced by esterification of LA with alcohol. The alkyl component from alcohol dictates the variability in the physical properties of LE. Methyl levulinate (ML) which has the shortest alkyl chain is a potential gasoline additive, whereas ethyl and higher alkylated levulinates which have better solubility in aromatics-rich diesel range fuels [25], are potential diesel blend components and biodiesel [26]. In particular, ethyl levulinate (EL) has similar boiling points to those of heavy gasoline compounds (over 475 K) or of the middle diesel fuel boiling range [27]. Thus, EL blending with diesel would neither significantly alter the volatility of diesel fuel nor require any modification to existing engine designs [26]. EL also serves as a solvent, plasticizer or precursor in the production of various synthetic materials [19]. The keto ester

functional groups of EL allow various condensation and addition reactions in the synthesis pathways [28], [29]. In summary, EL offers a promising prospect as an important platform chemical in the portfolio of a futuristic biorefinery.

Although the utilisation of renewable biomass feedstock allows both LA and EL to be produced at a lower cost, improvements in the use of more environmentally benign catalysts and in the reduction of process energy requirements are essential to develop a more sustainable production route. LA and EL are conventionally produced with the aid of mineral acid catalysts which are corrosive and thus pollute the environment [16]. The used acid are difficult to separate and recover from the final reaction mixture upon completion [5]. Hence, replacement of mineral acid catalysts with heterogeneous acid type catalysts which are more easily separable and reusable could be an advantage [30]. However, deactivation of heterogeneous catalysts upon recycling was usually observed if they were used without re-treating, due to the adsorption of formed carbonaceous products on the solid acid surface and the gradual loss of acid sites [19]. These challenges have prompted researchers to seek alternative, environmentally benign catalysts for biomass processing.

Recent LA and EL productions via green chemistry have focussed on the utilisation of novel and promising ionic liquids (ILs). ILs are typically composed of an organic cation and an inorganic anion, which could act as dual solvent-catalysts that offer numerous advantageous over conventionally used organic solvents [31]. ILs possesses several remarkable properties such as negligible vapour pressure, non-flammability, high thermal stability, recyclability, broad liquid range and excellent dissolving capacity [31]–[33], all of which support sustainable production. The potential of ILs is further emphasised by the fact

that their structural functionalities on the cationic or anionic part can be finely tuned which has made it possible to design new ILs, or normally known as task-specific ILs (TSILs), with the desired targeted properties [34]. Meanwhile, these ILs could introduce specific features such as dual hydrophobicity-hydrophilicity ends, control of solute solubility and additional functional groups for catalysis or reactivity purposes [35]. This flexibility offers a broad room for further exploration and improvements.

Lignocellulose consists of three main compositions, i.e. cellulose, hemicellulose and lignin. These made up its complex structure with distinctive chemical and physical properties that resist various chemical and biological microbial attacks [36]. Considerable efforts have been made to reduce the structural complexity of the lignocellulose without destroying its fermentable sugar content, prior to further conversion into various bio-based materials. There are four main pretreatment strategies developed for lignocellulose, which include physical, chemical, physicochemical and biological methods [33]. However, all these pretreatments exhibit varying degrees of drawbacks, such as the need for specialised equipment and extreme operating conditions or the release of toxic pollutants [33]. To address these problems, recent progress has concentrated on ILs dual solvent-catalysts system which allows several reactions to be conducted concurrently (i.e. biomass pretreatment, catalytic chemical conversion and purification steps) in one-pot [37]. This is regards to the ILs have high potential for energy efficient in both processes, i.e. biomass pretreatment and catalytic conversion, owing to their low vapour pressure, emission profile, recyclability and tuneable properties [38]. In one-pot conversion strategy, after the biomass pretreatment, the reluctant nature and complex ultra-structure of the

biomass cell-wall material, i.e. cellulose and hemicellulose, is responsible for the sluggish yield of the LA and EL, through their corresponding pathway [39].

In this context, ILs are viewed as prospective dual solvent-catalysts for one-pot production approach (i.e. biomass pretreatment and various bio-based production steps) where the technical, economic and environmental aspects were addressed through their inherent characteristics of being less corrosive, easily separable, recyclable, applicability to continuous process and lesser waste water production. Among the different types of ILs, considerable efforts have been made to design acidic ionic liquids (AILs) as potential alternative catalysts for the processing of energy conversion materials [40]. The acidic nature of AILs makes it a more efficient catalyst in various catalytic chemical conversions. Among the available AILs, Bronsted-Lewis acidic ionic liquids (BLAILs) was developed to provide a mixed acids catalytic system. BLAILs catalytic system has been reported to demonstrate promising results in depolymerisation, esterification, transesterification and oxidation reactions [41]–[43]. The addition of Lewis acidic site to the catalyst lead to a stronger and more controllable acidity than solely Bronsted acid ILs (BAILs) [44], owing to the positive and strong synergistic effect from both Bronsted and Lewis acidic sites in promoting the catalytic chemical reactions concurrently. Therefore, the development of technically feasible and environmentally friendly ion pairs of BLAILs for biomass pretreatment and catalytic conversion into LA and EL, via one-pot, is highly demanded.

A dynamic guidance towards the development of technology could provide commercial success through the proper integration of biofuel with the readily available agricultural residues. As such, oil palm biomass allows for a

flexible and integrated processing approach in advanced biorefinery operations thus allowing greener industrial commercial biomass processing to become a reality.

## 1.2 Problem Statement

In the exploitation of ILs utilisation in LA and EL productions, most ILs applied were halide based ILs such as $[Cl]^-$, $[Br]^-$, $[PF_6]^-$, $[BF_4]^-$, $[(CF_3SO_2)_2N]^-$ and their derivatives [45]. These ILs are well acknowledged for the biomass and/ or cellulose dissolution competency, prior the subsequent conversions into LA and EL via homogeneous and/ or heterogeneous catalysts. Nonetheless, the presence of halide based ILs results in catalyst poisoning and deactivation [46]. Therefore, an alternative approach that is capable of overcoming these drawbacks is the development of newly emerged and promising ILs such as AILs.

AILs have been utilised for the production of LA and EL [47]–[52], owing to the acidic nature of the ILs for the catalytic conversion to be possible [53]. As such, most of the research works on the biomass and its derivatives conversions to LA and EL were catalysed by a single acid catalytic system, i.e., a Bronsted acid ILs (BAILs) or a Lewis acid ILs (LAILs) [54]–[56]. Nonetheless, neither sole BAILs or LAILs catalytic system gave satisfactory yields. Solely BAILs catalytic system gave slow conversion of glucose and thus prolonged reaction time is normally required [44]. This is owing to the poor isomerisation of glucose to fructose [57]. In fact, fructose consistently gave better yields of LA and EL, as compared to the glucose [58], due to the dehydration of fructose to 5-HMF producing lesser soluble polymer than glucose [59]. Conversely, solely

LAILs catalytic system contributes to low selectivity of LA and EL, as glucose tends to convert into other by-products [60]. To seek out a solution, the coexistence of both Bronsted and Lewis acidic sites, i.e. BLAILs, thereby led to a positive synergistic catalytic effect. The stronger and more controllable acidity of Lewis acid catalyst could overcome the weaker acidity of BAILs [61], by achieving the equilibrium limitations of glucose-fructose isomerisation from the Lewis acidic site. Nevertheless, the existing BLAILs catalytic system developed such as 1-sulphonic acid-3-methyl imidazolium tetrachloroferrate ([SMIM][$FeCl_4$]) [7], involved alkyl sulphonic acid (-$SO_3H$) functionalised group, which is not eco-friendly. This is owing to the presence of (-$SO_3H$) in the ILs, or commonly known sulfonic acid functionalised ILs (SFILs) are extremely acidic, and thus could cause serious equipment corrosion [62]. Nonetheless, to date, SFILs are among the most popular type of AILs utilised in the productions of LA and EL to date [7], [47], [48], [58].

As for the Lewis acidic site of BLAILs, Lewis acid metal salt [64] or zeolites [49] coupled with BAILs co-catalytic system, were the most common BLAILs reported to date. The deactivation of zeolites due to acid site solvation or leaching [65] have necessitated the search of alternative catalyst. Furthermore, Lewis acid $CrCl_2$ and $CrCl_3$ are among the most popular Lewis acid metal salts either used as a sole catalyst for LA production [66] or coupled with BAILs co-catalytic systems for 5-HMF production [67]–[69], followed by dehydration to LA [64]. Nonetheless, the high price, instable nature, toxicity and environmental pollution derived from Lewis acid $CrCl_2$ and $CrCl_3$ have necessitated the search for non-toxic and low cost metal salts. Hence, in a recent work, Lewis acid $FeCl_3$ is used to couple with BAILs co-catalytic systems for the production of LA and

EL [7]. However, the BAILs applied was an SFILs group, and thus was not eco-friendly.

The realisation for the production of LA and EL in the marketplace is challenging due to the high costs associated with complex process engineering configurations, which limit application to large scale specialised processes [63]. Increasing ILs recycling ability could be an option to offset the high cost ILs synthesised materials. Therefore, for feasible operation, the ILs recovery for the recycling purposes has to be as efficient as possible. In addition, biomass pretreatment by using ILs has been recognised as the second largest cost contributor in sugar-based biofuel production [70]. This is owing to the pretreatment process requires a water-wash step which result in losses of sugars and generate large volumes of wastewater or solid waste [37]. Hence, combination of biomass pretreatment step and subsequent chemical conversions to LA and EL into one-pot production would be a feasible approach. Besides, the environmental impacts of ILs is also one of the concerns, although ILs has been tagged as "green reaction media" in the catalytic processes [40]. This is owing to certain ILs, i.e. halide based ILs and SFILs are toxic and corrosive, thus is not environmentally friendly [62], [71].

For these reasons, a feasible, low cost, environmentally friendly one-pot production approach with efficient catalytic activity, as well as easy separable and recyclable BLAILs catalytic system is imperative for the conversion of biomass to LA and EL.

## 1.3 Significance of Study

A substantial body of literature exists for the conversion of biomass and its derivatives to LA and EL via various SFILs catalytic system [7], [47], [72]–[74]. Nonetheless, to date, there is still no research evaluated on the performance of sole acidic [$HSO_4$] anion based BAILs catalytic system, without the (-$SO_3H$) functionalised group in the cation (SFILs). As such, the novelty of the present study focused on using sole acidic [$HSO_4$] anion based BAILs catalytic system for the oil palm biomass conversion to LA and EL. Herein, three types of imidazolium based ILs were proposed, i.e. 1-butyl-3-methylimidazolium chloride ([BMIM][Cl]), 1-butyl-3-methylimidazolium hydrogen sulphate ([BMIM][$HSO_4$]) and 1-methylimidazolium hydrogen sulphate ([HMIM][$HSO_4$]). Chloride $[Cl]^-$ based ILs is neutral and acted as a control, whereas the latter two have a sole acid site but differ in alkyl chain length. It was expected that the sole acidic [$HSO_4$] anion based BAILs proposed could contribute to the following potential aspects.

Sole acidic [$HSO_4$] anion based BAILs have been regarded as noncorrosive [62] and thus is an environmentally friendly catalyst [75], owing to the absence of the corrosive (-$SO_3H$) functionalised group in the cation [70]. As for the synthesis, these ILs can be synthesised through a simple acid–base neutralisation of an organic amine (imidazolium cation based) with a mineral acid (Bronsted acidic salts ($H_2SO_4$)). These starting materials are relatively cheap and the process does not require a purification [70]. Besides, a large reduction in synthetic steps in the production of these ILs has lowered the environmental impact via reduction in the waste by-products, solvent losses, energy usage and $CO_2$ generation [70]. These elements have thus contribute to

an added benefit for its use in commercial industrial processes. The Bronsted acidity of [$HSO_4$] anion also contributes to significant rate enhancements and improved yields of esterification reaction, for instance in the production of ethyl acetate [76]. Besides, ILs composed of [$HSO_4$] anion have the ability to bind with the formed water and contemporaneously to give a biphasic system with the formed products (e.g. ester), that favourably shift the equilibrium towards products, thus increasing the process efficiency [61]. Lastly, these ILs are also technically designed to be thermally stable at processing conditions [70]. The higher stability of [$HSO_4$] anion complexes could avoid occurrence of hazardous vapours and structural damage to the ILs. This suggests that their long-term use in a continuous process would be feasible, with an added benefit of being recyclable [75].

Apart from that, this study also investigated the potential of a co-catalyst, Lewis acid indium trichloride ($InCl_3$), to promote the hydrolysis of polysaccharide [77] and the isomerisation of glucose to fructose [78], which could potentially boost the conversions of LA and EL, in BLAILs catalytic system (i.e. coupling of Lewis acid $InCl_3$ and BAILs, $InCl_3$-BAILs). Lewis acid $InCl_3$ was chosen as a co-catalyst due to their excellent properties, as follow: (1) a newly emerged environmentally friendly catalyst that is easily-handled and imparts high region-selectivity and chemo-selectivity in various chemical conversions [79]; (2) low toxicity, operational simplicity and remarkable ability to suppress side reactions in acid-sensitive substrate [77]; (3) a water-compatible Lewis acid catalyst [80] and is thus suitable for the use in biphasic ILs/water system. To date, the literature on using $InCl_3$-ILs catalytic system is still at a newly developing stage. For instance, the study showed that in $InCl_3$-SFILs

catalytic system, Lewis acid site highly favoured the production of 5-HMF intermediate (+28.3% compared to sole SFILs), signifying the enhancement of the isomerisation of glucose to fructose [77]. Hence, LA yield was increased.

As for the production aspect, the proposed coupling of BLAILs ($InCl_3$-BAILs) catalytic system could facilitate the biomass pretreatment steps, hydrolysis, isomerisation, dehydration and rehydration reactions in the conversion to LA, followed by the upgrading esterification reaction to EL via one-pot. One-pot production approach could render the process to be more economically competitive [81], by reducing the number of products recovery after each steps, alongside with a reduction of unwanted liquid and solid waste by-products [82]. In addition, it allows the discarding of the high cost biomass pretreatment step [70], thereby giving the overall conversion process into a simple and convenient one-pot conversion strategy. To date, one-pot production approach of LA and EL via SFILs is still at a developing stage with only a few literatures reported [7], [73], [74], [83].

To date, a feasible, low cost, environmentally friendly one-pot production approach with efficient catalytic activity, as well as easy separable and recyclable BLAILs catalytic system has yet to be developed. Herein, the present study aims to address this knowledge gap by developing a new environmentally friendly BLAILs ($InCl_3$-BAILs), i.e. coupling of Lewis acid $InCl_3$ and sole acidic [$HSO_4$] anion based BAILs, for the oil palm biomass conversion to LA and upgrading to EL. The results obtained are critically compared with other ILs catalytic system, with the aim to assess the effectiveness of the LA and EL production yields as well as the "greenness and energy saving" perspectives of the system.

## 1.4 Objectives

The proposed research aims to develop and evaluate the sustainable production of LA and upgrading to EL from oil palm biomass, i.e. OPEFB and OPMF, via a new environmentally friendly coupling mixed acids $InCl_3$-BAILs catalytic system. The specific objectives of the research are:

1) To characterise the extractive compositions of OPEFB and OPMF biomass, as well as the physical properties of the proposed imidazolium based ILs.
2) To screen and select the best catalytic activity of ILs for the catalytic conversion of OPEFB and OPMF biomass to EL.
3) To optimise the operating reaction conditions for the catalytic conversion of OPEFB and OPMF biomass to LA and upgrading to EL via $InCl_3$-BAILs catalytic system.
4) To evaluate the kinetic and thermodynamic parameters for the catalytic conversion of OPMF biomass to LA and upgrading to EL via $InCl_3$-BAILs catalytic system.
5) To investigate the catalyst recyclability for the $InCl_3$-BAILs catalysed conversion of OPEFB and OPMF biomass to EL.

## 1.5 Research Approach and Scope

The research scope comprises five main sections as follows:

**1) Characterisation studies of oil palm biomass and ionic liquids**

Oil palm biomass characterisation study by using thermal gravimetric analysis (TGA) method was performed for the determination of the

lignocellulose compositions, i.e. holocellulose (cellulose and hemicellulose), lignin, etc. Holocellulose, which is the sum of cellulose and hemicellulose, was analysed according to the method reported by Teramoto et al. [84] (refer to **Appendix 1**). The percentages of holocellulose content from the biomass samples were adopted from the TGA analysis. Subsequently, the studies on the physical properties of ILs, which included density, viscosity, thermal decomposition and Hammett acidity function were examined for the reliable data on the proposed ILs.

**2) Screening of ILs for the conversion of oil palm biomass to EL**

Three types of ILs were proposed for the conversion of oil palm biomass (OPEFB and OPMF) to EL. A two-step sequential reaction was conducted, i.e. the depolymerisation to LA, followed by the upgrading esterification to EL. The ILs involved in this study were made up of imidazolium based ILs, i.e. [BMIM][Cl], [BMIM][$HSO_4$] and [HMIM][$HSO_4$]. The best catalytic activity of ILs, i.e. [HMIM][$HSO_4$], was then chosen for the subsequent studies.

**3) Optimisation studies on the conversion of oil palm biomass to LA and upgrading to EL via $InCl_3$-[HMIM][$HSO_4$]**

Statistical analysis and reaction optimisation studies by using a response surface methodology (RSM) based on a central composite design (CCD) method was conducted. A preliminary parametric study for the conversion of OPEFB and OPMF biomass to LA and upgrading to EL was first conducted (Tiong et al. [78], refer to **Appendix 2**), in order to obtain the desired

experimental parametric range for the statistical analysis and optimisation studies. This study was conducted to understand the effects of process parameters and to obtain statistical models for the associated responses. Subsequently, the research further investigated the potential of Lewis acid $InCl_3$ to boost the catalytic activity of the optimised sole [HMIM][$HSO_4$] catalytic system. On top of that, other by-products produced from the both LA and EL syntheses were also discussed, to have a deep understanding on all the bio-based chemical products produced. Finally, the results of the present studies on both LA and EL yields via $InCl_3$-[HMIM][$HSO_4$] catalytic system were critically compared with other ILs catalytic system reported in the literature.

**4) Kinetic and thermodynamic studies on the conversion of oil palm biomass to LA and upgrading to EL via $InCl_3$-[HMIM][$HSO_4$]**

Kinetic and thermodynamic studies were conducted to investigate the mechanistic elucidation of chemical reactions and their energetic feasibility. The biomass conversion reactions via hexose (cellulose) pathway, i.e. cellulose depolymerisation to LA, and the subsequent upgrading esterification to EL, were conducted within temperature ranges of 135-175°C and 65-105°C, respectively. Pseudo-homogeneous kinetic models were adapted to evaluate the best reaction order. The kinetic parameters, such as the reaction rate constants at various temperatures, pre-exponential factor and activation energy were investigated. The thermodynamic energy was assessed by examining the activation enthalpy, activation entropy and Gibbs free energy of activation. This work exhibited the inputs and important basic information for both kinetic and thermodynamic

models on the oil palm biomass conversion to LA and upgrading to EL via $InCl_3$-[HMIM][$HSO_4$] catalytic system . Finally, the results were critically compared to the literature data to assess the "greenness and energy saving" perspectives of the system.

**5) Recyclability of $InCl_3$-[HMIM][$HSO_4$]**

The main reason that hindered the application of ILs in a large scale process is due to high costs in comparison to conventional catalysts. Hence, an option to offset this drawback is by recycling them for the next process. Herein, $InCl_3$-[HMIM][$HSO_4$] catalytic system was assessed through a series of consecutive recyclability test runs on the optimised reaction conditions of biomass conversion to EL. In addition, the stability of used $InCl_3$-[HMIM][$HSO_4$] was assessed by comparing its viscosity and molecular structure with the fresh one if any deterioration incurred. The molecular structure was examined by using $^1$H NMR, and FTIR/ATR analyses.

## 1.6 Limitations of Study

It is acknowledged that there exist many types of oil palm biomass residue generated by the palm oil industry, as mentioned in **Chapter 1.1**. Among these, OPF and OPEFB biomass were the most utilised and reported biomass type in biomass conversion to LA and EL [7], [85]–[90]. In contrast, OPT, OPMF, OPKS and OPS biomass have not been reported for this particular biomass conversion to date. Nonetheless, this study focuses on using OPEFB and OPMF biomass only, for the catalytic conversion to LA and upgrading to

EL via the proposed ILs, due to the availability as well as easier handling and processing. As such, the results on the production yields of LA and EL from the commonly used OPEFB biomass conversion could be justified, along with the comparison to the first use OPMF biomass. Furthermore, for the novel coupling mixed acids BLAILs ($InCl_3$-BAILs) catalytic system, the environmentally friendly Lewis acid $InCl_3$ was directly selected, for the novel coupling with the best catalytic activity of noncorrosive BAILs, i.e. [HMIM][$HSO_4$], without screening a series of various Lewis acid catalysts, due to budget constraints and insufficient time. As for the kinetic and thermodynamic studies, only OPMF biomass was conducted, owing to OPMF biomass exhibiting higher production yields of LA and EL in the prior reaction optimisation studies. Finally, only EL yield was taken into consideration in the recyclability test runs, as EL is the main target and final bio-based chemical product produced in this study as it is a high potential biofuel.

# Chapter 2

# Literature Review

## 2.1 Oil palm

Unlike crops that are grown in temperate climates, oil palm is a perennial crop that grows in tropical regions of the world. Oil palm (*Elaeis guineensis*) is a tropical palm tree native to Africa [91], and is the most important monecious species in the *Elaeis* genus which belongs to the family of Palmae [92]. The original African oil palm was brought to the Malaya region (the now Sumatera, Indonesia and Peninsular Malaysia) in the beginning of the 20$^{th}$ century [93].

Oil palm is the second most traded vegetable oil crop and the majority of the world's oil palm exports originate from South East Asia countries [94]. In a recent review [95], in the year of 2015, Indonesia had the highest global palm oil production (33,000,000 t), followed by Malaysia (20,500,000 t), Thailand (2,250,000 t), Columbia (1,108,000 t), Nigeria (930,000 t), Papua New Guinea (630,000 t), Ecuador (575,000 t) and Ghana (495,000 t). As observed, the production of palm oil is majorly dominated by Indonesia, Malaysia and Thailand, together accounting for approximately 95% of Asia's total palm oil production. Generally, the expansion of production in Asia is due to good growth conditions, greater productivity of oil palm over potential alternatives and advances in cultivation, refining and transport technologies. This is especially true for Malaysia due to the global demand for palm oil as an edible oil, where about 25% of edible oil production is dominated by palm oil [93].

According to a review reported by Sumathi et al. [96], the physical characteristic of oil palm trees are illustrated as follow. The mature oil palm trees are single-stemmed, and grow up to 20 m tall. The leaves are pinnate or "feather-like" shape with lengths of 3 to 5 m long. The flowers are produced in dense clusters with three sepals and three petals. Morphologically, oil palm fruits come in a bunch weighing around 10-40 kg each and are reddish in colour. The oil palm fruit or normally known as fresh fruit bunch (FFB) takes around five to six months to mature from pollination to maturity. FFB comprises an oily, fleshy outer layer (the pericarp), shell and kernel which contain 45-55% edible oil. Crude palm oil (CPO), palm kernel oil (PKO) and palm kernel cake (PKC) are the main products of FFB [91].

### 2.1.1 Availability of oil palm biomass

Apart from CPO, PKO and PKC, the palm oil agroindustry generates a significant amount of residual biomass at an estimation of around 87 million tonnes annually worldwide [97]. For instance, the production of CPO in Malaysia has recorded a large increment from 2.6 million tonnes in 1960 to 19.7 million tonnes in 2013 [98]. Consequently, this massive production also contributed to an even larger amount of palm oil mill effluent (POME) [99]. In fact, the palm oil industry in Malaysia is one of the major agricultural industries that contribute to the highest biomass residues. Although POME is a non-toxic liquid, it contains soluble materials that are harmful to the environment, either in the form of soluble gases (such as methane ($CH_4$), sulphur dioxide ($SO_2$) and ammonia ($NH_3$)), soluble liquids or solids, with concentrations above the

threshold limit values [95]. Hence, it has become necessary to treat the effluent to the highest degree possible before it is discharged into the environment.

As for the biomass residues generated from the palm oil industry, the biomass residues can be generated in two ways, i.e. from the plantation and the mill sites. Awalludin et al. [91] highlighted that the solid biomass wastes comes from the oil palm plantations in the form of harvested trunks (OPT) and pruned fronds (OPF). These are the major residues obtained from the plantation during cut-down. The OPF are left rotting between the rows of palm trees, mainly for soil conservation, erosion control and long-term nutrient recycling [100]. Moreover, both OPT and OPF are applied in wood manufacturing industry for pulp, paper and fibreboard [100]. On the other hand, the palm oil extraction mills produce various oil palm biomass wastes such as OPEFB, OPKS, OPMF and POME. These main residues are produced during the milling process of CPO production [101]. The FFB are pressurized cooked and stripped from the bunch for oil extraction purpose and thus generates the production of OPEFB. During the palm oil extraction process, the OPMF is produced while the process of nut separation from its kernel produces OPKS. All the palm biomass wastes are rich in fibre content except POME.

Following the trend of oil palm production in Malaysia, the biomass from oil palm displays a positive slope from year 2009 to 2014. In 2014, the generation of OPKS was as much as 5,525,154 t; OPMF was 13,561,741 t; OPF and OPT were 16,176,705 t; OPEFB was 22,100,614 t, being the most generated biomass, while POME was 72,767,726 t [93]. Therefore, there is potential in harnessing the widely available oil palm biomass for the development of more

sustainable and greener biofuels and highly valuable biochemical-based products production. With Malaysia's high capacity of oil palm plantation, Malaysia could enhance this sector into a renewable energy sector as an effort towards sustainability.

### 2.1.2 Oil palm biomass for energy

Concerns regarding the price fluctuation of oils, high energy demand and climate change have been the focus of international policy discussion. The fundamental principle of making the palm oil industry more sustainable is to reduce and recycle the waste with possibility of converting the wastes into useful energy. Hence, the use of oil palm biomass as a renewable energy source is highly promising. Energy is important for increasing productivity, enhancing competitiveness and promoting economic growth such as in the case of promoting bioethanol derived from plant-biomass based feedstock and biodiesel derived from oil crops and animal fats [102].

In 2012, 106 billion litres of biofuels were produced globally, of which 22.5 billion litters were in the form of biodiesel [102]. The growing market for biofuel has created great opportunities for several countries in South East Asia that find themselves poised as major producers, consumers and exporters. Specifically, Malaysia and Indonesia have proceeded as large agribusinesses enterprises due to the large availability of oil palm biomass. For instance, Indonesian biodiesel exports recorded a 117% growth over 2010 that has encouraged the national government to allocate 20 million hectares of land

towards establishing new oil palm plantations, which represents a 330% increase over present land area under cultivation [102].

Oil palm biomass is considered as a clean source of energy where the environmental impacts are reduced and lesser secondary wastes are produced. Furthermore, oil palm biomass is a renewable source of raw material and energy by reducing the utilisation of the carbon reservoir in the form of crude petroleum oil beneath the earth [91]. Structural analysis of oil palm biomass wastes shows that they are rich in lignocellulose content (cellulose, hemicellulose and lignin) which are important for the development of fuels and chemicals [101]. There is a high potential in converting oil palm biomass efficiently and effectively to other value added by-products [92]. For instance, Sime Darby in Malaysia has been utilising OPEFB and POME from the oil mill to produce 26,000 t of enriched organic fertiliser annually at Lavang Oil Mill [103]. Therefore, the utilisation of oil palm biomass as feedstock is an excellent way to reduce waste management problems and decrease the emission of toxic compounds such as $CH_4$ and nitrous oxide ($N_2O$) from the degradation of dumped palm wastes [104]. Apart from that, in Indonesia, the estimation of biomass-based renewable energy potential generated from oil palm biomass was approximately 54.8 GJ/year [105].

In summary, the use of oil palm biomass as the substitute lignocellulosic material can enhance the status of oil palm industry as an environmentally friendly and sustainable industry [106].

## 2.2 Approaches for conversion of biomass to biofuels: Thermochemical and depolymerisation pathway

According to a review reported by Alonso et al. [107], there are two major routes of biomass conversion to liquid biofuels, as depicted in **Figure 2.1**. The first pathway is thermochemical route, where biomass is processed at high temperatures and/or pressures (e.g. pyrolysis, gasification, liquefaction). The thermal deconstruction of biomass yields upgradeable intermediates such as bio-oils by pyrolysis and synthesis gas (syn-gas) by gasification. The second pathway is depolymerisation route, where lignin is isolated from biomass and processed selectively through either biological or catalytic chemical pathways, to produce sugar monomers which are then deoxygenated to form upgradeable intermediates. In both pathways, the functional species from each platform are subsequently upgraded by C–C coupling reactions to form the desired liquid hydrocarbon fuel. Generally, biomass depolymerisation is rather complex than the thermochemical conversion, alongside incurring at a higher cost. Nonetheless, depolymerisation based strategy offers a more selective processing options for the productions of desired chemical intermediates or targeted hydrocarbons for transportation biofuels [108]. In any case, depending on the renewable biomass feedstock and desired chemical product, thermochemical and depolymerisation pathways are both important for the production of sustainable biofuels and bio-based chemicals.

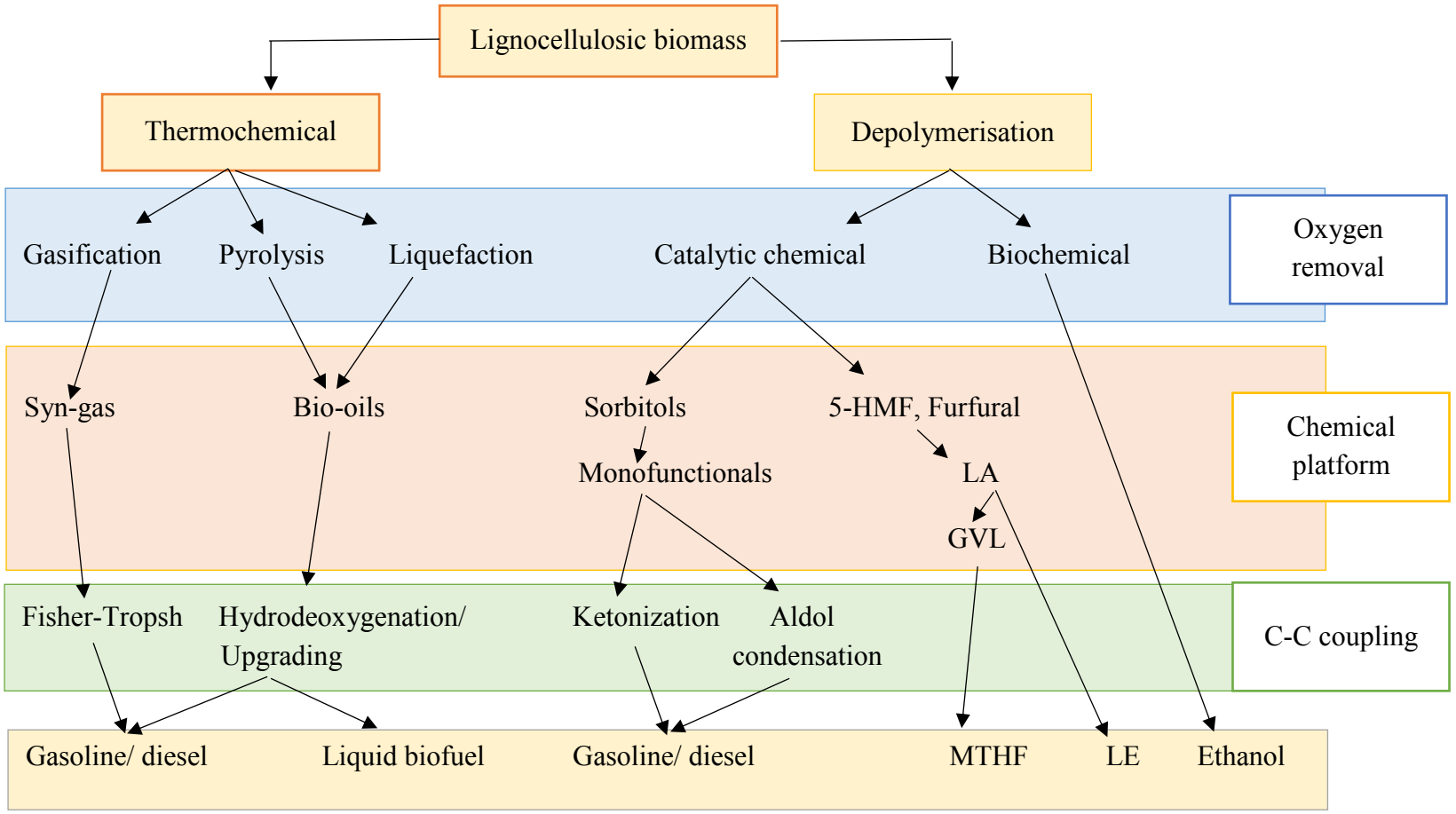



**Figure 2.1** Strategies for conversion of lignocellulosic biomass to liquid biofuels via thermochemical and depolymerisation routes. Adapted from Alonso et al. [107].

## 2.3 Bio-based Chemicals: Levulinic acid (LA) and Levulinate esters (LE)

LA and LE are attractive chemicals for potential value-added chemicals, biofuels or fuel additives. The shift from non-renewable to renewable (from petroleum-based to biomass-based) resources for the production of LA and LE is generally viewed as a viable solution to develop a "Green-Sustainable Society" [109]. In this regard, there is great research interest in the sustainable and greener production of biomass derived energy such as biofuels and valuable bio-chemical products (LA and LE).

### 2.3.1 Levulinic acid (LA)

LA, also known as 4-oxopentanoic acid or gamma-ketovaleric acid, is a $C_5$ short chain fatty acid with an acidic carboxyl group (COOH) and ketone carbonyl group (C=O) [18], as shown in **Figure 2.2**.

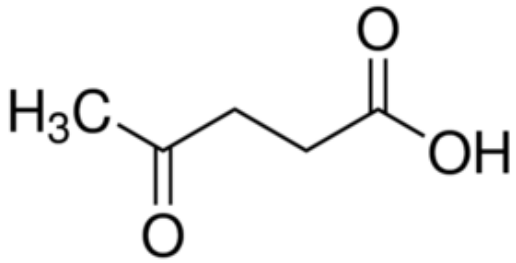



**Figure 2.2** Chemical structure of LA.

LA is a crystalline compound. It melts at 37˚C into a clear yellow to brownish liquid with a caramellic odour [18]. It has a boiling point of 245-246ºC and a density of ~1.14 g/cm$^3$ [2]. The ketone and carboxyl functional groups of

LA imparts the ability to react in various organic syntheses such as esterification, hydrogenation, condensation, oxidation and halogenation into a wide range of chemicals or derivatives [2], [110]. LA is a polar compound and thus is soluble in water and polar organic solvents such as alcohols, ethers, acids, chloroform, etc [18]. LA is water soluble with $pK_a$ of 4.59 at 25$^oC$, which means that its acidity is comparable to that of lower alkane carboxylic acids [2].

LA is an ideal platform chemical for various high-value organic chemicals such as succinic acids, resins, polymers, herbicides, pharmaceuticals, flavouring agents, solvents, plasticisers, anti-freeze agents and fuel additives with wide potential industrial applications [17], [111]. It can also be an intermediate product for applications in medical supplies or materials for producing some other value-added chemicals such as approved skin cancer treatments [112]. Moreover, the designation of LA is recognised as safe for specific uses in foods and it acts as a potential sanitizer for large-scale food processing facilities [110].

The high yield of LA from renewable feedstock has been practiced in several new chemical industries such as the facility in South Glens Falls, New York where the LA production is at a 1 ton/ day scale [112]. There is another existing LA production industry developed by Biofine Corporation [113]. This Biofine process reaction involved the use of lignocellulose as starting material with sulphuric acid (1.5-3% (w/w)) as catalyst to perform the hydrolysis process in the production of 5-HMF, followed by the production of LA in yields within 70-80% of the theoretical maximum [114]. Although the utilisation of inexpensive lignocellulosic wastes in the processes allows LA to be produced at

a moderate cost, improvements in environmentally benign catalysts and energy efficient processes are essential.

#### 2.3.1.1 LA in the production of biofuel or fuel additive

Due to its high functionality (keto and carboxyl groups), LA is an attractive platform chemical for obtaining higher value-added chemicals, biofuels or fuel additives. Hydrogenation and esterification of LA produces a variety of biofuel additives such as GVL, MTHF, LE and long chain hydrocarbon alkanes [115], [116]. These biofuels can be readily blended with petroleum products to make cleaner burning fuels [17] and used as diesel additives [117]. One of the most vital processes is the hydrogenation of LA into 4-hydroxy LA, followed by its ring cyclization to GVL, along with LE formation where they can be used in producing sustainable liquid transportation fuels as an alternative to ethanol in a gasoline ethanol blend [118]. Moreover, the conversion of LA to MTHF can also be applied in the petrochemical industries as gasoline [119]. The production of MTHF is a single stage catalytic hydrogenation process where it is produced with over 80% molar yield for the application of solvent and fuel extender [112]. MTHF and LE have been approved by the US-DOE as a component of P Series type fuels [118]. **Figure 2.3** shows a variety of derivatives of LA for various end products application.

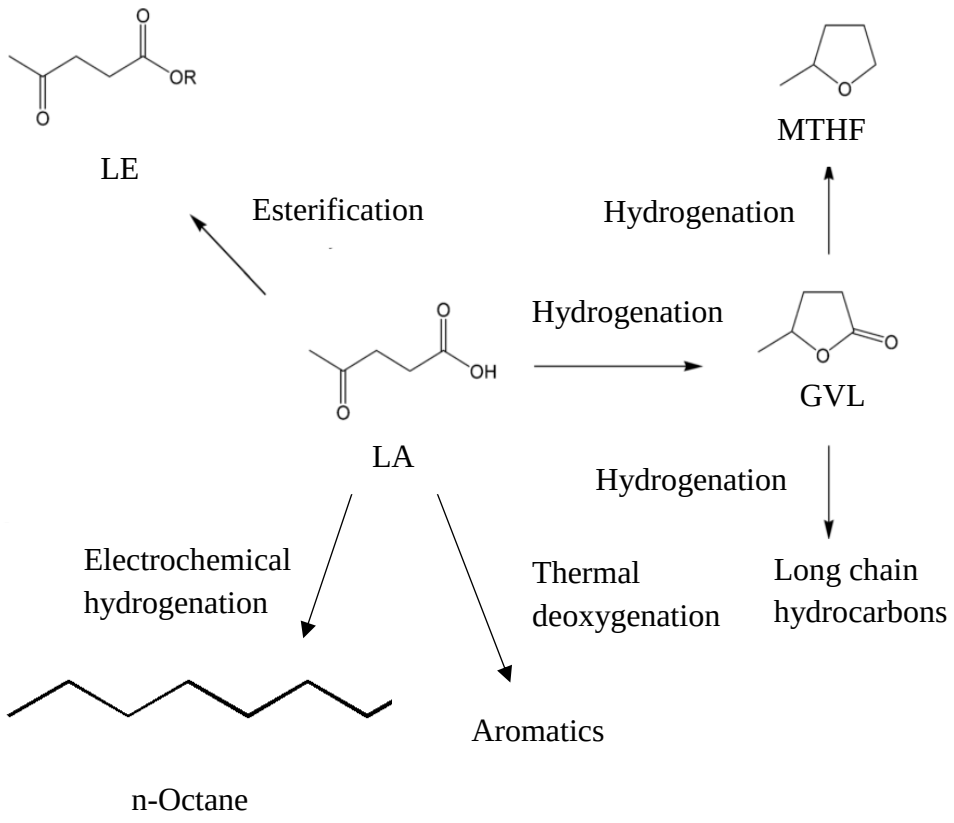



**Figure 2.3** Derivatives of LA from the lignocellulosic biomass as a platform for liquid fuels and additives. Modified from Démolis et al. [15] and Mariscal Lopez et al. [120].

### 2.3.2 Levulinate esters (LE)

LE are produced by the esterification of LA with alcohol. The alkyl component from the alcohol dictates the variability in the physical properties of LE. As such, EL, being one of the LE, is under the keto ester group, which is also known as ethyl 4-oxopentanoate. EL has a high flash point of 90$^{o}$C, a boiling point temperature of 206$^{o}$C which is similar to typical diesel fuel, and a high energy content compared to other diesel fuel oxygenate candidates such as ethyl palmitate, ethyl sterate, ethyl oleate and ethyl linoleate [26].

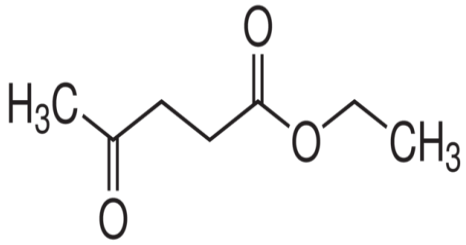



**Figure 2.4** Chemical structure of EL.

### 2.3.2.1 LE as potential biofuel or fuel additive

LE are known to be viable biofuel molecules for diesel engines. The different alkyl group of levulinate differentiate each LE properties. For instance, ML is the shortest alkyl group which can be used as gasoline additives, whereas ethyl and higher alkyl levulinates are potentially used as diesel blend components [11]. For instance, with a short chain fatty esters structure of EL, it contains no sulphur which leads to lower sulphur emissions then the regular diesel as well as lower cloud point than biodiesel [112]. Additionally, the excellent performance attributes of LE including low toxicity, high lubricity, flashpoint stability and superior moderate flow properties under low temperature conditions have make it a suitable alternative source for additives to biodiesel transportation fuels [121]–[123].

EL has been highly prospected as a better choice among the levulinates. For instance, Christensen et al. [27] has demonstrated an experimental study with both EL and butyl levulinate (BL) as diesel blends in a 2008 model year Cummins ISB engine. No change in total hydrocarbon, carbon monoxide or particulate matter exhaust gas emissions were observed from the 10% and 20% (v/v) of EL and BL, respectively. The engine-out smoke number was reduced by

41.3% and 55% from EL and BL, respectively while oxides of nitrogen emissions, which are greenhouse gases, were increased for BL with 4.6%. Nonetheless, there were no oxides of nitrogen observed from the EL and thus it was a better choice in terms of environmental concern. Furthermore, Joshi et al. [124] reported that diesel blends with EL satisfied the ASTM D6751 with up to 15% (v/v) and have been proven in improving the cloud point, pour point and cold filter plugging point with a reduction of 4-5°C, 3-4°C and 3°C, respectively, as compared to diesel fuel prepared from cottonseed oil and poultry fat. Moreover, EL has also been applied as a fuel extender for diesel [125], [126] as it can be used up to 5% (w/w) as a diesel miscible biofuel (DMB) directly in regular diesel car engines [8]. This is attributed to the similar properties of EL to biodiesel fatty acid ethyl esters (FAEEs), and thus it has been highly proposed to be used as an oxygenate diesel additive.

## 2.4 Synthesis route of LA and LE from biomass

Lignocellulose primarily contains cellulose, hemicellulose and lignin. Cellulose and hemicellulose are highly functionalised polysaccharides that constitute a major portion of plant biomass [113], and play a decisive role in depolymerisation and esterification routes for the production of LA and LE, respectively. Upon hydrolysis, they are macro sugar polymers that depolymerise into $C_5$ and $C_6$ sugar monomers and/or oligomers, prior to further conversion to intermediate products (i.e. furfural, 5-HMF), and finally, to LA in the presence of an acid catalyst [127], [128].

Cellulose is the major substrate in the conversion to LA and LE where it breaks down into $C_6$ sugars (glucose, galactose and mannose). To a lesser extent, hemicellulose also breaks down into $C_6$ sugars, apart from the major components of $C_5$ sugars (xylose and arabinose). Aside from that, lignin is a phenolic polymer that may be dissolved in the reaction solution as an acid soluble lignin [129]. **Figure 2.5** shows a schematic diagram for the conversions of each component of lignocellulosic biomass to LA and LE.

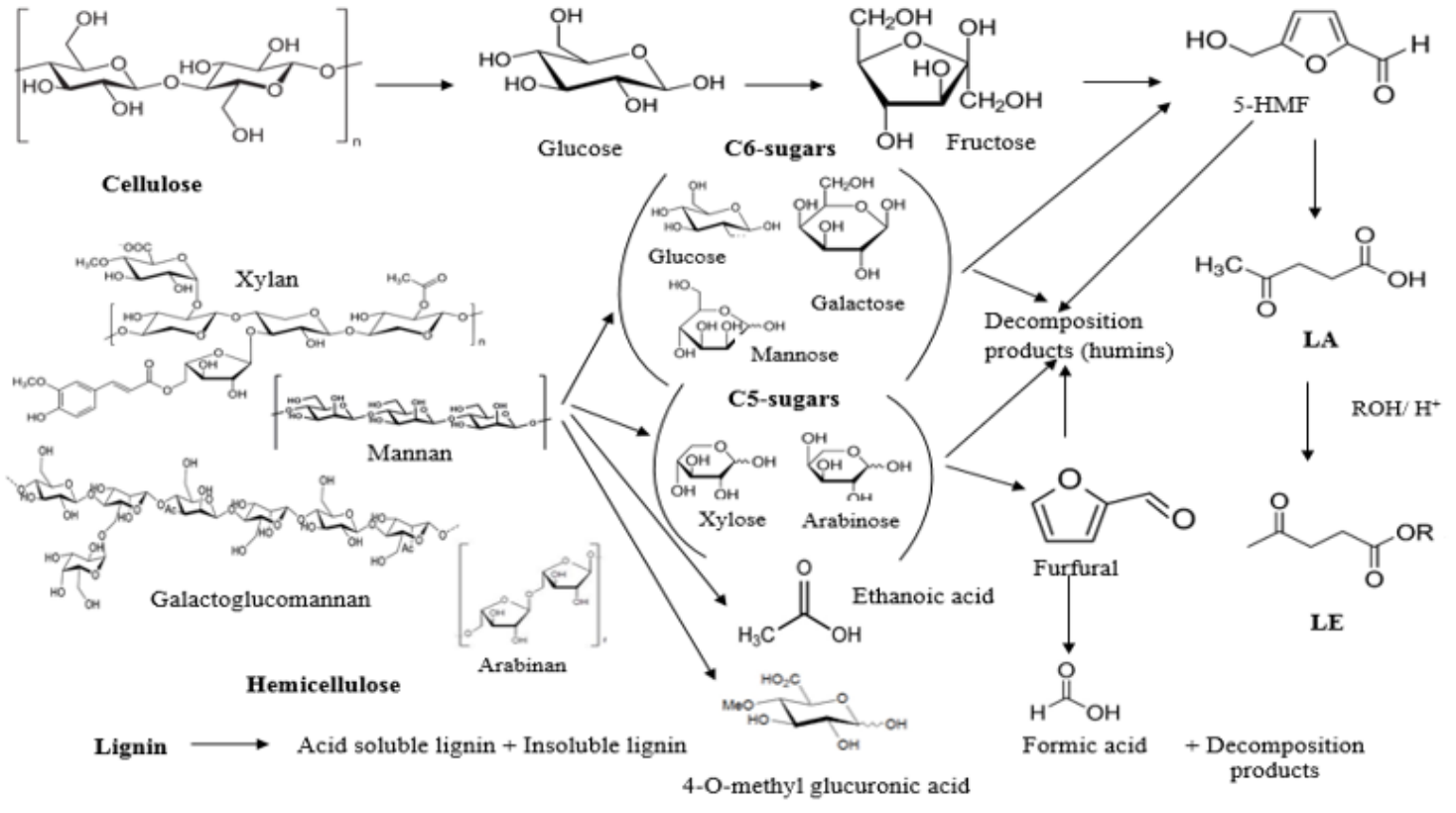



**Figure 2.5** Conversion of lignocellulosic biomass components to LA and LE. Adapted from Girisuta et al. [130].

Specifically, LA and LE are synthesised via two major routes, i.e. hexose (cellulose) and pentose (hemicellulose) routes [131]. The hexose sugars route is more common and is related to the degradation of cellulosic carbohydrate of lignocellulosic biomass [132] in which 5-HMF is the key intermediate compound. This route involves five major steps as follows: (1) hydrolysis of polymeric cellulose into monosaccharides, (2) isomerisation of aldose-type sugars (glucose) to ketose-type sugars (fructose) by allowing five-membered ring formation, (3) dehydration of fructose to generate 5-HMF, (4) rehydration of 5-HMF to produce LA, then (5) esterification of LA with alcohol to produce LE [129], [131]. Meanwhile, the pentose route is based on the degradation of hemicellulosic carbohydrate of lignocellulosic biomass [132] in which furfural and furfuryl alcohol are intermediate products. Due to the branched and amorphous structure, hemicellulose is easily hydrolysed and converted into end products as follows: (1) hydrolysis of hemicellulose into $C_5$ sugars (mainly xylose), (2) dehydration of xylose to furfural, (3) separation and transformation of furfural into furfuryl alcohol via a gas-phase hydrogenation step, (4) acid catalysed ring-opening of furfuryl alcohol in water to produce LA, then (5) esterification of LA with alcohol to produce LE [133]. In certain circumstances, the ring opening of furfuryl alcohol can also be achieved in the presence of alcohols where the alcoholysis subsequently affords LE and the hydrolysis process is skipped to furnish LA [120], as shown in **Figure 2.6**. However, under the severe reaction conditions, the intermediate products (sugars, 5-HMF and furfural) may further react with sugars to form dark-brownish decomposition products (humins) [129], as shown in **Figure 2.5**. The pentose route is an alternative to the hexose route in the conversions of cellulose-derived substrates.

The details of the reaction pathways of hexose and pentose routes are shown in **Figure 2.6**.

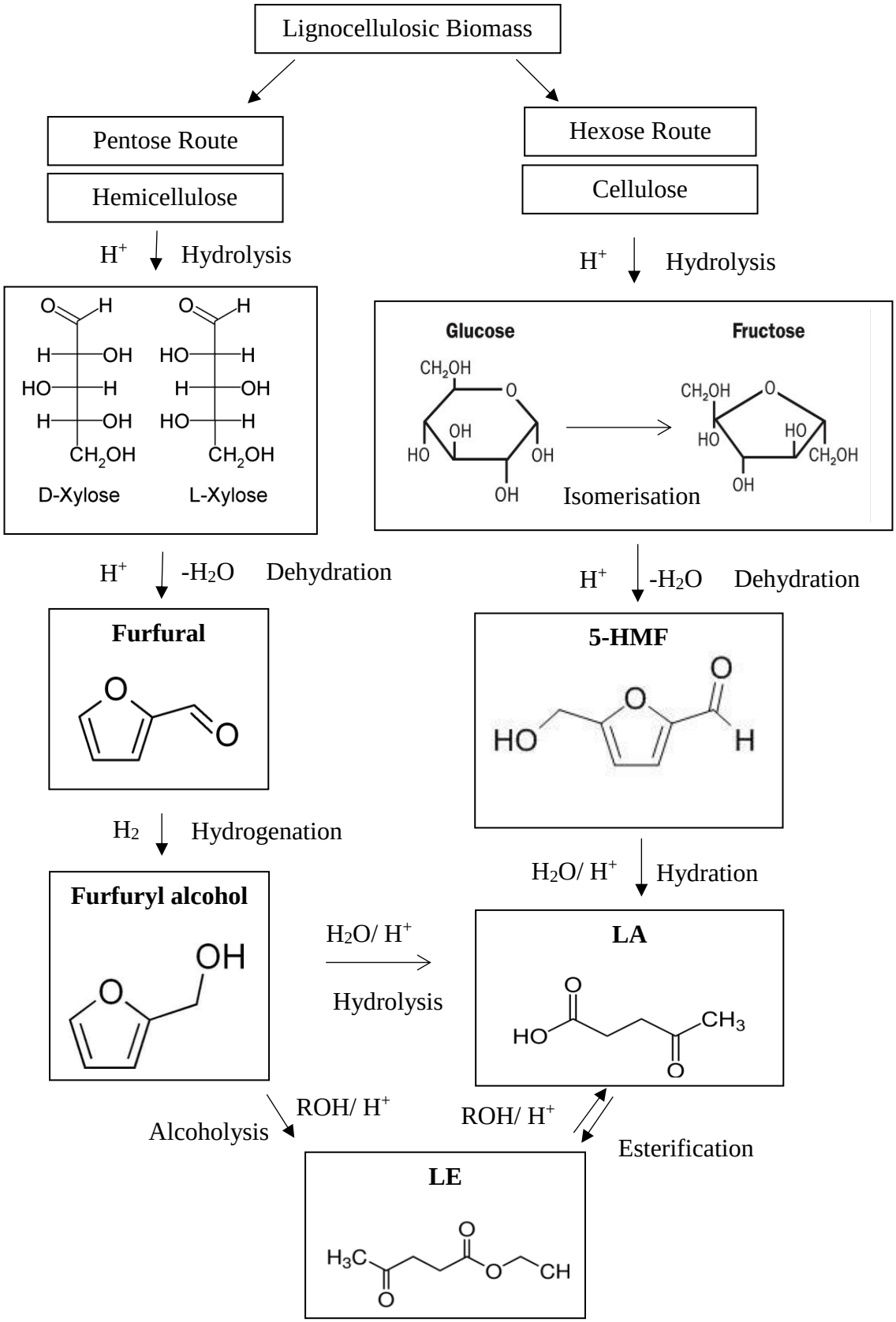



**Figure 2.6** Reaction pathways of hexose and pentose route for production of LA and LE. Adapted from Neves et al [134].

## 2.5 Ionic Liquids (ILs)

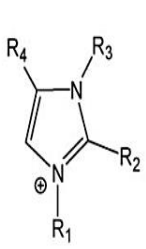
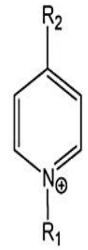
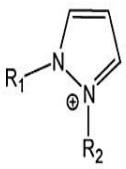
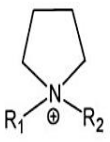
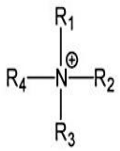
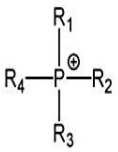
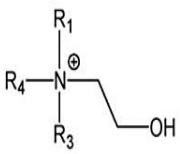
ILs refer to a Newtonian liquid composed of ionic species which comprises organic cations and organic or inorganic anions [32]. ILs have melting points below the boiling point of water, however, it is non-volatile and non-flammable. Thus, it is considered as environmentally friendly. Additionally, IL is a good solvent for a variety range of polar organic molecules and inorganic salts materials [135]. Most of the ILs are immiscible with apolar compounds resulting in the formation of biphasic layer thus benefitting the chemical separation process by simple decantation. The isolation of desired organic compounds from the ILs could be achieved relatively easier [76], [135], [136]. Furthermore, the nature of the intermolecular and intramolecular interactions between the cation and anion species in ILs makes them as an arbitrary upper limit temperature and strong stability catalyst [137]. This enables ILs to be recycled without significant loss of catalytic efficiencies [136], [138].

Apart from that, ILs enhance the catalytic activities with high efficiency and products selectivity yield in the desired organic unit reactions [139]. As such, the concepts of conventional heterogeneous catalysts have gone beyond to the concepts of solid catalysts with ILs (SCILs) and supported ILs phase catalysts (SLIPCs) to integrate heterogeneous catalysts with the ILs with better efficiency and products selectivity yield. For instance, Gu et al. [140] investigated the etherification of 1-tolyl-1-ethanol catalysed by $SiO_2$-$SO_3H$ leading to 30% of 4-methylstyrene as side product and thus reducing the desired ether yield to 61%. To overcome this limitation, coating of $SiO_2$-$SO_3H$ with 25% (w/w) of ILs, 1-methyl-3-octylimidazolium amide $[C_8MIM][NTf_2]$, led to a significant

selectivity improvement of up to 96% ether yield under similar reaction conditions.

The commonly used cations and anions of ILs are shown in **Table 2.1**.

**Table 2.1** Main cations and anions of ILs.

| Cations | Anions |
|---|---|
|  Imidazolium | $Cl^-$, $Br^-$, $I^-$ |
|  Pyridinium | $Al_2Cl_7^-$, $Al_3Cl_{10}^-$ |
|  Pyrazolium | $Sb_2F_{11}^-$, $Fe_2Cl_7^-$, $Zn_2Cl_5^-$, $Zn_3Cl_7^-$ |
|  Pyrrolidinium | $CuCl_2^-$, $SnCl_2^-$ |
|  Ammonium | $NO_3^-$, $PO_4^{3-}$, $HSO_4^-$, $SO_4^{2-}$ |
|  Phosphonium | $CF_3SO_3^-$, $ROSO_3^-$, $CF_3CO_2^-$, $C_6H_5SO_3^-$ |
|  Cholinium | $PF_6^-$, $SbF_6^-$, $BF_4^-$, |
| | $(CF_3SO_2)_2N^-$, $N(CN)_2^-$, $(CF_3SO_2)_3C^-$ |
| | $BR_4^-$, $RCB_{11}H_{11}^-$ |

Some cations based are attached with alkyl substituents such as the addition of functionalised cations group with the aim of providing an acidic nature to the ILs such as sulphonic acid and carboxylic acid functionalised groups [141]. On the other hand, the anions are weakly basic inorganic or organic compounds which constitute a diffuse or protected negative charge [137]. Most

of the research studies have been utilising ILs based on halides such as $[Cl]^-$, $[Br]^-$ and $[I]^-$ due to their strongly hydroscopic nature [141].

### 2.5.1 Task specific ionic liquids (TSILs)

TSILs contain functional group(s) that is covalently tethered to the cations or anions or even both sides of the ILs [61] to confer particular properties or reactivity for certain chemical reactions [142]. They also refer to the non-solvent applications of ILs as catalysts in organic syntheses [143], which includes hydrolysis, dehydration and esterification [144] etc. TSILs have been considered as the liquid version of solid-supported catalyst with the advantage of having kinetic mobility and a large operational surface area [139]. Other specific purposes in using TSILs are separation of specific materials as well as for the construction of nanostructure materials and ion conductive materials [145].

According to a review reported by Yue et al. [61], there are many types of TSILs (**Figure 2.7**). TSILs are of much interest to researchers from a wide variety of fields, particularly in the area of organic synthesis, and some of them have been utilised in the commercialised chemical industry. However, the scope of this study is focusing on the organic synthesis of LA and LE from biomass which requires the acidic nature of ILs, or normally known as acidic ionic liquids [53] (AILs*, **Figure 2.7**).

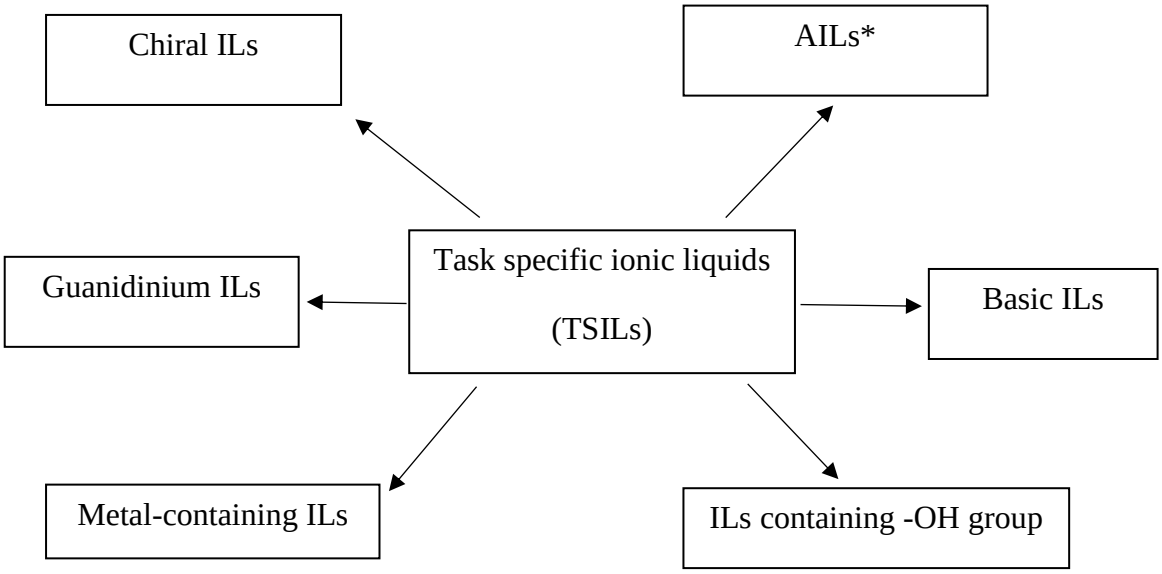



**Figure 2.7** Main evolution of TSIL generations. Modified from Yue et al. [61].

### 2.5.2 Acidic ionic liquids (AILs)

Conversions of biomass and its derivatives to LA and LE have been achieved via AILs. The acidic nature of ILs is the main criteria for the catalytic dehydration of carbohydrates to a variety of bio-based compounds which includes furan derivatives (5-HMF, furfural), LA, LE and other related compounds [53]. AILs are a group of functionalised TSILs which possess a functional group covalently tethered to the cation or anion (or both) of the ILs. AILs are low melting ionic salts with acidic characteristics. Their acidic character can be categorised into three major groups:[53], [61] (1) Bronsted, (2) Lewis, or (3) a combination of Bronsted and Lewis acids. The acidic function(s) or group(s) can be either cation, anion or both. Lewis acidic ionic liquids (LAILs) possess a Lewis acid site which can accept lone pair electrons from a Lewis base, whilst, BAILs possess a Bronsted acid site which can transfer a proton to a Bronsted

base. BAILs are further divided into sole acid site and multi-acid sites. Basically, there are two types of BAILs with sole acid site, as follows: (1) BAILs with acidic cation such as sulphonic acid (–$SO_3H$), carboxyl acid (–COOH) or hydroxyl acid (–H), which are covalently bonded to the anion, and (2) BAILs with monoacid anion such as hydrogen sulphate [$HSO_4$], dihydrogen phosphate [$H_2PO_4$], etc. BAILs with multi acid sites can also be separated into two types, as follows: (1) BAILs with two acidic sites, of which the acidity is contributed by the same or different type of functional groups, either solely from cation such as -$SO_3H$ or -COOH or -H groups, or solely from anion, such as [$HSO_4$], [COOH] and [$H_2PO_4$], (2) BAILs with three or more acidic sites, of which the acidity is contributed by various combinations of functional groups, such as -$SO_3H$, [$HSO_4$], [COOH], and [$H_2PO_4$] [146]. BLAILs possess both Bronsted and Lewis acidic sites. The addition of Lewis acidic site to the catalyst gives a better catalytic activity than solely Bronsted acid site [44], presumably caused by the synergistic effect between both acidic sites in promoting the catalytic chemical reactions. Moreover, the organic units of LAILs and BAILs can couple with various supporters to form heterogeneous catalysts with solid carriers, which are known as supported LAILs and supported BAILs, respectively. A detailed categorisation of AILs is illustrated in **Figure 2.8**.

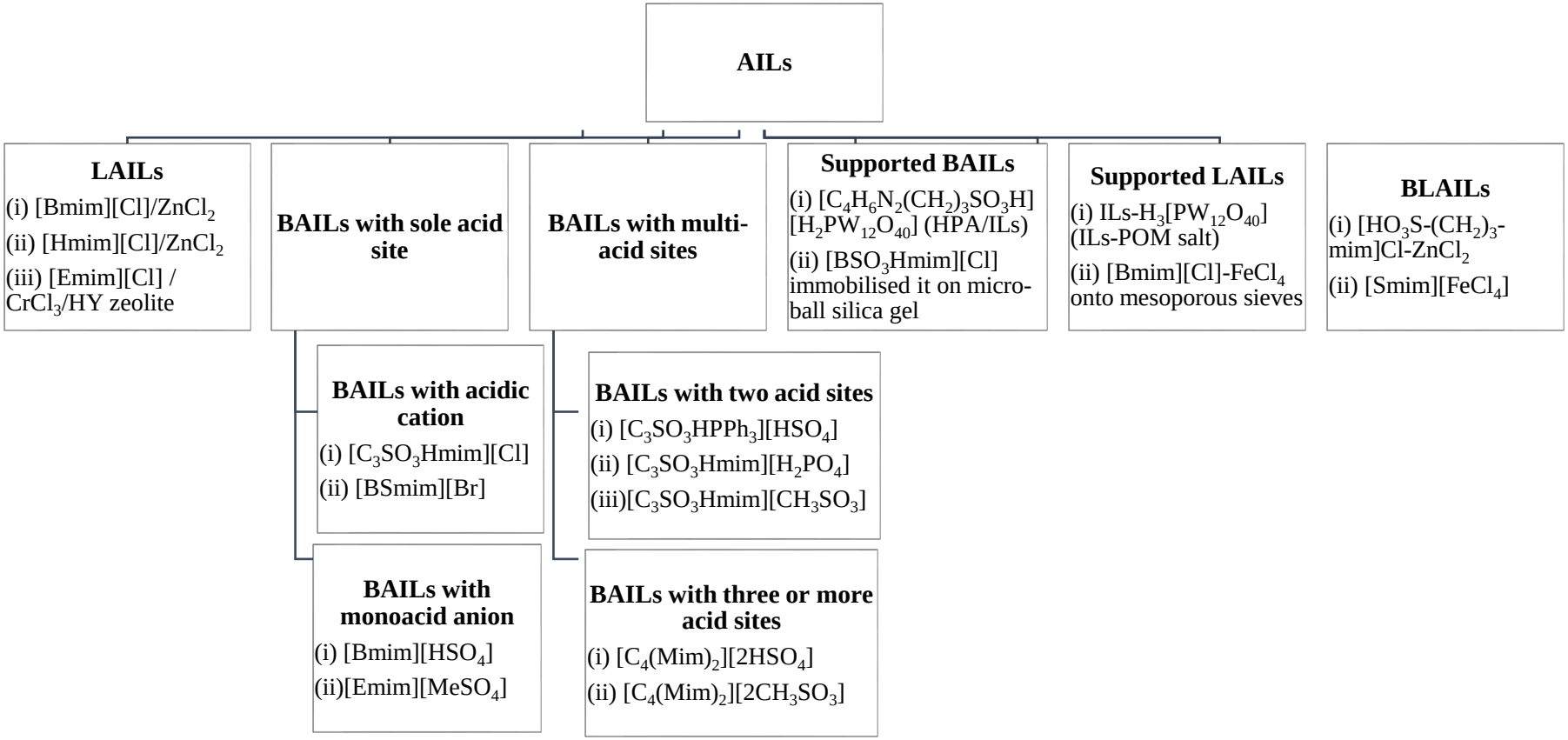



**Figure 2.8** Main categories of AILs with examples given in each category.

### 2.5.3 Comparison of ILs with other catalysts

The conversions of biomass and its derivatives to LA and LE can be catalysed by various catalysts which include mineral acids, heterogeneous catalysts and ILs. Mineral acids such as $H_2SO_4$ and HCl are the conventional catalysts for the production of LA and LE. However, these catalysts are unrecyclable and can cause equipment corrosion. The production catalysed by mineral acid requires harsh reaction conditions, and the waste generated needs a large volume of base for neutralisation. Thus, replacement of such mineral acids by heterogeneous acid type catalysts that are separable and reusable is highly desirable [30]. Nonetheless, heterogeneous catalysts are easily deactivated due to the adsorption of carbonaceous products on the solid acid surface and the gradual loss of acid sites [147], hence, re-treatment is often needed in recycling runs. With regard to this, efforts have been made to develop environmentally benign processes for conversion of biomass and derivatives to LA and LE using ILs as a greener and sustainable option. Additionally, since ILs play the dual role of solvent-catalysts, a biphasic system is readily formed at the end of the production (refer to **Chapter 2.7.5**), thereby the catalyst separation becomes favourable with no organic solvent needed. Nevertheless, the high cost of ILs remains a challenging issue. This can be overcome by synthesising ILs from low cost raw materials and recycling the ILs for subsequent catalytic runs [47], [50], [148]. A comparison of the advantages and disadvantages of ILs with mineral acids and heterogeneous catalysts is listed in **Table 2.2**.

**Table 2.2** Comparison of ILs with mineral acid and heterogeneous catalysts.

| Catalyst | Advantages | Disadvantages |
|---|---|---|
| Mineral acid | • High process effectiveness [86] | • Corrosive [62]<br>• Used acid is difficult to recover [62]<br>• Contaminated end-products [111]<br>• Large amount of acidic wastes generated [135] |
| Heterogeneous catalysts | • No corrosion and erosion [115]<br>• Easy to handle [149]<br>• Recyclable [149] | • Leaching of acidic groups of the catalyst [115]<br>• Extreme reaction conditions are required which results in deactivation due to coking [135]<br>• Restricted accessibility of the matrix-bound acid sites [150]<br>• High molecular weight to active-site ratios [150] |
| ILs | • Greener [151]<br>• Milder reaction conditions [151]<br>• Higher process effectiveness [151]<br>• Recyclable [151]<br>• Recoverable [152] | • High material cost [88], [151] |

## 2.6 Biomass pretreatment with ILs

Lignocellulosic biomass has been recognised as the only fixed carbon alternative source to first generation feedstock such as starch and edible triglycerides [153]. The majority of carbon content of lignocellulosic biomass is stored within the structures of cellulose and hemicellulose which are enclosed by lignin, by strong covalent, and intra- and inter-molecular hydrogen bonding [154]. They form a network of fibres that provide mechanical tensile strength to the plant cell wall that could hinder the digestibility of the structures and physically barrier surface accessibility [90], [155]–[157].

Pretreatment is key to unlocking the recalcitrance of lignocellulosic biomass towards various chemical processes in the production of platform chemicals. ILs acts as dual solvent-catalysts to dissolve the lignocellulosic matrix by breaking apart its structure, thereby enabling an easier extraction of cellulose components, as shown in **Figure 2.9**. An example of the dissolution mechanism of cellulose by imidazolium based ILs is illustrated in **Figure 2.10**.

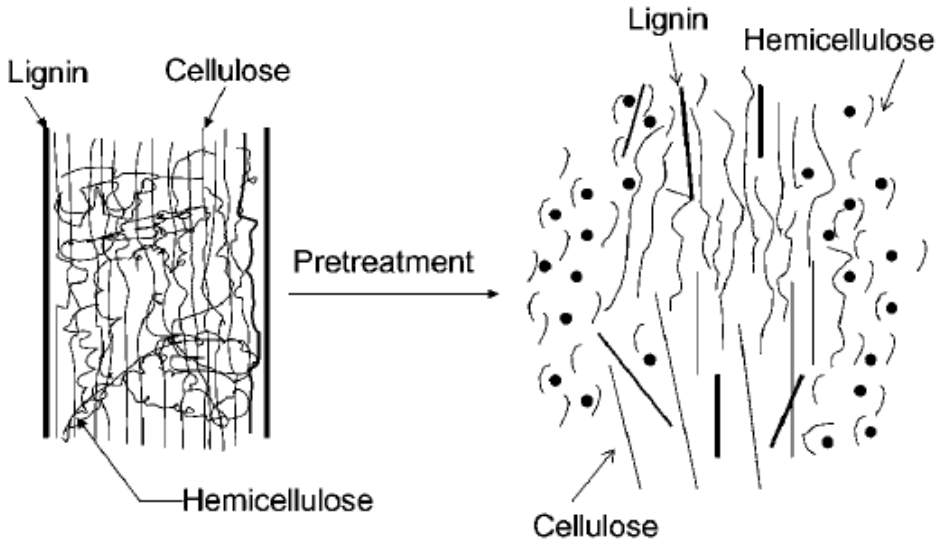



**Figure 2.9** Schematic representation of pretreatment effect on lignocellulosic biomass. Adapted from Tadesse and Luque [158].

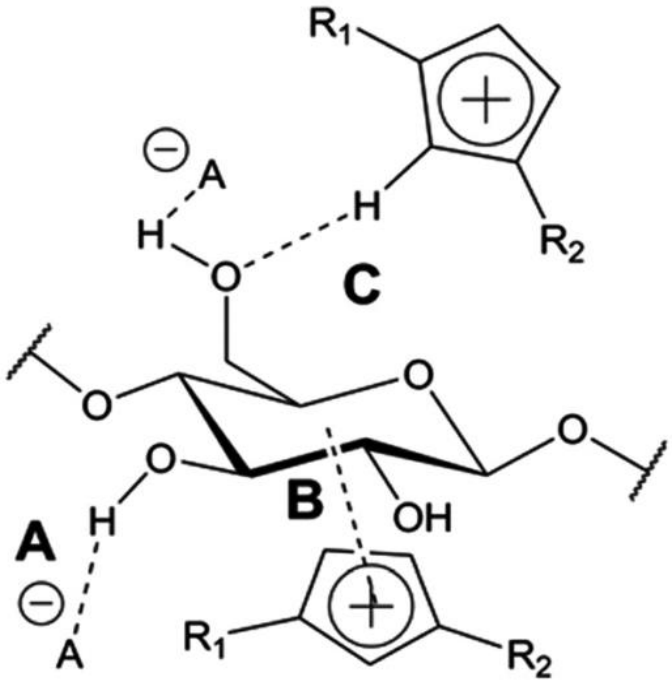



**Figure 2.10** Proposed dissolution mechanisms of cellulose by imidazolium based ILs: (A) interactions between the basic anion and the cellulose hydroxyl groups break up the hydrogen bond network between the cellulose chains. (B) Hydrophobic interactions take place between the hydrophobic face of cellulose and the imidazolium ring. (C) The acidic proton at the C-2 position on the

imidazolium ring interacts with the cellulose hydroxyl groups. Adapted from Wahlstrom and Suurnakki [159].

The degree of dissolution in ILs is positively related to the hydrogen bond accepting ability of the anion [160]. The most prevalent ILs used in pretreatment processes are those of imidazolium cation based attached with various anions, which fall into three groups: (1) halide based ILs such as 1-butyl-3-methylimidazolium chloride ([BMIM][Cl]), 1-ethyl-3-methylimidazolium chloride ([EMIM][Cl]) and 1-octyl-3-methylimidazolium chloride ([OMIM][Cl]), (2) acetate based ILs such as 1-ethyl-3-methylimidazolium acetate ([EMIM][OAc]) and 1-butyl-3-methylimidazolium acetate ([BMIM][OAc]), and (3) the large coordinating anion based ILs such as 1-butyl-3-methylimidazolium tetrafluoroborate ([BMIM][$BF_4$]) and 1-butyl-3-methylimidazolium hexafluorophophate ([BMIM][$PF_6$]) [159], [161]. Among these, [Cl] anion imidazolium based ILs are an excellent combination that exhibits excellent solubility for both biomass and cellulose, causing a powerful breaking down of the intramolecular hydrogen bonds of the cellulose structure network without further derivatisation [162]. The non-derivatising nature of ILs produces no fermentation inhibitors and thus the products are easily recovered [163]. Additionally, their solubility is further enhanced by the formation of hydrogen bonds between [Cl] anions of ILs and the hydroxyl groups of sugars in biomass [164]. For instance, [BMIM][Cl] gave an Avicel cellulose dissolution up to 25% under microwave heating, whilst, 10% solubility was achieved at 100°C [164]. Pyridinium based ILs, 3-methyl-N-butylpyridinium chloride ([BmPy][Cl]), were more efficient than those of imidazolium based, in which up to 39% Avicel cellulose dissolution could be achieved [165]. In contrast, [$BF_4$]

and [$PF_6$] anions are large and noncoordinating [165], with weak hydrogen-bonding basicity [166], leading to a poorer dissolving ability for biomass [158]. Furthermore, the smaller size anions of the ILs favour cellulose dissolution due to its flexible dipoles arrangement in combination with cellulose [167].

In this context, ILs was recently extended to dissolve natural lignocelluloses and to separate its constituents. Kilpelainen et al. [168] reported that both hardwoods and softwoods such as Norway spruce, Southern pine, and their thermomechanical pulp fibres were readily soluble in various [Cl] anion imidazolium based ILs, which were functionalised by strong hydrogen bond acceptors such as aromatic rings and allyl groups. The authors found that the solubility of biomass was highly dependent on the particle size and moisture of the wood sample, in which the former served as the dominant factor. To date, ILs pretreatment has been studied on various biomass such as giant silver grass, pine and willow [154], oil palm such as empty fruit bunch and oil palm fronds[88], [169]–[172], switchgrass [173]–[175] and sugarcane bagasse [176]–[179]. They have been proven to be superior to conventional methods, particularly in altering the physicochemical properties of the biomass macromolecular components such as cellulose, to ease their extraction. Sugars released from ILs pre-treated wood has also been discovered, particularly with dialkylimidazolium based ILs containing [Cl], [$MeCO_2$] and [$MeSO_4$] anions [180]. Aside from that, Brandt et al. [154] reported that ILs with strong hydrogen acceptance ability such as those of [$MeSO_4$], [$HSO_4$] and [$CH_3SO_3$] anions based could disrupt the intra and inter-molecular hydrogen bond in the covalent structure of cellulose or biomass, enhancing the biomass dissolution. In the biomass dissolution process, lignin and hemicellulose are partially removed

from the pretreatment solution. Hence, the lignin fraction could be recovered and converted to value-added aromatic chemicals. In addition, pretreatment with 1-butyl-3-methylimidazolium alkylbenzene sulfonate ([EMIM][ABS]), an ILs mixture containing aromatic sulphonate anions, mainly xylenesulfonate [181], was found to be able to dissolve lignin of sugarcane bagasse. Lignin solubilisation has also been reported after pretreatment with acetate based ILs, [EMIM][OAc], when the solvent was a mixture of water and acetone [182]. Furthermore, the cellulose dissolving ILs ([EMIM][OAc]) has been used for the solubilisation of paper-grade kraft pulp into a separated cellulose and hemicellulose fraction. The products were of high purity, and no yield loss was observed as it might, resulting from depolymerisation [183]. Overall, ILs enable the selective separation of biomass fractions, i.e. cellulose, hemicellulose and lignin, with high yield.

Biodegradable ILs have been recently developed for biomass pretreatment [184]. Among these, amino acid based bio-ILs, 1-ethyl-3-methylimidazolium glycinate ([EMIM][Gly]), could effectively dissolve the biomass completely by converting the type I cellulose (native cellulose) to type II (crystalline and amorphous cellulose) [185], [186]. Cholinium based ILs, could effectively treat lignocellulose as observed from their high total reducing sugars yields in the subsequent hydrolysis. Examples of cholinium based ILs used in biomass pretreatment include cholinium argininate ([Ch][Arg]) in rice straw [187], choline acetate ([Ch][OAc]) in bamboo [188] and bagasse [152] as well as cholinium taurate ([Ch][Tau]) in wheat straw [184]. All these studies reported significant improvements in the subsequent hydrolysis of biomass after the ILs pretreatment presumably caused by the extensive removal of lignin.

Besides, renewable ILs which are synthesised from biomass "wastes", i.e. lignin monomers and hemicellulose are also an alternative to conventional ILs for the pretreatment use. For instance, Socha et al. [189] synthesised a series of tertiary amine-based ILs from aromatic aldehydes derived from lignin and hemicellulose. These ILs were used to pretreat switchgrass biomass. High yields of total reducing sugars were generated, which are comparable to those of conventional ILs, [EMIM][OAc]. These concepts of using low environmental impact bio-ILs and biomass-derived ILs show significant potential for future lignocellulosic biorefineries development.

However, biomass pretreatment has been recognised as the second largest cost contributor in sugar-based biofuel production [70]. This is primarily caused by the ILs water-wash step in the pretreatment process which generates large volumes of wastewater. To address this problem, Xu et al. [37] have recently developed a high gravity biomass conversion in which all catalytic conversions were included in a one-pot production approach. The process allowed ILs pretreatment and subsequent chemical conversion to occur in one-pot for the production of concentrated cellulosic bioethanol. The optimised one-pot configuration managed to reduce the ILs amount by ~90% and pretreatment related water inputs and wastewater generation by ~85%. For multi-ton ILs production, the use of protic ILs (ILs with a protonated amine for cation) would be an option, as the synthesis method involved is solely a simple neutralisation that does not require any purification step [190]. Hence, protic ILs is of lower cost than traditional dialkylimidazolium based ILs [70]. For example, the bulk production of triethylammonium hydrogen sulphate ($[HNEt_3][HSO_4]$) is estimated as \$1.24 $kg^{-1}$. This compares favourably with organic solvents such

as acetone or ethyl acetate, which sell for \$1.30–\$1.40 $kg^{-1}$ [63]. The cost of protic ILs is predominated by the type of amine attached, since the price of sulphuric acid used is less costly and the synthesis process of the ILs is relatively simpler. For instance, the synthesis step of protic ILs, e.g. $[HNEt_3][HSO_4]$, only involves 7 steps, whilst, acetate based ILs, e.g. [EMIM][OAc], consists as much as 30 steps [70]. Overall, protic ILs appear to be more environmentally friendly with a reduction of unwanted waste by-products, solvent losses, energy usage and carbon dioxide generation.

Recent studies showed the possibility of one-pot production of LA and LE from various lignocellulosic biomasses via various catalytic methods, including wheat straw [8], [54], [65], bamboo [9], [51], [52], oil palm biomass such as empty fruit bunch, fronds and kenaf [85]–[90], sorghum grain [157], marine biomass [16], [191], bagasse [110], [192], rice husk [193], rice straw [194], switchgrass, wood chips and paper pulp [10] as well as paper waste [112]. Nevertheless, the use of ILs for the one-pot production of LA and LE from lignocellulosic biomasses is still at the developing stage, with limited research reported [7], [51], [52], [85], [89] which will be critically discussed in **Chapter 2.7.3**. As shown in **Figure 2.11**, the ILs-catalysed strategy allows the discarding of biomass pretreatment step, thereby giving a shorter process compared to the conventional strategy. It reduces the time, cost and energy consumption of the conversions, signifying a technological breakthrough in the organic synthesis of LA and LE.

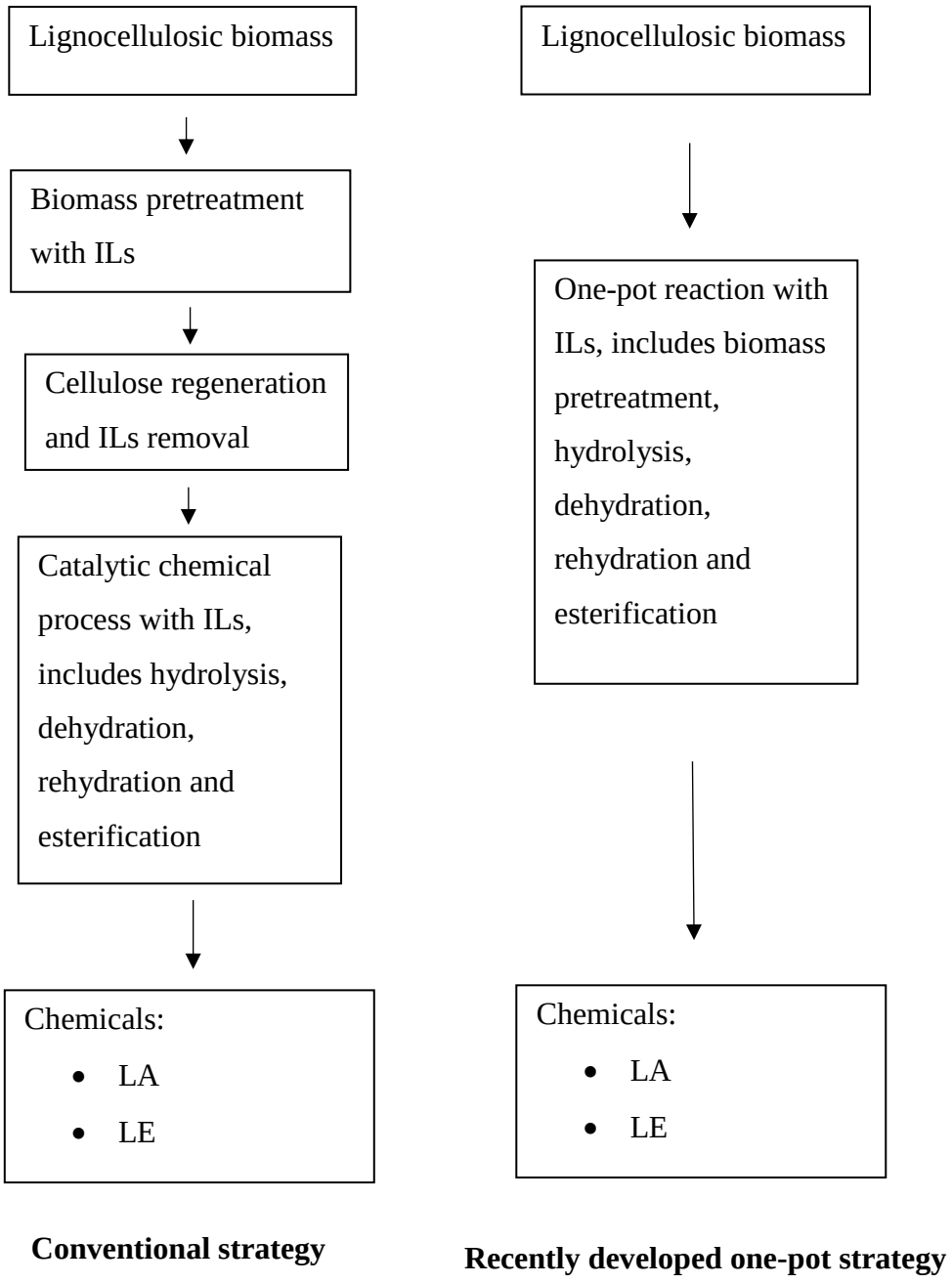



**Figure 2.11** Comparison of conventional strategy and recently developed one-pot strategy, for the production of LA and LE from biomass feedstock. Adapted from Xu et al. [37].

## 2.7 Conversions from biomass and its derivatives to LA and LE

In general, the preparations of both LA and LE from biomass or its derivatives require the presence of an acid catalyst. LE is typically synthesised using a conventional esterification method, i.e. by reacting the biomass or its derivatives with alcohol under reflux condition. The feedstock of biomass and its derivatives include sugars, cellulose and furfuryl alcohol. Monosaccharide, disaccharide and polysaccharide are the building blocks of the complex carbohydrate network. In the case of lignocellulosic materials, the recalcitrance and insolubility of the reactants in the reaction medium add to the necessity of having a depolymerisation step which consists of hydrolysis, dehydration and rehydration, entailing a series of complex reactions and drastic reaction conditions.

The following discussion begins with the conversions from the simple structure of sugar, followed by that of cellulose, and lastly from the complex structure of biomass, for both productions of LA and LE. Then, the synthesis of LE from furfuryl alcohol and LA conversion to LE were further discussed. Furfuryl alcohol is formed by the reduction of furfural, obtained from the xylan hemicellulose component of lignocellulosic biomass (refer to **Figure 2.6**). The conversion from furfuryl alcohol to LA and LE via the pentose pathway is therefore an alternative method to those conversions from cellulose-derived feedstock via the hexose pathway. The mechanistic insights on both pentose and hexose routes for the syntheses of LA and EL have been widely discussed in **Chapter 2.4**. In the final process, LA can be upgraded to LE by undergoing a conventional esterification with alcohol under reflux condition.

### 2.7.1 Sugars to LA and LE

**Figure 2.12** shows how these compounds are oxidised into LA and LE. To date, there are limited studies reported on sugar conversion to LA and EL via ILs [58], [195]–[197]. As this conversion is a simple process, cheaper options such as heterogeneous catalysts [198]–[200] is generally preferable over ILs. Since ILs is of higher cost, it is more catered for complicated conversions such as those from biomass feedstock. In addition, sugar is not renewable and sustainable so it is less preferred compared to other feedstock. The utilisation of ILs for the conversion of sugars into LA [195], [196] and LE [58], [197] are shown in **Table 2.3**. Glucose and fructose are the two common monosaccharides that have been used to produce LA and its esters [58], [195]–[197]. In addition, a disaccharide of sucrose and a polysaccharide of inulin have also been investigated for the conversions to LE [58], [197].

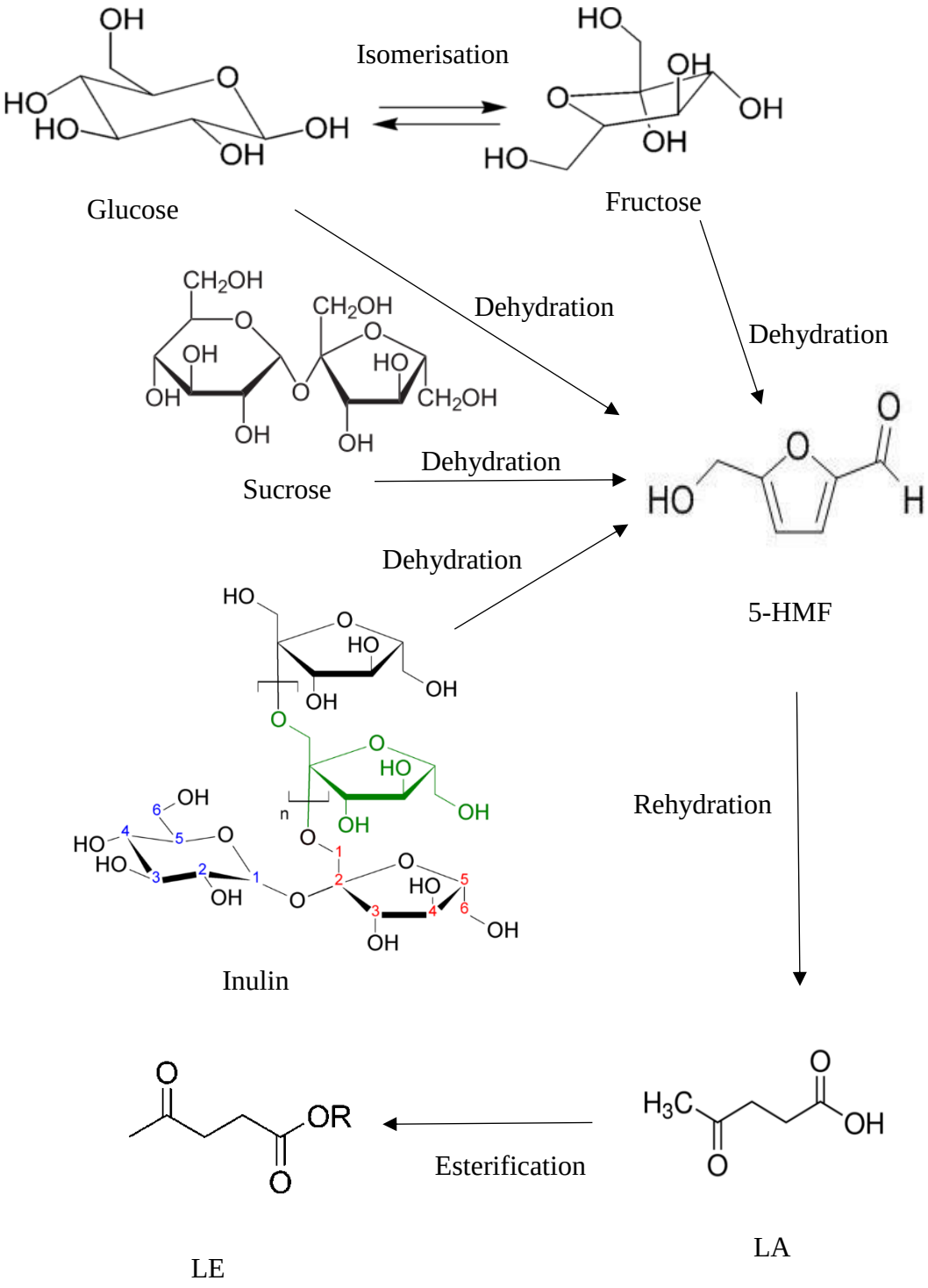



**Figure 2.12** Conversion of sugars to LA and LE.

**Table 2.3** Studies on the conversion of sugars to (a) LA and (b) LE via ILs at various reaction conditions.

| Feedstock | Reaction conditions | ILs | Percentage yield (%) | Ref. |
|---|---|---|---|---|
| **(a) LA yield** | | | | |
| BAILs with sole acid site and BLAILs * | | | | |
| Glucose | Sugars: 0.1 g<br>ILs: 10 g<br>Water: 10 ml<br>Temp: 150°C<br>Time: 4 h | [BMIM][$HSO_4$]<br>[SMIM][Cl]<br>[SMIM][$FeCl_4$]* | 22.4<br>25.8<br>67.8 | [195] |
| Glucose | Sugars: 0.56 mmol<br>ILs: 1 g<br>Metal salts: 1.8% (w/w)<br>Temp:155°C<br>Time: 5 h | IL-$SO_3H$<br>IL-$SO_3H$–$NiCl_2$*<br>IL-$SO_3H$–$NiSO_4$* | 46.6<br>49.6<br>56.3 | [196] |
| **(b) LE yield** | | | | |
| Supported BAILs | | | | |

| | | | | |
|---|---|---|---|---|
| Fructose | Sugars: 150 mg<br>ILs: 29.0 mg<br>Alcohol: 3.4 ml<br>Temp: 140°C<br>Time: 4 h | $[C_3N][SO_3CF_3]$-HCSs<br>($C_3$= *Pr*$SO_3H$) | 89.7 | [201] |
| Supported LAILs | | | | |
| Fructose<br>Sucrose<br>Inulin | Sugars: 50 mg<br>ILs: 5.0 mg<br>Alcohol: 4 ml<br>Temp: 120°C<br>Time: 12 h | IL-$H_3[PW_{12}O_{40}]$ | 82.0<br>45.0<br>67.0 | [197] |
| BAILs with multi-acid sites | | | | |
| Fructose | Sugars: 380.2 mg<br>ILs: 45.0-55.0 mg<br>Ethanol: 5.6 g<br>Temp: 140°C<br>Time: 24 h | [BMIM-$SO_3H$][$HSO_4$]<br>[BPyr-$SO_3H$][$HSO_4$]<br>[$NEt_3B$-$SO_3H$][$HSO_4$]<br>[BMIM-$SO_3H$][$NTf_2$]<br>[BMIM-$SO_3H$][OMs]<br>[BMIM-$SO_3H$][OTf] | 68.0<br>70.0<br>74.0<br>77.0<br>67.0<br>69.0 | [58] |
| Glucose | | [BMIM-$SO_3H$][$HSO_4$] | 8.0 | |

| | | |
|---|---|---|
| | [BPyr-$SO_3H$][$HSO_4$] | 13.0 |
| | [$NEt_3B$-$SO_3H$][$HSO_4$] | 6.0 |
| | [BMIM-$SO_3H$][$NTf_2$] | 8.0 |
| | [BMIM-$SO_3H$][OMs] | 3.0 |
| | [BMIM-$SO_3H$][OTf] | 8.0 |
| Sucrose | [BMIM-$SO_3H$][$HSO_4$] | 41.0 |
| | [BPyr-$SO_3H$][$HSO_4$] | 43.0 |
| | [$NEt_3B$-$SO_3H$][$HSO_4$] | 41.0 |
| | [BMIM-$SO_3H$][$NTf_2$] | 43.0 |
| | [BMIM-$SO_3H$][OMs] | 40.0 |
| | [BMIM-$SO_3H$][OTf] | 42.0 |

Among the monosaccharides, fructose gives significant LE yield, which makes it the most desirable feedstock for the conversion. Hu et al. [59] claimed that fructose consistently gave better yields for LA and LE compared to glucose during acid-catalysed conversion of sugars. Saravanamurugan et al. [58] studied the reactivity of different carbohydrates (i.e. fructose, glucose and sucrose) in a series of acidic anion based SFILs. Fructose gave the highest yields of 67-77% of LE, whereas glucose gave limited yields of only 3-13%. Almost all glucose stopped at the alkyl glucoside step in the reaction, thereby was unlikely to be isomerised into fructose. The acidity of ILs thereby could not be fully unleashed for the successive dehydration and rehydration of the substance into LA and further esterification into LE. Moreover, glucose reacted with alcohol to form other by-products such as pyranoside esters. However, Ramli and Amin [195] reported that glucose conversion could achieve 67.8% LA yield via [SMIM][$FeCl_4$]. Both counterparts of the ILs structures contained acidic properties (Bronsted acid and Lewis acid sites), and were thus able to fulfil the acidity requirements of the successive conversion reactions. This work was in agreement with recent studies conducted by Kumar et al. [196]. The synergistic effect of the Lewis acid $NiCl_2$ and $NiSO_4$ aided in improving the LA yield by 3% and 9.7%, respectively, as compared to solely Bronsted acidic ILs. These observations further indicated that solely Bronsted acidity was not sufficient to achieve optimum efficiency for the conversion of glucose to LA. Among these two Lewis acid metal ions, the sulphate salts co-ordinated with the -OH groups of the α-anomers of glucose, forming stronger hydrogen bonds than the chloride salts. Hence, this result suggested that the extent of hydrogen bonding ability of the Cl-atom was not high enough to alter the process to a greater extent.

Moreover, the higher activity of the sulphates could also be attributed to a reduced side product formation [196]. The synergistic catalytic effect of using mixed acid catalytic system will be extensively discussed in **Chapter 2.7.2** and **2.7.3**.

Apart from the use of glucose and fructose as feedstock, Chen et al. [197] attempted to use inulin as feedstock for the LE synthesis via IL-based polyoxometalate salts (IL-POMs), IL-$H_3[PW_{12}O_{40}]$, and obtained a high yield of 67% [197]. However, fructose was still superior to inulin with the highest yield of 82% of LE production, which was in agreement with Hu et al. [59]. The modified ILs (IL-POMs) was not considered as conventional ILs due to their melting points of over 100°C [202]. The extended hydrogen bonding networks between cations and anions of the ILs could be the reason for its existence in solid state. POMs are heterogeneous acidic catalysts that act as a support for ILs. The coupling provides flexible adaptability of both inorganic and organic groups. The functional propyl sulphonic acid group in the organic cation of IL-POMs also provides active acid sites which favours the esterification reaction [202]. Furthermore, tethering organic groups to POMs enhances heterogenisation of heteropolyacid (HPA)-promoted reactions, which favours catalyst recycling. [197] This catalytic system also simplify a multi-stage process into one-pot production by omitting isolation and purification steps, in addition to providing promising production yields [197]. On top of that, in a recent research, a nitrogen-doped carbon-based BAILs hollow nanospheres, $[C_3N][SO_3CF_3]$-HCSs ($C_3$ = $PrSO_3H$), was applied for the conversion of fructose to LE with excellent yield [201]. This supported BAILs, which made of unique hollow

spherical nanostructures and BAILs exhibited the highest LE yield of 89.7% (**Table 2.3**). Additionally, this catalytic system could facilitate fructose ethanolysis reaction to proceed rapidly, and thus effectively avoid self-polymerization of the intermediates. This is owing to the inhibition of carbonaceous side products leading to negligible yields [203]. Meanwhile, the chemical interactions between the $[C_3N][SO_3CF_3]$ groups and nitrogen-doped carbon framework are able to avoid acid site leaching [201]. In fact, this catalytic system favours accessibility to acid sites, mass transfer and diffusion, owing to their inherent super strong Bronsted acid nature and unique hollow spherical nanostructures.

### 2.7.2 Cellulose to LA and LE

**Table 2.4** summarise the studies on the ILs catalysed one-pot conversion of cellulose to LA [47], [49], [50], [64], [85], [148], [204] and LE [47]–[49].

**Table 2.4** Studies on conversion of cellulose to (a) LA and (b) LE via ILs at various reaction conditions.

| Reaction Conditions | ILs | Percentage yield (%) | Ref. |
|---|---|---|---|
| **(a) LA yield** | | | |
| Supported BAILs | | | |
| Cellulose: 0.1 g<br>ILs: 0.22 g<br>0.5 ml water | $[C_4H_6N_2(CH_2)_3SO_3H][H_2PW_{12}O_{40}]$ (HPA/ILs) | 63.1 | [204] |

| | | | |
|---|---|---|---|
| Temp: 140°C<br>Time: 5 h | | | |
| BAILs with sole acid site* and BAILs with multi-acid sites | | | |
| Cellulose:<br>0.15 g<br>ILs: 0.6-1.2 g<br>6.0 g water<br>Temp: 170°C<br>Time: 5 h<br>(Hydrothermal conditions) | $[C_3SO_3HMIM][HSO_4]$<br>$[C_4SO_3HMIM][HSO_4]$<br>$[C_3SO_3HN_{222}][HSO_4]$<br>$[C_3SO_3HPy][HSO_4]$<br>$[C_3SO_3HPPh_3][HSO_4]$<br>$[C_3SO_3HMIM][H_2PO_4]$<br>$[C_3SO_3HMIM][CH_3SO_3]$<br>$[C_3SO_3HMIM][1\text{-NS}]$<br>$[C_3SO_3HMIM][Cl]$* | 63.0<br>57.6<br>54.5<br>56.9<br>55.2<br>16.7<br>53.9<br>53.8<br>66.2 | [50] |
| Cellulose:<br>0.25 g<br>ILs: 0.6-1.2 g<br>2.0 g water<br>Temp: 160°C<br>Time: 0.5 h<br>(Microwave-assisted synthesis) | $[C_3SO_3HMIM][HSO_4]$<br>$[C_4SO_3HMIM][HSO_4]$<br>$[C_3SO_3HPy][HSO_4]$<br>$[C_3SO_3HN_{111}][HSO_4]$<br>$[C_3SO_3HMIM][H_2PO_4]$<br>$[C_3SO_3HMIM][CH_3SO_3]$ | 44.5<br>41.4<br>40.5<br>43.2<br>3.5<br>36.3 | [148] |
| Cellulose:<br>0.15 g<br>ILs: 0.05 g<br>54% (w/w) water<br>Temp: 150°C<br>Time: 48 h | $[C_3SO_3HMIM][Cl]$* | 23.7 | [47] |
| Cellulose:<br>25 mg<br>ILs: 750 mg<br>Temp: 100°C | $[C_4(MIM)_2][(2HSO_4)(H_2SO_4)_2]$ | 55.0 | [72] |

| | | | |
|---|---|---|---|
| Time: 3 h | | | |
| BAILs with multi-acid sites and BLAILs* | | | |
| Cellulose: 0.05 g<br>ILs: 1.5 g<br>20% (w/w) water<br>Temp: 120°C<br>Time: 2 h | [BSMIM][$HSO_4$] | 25.5 | [64] |
| | [BSMIM][$HSO_4$] and $InCl_3$* | 28.8 | |
| BAILs with sole acid site and supported BAILs* | | | |
| Cellulose: 0.15 g<br>ILs: 0.05 g<br>40% (w/w) water<br>Temp: 180°C<br>Time: 24 h | [$C_3SO_3HMIM$][Cl] | 19.0 | [49] |
| | [$C_3SO_3HMIM$][Cl] and zeolite (ZSM-5)* | 25.0 | |
| LAILs | | | |
| Cellulose: 0.1 g<br>ILs: 2.0 g<br>Temp: 120°C<br>Time: 6 h | [BMIM][Br] and $FeCl_3$/HY zeolite | 27.7 | [85] |
| Cellulose (hydrolysis to TRS):<br>0.1 g<br>ILs: 2 g<br>Temp: 120°C<br>Time: 3 h | | 43.8 | |
| **(b) LE yield** | | | |
| BAILs with sole acid site | | | |

| | | | |
|---|---|---|---|
| Cellulose: 0.15 g<br>ILs: 0.05 g<br>38.5% (v/v) aq. ethanol<br>Temp: 170°C<br>Time: 12 h | $[C_3SO_3HMIM][Cl]$ | 19.0 | [47] |
| BAILs with sole acid site and supported BAILs* | | | |
| Cellulose: 0.15 g<br>ILs: 0.05 g<br>40% (v/v) aq. ethanol<br>Temp: 180°C<br>Time: 24 h | $[C_3SO_3HMIM][Cl]$<br>$[C_3SO_3HMIM][Cl]$ and zeolites (ZSM-5)* | 16.3<br>29.5 | [49] |
| BAILs with sole acid site* and BAILs with multi-acid sites | | | |
| Cellulose: 1.62 g<br>ILs: 0.13-0.16 g<br>20 ml butanol<br>Temp: 180°C<br>Time: 45 min | $[C_4H_8SO_3HMIM][HSO_4]$<br>$[C_4H_8SO_3HMIM][H_2PO_4]$<br>$[C_4H_8SO_3HMIM][Cl]$* | 31.1<br>2.6<br>1.1 | [48] |

Ren et al. [50], [148] conducted a study for the cellulose conversion to LA via ILs composed of $-SO_3H$ functionalised group cation and acidic anion. These ILs are made up of BAILs with multi-acid sites, of which both counterparts contain acidic properties, known as acidic anion based SFILs. The introduction of $-SO_3H$ functionalised groups evidently enhanced the acidity of ILs, providing a promising alternative to mineral acid catalyst (i.e. HCl, $H_2SO_4$,

etc.). Hence, the reaction catalysed by acidic anion based SFILs exhibited a higher LA yield than the acidic anion based ILs, as the former ILs have multi-acid sites in both cation and anion. Among the acidic anions tested, [$HSO_4$] gave the highest catalytic activity. [$HSO_4$] anion has high viscosity property attributed to the strong cation-anion interactions arising from the absence of alkyl chain in the structure [205]. The strong forces between cation and anion trigger the molecules to interact intensively and thus increase the ILs capability in promoting a higher turnover synthesis. Moreover, the acidic anions could possibly undergo glycosidic oxygen protonation during the catalytic cleavage of cellulose [159]. With reference to the relative acidity order of acidic anion based SFILs, i.e. [$HSO_4$] > [$CH_3SO_3$] > [1-NS] > [$H_2PO_4$], higher acidity of anions significantly favours the production of LA [158]. This is in agreement with the conversion of cellulose to LE [48]. Nonetheless, in a recent research on using multiple [$HSO_4$] ions, without the -$SO_3H$ functionalised group in the cation of ILs, the catalytic conversion activity to LA was not favoured, where slightly lesser LA yield was obtained [72], as compared to [$HSO_4$] acidic anion based SFILs [50]. In this regard, the results further suggested that excessive [$HSO_4$] ions in the ILs were not able to promote the efficiency of the turnover synthesis of LA. Apart from that, the cation of the ILs also contribute to its acidity strength although to a lesser extent. Specifically, the strength of Bronsted acidity of an ILs is dependent on the nitrogen group and the carbon chain length of the cations [206]. Increasing Bronsted acid strength would subsequently improve the ILs catalytic activity. In the context of the cations of ILs, the LA yields decrease in the order of imidazolium > pyridinium > phosphonium > ammonium [50], [148]. The elongating alkyl carbon chain linked with the -$SO_3H$ functionalised group

from methyl to butyl could also reduce the acidity strength of the ILs. In any case, the acidity of an ILs is most dependent on its anions, rather than its cations [50]. In terms of methods applied, the hydrothermal method [50] gave higher LA yields than the microwave-assisted synthesis method [148]. Different operating conditions, particularly the reaction temperature and time (refer to **Chapter 2.8**), also affect the catalytic activity of LA production [85].

An exceptional case was observed on halide based SFILs, $[C_3SO_3HMIM][Cl]$, in which it gave the highest LA yield (66.2%) [50] irrespective of its lower acidity relative to $[HSO_4]$ anion based SFILs. The formation of hydrogen bonding between [Cl] counterpart and hydroxyl protons of the carbohydrates could have promoted the breaking of the extensive hydrogen bonding networks of cellulose and hence facilitated the cellulose dissolution [207]. In this regard, the stronger hydrogen bond acceptor on ILs such as [Cl] may promote the catalytic activity of LA production by increasing the accessibility of the acid sites rather than the usual acidity strength. However, [Cl] based SFILs was unsuitable for the conversion into LE, as indicated by an extremely low yield of 1.1% [48]. This could perhaps be linked to the inefficiency of [Cl] based SFILs in esterification reaction [48] and their role in only favouring the prior depolymerisation reaction [49], [50], [148]. Furthermore, ILs bearing highly coordinating anions such as [Cl], $[BF_4]$ and $[PF_6]$ might impede the catalytic function of the cation of ILs on esterification, even in the presence of $–SO_3H$ acid functionalised group. These ILs are hygroscopic, hence, in the production of LE, the anions of ILs tend to interact with the water molecules in the water-ethanol medium to form hydrogen bonds [208]. This

strong interaction not only stabilises the absorbed water molecules, but also leads to structural changes on ILs [208], thereby possibly reducing the catalytic ability of ILs in the esterification. In contrast, Amarasekara and Wiredu [47] and Wiredu et al. [49] achieved low LA yields despite using the same [Cl] based SFILs ([$C_3SO_3HMIM$][Cl]). This was presumably attributed to the high loadings of cellulose and ILs used in the catalytic systems that caused undesired cross polymerisation resulting in by-products.

Apart from that, supported BAILs (heterogeneous catalyst coupled with BAILs) have also been used to catalyse the conversions. Sun et al. [204] conducted a cellulose conversion via heteropolyacid (HPA) ILs in a water-methyl isobutyl ketone (MIBK) catalytic system and obtained a significant LA yield of 63.1%. The high performance was mainly due to (1) HPA ILs dissolve in water, forming a homogeneous catalytic system that favours the contact of the catalyst and cellulose, (2) HPA molecule being sterically constrained, thereby having less interaction with the anions of the ILs, but becomes more available for hydrogen bonding with cellulose and hence increases its solubility, and (3) HPA offering a Bronsted acid property which enhances the catalytic activity. In general, HPA ILs exhibited higher catalytic activity than sole HPA catalyst, as the former has strong Bronsted acidity with double acid sites in the cation. Furthermore, the recycled catalyst performed efficiently with up to six recycling runs, without appreciable loss of production yield [204].

Aside from that, Wiredu et al. [49] utilised another supported BAILs (i.e. ZSM-5 coupled with halide based SFILs ([$C_3SO_3HMIM$][Cl])) to catalyse the conversion and managed to improve the LA (+6%) and LE (+13.2%) yields

significantly, in comparison with solely [$C_3SO_3HMIM$][Cl] catalytic system. This enhancement of product yields might be due to the co-existence of both Lewis and Bronsted acidic sites that leads to the synergistic catalytic effect of the catalysts, and thus facilitates the isomerisation of glucose to fructose (refer to **Chapter 2.7.3**) which is an essential step in the LA production. A proposed mechanism of this catalytic conversion is as follows: (1) the breakdown to glucose from cellulose is completely dissolved in [$C_3SO_3HMIM$][Cl] to form a homogeneous solution, (2) Cl in [$C_3SO_3HMIM$][Cl] favours the Lewis acid sites of ZSM-5 to isomerise the glucose into fructose, (3) the ion-exchange of [$C_3SO_3HMIM$][Cl] with Bronsted acid sites of ZSM-5 promotes the release of $H^+$ , which could readily contact fructose, and finally (4) $[C_3SO_3HMIM]^+$ in [$C_3SO_3HMIM$][Cl] facilitates the stabilisation of 5-HMF and LA, thereby preventing them from further decomposition into waste by-products [209]. In another study, Shen et al. [64] utilised BLAILs (i.e. Lewis acid $InCl_3$ coupled with BAILs with multi-acid sites ([BSMIM][$HSO_4$])), to further enhance the LA yield (+3.3%), in comparison with solely [BSMIM][$HSO_4$] catalytic system. The addition of Lewis acid $InCl_3$ facilitated the hydrolysis of glucose, in which the metal ions-ILs system favoured the isomerisation of glucose to fructose. Specifically, the complexes $[InCl_m(SO_4)_n]^{2n-}$ enhanced the isomerisation of the α-anomers to the β-anomers through the formation of hydrogen bonding between oxygen atom in $[SO_4]^{2-}$ or $[Cl]^-$ in metal chlorides and the hydroxyl groups in glucose [210].

### 2.7.3 Lignocellulosic biomass to LA and LE

**Table 2.5** summarise the pertinent references on the direct conversions of biomass to LA [7], [51], [52], [85], [89] and LE [7] via ILs. The theoretical yield refers to the theoretical assumption of total LA/LE yield obtained based on the cellulose content of biomass (**Eq. 2.1**), whereas the process efficiency refers to the efficiency of biomass conversion to LA/LE based on the theoretical yield. ILs can act as dual solvent-catalysts that enable all the catalytic conversions, i.e. biomass pretreatment, depolymerisation and esterification, in one-pot [37]. Nonetheless, due to the structural complexity and recalcitrance of lignocellulose, the functionality of catalysts will be reduced somewhat [15]. Thereby, the production with a separate biomass pretreatment process in any case would still give a better turnover synthesis of LA compared to without it [85].

$$\text{Theoretical LA/EL yield (\%)} = \frac{\text{Cellulose content in biomass (g) x } 0.71/\ 0.89}{\text{Initial biomass loading (g)}} \text{ x } 100\% \quad (2.1)$$

$$\text{where } \frac{\text{Molecular weight of LA/EL (g } mol^{-1})}{\text{Molecular weight of cellulose (g } mol^{-1})} = \frac{116/\ 144}{162} = 0.71/\ 0.89$$

**Table 2.5** Studies on the direct conversion of various biomass to (a) LA and (b) LE via ILs at various reaction conditions.

| Type of biomass | ILs | Reaction conditions | Cellulose content of biomass (%) | Yield (%) based on | | Process efficiency (%) | Ref. |
|---|---|---|---|---|---|---|---|
| | | | | Biomass | Theoretical | | |
| **(a) LA yield** | | | | | | | |
| BLAILs | | | | | | | |
| Oil palm fronds | [SMIM][$FeCl_4$] | Temp: 154.5°C<br>Time: 3.7 h<br>ILs: 7.27 g<br>Biomass: 0.18 g | 45.2 | 24.8 | 32.1 | 77.3 | [7] |
| BAILs with sole acid site | | | | | | | |
| Bamboo shoot shell | [BMIM][$HSO_4$] | Temp: 145°C<br>Time: 1.7 h<br>ILs conc:<br>0.9 $molL^{-1}$<br>Biomass: 2.04 % (w/w) | 37.8 | 17.9 | 26.8 | 66.8 | [52] |
| BAILs with multi-acid site | | | | | | | |
| Bamboo | [$C_4(MIM)_2$] [$(2HSO_4)(H_2SO_4)_4$] | Temp: 110°C<br>Time: 1 h<br>ILs: water ratio of 10:1 (w/w)<br>Biomass: 25 mg | 40.3 | 13.6 | 28.6 | 47.5 | [73] |
| Straw | [$C_3SO_3HMIM$][$HSO_4$] | Temp: 180°C | 34.7 | 5.3 | 24.6 | 21.6 | [83] |

| | | | | | | | |
|---|---|---|---|---|---|---|---|
| | | Time: 1.5 h<br>ILs: 1 g<br>Water: 2 g<br>Biomass: 250 mg | | | | | |
| LAILs | | | | | | | |
| Bamboo shoot shell | [BMIM][Cl] and $ZnCl_2$ | Temp: 132.7°C<br>Time: 1.4 h<br>3.3 molar ratio of $ZnCl_2$: ILs<br>Biomass: 1.1 (w/w) | 41.5 | 29.5 | 38.2 | 77.2 | [51] |
| Empty fruit bunch | [EMIM][Cl] and $CrCl_3$/HY zeolite | Temp: 176.5°C<br>Time: 2.3 h<br>Biomass: 0.1 g<br>ILs: 1.5 g | 41.1<br>32.0 | 20.0<br>17.0 | 29.2<br>22.7 | 68.5<br>74.9 | [89] |
| Kenaf | | | | | | | |
| Oil palm fronds | [BMIM][Br] and $FeCl_3$/HY zeolite | Temp: 120°C<br>Time: 6 h<br>Biomass: 0.1 g<br>ILs: 2 g | 45.2<br>41.1 | 11.1<br>9.3 | 32.1<br>27.1 | 34.6<br>34.3 | [85] |
| Empty fruit bunch | | | | | | | |
| Oil palm fronds (hydrolysis to TRS) | | Temp: 120°C<br>Time: 3 h<br>Biomass: 0.1 g<br>ILs: 2 g | 45.2 | 18.6 | 32.1 | 57.9 | |
| Empty fruit bunch | | | 38.2 | 17.6 | 27.1 | 64.9 | |

(hydrolysis to TRS)

| | | | | | | | |
|---|---|---|---|---|---|---|---|
| **(b) LE yield** | | | | | | | |
| BLAILs | | | | | | | |
| Oil palm fronds | [SMIM][$FeCl_4$] | Temp: 154.5°C[a] 78.4°C[b] Time: 3.7 h[a] 5 h[b] ILs: 7.27 g Biomass: 0.18 g Ethanol: 30 ml[b] | 45.2 | 20.1 | 32.1 | 77.3 | [7] |
| BAILs with multi-acid sites | | | | | | | |
| Wheat straw | [$HSO_3$-BMIM][$HSO_4$] | Temp: 200°C Time: 1 h ILs: 1.3 g Biomass: 5 g Ethanol: 75 g | N.A. | 16.2 | N.A. | N.A. | [74] |

*TRS= Total reducing sugar

[a]Depolymerisation reaction

[b]Esterification reaction

Among the available ILs, the AILs which possess both Lewis and Bronsted acidities (BLAILs) have been reported to demonstrate promising results in polymerisation, transesterification and oxidation reactions [41]–[43]. With regard to this, a recent study introduced 1-sulphonic acid-3-methylimidazolium tetrachloroferrate ([SMIM][$FeCl_4$]), a BLAILs, for the conversion of oil palm frond to LA and LE [7]. The findings showed that BLAILs in general performed better than other types of AILs. The co-existence of both Bronsted and Lewis groups on BLAILs presumably led to a stronger and more controllable acidity of LAILs which overcame the weaker acidity of BAILs [61]. This was in agreement with Antonetti et al. [44] who reported that although Bronsted acid sites played a greater role than Lewis acids in a catalytic reaction, solely BAILs in the reaction proceeded very slow under the Bronsted acid conditions. In the conversion, the biomass was first broken into glucose by the Bronsted acid sites ([SMIM]), followed by the isomerisation into fructose by the Lewis acid sites ($FeCl_4$). The fructose was then simultaneously dehydrated to 5-HMF, and rehydrated again into LA by Bronsted acid sites ([SMIM]) [7]. Nonetheless, excess Lewis acid sites (high Lewis/Bronsted ratio) can lead to the transformation of glucose to undesirable waste by-products, the so-called humins [211]. These dark, tarry to solid, insoluble polymeric structures are favoured by the aqueous acidic media of most lignocellulosic biomass transformations [212]. Humin formation results in tedious separation of catalyst and product [118]. Hence, appropriate Lewis/Bronsted ratio of ILs is vital to achieve a full turnover of organic synthesis.

However, Zhou et al. [51] showed that LAILs (i.e. Lewis acid $ZnCl_2$ coupled with [BMIM][Cl]) exhibited slightly better catalytic activity than BLAILs (e.g. [SMIM][$FeCl_4$] [7]) for the production of LA. This was presumably caused by the presence of Lewis acid $ZnCl_2$ on the ILs. Lewis acid metal salt is well known for the breakdown of cellulosic biomass [213], mainly due to the chelation of metal ion on the glycosidic oxygen of the cellulosic biomass structure. Williams and Horne [214] revealed that $Zn^{2+}$ is among the most effective metal chlorides in cellulose degradation for biochar production through pyrolysis. This suggested that the coupling of Lewis acid metal salt with neutral halide based ILs, especially Lewis acid $ZnCl_2$, could presumably improve its catalytic activity in the synthesis of LA.

Lewis acid metal salt also has an added advantage of being easy to separate from the reaction products [66]. Some types of Lewis acid metal salts (i.e. $CrCl_3$ and $FeCl_3$) have been coupled with HY zeolite to make a new hybrid catalyst, which is then coupled with neutral halide based ILs [85], [89]. With respect to this, lower LA yield was reported for the system catalysed by Lewis acid $FeCl_3$/HY zeolite coupled with [BMIM][Br] [85] than Lewis acid $CrCl_3$/HY zeolite coupled with [EMIM][Cl] [89]. However, the results might be affected by the discrepancies in reaction temperature and reaction time adopted (refer to **Chapter 2.8**). In any case, the purpose of implementing a combination of catalysts (i.e. zeolite and metal salts) is to enhance the performance of the organic synthesis. The use of solely zeolite or metal salt was proven to give rise to low LA and LE yields [66], [149], [215], [216], likely due to the formation of intermediate compound, 5-HMF, which allows the omission of ring cleavage

process to form linear-type LA and formic acid [149]. In addition, the low acidity and porosity of the catalysts could also partially account for the poor catalytic activity on LA yield. In this regard, the hybrid catalysts which formed from the combination of porous zeolite catalyst and acidic metal salt have been shown to enhance the catalytic activity of LA yield [85], [89]. Earlier researchers mainly used Lewis acid $CrCl_2$, as a part or a whole catalyst for biomass hydrolysis [149], [217], [218]. However, $CrCl_2$ would pollute the environment due to it is toxicity. Current research has moved towards the use of another commercially available metal salt, Lewis acid $FeCl_3$, which is environmentally friendly [219]. The biomass conversion catalysed by the common hybrid catalyst i.e. Fe-zeolite based, coupled with neutral halide based ILs such as [BMIM][Br], exhibited a moderate LA yield [85]. Impregnating the metal on a zeolite as a support could possibly improve their separation from the reaction products [85]. However, the environmentally friendly Lewis acid $FeCl_3$/HY zeolite coupled with neutral halide based ILs [85] gave a slight lower LA yield than Lewis acid $CrCl_3$/HY zeolite coupled with neutral halide based ILs [89]. These works are in agreement with Peng et al. [66] whereby Lewis acid $CrCl_3$ alone could catalyse efficiently to produce 67 mol% of LA, which was better than Lewis acid $FeCl_3$. In general, the efficiencies of LA yield with various types of metal salts could be summarised as: $ZnCl_2 > CrCl_3 > FeCl_3$. This is in accordance with Adnan et al. [220] who reported that among the LAILs tested (i.e. $ZnCl_2$, $FeCl_3$, $SnCl_2$ and $CuCl_2$ coupled with choline chloride (ChCl) based ILs), ChCl-$ZnCl_2$ exhibited the highest activity in oleic acid conversion. Similarly, Sunitha et al. [221] obtained a high product yield when the same LAILs (i.e. ChCl-$ZnCl_2$) was applied for esterification of long chain carboxylic acids.

Apart from that, Zhou et al. [52] reported that BAILs with sole acid site, [BMIM][$HSO_4$], was less efficient with a moderate LA yield of 17.9%. This further suggested that Bronsted acidic site (e.g. $HSO_4$) alone did not fulfil the full turnover synthesis as compared to BLAILs [7] and LAILs [51]. This result was in agreement with recent works reporting on the use of multiple Bronsted acidic sites in the ILs for both LA and LE yields [73], [74], [83], whereby the excess Bronsted acidic sites did not further increase the catalytic conversion activity. In this regard, this also confirmed that the absence of Lewis acid site on ILs may reduce the catalytic isomerisation of glucose to fructose [66]. Reduction in fructose formation reduces the overall reaction process.

To sum up, Lewis acid sites on ILs are essential in the catalytic conversions of biomass to LA and LE. They play the roles of (1) chelating and weakening the glycosidic bonds of polysaccharides of biomass, (2) enhancing the hydrolysis of polysaccharides into monosaccharides, and (3) isomerising glucose to fructose via enediol form [222]. From a mechanistic aspect, couplings of Lewis acid metal salt-ILs complex would promote the rapid conversion of α-anomer to β-anomer of glucose through hydrogen bonding between hydroxyl groups of ILs [209]. The β-anomer of glucose is a cyclic aldose, which would revert to acyclic form by combining with the Lewis acid complex to form an enolate structure. This allows the conversion of the aldoses to ketoses, followed by isomerisation into fructose [209].

By far, the most successful families of ILs for biomass dissolution are alkyl imidazolium cations based, such as [EMIM][Cl] [89] and [BMIM][Br] [85], owing to the unusually low melting points of many imidazolium salts [167]. The

alkyl side chain of ILs does not directly affect the biomass dissolution to a large extent, but it alters the dissolving ability of ILs towards it [223]. Biomass solubility is decreased with the increase in the carbon chain length [224], [225]. As the carbon chain length increases, the hydrophilicity of ILs decreases and the affinity between the ILs and biomass is weakened. Moreover, the larger size of the ILs leads to higher melting temperature, as the van der Waals interactions between the alkyl side chains start outweighing the symmetry effect [226]. As the results, smaller alkyl groups (e.g. [EMIM][Cl] [89]) performed better than larger alkyl group (e.g. [BMIM][Br] [85]) in LA production.

### 2.7.4 Furfuryl alcohol to LE

The production of LA from furfuryl alcohol conversion via ILs is still absent, and only two studies have reported this for LE production [118], [227], as shown in **Table 2.6**. In accordance with the conversions from cellulose [50], [148] and sugars [58], LE yield also increases with the acidity of the anions of ILs in furfuryl alcohol conversion.

**Table 2.6** Studies on the direct conversion of furfuryl alcohol to LE via ILs at various reaction conditions.

| Reaction Conditions | ILs | Percentage yield (%) | Ref. |
|---|---|---|---|
| BAILs with sole acid site and BAILs with multi-acid sites* | | | |
| Furfuryl alcohol: 4.5 g | [MIM][$HSO_4$] | 65.0 | [118] |
| ILs: 0.3 g | [MIM] [$CF_3COO$] | 1.0 | |

| | | | |
|---|---|---|---|
| Methanol: 95 ml | [NMP][$HSO_4$] | 98.0 | |
| Temp: 130°C | [NMP] [$CF_3COO$] | 2.0 | |
| Time: 2 h | [BMIM-SH][$ClSO_3H$]* | 90.0 | |
| | [BMIM-SH][PTSA]* | 76.0 | |
| | [BMIM-SH][$HSO_4$]* | 95.0 | |
| Furfuryl alcohol: 2 g | [($HSO_3$-p)$_2$im] [$HSO_4$]* | 95 | [227] |
| ILs: 0.1-0.2 g | [BSMIM][$HSO_4$]* | 92 | |
| Ethanol: 40 ml | [BSTmG][$HSO_4$]* | 93 | |
| Temp: 110°C | [BSPy][$HSO_4$]* | 93 | |
| Time: 2 h | [BMIM][$HSO_4$] | 34 | |
| | [BSTmG][$CF_3COO$]* | 24 | |

As shown in **Table 2.6**, the efficiencies of ILs for LE production are in accordance with the increase in the acidity strength of their anions, as follows: [$CF_3COO$] < [PTSA] < [$ClSO_3H$] < [$HSO_4$]. ILs with weak acidity anion, [$CF_3COO$], performed the poorest in LE production, whereas, ILs with strong acidity anion, [$HSO_4$] performed the best, in agreement with other feedstock conversions [48], [50], [58], [148]. Apart from that, [MIM] cations based ILs performed poorer than those of [NMP] cations. The mono-alkyl $CH_3$ structure of [NMP] cation highly promotes the formation of LE intermediates [228]. [NMP] cation possesses superior catalytic activity, is easier to synthesise and purify and is more economical compared to pyrrolidine and imidazolium cations based ILs [229]. In addition, extending the cation alkyl chain with 1,4-butane sultone increases the stability and enhances the Bronsted acidity of ILs, especially for [$HSO_4$] anion based SFILs, [BMIM-SH][$HSO_4$], in which a high

LE yield has been observed (95%) [118]. [BMIM-SH][$HSO_4$] offers the advantage of higher recyclability than [NMP][$HSO_4$], in which the efficiency of the latter fell to 50% upon reuse although it gave slightly higher LE yield [118]. In fact, an increase in both reaction temperature and catalyst concentration improved the furfuryl alcohol conversion and selectivity towards LE [230]. In contrast, as the substrate concentration increases from 5-15%, the conversion and selectivity towards LE was greatly reduced which could be due to the accumulation of ether intermediates of furfuryl alcohol [118].

Wang et al. [227] utilised multi-alkyl -$SO_3H$ functionalised groups on the cation of ILs to promote their Bronsted acidity for higher catalytic activity in LE production. In this catalytic activity, intermediates products (i.e. 2-alkoxymethylfuran and 4,5,5-trialkoxypentan-2-one) were produced from furfuryl alcohol conversion and thus led to a high LE yield of 95%. An advantage of this catalytic system was that undesired diethyl ether (DEE) formed by the side reaction of intermolecular dehydration with ethanol. The Hammett method acidity test of the ILs indicated that the acidity and the molecular structure have strong effects on the catalytic activity of ILs in LE production. Briefly, the acidity of ILs acids decreases in the order of: [$(HSO_3\text{-p})_2$im][$HSO_4$] > [BsMIM]-[$HSO_4$] ≈ [BsTmG][$HSO_4$] ≈ [BsPy][$HSO_4$] > [BMIM][$HSO_4$] > [BsTmG][$CF_3COO$], and the yield of LE follows the same trend.

### 2.7.5 LA to LE

In contrast to numerous studies utilising mineral acid and heterogeneous catalysts [79], [123], [231]–[233], there is currently no reported literature on the

utilisation of ILs for the conversion of LA to LE. Based on the literature [229], [234]–[236], AILs could be a potential catalyst as they provide sufficient acidic catalytic power for the esterification reaction. In the early stage, LAILs (i.e. coupling of aluminium (III) chloride and 1-butylpyridinium chloride) have been tested in the esterification of carboxylic acid [234], but the direction of AILs rapidly moved towards the more manageable BAILs with multi-acid sites (i.e. [$HSO_4$] anion based SFILs) [76]. Cole et al. [150] first synthesised a series of [$HSO_4$] anion based SFILs for the esterification of acetic acid with ethanol. Furthermore, Gui et al. [237] have further illustrated the merits of using [$HSO_4$] anion based SFILs for esterification as an efficient and recyclable catalytic system. Despite the excellent conversion and selectivity, the results were not entirely satisfactory. [$HSO_4$] anion based SFILs are costly and require complex preparation. High concentration is usually required in order to achieve a considerable conversion [62], [238]. Furthermore, the ILs being similar in nature to $H_2SO_4$ in terms of extreme acidity, can cause serious equipment corrosion [62], [239], [240].

To develop new classes of "greener" ILs with simple preparation procedures, BAILs with sole acid site such as the noncorrosive and environmentally benign [$HSO_4$] anion based ILs could be an option [78], [241]. Briefly, the Bronsted acidic salts are prepared by addition of an equimolar amount of strong inorganic acid (i.e. HCl, $H_2SO_4$, $HNO_3$, $CF_3COOH$ and $H_3PO_4$) to a commercial N-base, making up the Bronsted acidic salts, for instance, imidazolium, pyrrolidine, piperidine, morpholine and betaine [76]. However, sole acid site BAILs with anion other than [$HSO_4$] resulted in significantly lower

ester conversions [7], [50], [58], [76], [118], [148], [227]. This suggested that sufficient acidic protons on the anionic component (i.e. $[HSO_4]$) of ILs is essential in the activation of the reaction, since strong acidity would promote the reaction efficiently. With regard to this, some of the $[HSO_4]$ anion based ILs have been applied in common organic synthesis reactions, for instance, 1-methylimidazolium hydrogen sulphate ($[HMIM][HSO_4]$), 1-ethyl-3-butylimidazolium hydrogen sulphate ($[EMIM][HSO_4]$), 1-butyl-3-methylimidazolium hydrogen sulphate ($[BMIM][HSO_4]$), pyridinium hydrogen sulphate ($[Hpy][HSO_4]$), 2-methylpyridine hydrogen sulphate ($[Hmpy][HSO_4]$), triethylammonium hydrogen sulphate ($[Et_3NH][HSO_4]$), triethylammonium dihydrogen phosphate ($[Et_3NH][H_2PO_4]$) and N-methylpyrrolidinium hydrogen sulphate ($[HPyrr][HSO_4]$) have been proven to catalyse the esterification of carboxylic acid reactions [62], [75], [76], [236], through greener and sustainable chemical processes. In particular, certain BAILs with sole acid site have been tested in the esterification of acetic acid with butanol, octanol and methyl β-D-glucopyranoside [76], and thus these $[HSO_4]$ anion based ILs are presumed to be feasible in the esterification reaction of LA to LE. In any case, $[HSO_4]$ anion based ILs have been reported as feasible ILs in the production of LA and LE from biomass [52] and its derivatives [118], [195], which have been discussed (refer to **Chapter 2.7.1-2.7.4**). They also offer the advantages of having low environmental impacts and being nearly noncorrosive and recyclable [62]. Moreover, the characteristic $[HSO_4]$ acidic anion allows one end of the ILs to function as dual solvent-catalysts and another end to be immiscible with esters, forming a biphasic solution even at room temperature (**Figure 2.13**) [75], [236]. This allows the esters to be constituted at the upper layer, while the ILs residues

and substrate are retained at the lower layer, favouring the shift of the reaction towards products, and also the esters recovery [61], [76]. The removal of water during the reactions is unnecessary as it is miscible with ILs residues [237]. Hence, a solvent-free separation is applicable in this case. Moreover, this biphasic system is also applicable for the conversions of biomass [78], [241] and its derivatives (sugars, cellulose) [47], [195], [242] to both LA and EL via one-pot production.

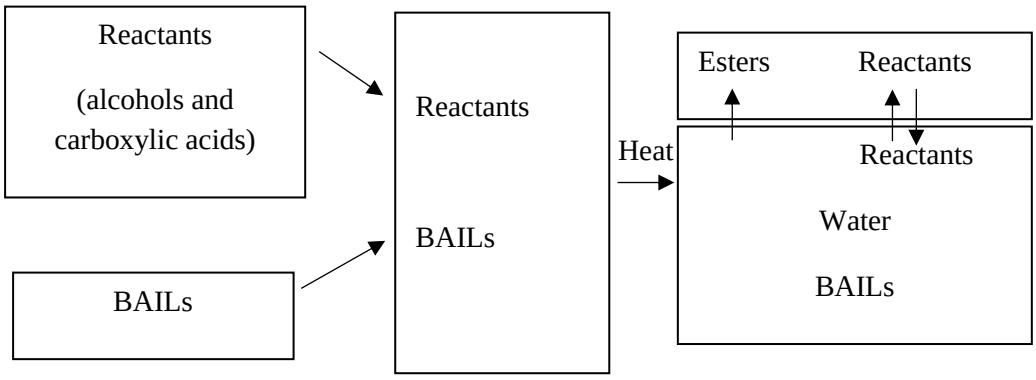



**Figure 2.13** Esterification of alcohols and carboxylic acid catalysed by BAILs. Adapted from Yue et al. [61].

## 2.8 Overview of the current ILs catalytic status and associated factors

Overall, LA yield, followed by its ester yield in the catalytic conversions can be improved by using ILs with (1) high acidity strength, (2) strong molecular interactions between cation and anion, (3) heterogeneous or hybrid catalyst supports, (4) the addition of Lewis acid co-catalysts, or (5) their combinations. In general, BAILs with multi-acid sites (i.e. acidic anion based SFILs) and BLAILs catalyse the conversions to both LA and LE more effectively as compared to the BAILs with sole acid site (i.e. acidic anion based ILs). However,

BAILs with multi-acid sites could be too corrosive for the reactor [62], [239]. Hence, BAILs with sole acid site, particularly [$HSO_4$] anion based ILs, offer a better option for an environmentally benign one-pot reaction conversion. Contrastingly, providing support to LAILs/ BAILs or mixed acid catalytic system (BLAILs) could be an alternative technique to enhance the LA and LE yield, since the pore structure of the support could exert significant influence on the reaction [243], [244].

In terms of feedstock, sugars (i.e. fructose) and furfuryl alcohol gave highest production yield at relatively mild temperatures (i.e. 110-150°C). However, lignocellulosic biomass is highly recommended for commercial-scale production from sustainability and economical viewpoints. Direct conversion from lignocellulosic biomass gave relatively lesser yields due to the recalcitrance of the biomass substrate. To address this problem, suitable ILs hold a promising dissolution ability that enable both biomass pretreatment and catalytic chemical conversion into LA and LE to occur in a one-pot system [245] (refer to **Chapter 2.6)**. Although multi-stage processes can be more complex, continuous processes in one-pot reaction with optimised operating conditions can be very effective in minimising labour, maintenance and energy costs associated with comparable batch operations.

The chemical conversion processes via ILs are versatile because of the wide selection of reaction conditions and range of ILs catalysts. ILs with long chain alkyl possess higher viscosity and thus require higher reaction temperature and vice-versa [245]. High temperature reduces viscosity by destabilising the H-bonding network between ILs, thereby making ILs molecules more readily to

solvate and dissolve the cellulosic molecules of biomass [32]. Zakrzewska et al. [246] reported that a 20-30$^{o}$C increase in temperature in dehydration of carbohydrates with ILs would double the intermediate yield (i.e. 5-HMF), which subsequently enhanced the LA and LE yields. However, elevated temperature produces side reactions and give rise to undesired by-products. Conversely, low temperature lengthens the reaction time and reduces the catalyst activity considerably [6]. The contact times of the starting material and its surrounding environment (solvent, catalyst) would also alter the product distribution profile [6]. Additionally, high loadings of substrate (i.e. biomass or derivatives) would increase the probability of the reactive compounds colliding with each other and causing cross polymerisation via self-condensation of furans in the substrate which lead to undesired products formation such as polyketones and humins [85], thereby reducing the conversions into LA and LE [6]. Apart from that, water acts as a base in the synthesis process which reduces the acidity strength as a catalyst in esterification, but it favours depolymerisation (i.e. hydrolysis, dehydration and rehydration) reaction for the formation of LA [246]. Precisely, when the β-1,4-glycosidic bonds of the dissolved cellulose are first attacked by ILs, the hydrolysis process is then initiated [246]. Hence, insufficient water in the catalytic system impedes proper integration of cellulose in the reaction [47], whilst, excessive water can precipitate the dissolved cellulose from the ILs which make the homogeneous hydrolysis of cellulose in ILs nearly impossible [85]. In any case, water favours the biphasic reactions as it is miscible with ILs at the aqueous phase (bottom layer), separated with the organic phase (upper layer) [247] (refer to **Chapter 2.7.5**: **Figure 2.13**).

## 2.9 Challenges

To date, the conversion of biomass to LA and LE via ILs has not proceeded beyond bench-scale. The cost of ILs is the most pronounced challenge and has been highly recognised as the major process cost driver. Seeking cheaper raw materials for ILs synthesis is vital for long-term production. For instance, inexpensive feedstock such as sulphuric acid, simple amines and imidazolium were combined into a range of [$HSO_4$] anion based ILs [63], [70]. In addition, for feasible operation, the ILs recovery for the recycling purposes has to be as efficient as possible. Nonetheless, the development of effective methods for the recovery of ILs remains another main hurdle for large scale process production. Specifically, the ILs recovery from the biomass hydrolysis step is complicated because the sugars produced have high affinity towards ILs. Additionally, both components of sugars and ILs have low volatility, hence, they are difficult to be separated [248]. Liquid-liquid extraction and distillation have been proposed for product recovery [249]. Since most of the by-products such as intermediate furanic compounds (i.e. furfural, 2-furancarboxyaldehyde and 5-HMF), fatty acid methyl esters (FAMEs) and phenolic compounds have close boiling points, distillation would not be an appropriate technique in extracting the target compounds (i.e. LA and LE) [9], [250]. This problem can be tackled by using biphasic catalytic systems (refer to **Chapter 2.7.5**: **Figure 2.13)**. Nonetheless, some LA and LE still remain in the ILs phase after reaction and further separation and purification processes might still be necessary for complete separation. Conversely, liquid-liquid extraction which is based on the concept of immiscibility of ILs with traditional solvents has facilitated the purification and extraction of the desired organic products. This could be the most appropriate

technique up-to-date [251]. Hu et al. [250] investigated the extraction of both LA and LE from reaction mixture with twelve different solvents. Ethyl acetate gave the best extraction efficiency, followed by 2-octanol, 1-butanol, ethyl butyrate, toluene, methyl acetate and ethyl ether. Some studies used methyl isobutyl ketone (MIBK) to extract LA [2], [50], [148], [203] and hexane to extract LE [148]. However, ethyl acetate is the most commonly used solvent in extracting these two compounds (i.e. LA and LE) [47], [49], [195], [242], [252]. Aside from that, recyclability of ILs is an important factor contributing to the cost of production. Most of the studies suggested that the ILs are capable of being recycled up to a maximum of seven consecutive runs, signifying their potential recycling ability [48], [62], [75], [204], [237], [246], [253]. The stability of the ILs can be examined by $^{1}$H-NMR spectra analysis [47]. However, although ILs are recyclable, the purification of recycled ILs remains problematic. In this regard, the ILs chemostability, thermostability, catalytic activity and recovery are still in the assessment stage for long term chemical industry processing conditions, particularly the challenges faced by the presence of contaminants derived from biomass processing. In any case, the information on the reusability of the ILs is still scarce [82]. Further research is also necessary to develop efficient processes that are able to manage the increase of substrate loading in order to improve the concentrations of the target products.

Finally, there is a growing concern over the environmental impacts of ILs, although ILs has been tagged as “green reaction media” in the catalytic processes. The ideal ILs are cited as nontoxic, biodegradable and recyclable. However, some [Cl] based ILs are toxic, corrosive and very hygroscopic [71],

although they have been reported to favour the conversion of biomass to LA and LE (refer to **Chapter 2.7**). El-Harbawi [254] reported that the estimated $LC_{50}$ toward aquatic organisms for some immidazolium based ILs ([BMIM][$HSO_4$], [BMIM][TFSI] and [HeMIM][$NTf_2$]) were 199.98 $mgL^{-1}$-374.11 $mgL^{-1}$, which were practically non-toxic. Wu et al. [255] claimed that the length of alkyl side chain has a more substantial influence than the methyl group in imidazolium ring on the toxicity of ILs. Longer alkyl chains impart higher toxicity. A number of non-toxic and generally recognised as safe (GRAS) anions with acidic nature are potential candidates for exploration in the production of LA and LE [256]. ILs with $[SO_4]^{2-}$ anion are highly suggested as an alternative environmentally benign ILs with the benefit of an acidic nature [46], which favours the catalytic conversion of biomass to LA and LE (refer to **Chapter 2.7**). Moreover, the $[SO_4]^{2-}$ anion based ILs with combination of alkyl group are stable under mild condition, have no toxic by-products formation and form a biphasic layer with the organic layer [257]. Therefore, the alkyl sulphate groups such as [$HSO_4$], [$MeSO_4$] and [$EtSO_4$] are newly developed ILs with the advantage of an acidic nature. In between, [$HSO_4$] anion based ILs have been studied for the conversion of biomass and derivatives, i.e. cellulose, sugars and furfuryl alcohol (refer to **Chapter 2.7**).

## 2.10 Concluding Remarks

LA and EL are promising biorefinery chemicals which can be synthesised from biomass and its derivatives via the newly emerging and promising ILs. The development of more selective ILs remains a key technical barrier to improve

the production efficiency and reduce by-products. Although ILs are traditionally recognised as “green reaction media”, the synthesis of more environmentally benign ILs, without the corrosive (-$SO_3H$) functionalised group in the cation (SFILs), alongside with the deployment of one-pot production approach, for the production of LA and EL has yet to be conducted. In light of this, this research aims to address this knowledge gap by revealing the potential and feasibility of using a new environmentally friendly coupling mixed acids ILs (BLAILs) catalytic system for the production of LA and EL. Thus, this research could establish a key challenging task toward emerging biorefineries for future sustainability via a greener and sustainable routes in generating future bio-based chemicals and biofuels.

# Chapter 3

# Characterisation studies of oil palm biomass and ionic liquids

## 3.1 Introduction

This chapter begins with the comprehensive oil palm biomass characterisation study for the determination of the lignocellulosic biomass compositions, i.e. cellulose, hemicellulose, lignin, etc. Subsequently, the focus moves towards the physical properties of the proposed ILs used in the catalytic conversion study. The proposed ILs were made of noncorrosive imidazolium based ILs, i.e. [BMIM][Cl], [BMIM][$HSO_4$] and [HMIM][$HSO_4$]. The studies on the physical properties of ILs included density, viscosity, thermal stability and Hammett acidity function.

## 3.2 Methodology

### 3.2.1 Materials

The oil palm biomass (OPEFB and OPMF) were collected from Seri Ulu Langat Palm Oil Mill, Dengkil, Selangor. The samples were dried in an oven at 105$^{o}$C for 24 h and ground with a high-speed rotor beater mill (SM 100 RETSCH, Germany) to particle sizes within the range of 0.4-1 mm. The samples were stored in a desiccator at room temperature for further use. The chemicals needed for further determination of cellulose and hemicellulose from the holocellulose content were acetic acid (95%), $NaClO_2$ (95%) and NaOH (95%), which were purchased from Sigma-Aldrich, USA. In addition, 4-nitroaniline dye, which act as an indicator was also purchased from Sigma-Aldrich, USA. As for the

imidazolium based ILs, i.e. [BMIM][Cl], [BMIM][$HSO_4$] and [HMIM][$HSO_4$], were also purchased from Sigma-Aldrich, USA, with a purity of ≥95%.

### 3.2.2 Biomass composition study

The compositions of OPEFB and OPMF biomass were determined by TGA using a Mettler Toledo (TGA/DSC1, Switzerland). This technique is effective in analysing the characterisation of lignocellulosic biomass materials based on reaction rates or volatility of components during processes [258]. The biomass samples (5.0-10.0 mg) were heated in a platinum cell with a scanning rate of 10°C $min^{-1}$, from 30-700°C, under a $N_2$ flow rate of 20 ml $min^{-1}$ [85]. Holocellulose, which is the sum of cellulose and hemicellulose, was analysed according to the method reported by Teramoto et al. [84] (refer to **Appendix 1**). The percentages of holocellulose content from both samples were adopted from the TGA analysis.

### 3.2.3 Physical properties of ILs

The physical properties of ILs such as density, viscosity, thermal stability and Hammett acidity function were determined. The density of the ILs was measured using an Anton Paar density meter (DMA 4500M, Austria), whilst the viscosity of the ILs was measured using a Brookfield AMETEK viscometer (LVDVE230, USA). Both the density and viscosity of the ILs were carried out at temperatures within the range of 293.15-353.15 K at atmospheric pressure with a control accuracy of ± 0.05 K. All the density and viscosity instruments

were calibrated by using deionised water and the measurements were conducted in triplicates with the mean values reported. The reproducibility of the density and viscosity measurements were ± 5 x $10^{-4}$ g $cm^{-3}$ and ± 0.5 mPa·s, respectively. The thermal decomposition temperature of ILs was determined by TGA using a Mettler Toledo (TGA/DSC1, Switzerland). In the thermal analysis measurement, each IL was placed in a platinum pan and was heated from 50-650°C in a $N_2$ atmosphere with a heating rate of 10°C $min^{-1}$. Lastly, Hammett acidity is an important index to measure the acidity of ILs. Hammett acidity was tested by a Shimadzu UV-vis spectrophotometer (UV1800, Japan) with 4-nitroaniline dye as an indicator to trap the dissociated protons of ILs in deionised water. This method was in accordance to previous works [72], [259]. The solutions of 4-nitroaniline and ILs having concentration 7.5 x $10^{-2}$ mol $L^{-1}$ and 3.0 x $10^{-3}$ mol $L^{-1}$, respectively, were prepared in deionised water. The solutions were stirred for 15 min [195] and their spectra were recorded accordingly. The Hammett acidity function of ILs was measured using the following **Eq. 3.1**:

$$H_0 = pK_a\,[I]_{aq} + \log\left(\frac{[I]}{[IH^+]}\right) \qquad (3.1)$$

where $H_0$ is Hammett acidity function, $pK_a$ is the electrolytic constant of 4-nitroaniline ($pK_a$ = 0.99), [I] and [$IH^+$] are molar concentration of un-protonated and protonated forms of 4-nitroaniline in the solvent, respectively.

## 3.3 Results and Discussion

### 3.3.1 Biomass composition study

**Figure 3.1** illustrates the TGA curves for both biomass. Three distinct stages of weight losses for both biomass were observed. The initial weight loss was recorded in the range of 30-100$^0$C, which was due to the evaporation of residual water in the biomass. The second stage of weight loss at a temperature range of 200-360$^0$C indicated the decomposition of holocellulose (i.e. cellulose and hemicellulose). The weight loss of last stage at 360-650$^0$C represented the degradation of lignin. The remaining amount is known as residue or commonly defined as the ash content. The temperature range was in line with the TGA study reported on lignocellulosic biomass by Ramli et al. [90].

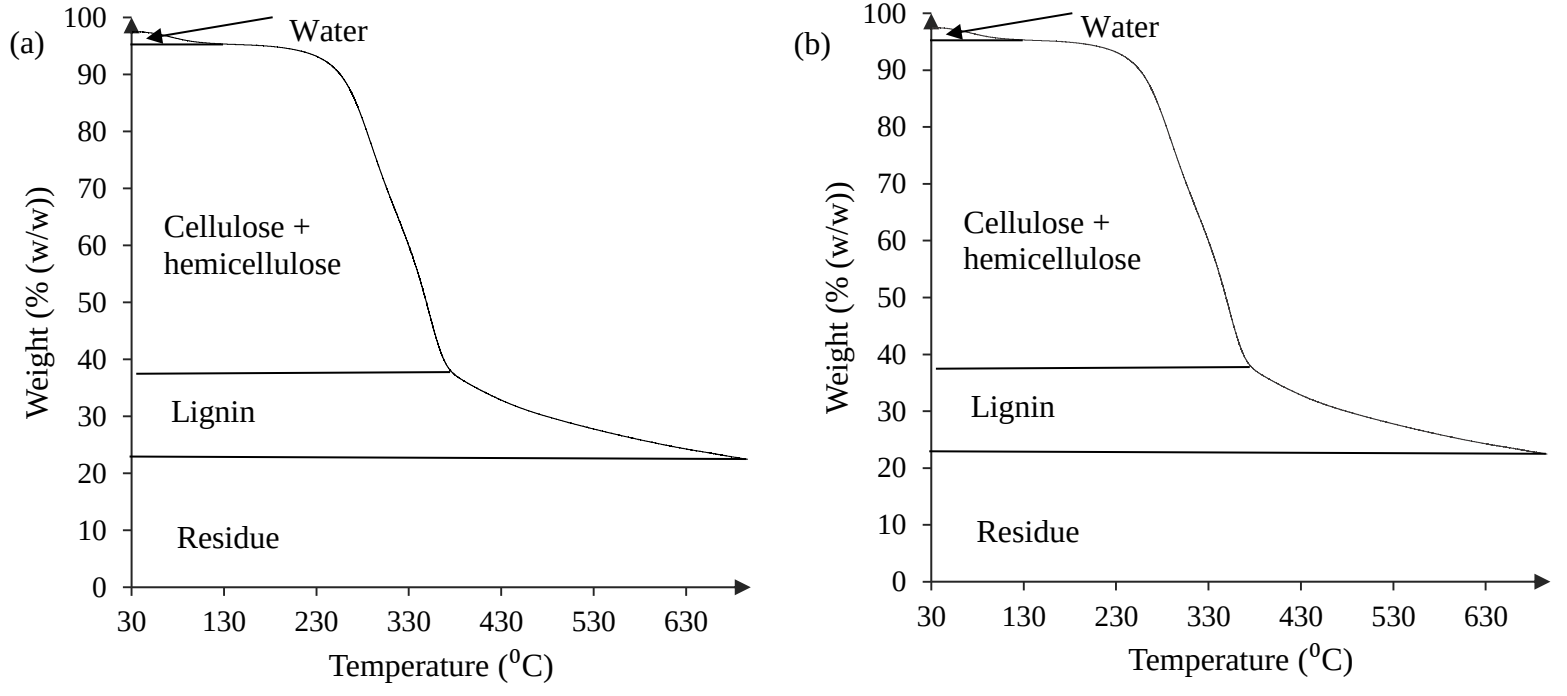



**Figure 3.1** TGA analysis of oil palm biomass (a) OPEFB and (b) OPMF.

**Table 3.1** summarises the composition of OPEFB and OPMF biomass. OPEFB biomass was found to contain a higher cellulose content and a lower lignin content than OPMF biomass. Higher lignin content in the biomass contributed to lower sugars yield, as lignin is naturally recalcitrant to chemical processes [85]. Lignin is linked by covalent bonds and cross-linked with hemicellulose and cellulose, respectively, which hindered the subsequent depolymerisation and esterification processes.

The present results obtained for the compositions of both samples were comparable to those reported in literature, as depicted in **Table 3.2**. To summarise, the composition range of OPEFB contains 4.4-10.6% moisture, 13-18.5% lignin, 16.7-18.9% ash, 31-33.2% cellulose and 23.3-25.3% hemicellulose, whilst OPMF contains 4.3-5.9% moisture, 16.3-17.4% lignin, 20.2-23.1% ash, 28.8-34.4% cellulose and 25.2-26.3% hemicellulose. Among these compositions, cellulose plays the major role in the catalytic conversion to LA and EL [57], where biomass materials with a higher cellulose content would contribute to higher LA and EL yields [260].

**Table 3.1** Composition of oil palm biomass.

| Components | Composition (% (w/w)) | |
|---|---|---|
| | OPEFB | OPMF |
| Moisture content | 4.4 | 4.3 |
| Holocellulose | 58.3 | 56.3 |
| Cellulose | 33.2 | 30.0 |
| Hemicellulose | 25.0 | 26.3 |
| Lignin | 18.5 | 16.3 |
| Residues | 18.9 | 23.1 |

**Table 3.2** A comparative study on the composition of oil palm biomass, in comparison with other literatures reported.

| Components | Composition (%(w/w)) | | | | | |
|---|---|---|---|---|---|---|
| | OPEFB | | | OPMF | | |
| Moisture content | 4.4 | 6.7 | 10.6 | 4.3 | 3.7 | 5.9 |
| Holocellulose | 58.3 | 63.6 | 54.3 | 56.3 | 59.6 | 54.1 |
| Cellulose | 33.2 | 38.3 | 31.0 | 30.0 | 34.4 | 28.8 |
| Hemicellulose | 25.0 | 25.3 | 23.3 | 26.3 | 25.2 | 25.3 |
| Lignin | 18.5 | 13.0 | 17.1 | 16.3 | 16.5 | 17.4 |
| Ash | 18.9 | 16.7 | 18.0 | 23.1 | 20.2 | 22.6 |
| Ref. | Present study | [261] | [86] | Present study | [261] | [262] |

### 3.3.2 Physical properties of ILs

#### 3.3.2.1 Density and viscosity

The effect of temperature on the density and viscosity of ILs are shown in **Table 3.3**.

**Table 3.3** Density and viscosity of ILs measured at various temperatures.

| T/K | ρ (g $cm^{-3}$)/ η (mPa·s) | | |
|---|---|---|---|
| | [HMIM][$HSO_4$] | [BMIM][$HSO_4$] | [BMIM][Cl] |
| 293.15 | 1.4727/ 240.42 | 1.2652/ 290.86 | 1.1357/ 349.14 |
| 303.15 | 1.4317/ 198.77 | 1.2435/ 274.93 | 1.1156/ 287.44 |
| 313.15 | 1.4252/ 143.65 | 1.2349/ 205.56 | 1.1123/ 231.87 |
| 323.15 | 1.4132/ 102.94 | 1.2234/ 134.27 | 1.1113/ 156.42 |
| 333.15 | 1.4065/ 73.25 | 1.2109/ 87.87 | 1.1043/ 105.66 |
| 343.15 | 1.3974/ 59.57 | 1.2056/ 65.97 | 1.0897/ 85.16 |
| 353.15 | 1.3877/ 36.44 | 1.1998/ 53.99 | 1.0702/ 70.07 |

The order of decreasing density for the ILs was [HMIM][$HSO_4$] > [BMIM][$HSO_4$] > [BMIM][Cl]. The results demonstrated that the presence of an acidic nature in the ILs, i.e. acidic [$HSO_4$] anion based ILs, resulted in a greater density, as compared to the neutral halide based ILs ([BMIM][Cl]). This was attributed to the formation of inter- and intramolecular H-bonds in the acidic hydrogen atoms of the imidazolium ring, leading to a denser packing than the non-functionalised acidic ILs [263]. Noteworthy, mono-alkylated ILs, [HMIM][$HSO_4$], had a slight higher density than the longer chain alkylated ILs, [BMIM][$HSO_4$]. This behaviour further suggested that a longer alkyl chain

length of the imidazolium cation determined a lower density value, which was mainly due to the insufficient close packing of the cations [264]. Moreover, De Santis et al. [263] highlighted the presence of more hydrogen bond forming groups in the longer alkyl chain length groups giving rise to an increase in density. Nonetheless, the replacement of a methyl group with a longer alkyl chain length group did not give a significant drop in density [265], which was in accordance with the present work. Additionally, the density decreased with a rise in temperature (**Figure 3.2**). This was mainly due to the decrease in the van der Waals forces of attraction [266], consequently causing an increase in the mobility of the ions [267]. In this regard, the molecules parted away from each other, and thus led to a reduction in the density value. The decrease in the density value of ILs with increasing temperature is common and also observed for other ILs reported [268].

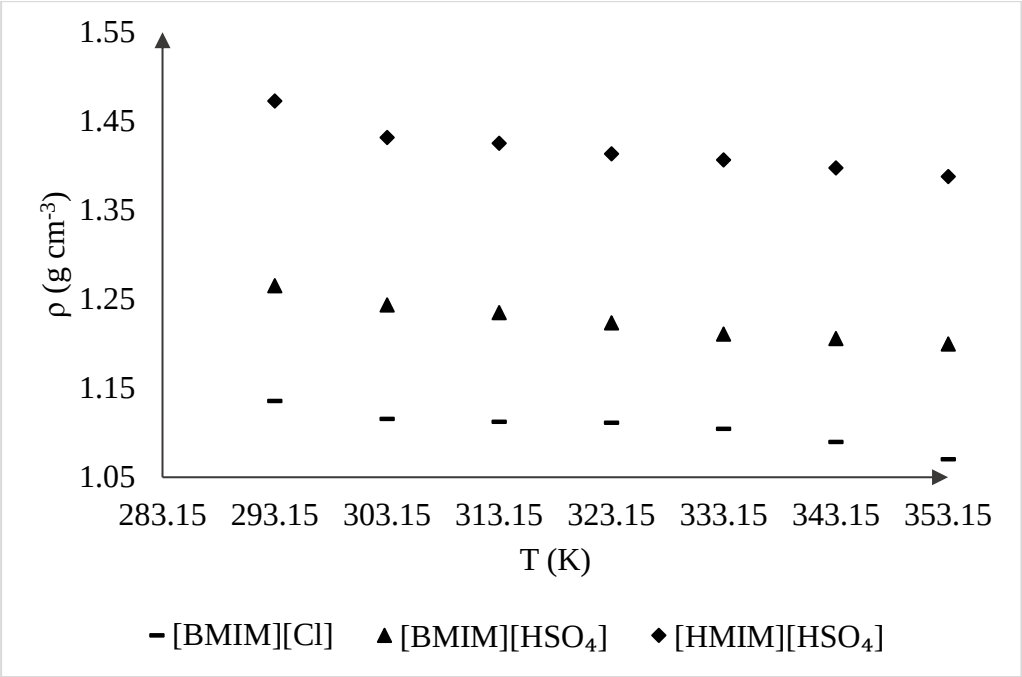



**Figure 3.2** Temperature effect on the density of ILs.

Meanwhile, the order of decreasing viscosity for the ILs was [BMIM][Cl] > [BMIM][$HSO_4$] > [HMIM][$HSO_4$]. Viscosity highly depends on the interactions of ions, such as hydrogen bonding and van der Waals interactions [269]. Moreover, anion plays a greater role in influencing the viscosity, as compared to cation [270]. As such, [BMIM][Cl] demonstrated the highest viscosity, signifying its strongest molecular interactions from the hydrogen bonding [271]. [BMIM][Cl] also readily crystallises at room temperature when exposed to even small amounts of water vapour [272]. Subsequently, longer chain alkylated ILs, [BMIM][$HSO_4$], had a higher viscosity than the mono-alkylated ILs, [HMIM][$HSO_4$]. This suggested that an increase in the alkyl chain length in the imidazolium ILs, produced a more viscous property, due to the increase in the internal resistance towards mobility of the ILs [273]. This behaviour agreed with Sánchez et al. [274]. This increase

might reflect increasing entanglement of the alkyl chains or possibly increased interaction between the N-based moiety and the −OH group of the imidazolium cation, with regard to the electron donating characteristic of the alkyl chain [247]. This effect might also be due to the longer alkyl chains that led to steric hindrance which prevented close associations between ions [275]. Furthermore, an increase in the viscosity also reduced the heat and mass transfer in the system [276]. Similarly to the density of ILs results, the decrease in the viscosity of ILs was also observed as the temperature rose (**Figure 3.3**). At higher temperatures, the molecules tended to move freely and the average intermolecular forces or internal resistance of the molecules in the liquid decreased thus reducing the viscosity of ILs [268]. This rapid decrease in the viscosity of ILs with increased temperature is common and has also been reported for other ILs [247], [270].

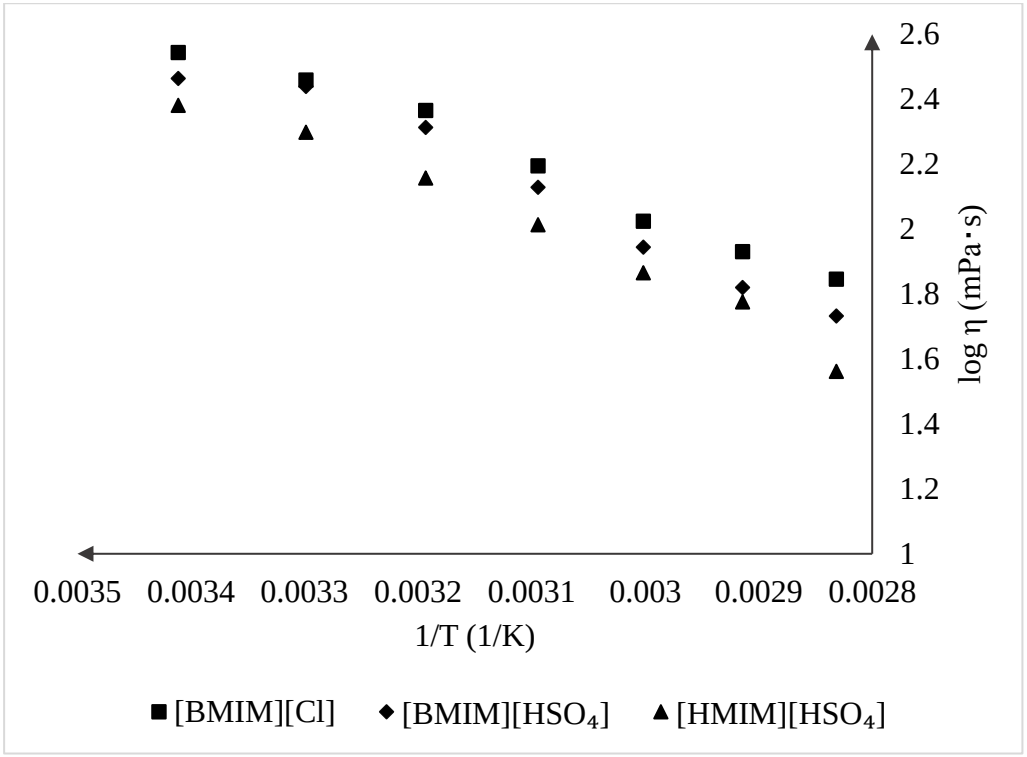



**Figure 3.3** Temperature effect on the viscosity of ILs.

### 3.3.2.2 Thermal stability

Generally, the two-step sequential reaction for the oil palm biomass conversions, i.e. depolymerisation to LA, then esterification to EL, are carried out within the temperature range of 40-200°C [7], [47], [49]. Hence, ILs with high thermal stability is necessary for the biomass catalytic conversion to be steadily accomplished. **Figure 3.4** showed the change in weight of ILs with temperature change within 50-650$^0$C with a heating rate of 10$^0$C min$^{-1}$.

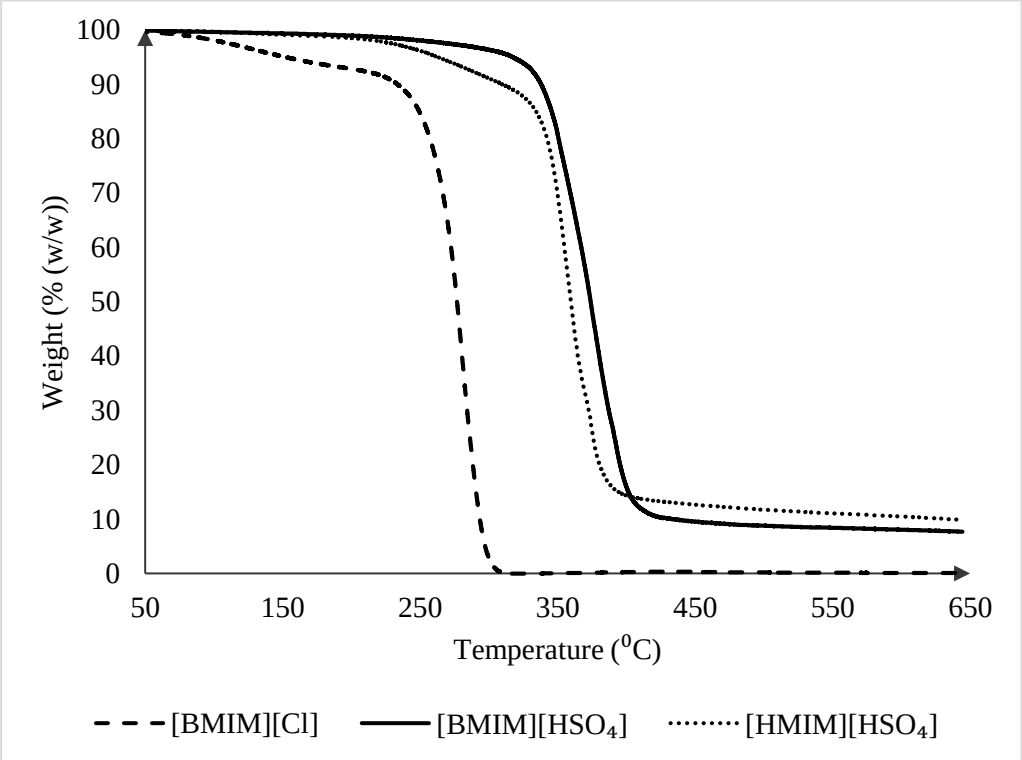



**Figure 3.4** Thermal analysis of the ILs.

The results demonstrated that all ILs were thermally stable >200$^0$C, which was appropriate for the reaction processes. Among the ILs, the loss of a small amount of water was noticeable for [BMIM][Cl]. Moreover, [BMIM][Cl]

was less thermally stable than the acidic ILs, where it decomposed totally at 300$^{o}$C. The other two acidic [$HSO_4$] anion based ILs were found to be sufficiently stable up to 350$^{o}$C, then weight loss occurred at 350-400$^{o}$C. At 650$^{o}$C, the weight losses of [BMIM][$HSO_4$] and [HMIM][$HSO_4$] remained at 8.9% and 10.3%, respectively. This further suggested that [HMIM][$HSO_4$] had a slight higher thermal stability, as compared to [BMIM][$HSO_4$]. This might be due to molecular interactions, i.e. $[HMIM]^+$ and $[HSO_4]^-$, which exhibited higher stability had stronger interaction between the molecules that mitigate the thermal effect when the external temperature approached the degradation temperature. This behaviour was in agreement with Muhammad et al. [273], whereby an increase in alkyl chain length on cation ([BMIM][$HSO_4$]) reduced the thermal stability of ILs. As for the mono-alkylated ILs, [HMIM][$HSO_4$], showed better thermal stability property. This was perhaps due to some additional stability that can be obtained by blocking the acidic hydrogen in the second position on the imidazolium ring with a methyl group [277]. This behaviour was agreed with another type of mono-alkylated ILs, [HMIM][$Tf_2N$], as reported by Crosthwaite et al. [275].

### 3.3.2.3 Hammett acidity function

The measurement of the acidic scale of ILs was conducted by using UV-Vis spectrophotometer with a basic indicator (4-nitroaniline). The maximum absorbance of the unprotonated form of an indicator was observed at 380 nm in the deionised water solution. When an acidic ILs was added, the absorbance of the unprotonated form of the indicator decreased, whereas the protonated form of the indicator could not be observed due to its small molar absorptivity and

location. The differences in the absorbance after the addition of ILs were determined, then the $H_0$ value was calculated based on **Eq. 3.1**. This value was regarded as the relative acidity of the ILs. A lower $H_0$ value indicates a stronger acidic strength of the ILs [195].

Herein, the maximum absorbance data for the unprotonated indicator in UV-vis spectra at 380 nm with the respective $H_0$ results are summarised in **Table 3.4**.

**Table 3.4** Hammett acidity function ($H_0$) data for the ILs studied.

| ILs | $A_{max}$ | [I] (%) | $[IH]^+$ (%) | $H_0$ |
|---|---|---|---|---|
| 4-nitroaniline (Blank) | 0.989 | 100 | 0.0 | - |
| [BMIM][Cl] | 0.989 | 100 | 0.0 | - |
| [BMIM][$HSO_4$] | 0.737 | 73.7 | 26.3 | 1.42 |
| [HMIM][$HSO_4$] | 0.657 | 65.7 | 34.3 | 1.25 |

Among the ILs evaluated, [HMIM][$HSO_4$] had the lowest $H_0$ value. This was reflected in the activity of the catalyst, as [HMIM][$HSO_4$] showed the maximum yield of 65.7%. Theoretically, the stronger the acidity (the lower the acidity value) of the [I], the more $H^+$ can be released. Hence, it could be observed that [HMIM][$HSO_4$] had the strongest acidity strength. In this regard, [HMIM][$HSO_4$] could favour catalytic activity, where it likely exhibited a better ion-dipole type interaction with the substrate molecule more easily by releasing $H^+$ from the ILs [278]. Moreover, the increase in the alkyl chain length (HMIM > BMIM) of the cation of the ILs signified the acidity of the ILs decreased. Lu et

al. [279] interpreted that the cation of ILs has a weak σ-π hyperconjugation effect between its substituent alkyl and imidazole ring, which associates with the number of C-H on alkyl adjacent to the imidazole ring. As the number of C-H bond on the alkyl increases, the effect becomes stronger, leading to a more difficult release of $H^+$ from ILs, and thus weaker acidity of ILs. This result was in accordance with Qi et al. [280], where the authors further claimed this scenario was mainly due to the aggregation effects. The imidazolium ILs with shorter alkyl chains (<4) are isotropic in their neat form and do not form definite aggregations, but those with longer alkyl chains (>4) gradually form well-defined and bigger aggregations [281]. These aggregations lead to non-uniform and co-adjacent structure of ILs systems, which is an obstacle for the transfer of electrons and protons in the molecular interior thus hindering the reaction. Moreover, aggregations also prevent hydrogen at the C2 position of the imidazolium cation from contacting with –OH of fructose molecules to dehydrate into 5-HMF [282], which could reduce the subsequent conversion efficiencies for both LA and EL. Lastly, [BMIM][Cl] did not exhibit any Bronsted acidity, which further confirmed its nature of being neutral based ILs. This result was the same as that reported by Matsagar and Dehepe [278].

## 3.4 Concluding Remarks

A biomass composition study was conducted to determine the insights composition of OPEFB and OPMF biomass. This composition of biomass samples, i.e. cellulose, hemicellulose, lignin, etc., are important for the calculation of production yields, alongside with the corresponding efficiencies of LA and EL. The thermal degradation TGA analysis, followed by cellulose

and hemicellulose characterisation studies revealed that OPEFB and OPMF contains 4.3-4.4% moisture, 16.3-18.5% lignin, 18.9-23.1% ash, 30-33.2% cellulose and 25-26.3% hemicellulose. Then, a series of physical properties of ILs were conducted, i.e. density, viscosity, thermal stability and Hammett acidity function, in order to present a reliable data on the proposed ILs. Among these, the mono-alkylated ILs, [HMIM][$HSO_4$] showed higher density and thermal stability, as well as stronger acidity and lesser viscosity, was foreseen to favour the catalytic conversion of biomass to LA and upgrading to EL.

# Chapter 4

# Screening of ionic liquids for the catalytic conversion

## 4.1 Introduction

This chapter describes the catalytic activities of the proposed ILs for the OPEFB and OPMF biomass conversion to EL. A two-step sequential reaction via one-pot production was conducted, i.e. depolymerisation to LA, followed by the upgrading esterification to EL. Three types of noncorrosive imidazolium based ILs were screened, as reported in **Chapter 3**. Chloride $[Cl]^-$ based ILs ([BMIM][Cl]) is neutral and acted as a control whereas the other two have a sole acid site, but differ in alkyl chain length ([BMIM][$HSO_4$] and [HMIM][$HSO_4$]). Apart from being environmental friendly [75], noncorrosive [62] and lower cost [63], the acidic nature of [$HSO_4$] anion would expectedly favour the production of EL. To the best of our knowledge, all the three ILs have never been explored in the production of EL from oil palm biomass resources or their derivatives.

## 4.2 Methodology

### 4.2.1 Materials

The oil palm biomass (OPEFB and OPMF) were collected and processed, as reported in **Chapter 3.2.1**. As for the proposed imidazolium based ILs, i.e. [BMIM][Cl], [BMIM][$HSO_4$] and [HMIM][$HSO_4$], have also been reported in **Chapter 3.2.1**. For calibration purpose, the standard for EL (Analytical standard, 99%) was purchased from Sigma-Aldrich, USA. Analytical graded ethanol and ethyl acetate (RCI Labscan) were supplied by EOS Scientific Limited (Selangor, Malaysia).

### 4.2.2 Two-step sequential reaction system in one-pot: Depolymerisation and esterification reactions

The experimental procedures of biomass conversion to LA and EL consists of two major reactions, i.e. depolymerisation to LA, followed by the upgrading esterification to EL. The depolymerisation reaction of biomass to LA was conducted in a pressure vessel (Chemglass, USA), followed by the transfer of the reaction mixture of LA synthesis to a single-neck round bottom flask (PYREX, UK) for the upgrading esterification reaction to EL, under reflux in excess ethanol. Upon the completion of (i) depolymerisation of LA synthesis, or (ii) the subsequent upgrading esterification of EL synthesis, the reaction mixture of LA/ EL was cooled to cease the reaction. Then, the reaction mixture of LA/ EL was processed for products isolation and analysis.

### 4.2.3 Products isolation

The reaction mixture was extracted three times with 1:1 (v/v) ethyl acetate and transferred into a centrifuge tube. The solution was centrifuged at 2,000 rpm for 5 min by using a Centrifuge 5430 (Eppendorf, Germany). This resulted in the formation of a two-layered solution: organic phase (upper layer) and aqueous phase (bottom layer). The organic liquid layer was withdrawn from the upper layer and evaporated to dryness at 50°C for 30 min using a rotary evaporator Laborota 4003 Control (Heidolph, Germany). The content was reconstituted to 2 ml of ethyl acetate, and further diluted with ethyl acetate whenever necessary. The sample was then sent for GC-MS analysis. All experiments were conducted in triplicate.

### 4.2.4 Products analysis

The EL was determined by using a GC (Perkin Elmer Clarus 680, USA) equipped with a MS detector and a fused silica capillary column (Agilent HP-FFAP, 30 m length x 0.32 mm diameter x 0.25 µm film thickness, USA). The autosampler injection volume was 1.0 µl in the split mode ratio of 50:1. The following GC temperature program for EL was developed in-house. The injection port was maintained at 240°C, while the oven operating temperature was initially set at 90°C for 3 min, then gradually increased to 230°C at a rate of 10°C $min^{-1}$, and held at the final temperature for 10 min. A solvent delay of 2 min was applied. Helium was used as carrier gas at a constant flow of 1.0 ml $min^{-1}$. The EL was identified using a GC-MS library system (NIST MS search library) and further confirmed with injection of standard solution. The quantitative analysis of EL was conducted with a 6-point calibration curve ($R^2$ > 0.99) (refer to **Appendix 3a**), by using an internal standard of 1-octanol (>99+%, Sigma-Aldrich, USA). The standard errors of triplicate data obtained for all yields ranged within 0.6-2.6%. The actual yield of EL was calculated by **Eq. 4.1**.

$$\text{EL yield (\%)} = \frac{\text{Amount of EL (g)}}{\text{Initital biomass loading (g)}} \text{ x } 100\% \qquad (4.1)$$

## 4.3 Results and Discussion

### 4.3.1 Conversion of oil palm biomass to EL via ILs

A two-step sequential reaction, i.e. depolymerisation, followed by esterification, was conducted to synthesise EL. For the depolymerisation reaction, biomass, ILs and 20% (w/w) water were heated at 160°C for 3 h with

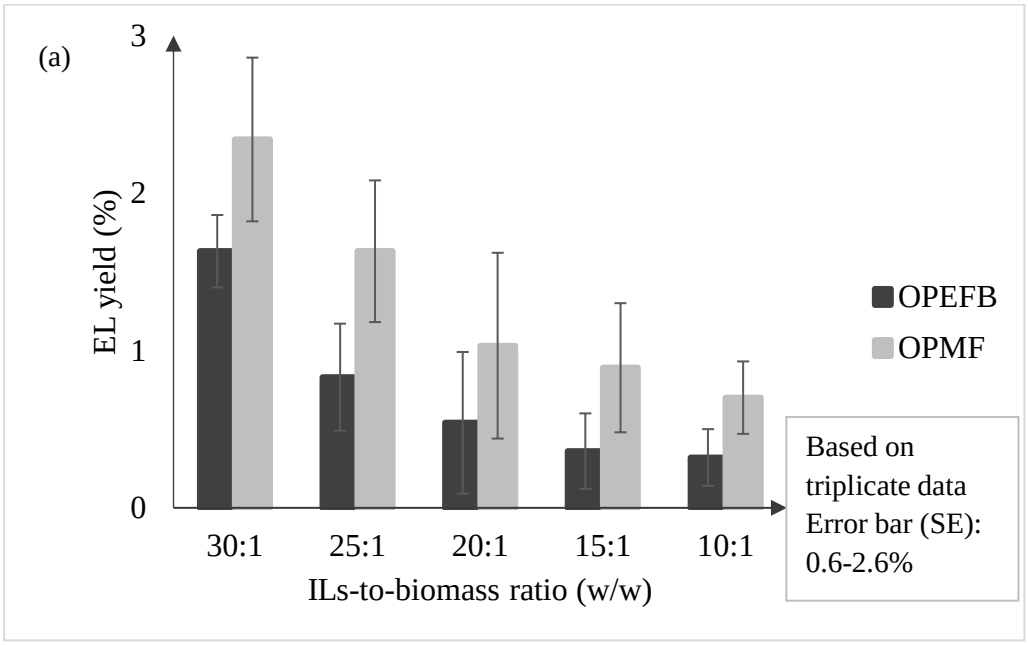
continuous stirring. The reaction mixture then proceeded to the esterification reaction under reflux at 90°C for 6 h in excess ethanol.

#### 4.3.1.1 Chloride $[Cl]^-$ imidazolium based ILs

There was no EL detected in both biomass conversions via the neutral based ILs, [BMIM][Cl]. Solely neutral based ILs, [BMIM][Cl], was incapable of converting the biomass to EL, despite being reported to successfully catalyse the production of LA in some coupling methods, i.e. coupling of neutral based ILs with metal halide [51]/ hybrid catalyst [89]. Neutral based ILs may favour the reaction by enhancing the dissolution of cellulose content of biomass. This is essential as cellulose is insoluble in solely water due to its extensive network of inter- and intramolecular hydrogen bonds, and van der Waals interactions between the cellulose fibrils [166]. Nonetheless, neutral based ILs lacked acidity, and thus the catalytic conversion was unlikely to be possible [53]. Protic ions ($H^+$) from acids play the role of initiating hydrolysis in depolymerisation reaction of biomass. $H^+$ ions attack the oxygen atom of 1,4-β-glycosidic linkage of cellulose in biomass, causing the bonds to break and form cyclic carbonium cations intermediates. The step is vital as it is the rate determining step of hydrolysis. Acidity again is necessary to promote the splitting of water into $H^+$ and hydroxide ($OH^-$) ions [283]. $H^+$ ions replenish the acidity in the catalytic system whereas $OH^-$ ions combine with carbonium cations to form glucose. Owing to these reasons, neutral based ILs are virtually inactive in the production of precursors of LA such as reducing sugars and 5-HMF [284], and thus may not catalyse the subsequent synthesis reactions of LA and EL.

#### 4.3.1.2 Hydrogen sulphate $[HSO_4]^-$ imidazolium based ILs

**Figure 4.1 (a)** shows that the longer chain alkylated BAILs, [BMIM][$HSO_4$], gave very low yields of EL (<2.5%) in both conversions. In contrast, the mono-alkylated BAILs, [HMIM][$HSO_4$] gave significant higher EL yields of 9.9% and 10.2% from the conversion of OPEFB and OPMF biomass, respectively, at ILs-to-biomass ratio of 10:1 (w/w) (**Figure 4.1b**).



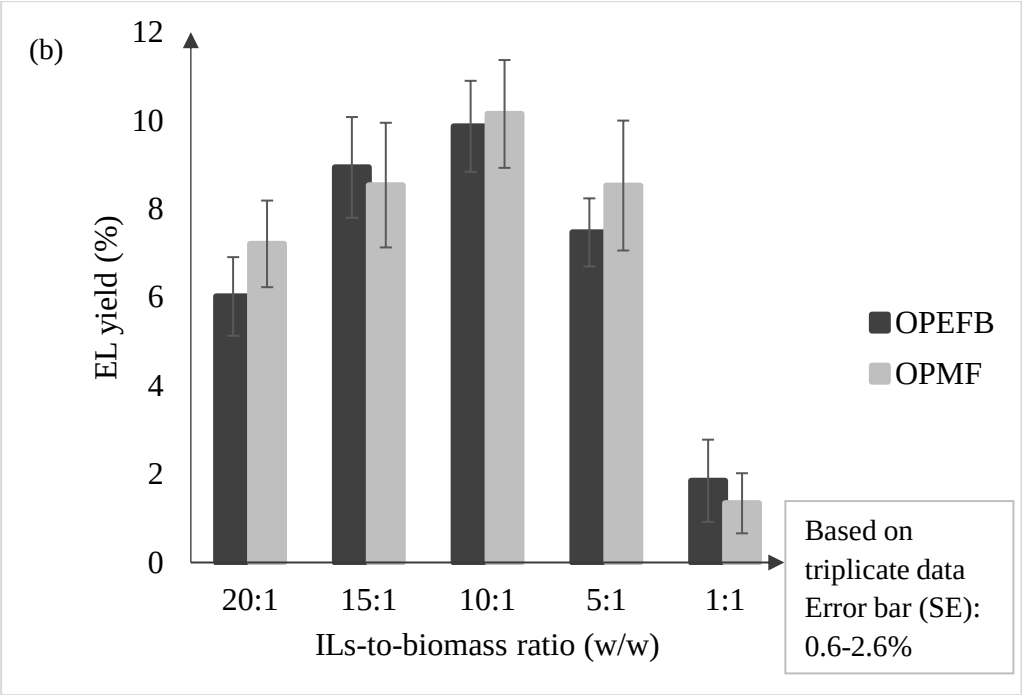



**Figure 4.1** EL yields from conversions of OPEFB and OPMF biomass via (a) [BMIM][$HSO_4$] and (b) [HMIM][$HSO_4$] at various ILs-to-biomass ratio (w/w). (Reaction conditions: Depolymerisation: 160$^o$C, 3 h; Esterification: 90$^o$C, 6 h, in 20% (w/w) water).

The results were in agreement with Naydenov et al. [236] who reported that the increase in alkyl chain length of cation in [BMIM][$HSO_4$] gave lower conversion of ethyl acetate from the esterification of acetic acid with ethanol. Better solubility of EL in longer chain alkylated BAILs, [BMIM][$HSO_4$], in the catalytic phase, could have promoted the undesirable reverse reactions that converted it back to LA. Conversely, an increased size of the two-phase region in HMIM systems creates larger miscibility gaps with lower mutual solubility of esters and ILs [236] thus the esters formed are less likely to convert back to LA in the catalytic system. Liu et al. [285] reported that the reaction rate decreased as the number of carbons in the alkyl chain of ILs increased due to both inductive and steric effects. The increase in the electron-releasing ability of longer chain

alkylated BAILs leads to a greater inductive effect. Despite facilitating the protonation of the carbonyl oxygen of LA, it also lowers the electrophilicity of the carbonyl carbon, resulting in a more energy-hindered rate-limiting nucleophilic attack by ethanol. On the other hand, steric hindrance increases with molecular size. This induces greater electronic repulsion between the non-bonded electrons of reacting molecules, lowering the electron density in the intermolecular region and disturbs bonding interactions. Owing to these factors, mono-alkylated BAILs, [HMIM][$HSO_4$], which had a stronger acidity and performed better in the production, was chosen for the subsequent studies.

## 4.4 Concluding Remarks

A two-step sequential reaction via one-pot production was conducted, i.e. depolymerisation to LA, followed by the upgrading esterification to EL, where the products extraction was only conducted after the two-step reaction. Meanwhile, multistep reaction refers to a non-sequential reactions, where products extraction step is required, prior proceeding for the subsequent esterification reaction. Herein, mono-alkylated BAILs, [HMIM][$HSO_4$], exhibited better catalytic activity of EL yields (+9.5-11.2%) than the longer chain alkylated BAILs, [BMIM][$HSO_4$]. In contrast, the neutral based ILs, [BMIM][Cl], was incapable of producing EL. Hence, [HMIM][$HSO_4$] catalytic system, exhibiting the best catalytic activity performance in EL production, was chosen for the subsequent studies on statistical analysis, reaction optimisation, kinetic, thermodynamic and recyclability test runs**.**

# Chapter 5

# Optimisation studies on the biomass conversion to levulinic acid

## 5.1 Introduction

Mono-alkylated BAILs, [HMIM][$HSO_4$], gave the best catalytic activity conversion efficiency of EL, as reported in **Chapter 4**. Herein, this chapter focuses on using [HMIM][$HSO_4$] for the statistical analysis and reaction optimisation studies by using a RSM based on a CCD method. A preliminary parametric study on using [HMIM][$HSO_4$] catalytic system for the conversion of OPEFB and OPMF biomass to LA was first conducted (Tiong et al. [78], refer to **Appendix 2**), in order to obtain the desired parametric range for the statistical analysis and optimisation studies. The "goodness fit" of the model was assessed based on ANOVA analysis. The quality of fit of the predicted model was expressed by the correlation coefficient ($R^2$), while its statistical significance was examined by the Fisher's F-test. Model terms were evaluated by the P-value (probability) at 95% confidence level. Then, the process variables were optimised by using the numerical optimisation method, generated from the Design-Expert 6.0.8 software. Lewis acid $InCl_3$ was further coupled with optimised sole [HMIM][$HSO_4$] catalytic system to examine the potential of co-catalytic system, i.e. $InCl_3$-[HMIM][$HSO_4$], to boost the conversions. Finally, the physical properties of $InCl_3$-[HMIM][$HSO_4$] was further examined to present reliable data on this novel coupling catalyst, in comparison with the other ILs without Lewis acid analogues studied in **Chapter 3**. To the best of our knowledge, $InCl_3$-[HMIM][$HSO_4$] catalytic system has never been reported for its physical properties and its capability in any catalytic conversion studies. As such, this study highlighted the potential of the proposed new environmentally

friendly coupling mixed acids $InCl_3$-[HMIM][$HSO_4$] catalytic system for biorefinery processing of renewable feedstock.

## 5.2 Methodology

### 5.2.1 Materials

The preparation of oil palm biomass (OPEFB and OPMF) and chemicals involved have been reported in **Chapter 3.2.1** and **4.2.1**. For calibration purpose, the standards for LA (Analytical standard, 99%) was purchased from Sigma-Aldrich, USA.

### 5.2.2 Biomass conversion reaction and products isolation

The experimental procedures of biomass conversion reaction, i.e. depolymerisation to LA, and the subsequent products isolation, have been reported previously, as in **Chapter 4.2.2** and **4.2.3**, respectively.

### 5.2.3 Products analysis

LA content was determined by using a GC-MS (Perkin Elmer Clarus 680, USA). The operating temperature setting for LA was developed in house, which is the same as those of EL, as described in **Chapter 4.2.4**. The quantitative analysis of LA was conducted with a 6-point calibration curve ($R^2 > 0.99$) (refer to **Appendix 3b**), by using an internal standard of butyric acid (>99+%, Sigma-Aldrich, USA). The standard errors of triplicate data obtained for all yields ranged within 0.6-3.6%. The actual yield, theoretical yield and efficiency of LA were calculated by **Eq. 5.1**-**5.3**, accordingly.

$$\text{LA yield (\%)} = \frac{\text{Amount of LA (g)}}{\text{Initial biomass loading (g)}} \text{ x } 100\% \quad (5.1)$$

$$\text{Theoretical LA yield (\%)} = \frac{\text{Cellulose content in biomass (g) x } 0.71}{\text{Initial biomass loading (g)}} \text{ x } 100\% \quad (5.2)$$

where $\frac{\text{Molecular weight of LA (g } mol^{-1})}{\text{Molecular weight of cellulose (g } mol^{-1})} = \frac{116}{162} = 0.71$

and the percentage of cellulose content in OPEFB and OPMF biomass were adapted from **Table 3.1**.

$$\text{LA efficiency (\%)} = \frac{\text{LA yield (\%)}}{\text{Theoretical LA yield (\%)}} \text{ x } 100\% \quad (5.3)$$

where the efficiency refers to the efficiency of biomass conversion to LA calculated based on cellulose content.

### 5.2.4 Statistical analysis

A RSM based on a CCD approach was used to illustrate the effect of independent variables on the response within the experimental region with the aid of Design-Expert 6.0.8 software (STAT-EASE, Inc., Minneapolis, USA). In the depolymerisation reaction, four independent variables were considered, i.e. reaction temperature, reaction time, loadings of ILs-to-biomass ratio and water, coded as A, B, C, and D, respectively. Five levels were designated for each variable as -α, -1, 0, +1 and +α. The selection of the ranges was conducted based on the results obtained from preliminary studies (Tiong et al. [78], refer to **Appendix 2**). The variables and the experimental domain in the design are presented in **Table 5.1**.

**Table 5.1** Range of independent variables and experimental levels (LA yields).

| Factors | Symbol | Levels | | | | |
|---|---|---|---|---|---|---|
| | | -α | -1 | 0 | +1 | +α |
| Reaction temperature (°C) | A | 120 | 140 | 160 | 180 | 200 |
| Reaction time (min) | B | 90 | 180 | 270 | 360 | 450 |
| ILs-to-biomass ratio (w/w) | C | 1:1 | 3:1 | 5:1 | 7:1 | 9:1 |
| Water (%(w/w)) | D | 0 | 10 | 20 | 30 | 40 |

The CCD consists of 16 factorial points, 8 axial points and 6 replicates at the centre points which translate into a total of 30 experiments generated according to **Eq. 5.4**. The quadratic equation model for predicting the optimal conditions can be fitted to a second-degree polynomial design as expressed in **Eq. 5.5**.

$$N = 2^n + 2n + n_c = 2^4 + 2(4) + 6 = 30 \quad (5.4)$$

where N is the number of experiment, n is the number of factor and $n_c$ is the number of replicate at the centre point.

$$Y = \beta_0 + \sum_{i=1}^{n} \beta_i X_i + \sum_{i=1}^{n} \beta_{ii} X_i^{\,2} + \sum_{i=1}^{n} \sum_{j>1}^{n} \beta_{ij} X_i X_j \quad (5.5)$$

where $Y$ is the predicted response, n is the number of experiments, $\beta_0$, $\beta_i$, $\beta_{ii}$ and $\beta_{ij}$ are regression coefficients for constant, linear, quadratic and interaction terms, accordingly. $X_i$ and $X_j$ are coded independent factors.

An analysis of variance (ANOVA) was employed to assess the "goodness of fit" of the models. The quality of fit of the predicted model was expressed by the correlation coefficient ($R^2$), while its statistical significance was examined by the Fisher's F-test. Model terms were evaluated by the P-value (probability) at 95% confidence level. The three-dimensional plots and their respective contour plots were obtained for both OPEFB and OPMF biomass conversions based on the interactive effects of independent variables at the five levels. Furthermore, a response surface equation was optimised using a numerical evaluation for the maximum LA yield to determine the optimum operating conditions. The models were developed with an assumption of equal variance.

### 5.2.5 Physical properties of $InCl_3$-[HMIM][$HSO_4$]

The physical properties of $InCl_3$-[HMIM][$HSO_4$] such as density, viscosity, thermal stability and Hammett acidity function were determined, in comparison with the other ILs without Lewis acid analogues studied in **Chapter 3**. The experimental procedures of these physical properties have been reported previously, as in **Chapter 3.2.3**.

## 5.3 Results and Discussion

### 5.3.1 Statistical analysis

#### 5.3.1.1 RSM based on CCD method

**Table 5.2** shows a series of experiments conducted based on the matrix of the experimental design with the corresponding responses (LA yields) from both OPEFB ($Y_1$) and OPMF ($Y_2$) biomass conversions. The predicted results (the LA yields, $Y_1$ and $Y_2$) were assessed by considering the following variables, i.e. reaction temperature (A), reaction time (B), loadings of ILs-to-biomass ratio (C) and water (D), and calculated based on the empirical second-degree polynomial model as shown in **Eq. 5.6** and **5.7** below.

$$Y_1 = 10.07 + 1.30A + 0.71B + 1.38C + 0.62D - 1.58A^2 - 1.91B^2 - 1.57C^2 - 1.78D^2 + 0.026AB + 0.86AC - 0.12AD + 0.17BC - 0.23BD + 0.34CD \quad (5.6)$$

$$Y_2 = 10.64 + 1.84A + 0.79B + 1.72C + 0.75D - 1.36\ A^2 - 1.97B^2 - 1.33\ C^2 - 1.86D^2 - 0.34AB + 0.98AC + 0.26AD + 0.59BC - 0.28BD + 0.28CD \quad (5.7)$$

**Table 5.2** CCD experimental design matrix and responses (LA yields).

| Entry | Point type | Independent process parameters levels | | | | Responses (%) | |
|---|---|---|---|---|---|---|---|
| | | Temp (°C), A | Time (min), B | ILs-to-biomass ratio (w/w), C | Water (% (w/w)), D | $Y_1$ | $Y_2$ |
| 1 | Centre | 160 (0) | 270 (0) | 5:1 (0) | 20 (0) | 10.6 | 11.7 |
| 2 | Centre | 160 (0) | 270 (0) | 5:1 (0) | 20 (0) | 9.3 | 9.0 |
| 3 | Centre | 160 (0) | 270 (0) | 5:1 (0) | 20 (0) | 10.7 | 12.3 |
| 4 | Centre | 160 (0) | 270 (0) | 5:1 (0) | 20 (0) | 11.3 | 9.5 |
| 5 | Centre | 160 (0) | 270 (0) | 5:1 (0) | 20 (0) | 10.1 | 10.0 |
| 6 | Centre | 160 (0) | 270 (0) | 5:1 (0) | 20 (0) | 8.3 | 11.2 |
| 7 | Axial | 200 (+α) | 270 (0) | 5:1 (0) | 20 (0) | 7.6 | 9.8 |
| 8 | Axial | 160 (0) | 90 (-α) | 5:1 (0) | 20 (0) | 0.5 | 0.9 |
| 9 | Axial | 160 (0) | 270 (0) | 9:1 (+α) | 20 (0) | 7.3 | 9.9 |
| 10 | Axial | 160 (0) | 270 (0) | 1:1 (-α) | 20 (0) | 0.8 | 1.0 |
| 11 | Axial | 160 (0) | 270 (0) | 5:1 (0) | 40 (+α) | 5.7 | 5.9 |
| 12 | Axial | 160 (0) | 450 (+α) | 5:1 (0) | 20 (0) | 4.8 | 5.0 |
| 13 | Axial | 120 (-α) | 270 (0) | 5:1 (0) | 20 (0) | 0.4 | 0.9 |
| 14 | Axial | 160 (0) | 270 (0) | 5:1 (0) | 0 (-α) | 0.7 | 0.8 |

| | | | | | | | |
|---|---|---|---|---|---|---|---|
| 15 | Factorial | 180 (+1) | 360 (+1) | 7:1 (+1) | 10 (-1) | 7.3 | 9.3 |
| 16 | Factorial | 140 (-1) | 360 (+1) | 7:1 (+1) | 30 (+1) | 4.1 | 5.2 |
| 17 | Factorial | 180 (+1) | 360 (+1) | 3:1 (-1) | 30 (+1) | 1.8 | 3.3 |
| 18 | Factorial | 180 (+1) | 360 (+1) | 7:1 (+1) | 30 (+1) | 6.8 | 8.8 |
| 19 | Factorial | 140 (-1) | 180 (-1) | 3:1 (-1) | 10 (-1) | 1.1 | 0.8 |
| 20 | Factorial | 140 (-1) | 360 (+1) | 7:1 (+1) | 10 (-1) | 2.0 | 3.5 |
| 21 | Factorial | 140 (-1) | 180 (-1) | 7:1 (+1) | 10 (-1) | 1.3 | 1.5 |
| 22 | Factorial | 180 (+1) | 180 (-1) | 3:1 (-1) | 10 (-1) | 1.5 | 3.5 |
| 23 | Factorial | 180 (+1) | 180 (-1) | 3:1 (-1) | 30 (+1) | 1.9 | 3.6 |
| 24 | Factorial | 180 (+1) | 180 (-1) | 7:1 (+1) | 10 (-1) | 4.2 | 4.4 |
| 25 | Factorial | 140 (-1) | 360 (+1) | 3:1 (-1) | 30 (+1) | 2.1 | 2.1 |
| 26 | Factorial | 140 (-1) | 180 (-1) | 3:1 (-1) | 30 (+1) | 1.4 | 1.9 |
| 27 | Factorial | 180 (+1) | 180 (-1) | 7:1 (+1) | 30 (+1) | 6.8 | 9.8 |
| 28 | Factorial | 140 (-1) | 180 (-1) | 7:1 (+1) | 30 (+1) | 2.3 | 1.1 |
| 29 | Factorial | 140 (-1) | 360 (+1) | 3:1 (-1) | 10 (-1) | 2.0 | 2.5 |
| 30 | Factorial | 180 (+1) | 360 (+1) | 3:1 (-1) | 10 (-1) | 2.9 | 2.4 |

ANOVA analyses for each response model was performed to exhibit the significance and nature of interactions between the process variables, as shown in **Table 5.3**.

**Table 5.3** ANOVA results for response parameters of LA yields.

| Response | Model F-value | P | PLOF | $R^2$ | Adj. $R^2$ | Pred. $R^2$ | AP | SD | PRESS |
|---|---|---|---|---|---|---|---|---|---|
| $Y_1$ | 17.97 | < 0.0001 | 0.34 | 0.95 | 0.89 | 0.71 | 11.41 | 1.18 | 106.77 |
| $Y_2$ | 15.46 | < 0.0001 | 0.60 | 0.94 | 0.88 | 0.68 | 10.40 | 1.40 | 141.82 |

P: probability of error; PLOF: probability of lack of fit; Adj. $R^2$: adjusted $R^2$; Pred. $R^2$: predicted $R^2$; AP: adequate precision; SD: standard deviation; PRESS: predicted residual error sum of squares.

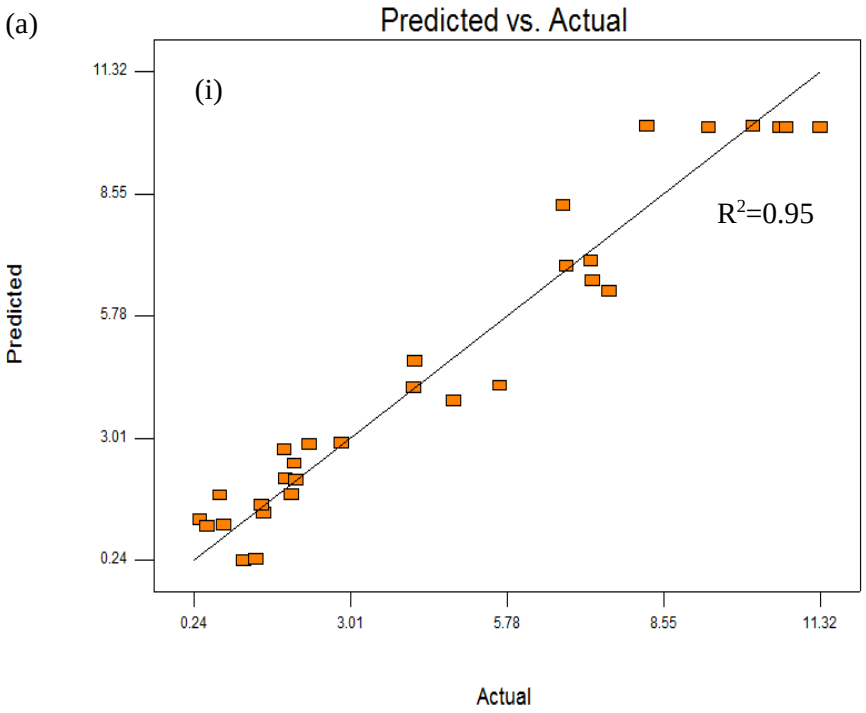
*Detailed data on the ANOVA regression model of LA yields (refer to **Appendix 5a**).

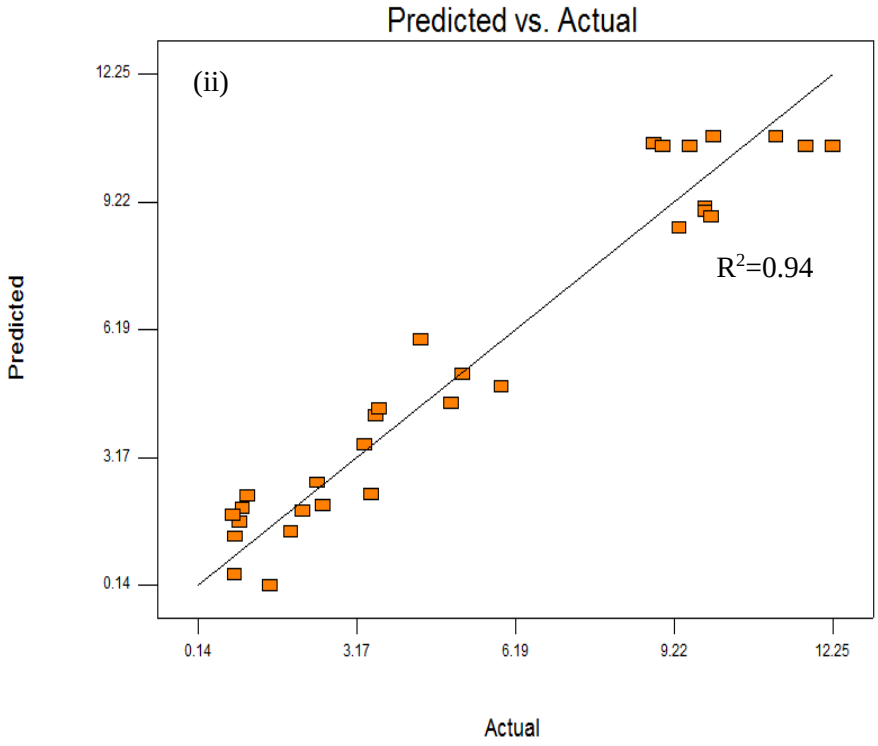
The results indicated that both models were statistically significant with only <0.01% chance that the models' F-values could occur due to noise. The lack of fit F-value for each response ($Y_1$, $Y_2$) was insignificant relative to the pure error, signifying a good fitting of the proposed model. This implies the proposed method is a reliable tool for predicting LA yields. High $R^2$ of 0.95 and 0.94 for $Y_1$ and $Y_2$, respectively, indicated that 95% and 94% of the total variability could be explained by the regression models. In addition, the adjusted $R^2$ and predicted $R^2$ of both models demonstrated a good agreement between the experimental and predicted LA yields. This allows a reliable estimation of response (LA yields) in the desired range of process conditions. The adequate precision values in both

responses had ratios greater than 4, confirming that all predicted models can be used to navigate the design space as defined by the CCD.

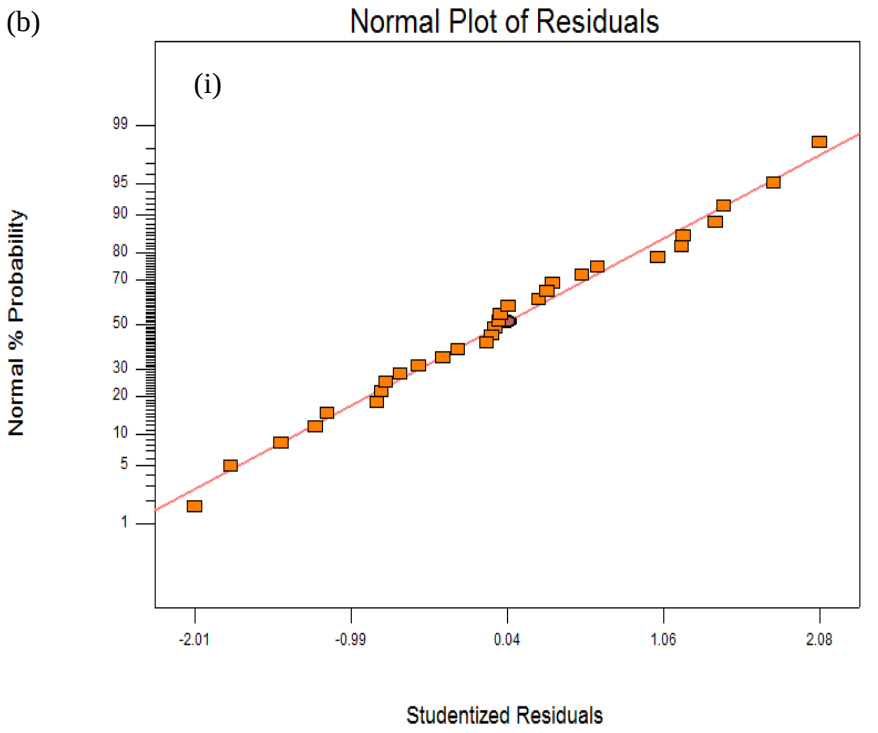
For further evaluation on the adequacy of quadratic models, a few diagnostic plots are presented. **Figure 5.1 (a)** shows the plots of actual responses (experimental LA yields) versus the predicted responses (predicted LA yields) with high $R^2$ of >0.9. **Figure 5.1 (b)** shows the normal % probability versus studentised residuals, where the data points are scattered along the straight line of the diagonal in both models. This trend further illustrates that the error terms are disseminated and independent of each other. **Figure 5.1 (c)** shows the outliers T versus run number, where the data points are randomly dispersed within the range of +3.5 to -3.5 in both models, denoting its homoscedasticity. These evaluations further suggested that both models are reliable and thus could initiate the relationship of the process variables for the depolymerisation reaction, along with the product distribution of LA yields.

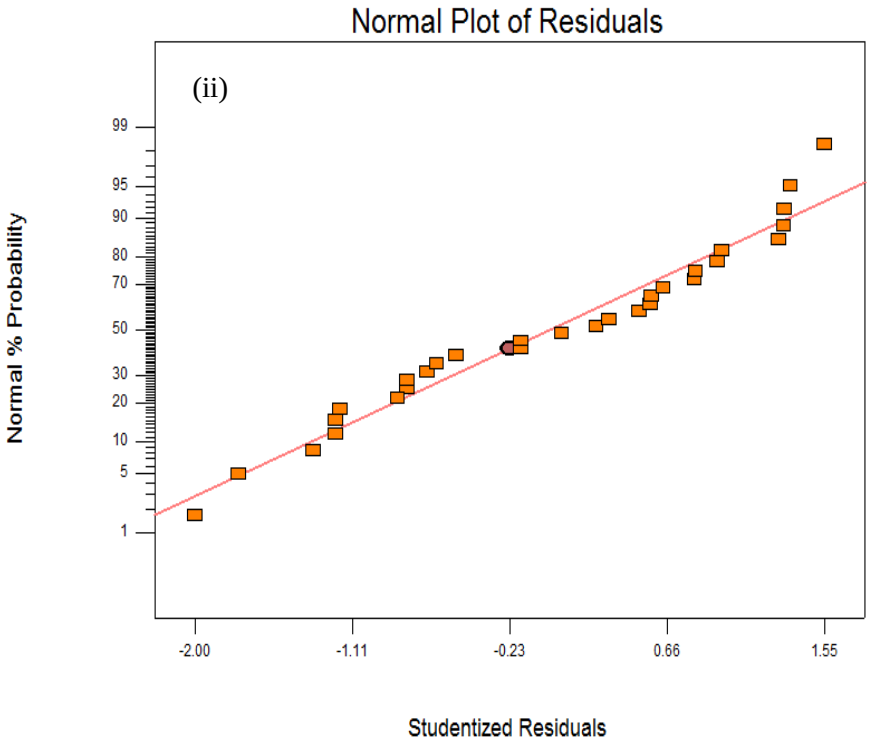
(a)


Predicted vs. Actual
(i)
$R^2$=0.95
Predicted
Actual
11.32
8.55
5.78
3.01
0.24
0.24
3.01
5.78
8.55
11.32


Predicted vs. Actual
(ii)
$R^2$=0.94
Predicted
Actual
12.25
9.22
6.19
3.17
0.14
0.14
3.17
6.19
9.22
12.25

(b)


Normal Plot of Residuals
(i)
Normal % Probability
99
95
90
80
70
50
30
20
10
5
1
-2.01
-0.99
0.04
1.06
2.08
Studentized Residuals


Normal Plot of Residuals
(ii)
Normal % Probability
99
95
90
80
70
50
30
20
10
5
1
-2.00
-1.11
-0.23
0.66
1.55
Studentized Residuals

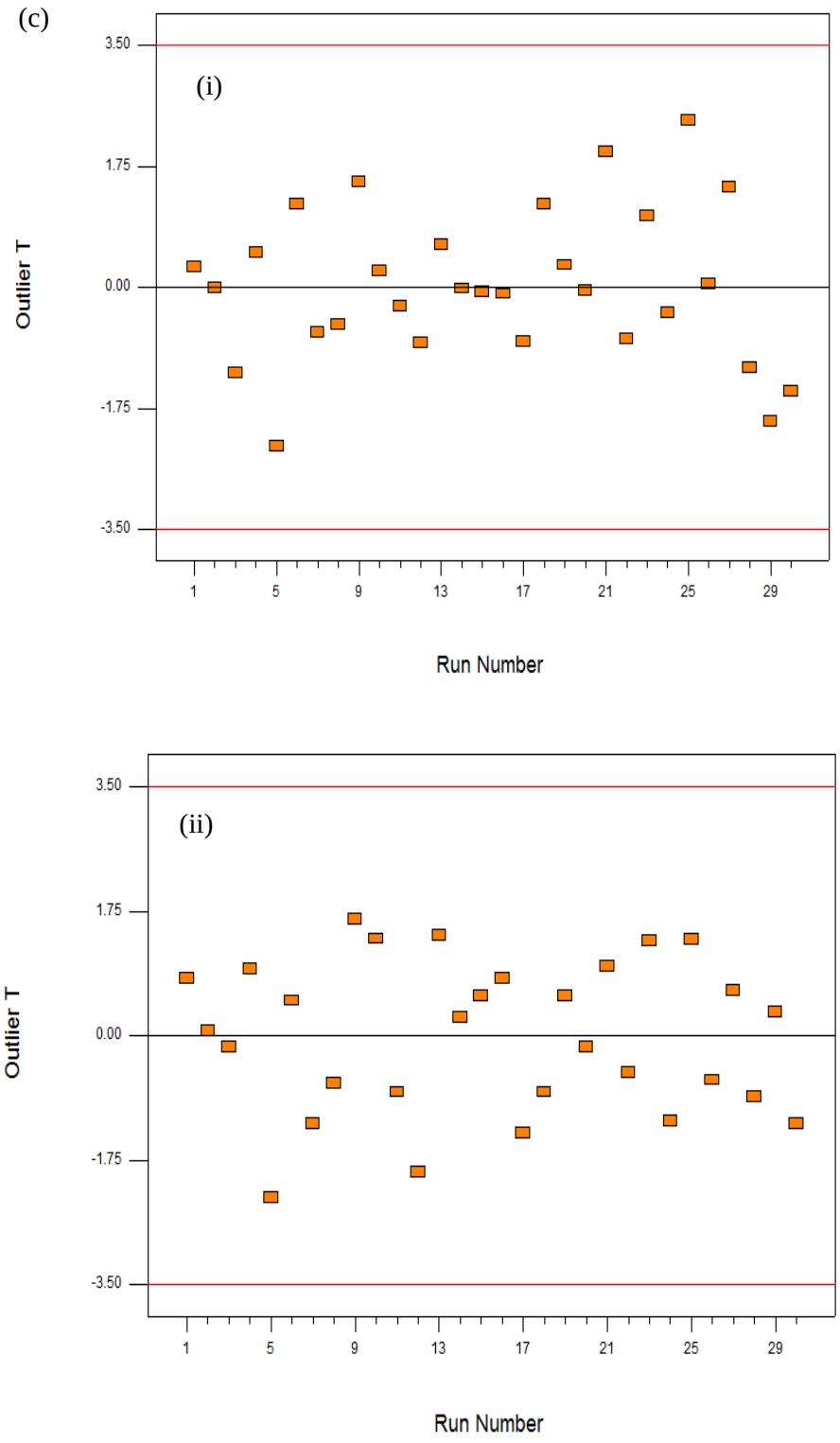



**Figure 5.1** Diagnostic of models (a) Relationship between predicted and actual values, (b) Normal % probability versus studentized residuals, and (c) Outliers T versus run number of LA yields from the conversions of (i) OPEFB ($Y_1$) and (ii) OPMF ($Y_2$).

### 5.3.1.2 Effect and interaction of variables on LA yields

**Table 5.4** shows the variable effects of the factors and associated p-values for the two responses. For both responses, the percentage of LA yields from the conversions of OPEFB ($Y_1$) and OPMF ($Y_2$) biomass were significantly affected by both the linear terms and quadratic terms of all variables tested. Among these, the linear term of A and C with higher F-values appeared to be the two most important variables affecting the LA yields, with very small P-values of <0.01. As for the interaction terms, only AC significantly enhanced the LA yields.

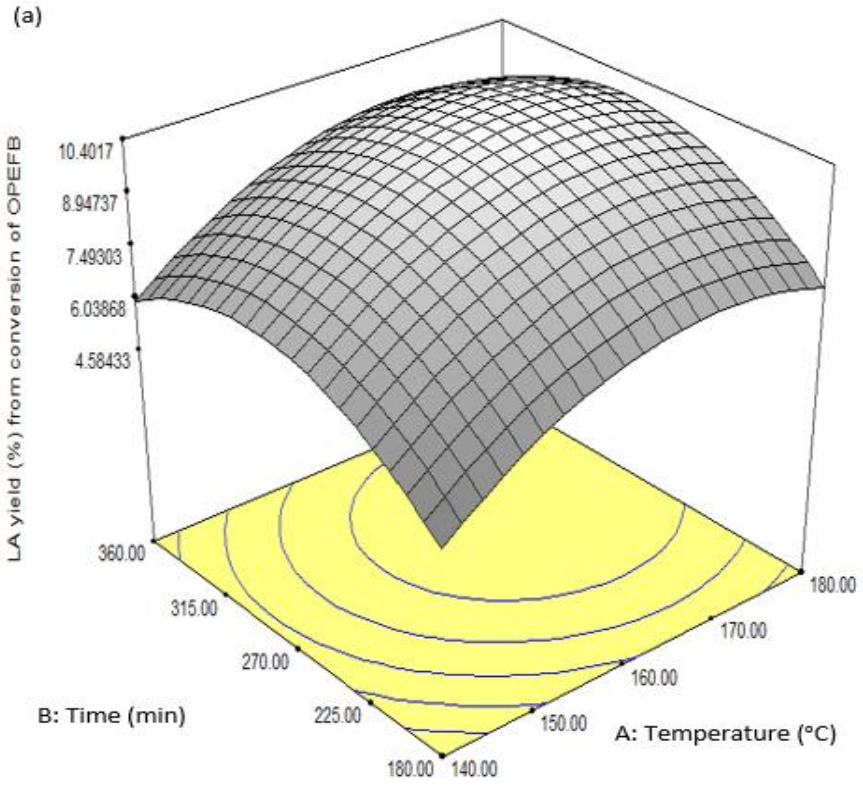
**Table 5.4** F-values and associated p-values for the responses of $Y_1$ (conversion from OPEFB) and $Y_2$ (conversion from OPMF).

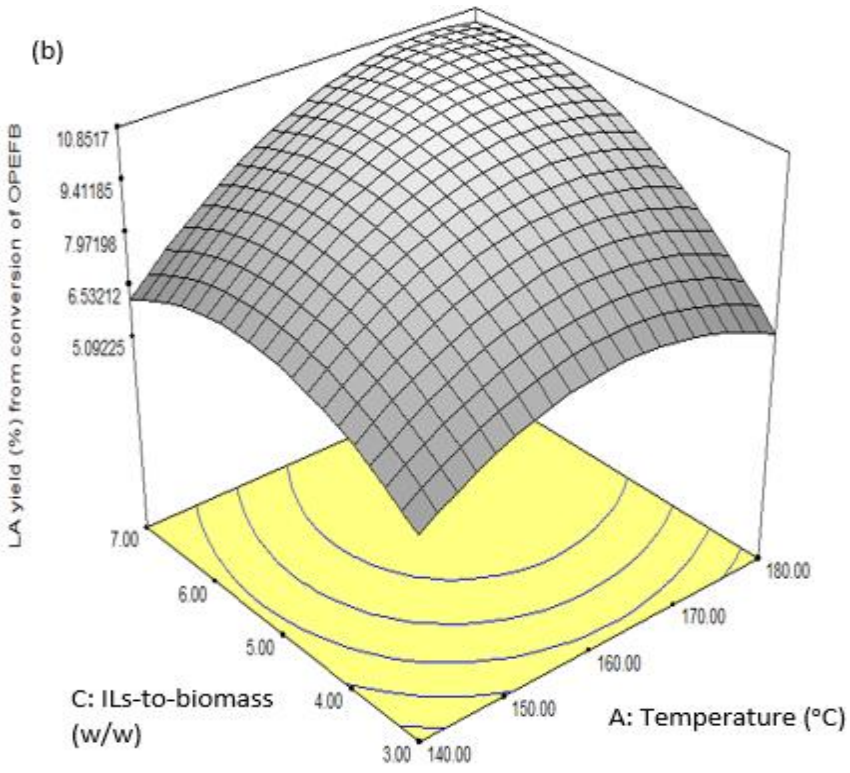
| Relationship | | Factor | Responses | | | |
|---|---|---|---|---|---|---|
| | | | $Y_1$ | | $Y_2$ | |
| | | | F-value | p-value | F-value | p-value |
| Main effects | Linear | A | 29.01 | <0.0001* | 41.71 | <0.0001* |
| | | B | 8.74 | 0.0104* | 7.64 | 0.0152* |
| | | C | 32.93 | <0.0001* | 36.53 | <0.0001* |
| | | D | 6.64 | 0.0220* | 7.01 | 0.0191* |
| Interactions | Pure quadratic | $A^2$ | 49.37 | <0.0001* | 25.87 | 0.0002* |
| | | $B^2$ | 71.88 | <0.0001* | 54.64 | <0.0001* |
| | | $C^2$ | 48.44 | <0.0001* | 25.02 | 0.0002* |
| | | $D^2$ | 62.53 | <0.0001* | 48.52 | <0.0001* |
| | Cross product | AB | 7.529E-003 | 0.9321 | 0.93 | 0.3520 |
| | | AC | 8.52 | 0.0112* | 7.85 | 0.0141* |
| | | AD | 0.16 | 0.6952 | 0.53 | 0.4773 |
| | | BC | 0.34 | 0.5671 | 2.89 | 0.1112 |

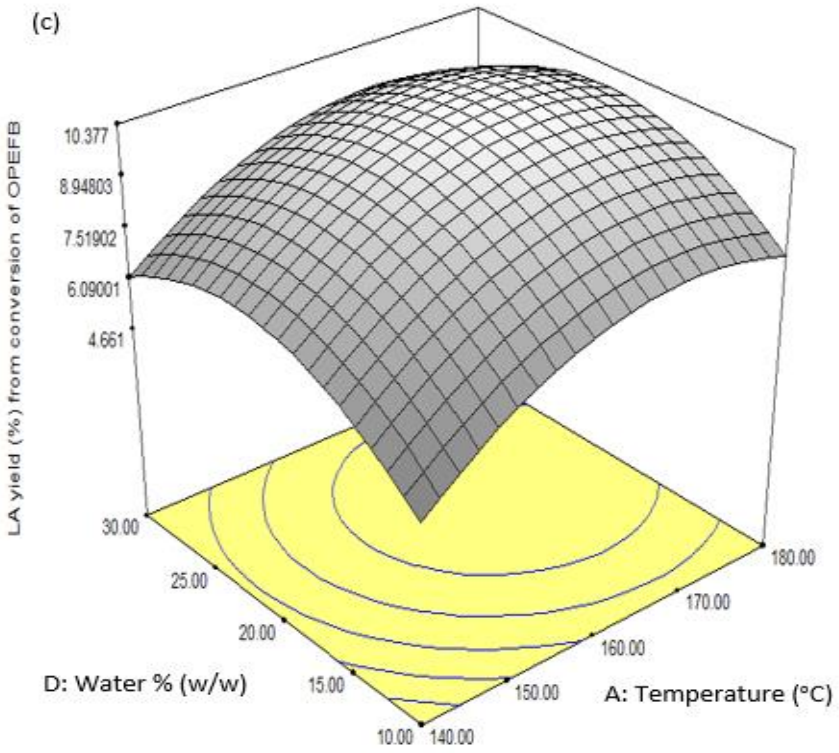
| | | | | | |
|---|---|---|---|---|---|
| | BD | 0.59 | 0.4551 | 0.65 | 0.4321 |
| | CD | 1.34 | 0.2664 | 0.63 | 0.4401 |

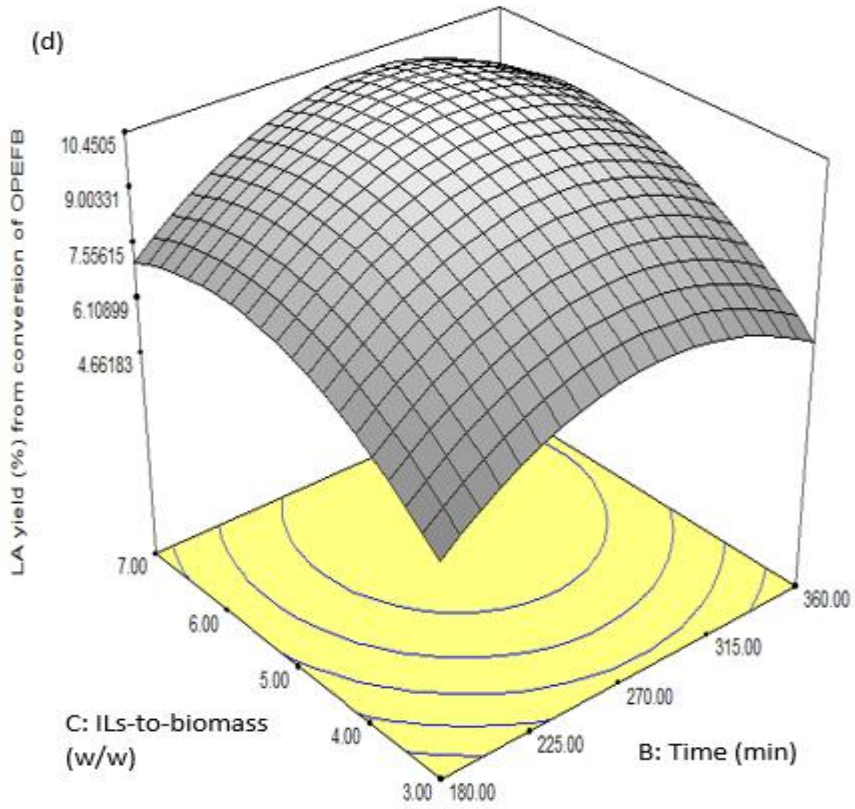
*Significant at 5% (p-value)

**Figure 5.2** and **5.3** show the interactions of the response surface with the corresponding contour plots among the four variables on LA yields. All interactions were observed attesting to the quadratic effect on each variable on LA yields. The plots were approximately symmetrical in shape with half-circular contours. All responses likely showed peaks, denoting that the optimum conditions for LA yields were imputed by the process variables close to the design space. The percentage of LA yields decreased when moving away from these points, signifying that either an increase or a decrease in any of the tested variables resulted in a reduction of yields.

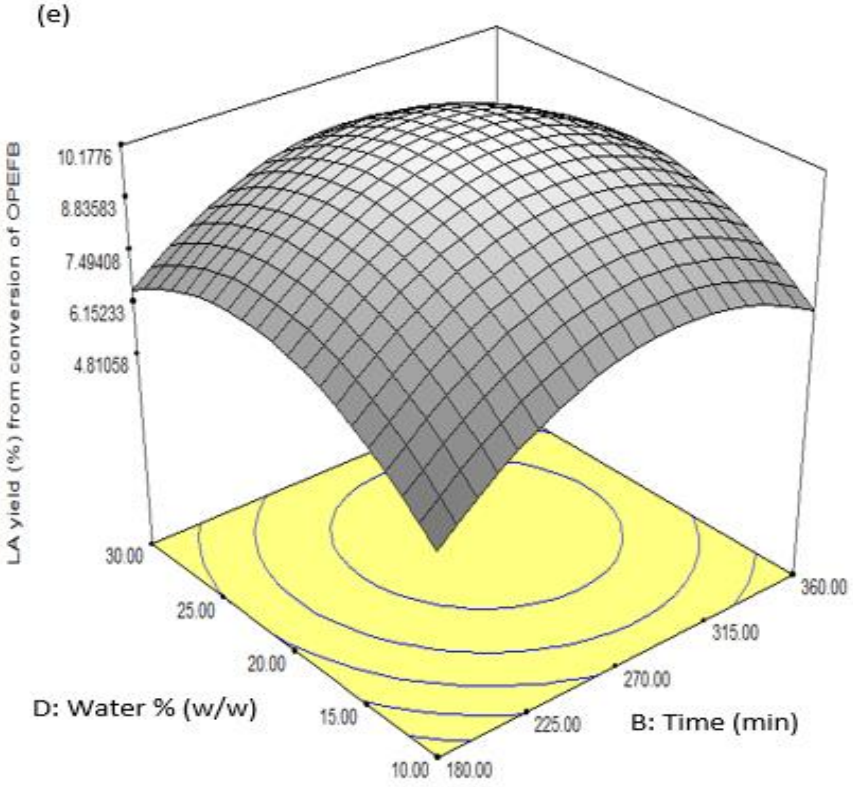

(a)
LA yield (%) from conversion of OPEFB
10.4017
8.94737
7.49303
6.03868
4.58433
360.00
315.00
270.00
225.00
180.00
B: Time (min)
140.00
150.00
160.00
170.00
180.00
A: Temperature (°C)


(b)
LA yield (%) from conversion of OPEFB
10.8517
9.41185
7.97198
6.53212
5.09225
7.00
6.00
5.00
4.00
3.00
C: ILs-to-biomass (w/w)
140.00
150.00
160.00
170.00
180.00
A: Temperature (°C)


(c)
LA yield (%) from conversion of OPEFB
10.377
8.94803
7.51902
6.09001
4.661
30.00
25.00
20.00
15.00
10.00
D: Water % (w/w)
140.00
150.00
160.00
170.00
180.00
A: Temperature (°C)


(d)
LA yield (%) from conversion of OPEFB
10.4505
9.00331
7.55615
6.10899
4.66183
7.00
6.00
5.00
4.00
3.00
C: ILs-to-biomass (w/w)
180.00
225.00
270.00
315.00
360.00
B: Time (min)

(e)


LA yield (%) from conversion of OPEFB
10.1776
8.83583
7.49408
6.15233
4.81058
30.00
25.00
20.00
15.00
10.00
D: Water % (w/w)
180.00
225.00
270.00
315.00
360.00
B: Time (min)

(f)

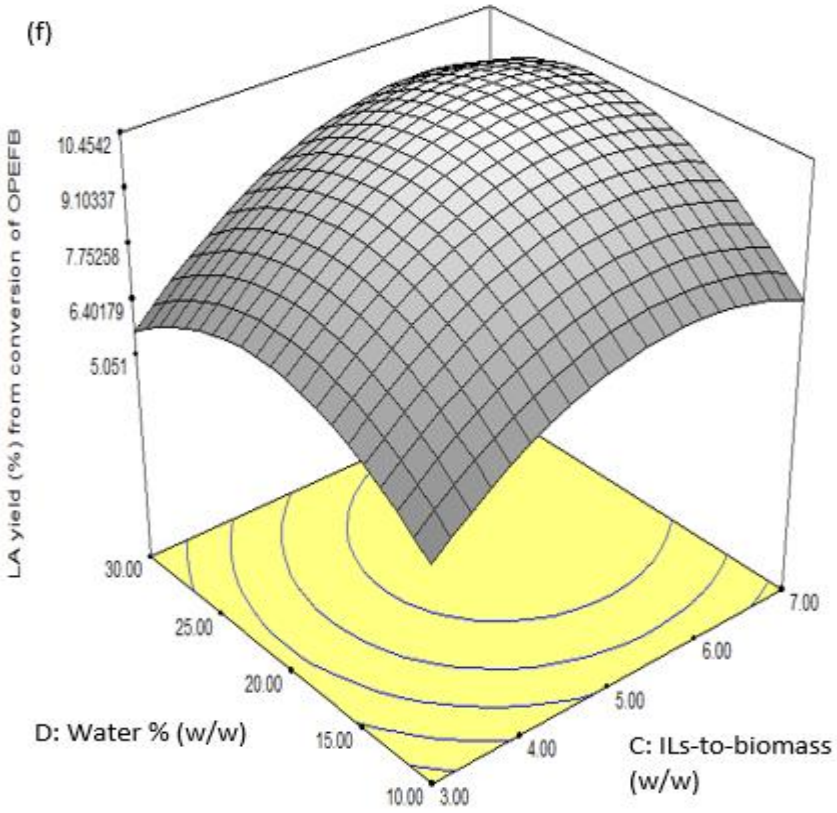
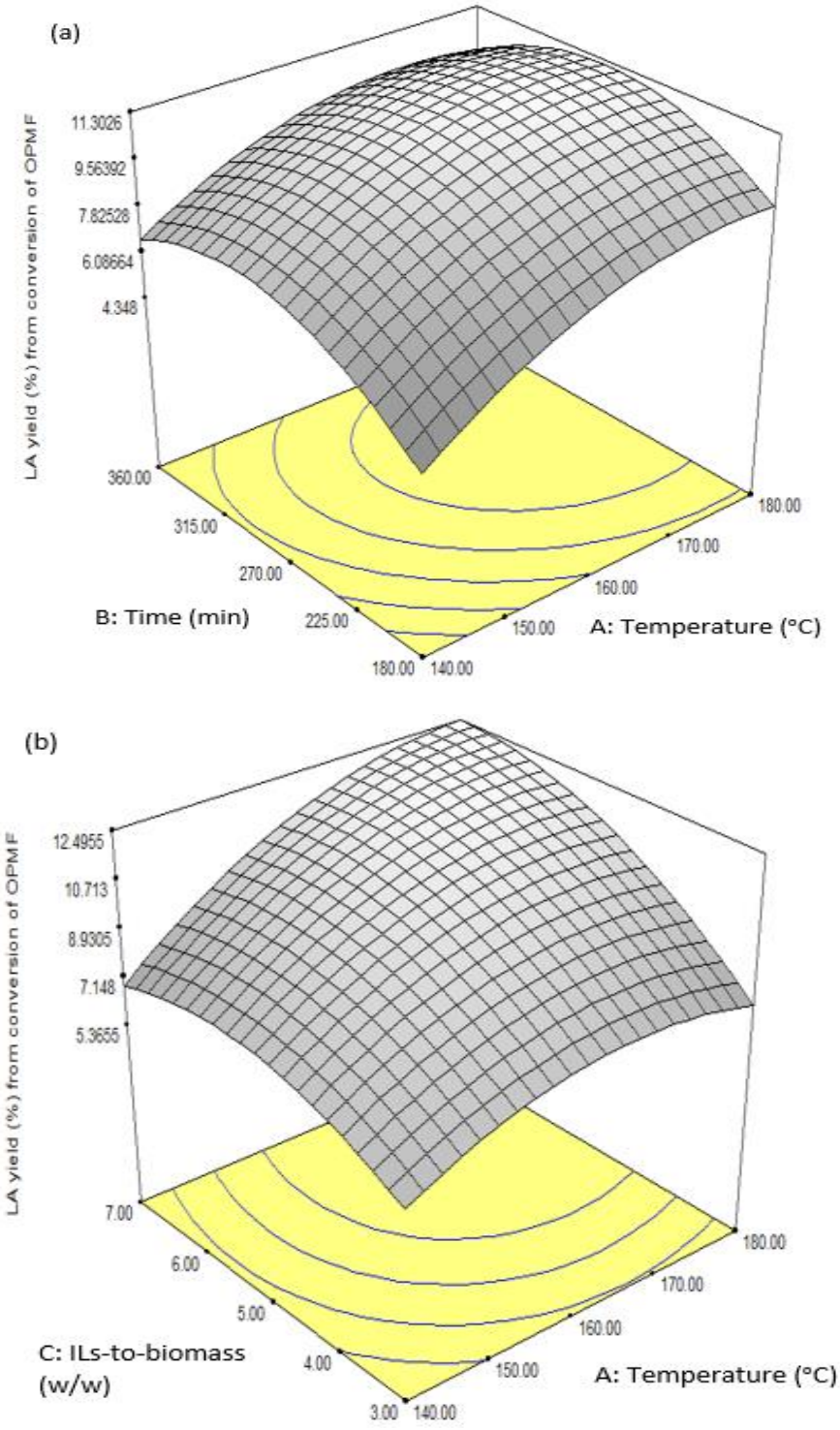
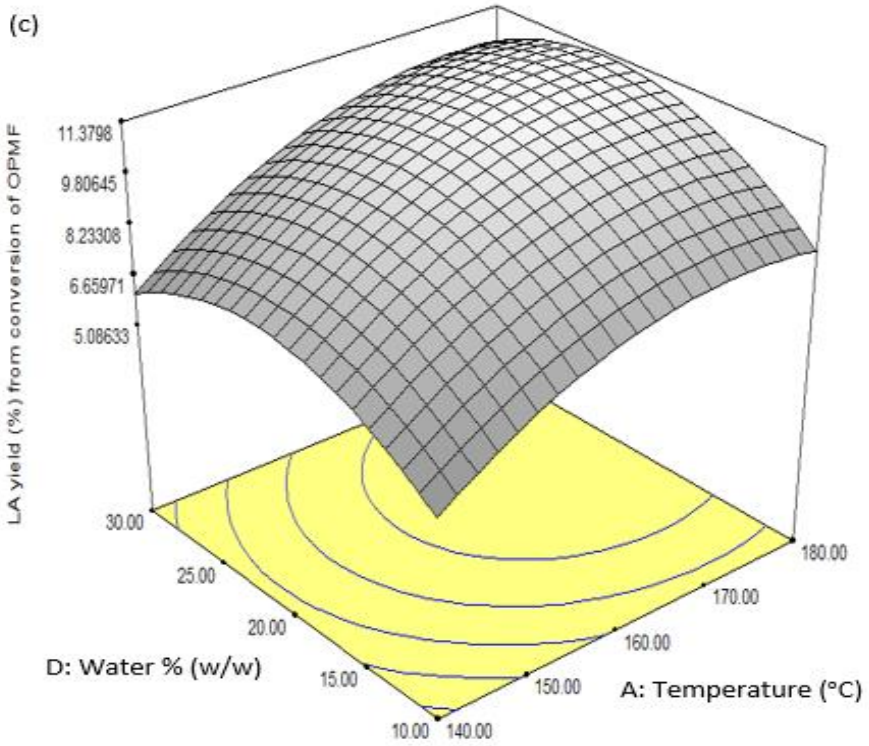
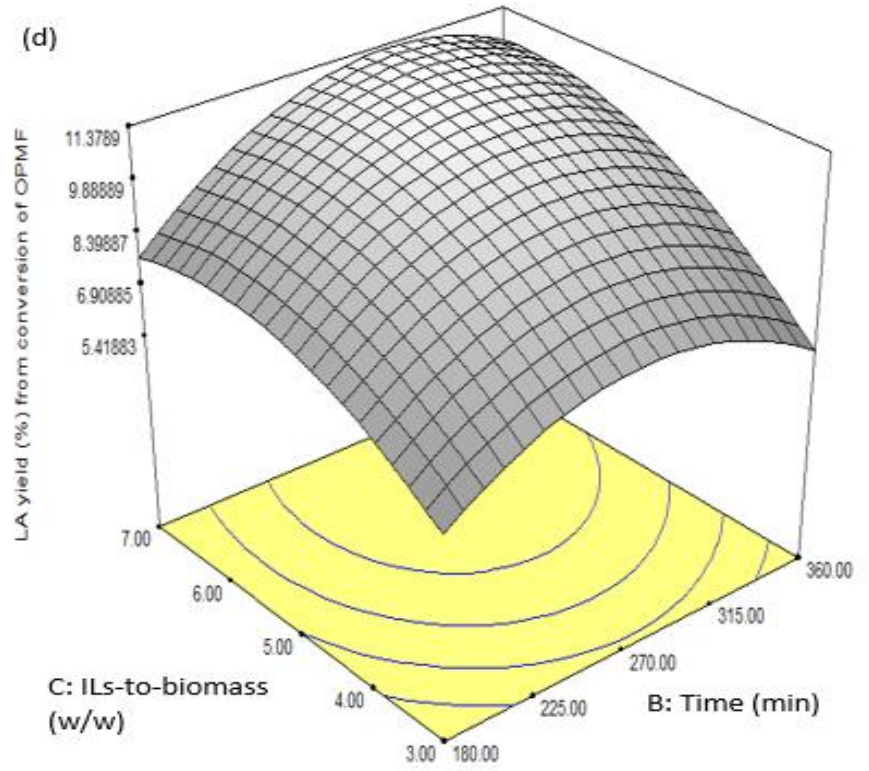
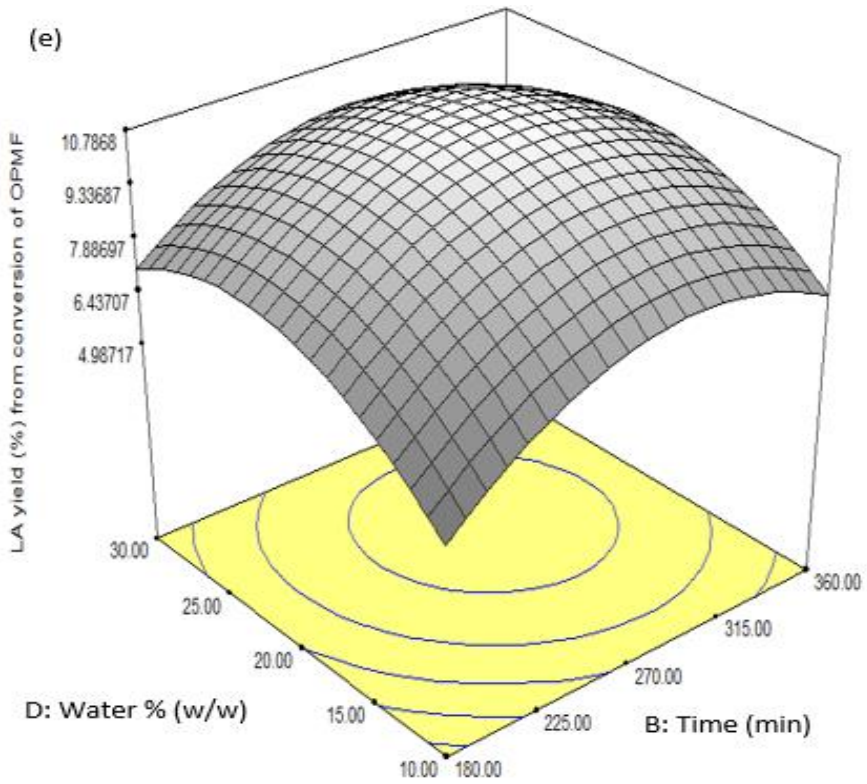

LA yield (%) from conversion of OPEFB
10.4542
9.10337
7.75258
6.40179
5.051
30.00
25.00
20.00
15.00
10.00
D: Water % (w/w)
3.00
4.00
5.00
6.00
7.00
C: ILs-to-biomass (w/w)

**Figure 5.2** Corresponding response surface and contour plots for LA yield from OPEFB conversion ($Y_1$), based on (a) temperature and time; (b) temperature and ILs-to-biomass ratio; (c) temperature and water; (d) time and ILs-to-biomass ratio; (e) time and water; and (f) ILs-to-biomass ratio and water.




(c)
LA yield (%) from conversion of OPMF
11.3798
9.80645
8.23308
6.65971
5.08633
30.00
25.00
20.00
15.00
10.00
D: Water % (w/w)
140.00
150.00
160.00
170.00
180.00
A: Temperature (°C)


(d)
LA yield (%) from conversion of OPMF
11.3789
9.88889
8.39887
6.90885
5.41883
7.00
6.00
5.00
4.00
3.00
C: ILs-to-biomass (w/w)
180.00
225.00
270.00
315.00
360.00
B: Time (min)


(e)
LA yield (%) from conversion of OPMF
10.7868
9.33687
7.88697
6.43707
4.98717
30.00
25.00
20.00
15.00
10.00
D: Water % (w/w)
180.00
225.00
270.00
315.00
360.00
B: Time (min)

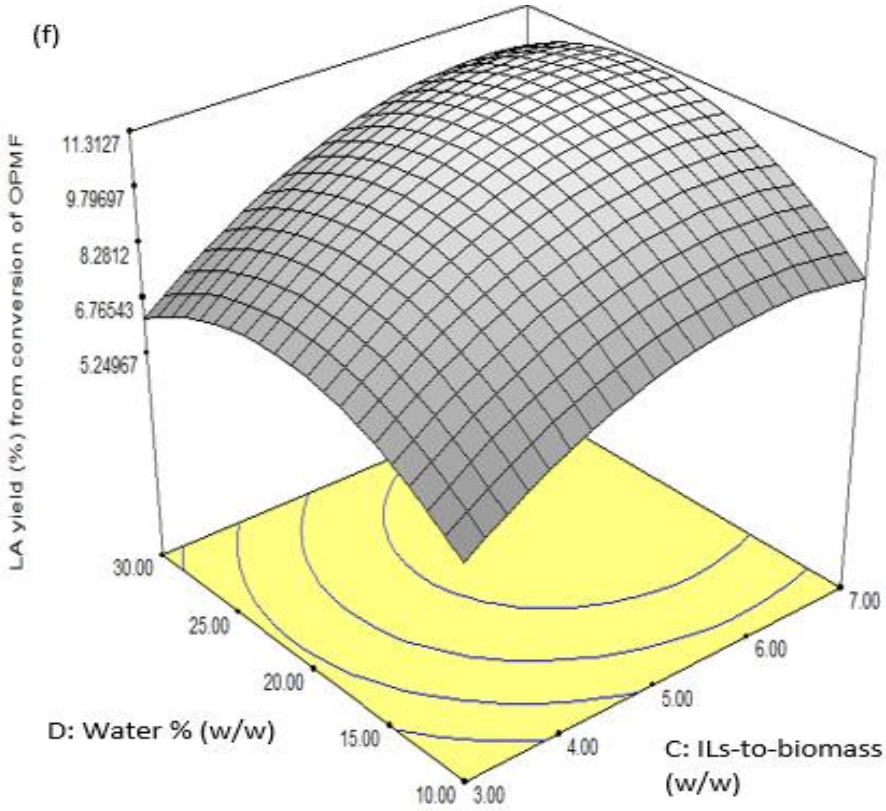

(f)
LA yield (%) from conversion of OPMF
11.3127
9.79697
8.2812
6.76543
5.24967
30.00
25.00
20.00
15.00
10.00
D: Water % (w/w)
3.00
4.00
5.00
6.00
7.00
C: ILs-to-biomass (w/w)

**Figure 5.3** Corresponding response surface and contour plots for LA yield from OPMF conversion ($Y_2$), based on (a) temperature and time; (b) temperature and ILs-to-biomass ratio; (c) temperature and water; (d) time and ILs-to-biomass ratio; (e) time and water; and (f) ILs-to-biomass ratio and water.

**Figure 5.2 (a)** and **5.3 (a)** show that LA yields were enhanced gradually along with an increase in reaction temperature and time, until the optimum conditions were reached. Reaction temperature and time are important factors that affect the destruction of hydrogen bonds in the cellulose network of the lignocellulosic biomass [85]. The catalytic system was favoured at higher temperature as it was easier to overcome the activation energy of the reaction. Higher temperature at a suitable reaction time frame theoretically gives a better turnover synthesis with significant LA yields as it highly disrupts the rigid structure of lignocellulosic materials [286] whereby atoms donate or receive electrons more readily. Increasing temperature decreases the viscosity in the catalytic system, accelerates the mass transfer and thus enhance the rate of reaction and the efficiency of conversion [64]. However, LA yields decreased when the reaction temperature was further increased to above an optimum point, implying that the unwanted side reactions might have occurred [85]. For instance, the sugar monomers of the biomass components particularly hemicellulose could be converted into furfural and humin at temperature exceeding the optimum [287]. Meanwhile, an adequate reaction time was essential for significant production of LA. At milder temperatures of <180°C, LA yields were increased with prolonged reaction times, whilst at elevated temperature of >180°C, the reversed trend was observed. Similarly, an excessive

reaction time could lead to the formation of by-products [288] due to the more rapid by-products reactions than the generation of LA [77]. This is owing to the prolonged reaction time promoting aldol condensation, etherification reactions, nucleophilic attack from 5-HMF and aggregation effects leading to the formation of insoluble polymers, especially at high 5-HMF yield [289]. These by-products subsequently could limit the interactions of reaction species with ILs where no substrate and product can form or migrate in and out of the ILs sites.

**Figure 5.2 (b)** and **5.3 (b)** show that the interaction between reaction temperature and loading of ILs-to-biomass ratio played a significant role in LA yields. In addition to being a catalyst, ILs could serve as an excellent solvent which enhance the mass transfer for the reaction to be viable. The Bronsted acidity developed by [HMIM][$HSO_4$] could facilitate the rapid depolymerisation of biomass, in the same way as Bronsted acidic based SFILs [196]. Nonetheless, when a ILs loading exceeds the optimum point, the viscosity of the reaction mixture increases thereby impeding the contact between the reactants [219]. This favours the formation of undesirable side products especially when the reducing sugars are degraded prior to the production of LA [216]. This result was supported from the findings of a preliminary work [78], where excess ILs loadings did not further convert 5-HMF to LA. This could be due to 5-HMF being an unstable molecule which easily condenses. Therefore, together with sugars and sugar degradation products, they may turn into black insoluble charred materials, so called "humins", especially at harsh reaction conditions, i.e. extremely high temperature of >190°C and prolonged reaction time of > 5h [44]. This restrained them from dehydrating into LA. Noteworthy, the interaction between loadings of ILs-to biomass ratio and reaction temperature was the most

significant among all interactions terms (**Table 5.4**), which markedly contributed to the catalytic reaction of LA production.

**Figure 5.2 (d)** and **5.3 (d)** demonstrate the interaction between reaction time and loading of ILs-to-biomass ratio. A limited amount of ILs with a prolonged reaction time favoured the gradual conversion of biomass to LA. This observation was in agreement with the use of homogenous acid catalysts for the conversions [16], [290]. However, certain unwanted products, i.e. humins, would be formed when the reaction was continued for too long, leading to a drop in LA yields. This result was in accordance with the work reported by Ramli and Amin [7]. Conversely, the surge of biomass loading in the catalytic system caused a decrease in LA yields, as the availability of ILs catalytic sites decreased [66]. Hence, this scenario would boost the probability of reactive intermediate compounds such as glucose, fructose and 5-HMF to collide with each other and enhance cross-polymerisation for undesired side products formation.

**Figure 5.2 (c, e, f)** and **5.3 (c, e, f)** illustrate the elliptical nature of the contour plots for water with reaction temperature, reaction time and loading of ILs-to-biomass ratio, respectively. The quadratic effect of water with all the three interactions on the responses suggested that neither insufficient nor excessive water in the catalytic system favoured the LA production. A small amount of water is dissolved with the ILs in the catalytic system to reduce the viscosity of ILs. This is because the high viscosity of ILs limits the ion-dipole interaction between catalyst and substrate [291], which can reduce the catalytic activity. Addition of water in the catalytic system increases the solubility of biomass and catalysts as well as promote the depolymerisation reaction and mass transfer

[292]. Moreover, as the dosage of water increases, the 5-HMF rehydration occurs progressively thus leading to higher LA formations. However, excessive water causes numerous drawbacks as follows: (a) water molecules would form hydrogen bonding with biomass and interact with ILs acidic sites, preventing them from functioning [85], (b) excessive water dilutes ILs and affects their purity [293], (c) excessive water encourages the reversed hydrolysis reaction, promoting the formation of undesirable products [86], and (d) water tends to precipitate out the dissolved biomass from participating in the catalytic reaction [85]. Conversely, a scarce amount of water gives a high viscous reaction mixture which results in poor catalytic efficiency of IL and decreases the mass transfer rate and may result in the occurrence of the rehydration reaction [294]. Herbst and Janiak [289] further reported that at low amounts of water, increasing the concentration of glucose substrate did not further enhance the 5-HMF yield significantly and thus reduced the subsequent LA yield. Hence, insufficient or excessive water should be avoided in the catalytic system for the synthesis of LA. In brief, this study proved that an appropriate amount of water is crucial for the catalytic system of LA production.

#### 5.3.1.3 Optimisation and validation

The process variables were optimised by using the numerical optimisation method. At the optimum conditions of 177°C in 4.8 h, with ILs-to-biomass ratio of 6.6:1 (w/w) and 22.7% (w/w) of water, the LA yields of 11.8% and 12.8% were achieved for both $Y_1$ (conversion from OPEFB ) and $Y_2$ (conversion from OPMF), respectively. **Table 5.5** presents a comparison

between the simulated and experimental results. The obtained experimental results were in reasonable agreement with the predicted values. The model was validated with errors less than 5%.

**Table 5.5** Optimisation and validation for LA yields.

| Experiment | Temp (°C) | Time (min) | ILs-to-biomass ratio (w/w) | Water %(w/w) | Responses (%) | | Error[a] (%) |
|---|---|---|---|---|---|---|---|
| | | | | | $Y_1$ | $Y_2$ | |
| CCD | 177 | 289 | 6.6:1 | 22.7 | 11.8 | 12.8 | $Y_1$: 4.5 |
| Validation (Trial 1) | 177 | 289 | 6.6:1 | 22.7 | 11.1 | 11.9 | |
| Validation (Trial 2) | 177 | 289 | 6.6:1 | 22.7 | 12.1 | 13.3 | |
| Validation (Trial 3) | 177 | 289 | 6.6:1 | 22.7 | 10.7 | 11.7 | |
| Validation[b] | 177 | 289 | 6.6:1 | 22.7 | 11.3 | 12.3 | $Y_2$: 4.4 |

[a]Error $= \left| \frac{\text{Validation result} - \text{CCD result}}{\text{CCD result}} \text{ x } 100\% \right|$

[b]Validation experiments were conducted thrice, and the averages of the responses are presented.

### 5.3.2 Addition of Lewis acidic $InCl_3$ coupled with [HMIM][$HSO_4$]

**Figure 5.4** shows that the addition of an optimum dosage of 0.15 mmol $InCl_3$ was able to boost the LA yields by additional 5.5-6% as compared to the sole optimised [HMIM][$HSO_4$] catalytic system, which gave maximum LA yields of 17.7% and 18.4% for the conversions from OPEFB and OPMF biomass, respectively. Similarly, the corresponding LA efficiencies were 74.1% and 86.4%, for the conversions from OPEFB and OPMF biomass, respectively. Further increase of $InCl_3$ dosage did not give a significant increase in LA yield as it reached a plateau.

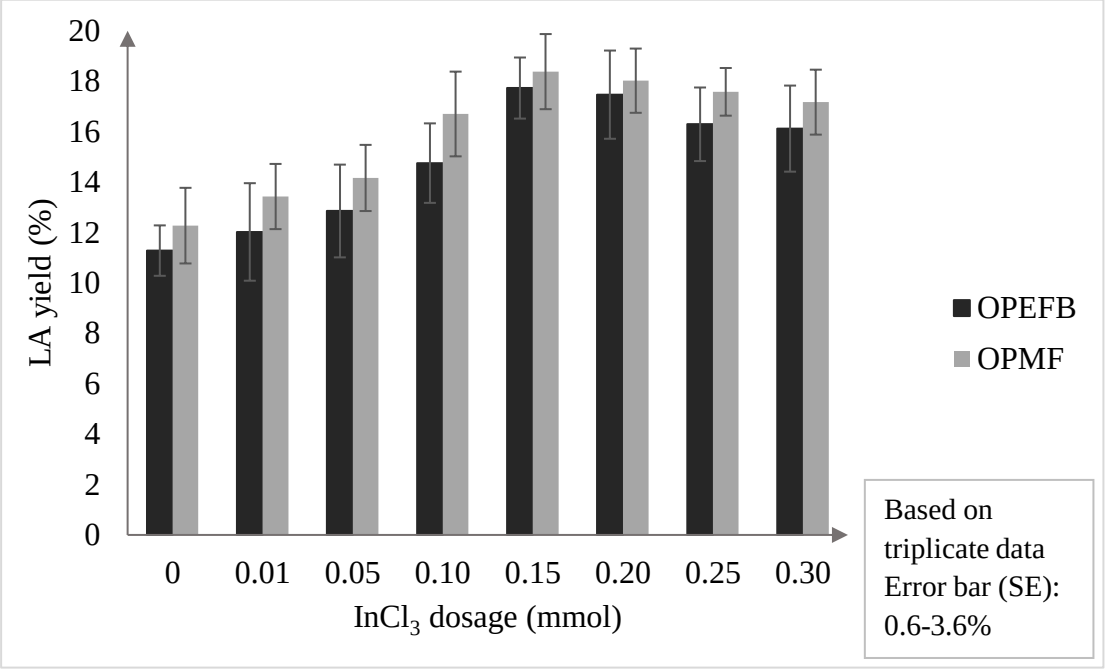



**Figure 5.4** Effect of $InCl_3$ dosage on LA yields from conversions of (a) OPEFB and (b) OPMF biomass via [HMIM][$HSO_4$]. (Depolymerisation: ILs-to-biomass ratio of 6.6:1 (w/w), 177°C, 4.8 h and 22.7% (w/w) water).

According to Li et al. [77], addition of $InCl_3$ weakens the glycosidic bonds of polysaccharides in biomass through binding with a glycosidic oxygen atom in a similar manner to protic acid. This enhances the hydrolysis of polysaccharides into monosaccharides. Likewise, Antonetti et al. [44] reported that although Bronsted acid sites play a greater role than Lewis acids in a catalytic reaction, solely BAILs in the reaction proceed very slowly under the Bronsted acid conditions. Isomerisation of glucose to fructose is commonly desirable for product formation and is enhanced in the presence of a Lewis acidic site via enediol form [222]. In the absence of a Lewis acidic site, this reaction proceeds very slow under the solely Bronsted acid conditions [44]. These lead to limited or even absence of formation of fructose from glucose, which suggests a different mechanism being involved [295]. Fructose consistently gives a significantly higher yield on a variety of acid catalysts as compared to other monosaccharides [260]. On the basis of these conversions, the results suggested that Lewis acid $InCl_3$ could serve as a co-catalyst that gives synergistic effect when combines with Bronsted acid sites ([HMIM][$HSO_4$]) for the conversion.

### 5.3.3 Physical properties of $InCl_3$-[HMIM][$HSO_4$]

The physical properties of $InCl_3$-[HMIM][$HSO_4$], i.e. density, viscosity, thermal stability and Hammett acidity were further analysed in order to present reliable data of this novel coupling ILs, in comparison with the other ILs studied in **Chapter 3**.

Noteworthy, $InCl_3$-[HMIM][$HSO_4$] had the highest density and lowest viscosity among the ILs studied at all temperatures, as shown in **Figure 5.5** and

**5.6**, respectively, alongside with the corresponding values listed in **Table 5.6**. This further suggested that in all cases, the density of the presence of Lewis acid $InCl_3$-ILs was higher than those without the Lewis acid analogues, foreseen to be the same case as in alkylnitrile ILs [269]. Incorporating the Lewis acidic group serves to increase the density of the ILs, which might favour separation from other solvents better, i.e. biphasic catalysis. Aside from that, adding in substituent groups (i.e. Lewis acid $InCl_3$) to the aromatic rings of ILs could reduce the viscosity, which might be due to steric hindrance from the substituent groups that prevents close associations between ions [275]. In this regard, being the least viscous, $InCl_3$-[HMIM][$HSO_4$] would favour the mass transfer rate during catalytic reactions and also easier handling [296].

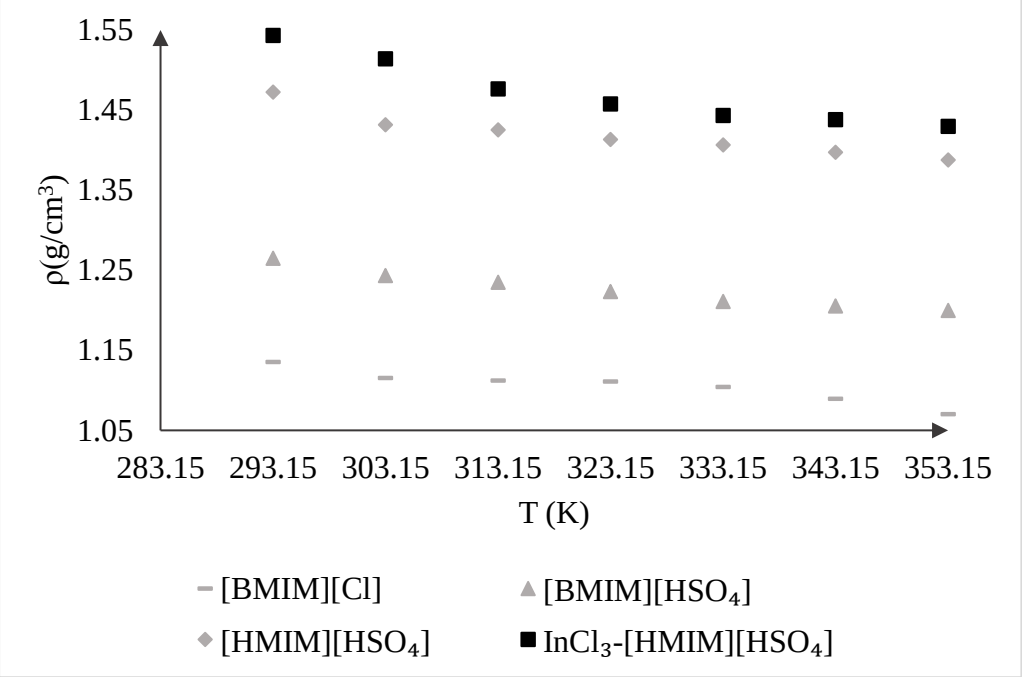



**Figure 5.5** Temperature effect of density of $InCl_3$-[HMIM][$HSO_4$] compared to other ILs without Lewis acid analogues.

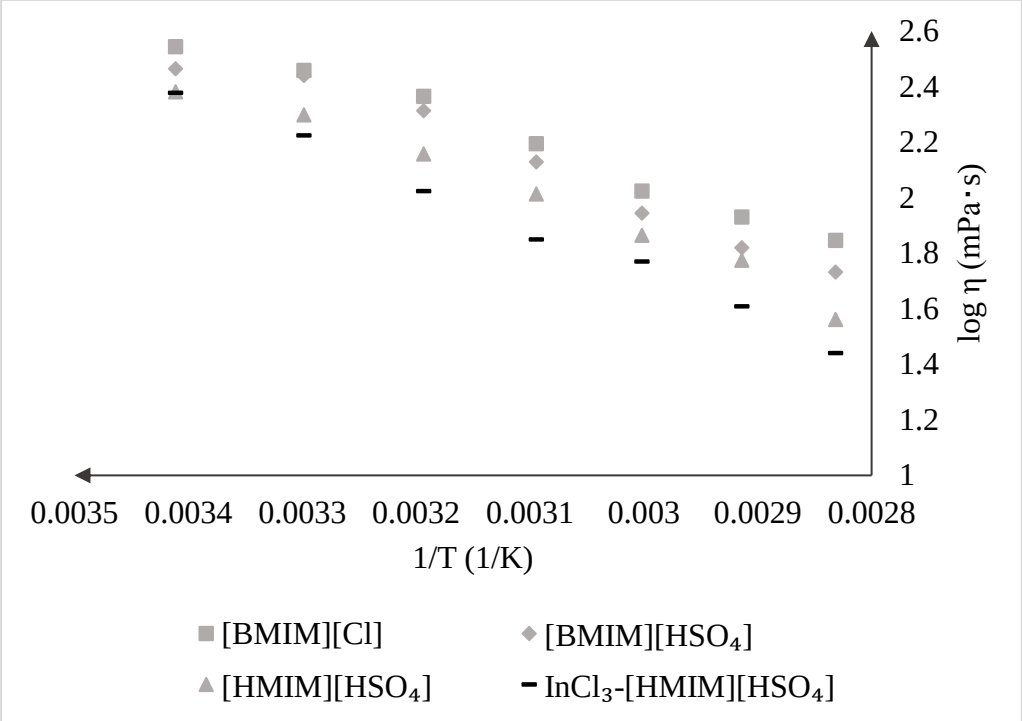



**Figure 5.6** Temperature effect of viscosity of $InCl_3$-[HMIM][$HSO_4$] compared to other ILs without Lewis acid analogues**.**

**Table 5.6** Density and viscosity of $InCl_3$-[HMIM][$HSO_4$] compared to other ILs without Lewis acid analogues at various temperatures.

| T/K | Density, ρ (g/cm$^3$) | Viscosity, η (mPa·s) |
|---|---|---|
| 293.15 | 1.5432 | 238.38 |
| 303.15 | 1.5141 | 167.73 |
| 313.15 | 1.4765 | 105.68 |
| 323.15 | 1.4577 | 70.67 |
| 333.15 | 1.4432 | 58.92 |
| 343.15 | 1.4381 | 40.56 |
| 353.15 | 1.4299 | 27.56 |

From the aspect of thermal stability, $InCl_3$-[HMIM][$HSO_4$] was among the most stable ILs in comparison to the other ILs studied (**Figure 5.7**). At the very final stage, the weight loss remained at 19.8%, signifying its highest stability. This further suggested that the presence of Lewis acid $InCl_3$ has increased its stability performance by strengthening the inter- and intramolecular hydrogen bonding between the $InCl_3$ and [HMIM][$HSO_4$]. In particular, $Cl^-$ anion forms a stronger hydrogen bond for the sake of Cl atom, much in the same way as in F atom, as reported by Aggarwal et al. [297]. This apparently lends some degree of attractiveness to this IL for high temperature applications.

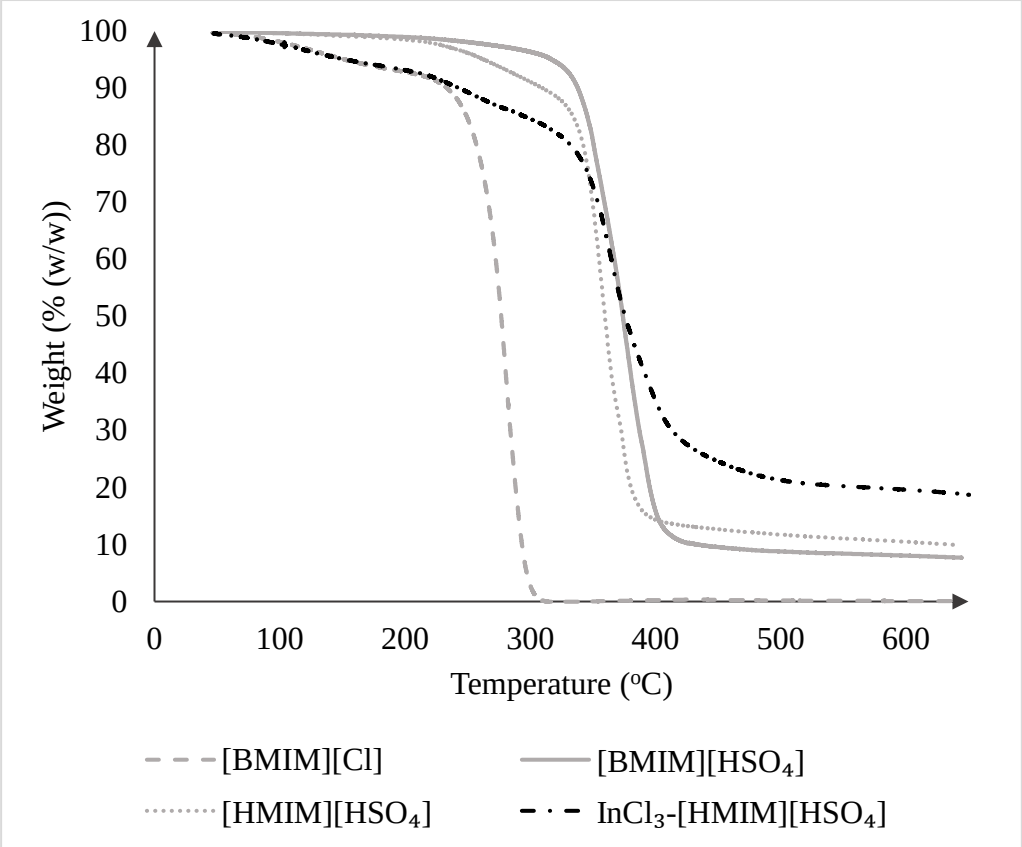



**Figure 5.7** Thermal analysis of the $InCl_3$-[HMIM][$HSO_4$] compared to other ILs without Lewis acid analogues.

As for the acidity of ILs evaluated by Hammett acidity function, $InCl_3$-[HMIM][$HSO_4$] exhibited the lowest $H_0$ value (1.10) in comparison to other ILs studied (**Table 5.7**). The additional Lewis acid $InCl_3$ coupled with [HMIM][$HSO_4$] further enhanced the acidity strength, mainly due to the coexistence of both Bronsted and Lewis acidic sites concurrently. Hence, this result further confirmed that $InCl_3$-[HMIM][$HSO_4$] would have better catalytic activity, since acidic strength plays a vital role for the conversion to be possible [53].

**Table 5.7** Hammett acidity function ($H_0$) data for $InCl_3$-[HMIM][$HSO_4$] compared to other ILs without Lewis acid analogues.

| ILs | $A_{max}$ | [*I*] (%) | $[IH]^+$ (%) | $H_0$ |
|---|---|---|---|---|
| 4-nitroaniline (Blank) | 0.989 | 100 | 0.0 | - |
| [BMIM][Cl] | 0.989 | 100 | 0.0 | - |
| [BMIM][$HSO_4$] | 0.737 | 73.7 | 26.3 | 1.42 |
| [HMIM][$HSO_4$] | 0.657 | 65.7 | 34.3 | 1.25 |
| $InCl_3$-[HMIM][$HSO_4$] | 0.577 | 57.7 | 42.3 | 1.10 |

## 5.4 Concluding Remarks

The present optimisation studies reported a new environmentally friendly coupling mixed acids $InCl_3$-[HMIM][$HSO_4$] catalytic system for the conversions of OPEFB and OPMF biomass to LA, by using a RSM based on a CCD approach. The ANOVA results indicated that both LA models ($Y_1$ and $Y_2$) were statistically significant. The lack of fit F-value for both responses were insignificant relative

to the pure error, indicating good fitting of the proposed models, and thus were reliable tools for predicting LA yields. The optimum conditions for the depolymerisation was achieved at a reaction temperature of 177°C in 4.8 h, with 0.15 mmol of $InCl_3$, 6.6:1 (w/w) of ILs-to-biomass ratio and 22.7% (w/w) of water content. The maximum LA yields were 17.7% and 18.4%, with the corresponding LA efficiencies of 74.1% and 86.4%, for the conversions from OPEFB and OPMF biomass, respectively. The synergistic effect of Lewis acid $InCl_3$ and Bronsted acid ([HMIM][$HSO_4$]) manifests an effective catalytic activity yield (+5.5-6%) as compared to the sole optimised [HMIM][$HSO_4$] catalytic system. $InCl_3$-[HMIM][$HSO_4$] also exhibited the highest density and lowest viscosity, as well as being the most stable with the strongest acidity property in comparison to the other ILs without Lewis acid analogues reported in **Chapter 3**. The results exhibited the potential of this new environmentally friendly coupling $InCl_3$-[HMIM][$HSO_4$] to serve as a greener dual solvent-catalyst in the production of LA from renewable oil palm biomass feedstock.

# Chapter 6

# Optimisation studies on the upgrading to ethyl levulinate

## 6.1 Introduction

This chapter focuses on the continuation study on the upgrading to EL in a two-step sequential reaction via one-pot production, i.e. depolymerisation to LA (**Chapter 5**), followed by the upgrading esterification to EL (**this Chapter**). Herein, statistical analysis and optimisation studies by using a RSM based on a CCD method on the esterification of LA to EL was further conducted. A preliminary parametric study on using $InCl_3$-[HMIM][$HSO_4$] catalytic system for the esterification of LA to EL was first conducted (Tiong et al. [78], refer to **Appendix 2**), in order to obtain the desired parametric range for the statistical analysis and optimisation studies. The determination on the ANOVA analysis, $R^2$, Fisher's F-test and P-value (probability) at 95% confidence level, followed by the optimisation studies method have been detailed in **Chapter 5.1**. Apart from the major LA and EL syntheses, the formation of by-products from the one-pot production were also discussed in-depth. Finally, the results of the present studies on LA and EL yields were critically compared with those reported in the literature.

## 6.2 Methodology

### 6.2.1 Materials

The preparation of oil palm biomass (OPEFB and OPMF) and chemicals involved have been reported in **Chapter 3.2.1** and **4.2.1**.

### 6.2.2 Biomass conversion reaction and products isolation

The experimental procedures of biomass conversion reactions, i.e. depolymerisation reaction into LA, then the subsequent upgrading esterification reaction to EL, followed by the subsequent products isolation, have been reported previously, as in **Chapter 4.2.2** and **4.2.3**, respectively.

### 6.2.3 Products analysis

EL content was determined by using a GC-MS (Perkin Elmer Clarus 680, USA), as described in **Chapter 4.2.4**. All the experiments were performed in triplicate. The standard errors of triplicate data obtained for all yields ranged within 0.6-3.4%. The calculation formula for the experimental yield of EL has been reported, as in **Eq. 4.1.** The theoretical yield and efficiency of EL were calculated by **Eq. 6.1** and **6.2**, respectively.

$$\text{Theoretical EL yield (\%)} = \frac{\text{Cellulose content in biomass (g) x } 0.89}{\text{Initial biomass loading (g)}} \text{ x } 100\% \quad (6.1)$$

where $\frac{\text{Molecular weight of EL (g } mol^{-1})}{\text{Molecular weight of cellulose (g } mol^{-1})} = \frac{144}{162} = 0.89$

and the percentage of cellulose content in OPEFB and OPMF biomass were adapted from **Table 3.1**.

$$\text{EL efficiency (\%)} = \frac{\text{EL yield (\%)}}{\text{Theoretical EL yield (\%)}} \text{ x } 100\% \quad (6.2)$$

where the efficiency refers to the efficiency of biomass conversion to EL calculated based on cellulose content.

### 6.2.4 Statistical analysis

For this subsequent upgrading esterification of LA to EL, a similar statistical analysis approach was performed, i.e. a RSM based on a CCD method, which has been described in **Chapter 5.2.4**. As such, in the esterification reaction, three independent variables were considered, i.e. reaction temperature, reaction time and volume of ethanol to substrate ratio, coded as E, F and G, respectively. The selection of the ranges was conducted based on the results obtained from preliminary studies (Tiong et al. [78], refer to **Appendix 2**). The variables and the experimental domain in the design are presented in **Table 6.1**.

**Table 6.1** Range of independent variables and experimental levels (EL yields).

| Factors | Symbol | Levels | | | | |
|---|---|---|---|---|---|---|
| | | -α | -1 | 0 | +1 | +α |
| Reaction temperature (°C) | E | 36 | 60 | 95 | 130 | 154 |
| Reaction time (min) | F | 176 | 360 | 630 | 900 | 1084 |
| Ethanol to substrate ratio (v/v) | G | 1:1 | 3:1 | 6:1 | 9:1 | 11:1 |

The CCD consists of 8 factorial points, 6 axial points and 6 replicates at the centre points which translate into a total of 20 experiments generated according to **Eq. 6.3**. The quadratic equation model for predicting the optimal conditions can be fitted to a second-degree polynomial design, similar to the previous chapter, as expressed in **Eq. 5.5**.

$$N = 2^n + 2n + n_c = 2^3 + 2(3) + 6 = 20 \quad (6.3)$$

where N is the number of experiment, n is the number of factor and $n_c$ is the number of replicate at the centre point.

The subsequent ANOVA, correlation coefficient ($R^2$), Fisher's F-test and P-value (probability) at 95% confidence level were further assessed, as described in **Chapter 5.2.4**. The three-dimensional plots and their respective contour plots were obtained for the esterification of LA to EL based on the interactive effects of independent variables at the five levels. Finally, the numerical evaluation for maximum EL yield was the same as those reported for LA yield, as in **Chapter 5.2.4**.

## 6.3 Results and Discussion

### 6.3.1 Statistical analysis

#### 6.3.1.1 RSM based on CCD method

**Table 6.2** shows a series of experiments conducted for the desired responses (EL yields) from both OPEFB ($Y_3$) and OPMF ($Y_4$) biomass conversions. The predicted results were assessed by considering the following variables, i.e. reaction temperature (E), reaction time (F) and volume of ethanol to substrate ratio (G), and calculated based on the empirical second-degree polynomial model as shown in **Eq. 6.4** and **6.5** below.

$$Y_3 = 18.80 + 1.04A + 0.89B + 1.98C - 2.47A^2 - 1.72B^2 - 2.25C^2 + 1.75AB - 0.50AC - 0.28BC \quad (6.4)$$

$$Y_4 = 20.16 + 1.25A + 1.32B + 2.04C - 2.56A^2 - 2.12B^2 - 2.32C^2 + 0.78AB - 0.75AC + 0.22BC \quad (6.5)$$

**Table 6.2** CCD experimental design matrix and responses (EL yields).

| Entry | Point type | Independent process parameters levels | | | Responses (%) | |
|---|---|---|---|---|---|---|
| | | Temp (°C), E | Time (min), F | Ethanol-to-substrate ratio (v/v), G | $Y_1$ | $Y_2$ |
| 1 | Centre | 95 (0) | 630 (0) | 6:1 (0) | 20.4 | 21.8 |
| 2 | Centre | 95 (0) | 630 (0) | 6:1 (0) | 22.0 | 20.2 |
| 3 | Centre | 95 (0) | 630 (0) | 6:1 (0) | 19.2 | 20.9 |
| 4 | Centre | 95 (0) | 630 (0) | 6:1 (0) | 18.9 | 22.3 |
| 5 | Centre | 95 (0) | 630 (0) | 6:1 (0) | 19.2 | 19.1 |
| 6 | Centre | 95 (0) | 630 (0) | 6:1 (0) | 17.3 | 20.9 |
| 7 | Axial | 95 (0) | 175.92 (-α) | 6:1 (0) | 8.9 | 8.2 |
| 8 | Axial | 153.86 (+α) | 630 (0) | 6:1 (0) | 11.5 | 12.8 |
| 9 | Axial | 95 (0) | 1084.08 (+α) | 6:1 (0) | 13.9 | 14.9 |
| 10 | Axial | 95 (0) | 630 (0) | 0.95:1 (-α) | 6.1 | 7.3 |
| 11 | Axial | 95 (0) | 630 (0) | 11.05:1 (+α) | 13.7 | 14.7 |
| 12 | Axial | 36.14 (-α) | 630 (0) | 6:1 (0) | 7.1 | 7.8 |
| 13 | Factorial | 130 (+1) | 360 (-1) | 9:1 (+1) | 14.8 | 16.2 |
| 14 | Factorial | 130 (+1) | 900 (+1) | 3:1 (-1) | 16.7 | 17.1 |

| | | | | | | |
|---|---|---|---|---|---|---|
| 15 | Factorial | 60 (-1) | 900 (+1) | 3:1 (-1) | 10.7 | 11.5 |
| 16 | Factorial | 130 (+1) | 900 (+1) | 9:1 (+1) | 18.9 | 19.5 |
| 17 | Factorial | 60 (-1) | 360 (-1) | 3:1 (-1) | 12.5 | 12.2 |
| 18 | Factorial | 60 (-1) | 360 (-1) | 9:1 (+1) | 17.8 | 16.7 |
| 19 | Factorial | 130 (+1) | 360 (-1) | 3:1 (-1) | 11.9 | 13.9 |
| 20 | Factorial | 60 (-1) | 900 (+1) | 9:1 (+1) | 14.5 | 17.7 |

ANOVA analysis for each response model was performed to establish its significance and nature of interactions between the process variables, as shown in **Table 6.3**.

**Table 6.3** ANOVA results for response parameters of EL yields.

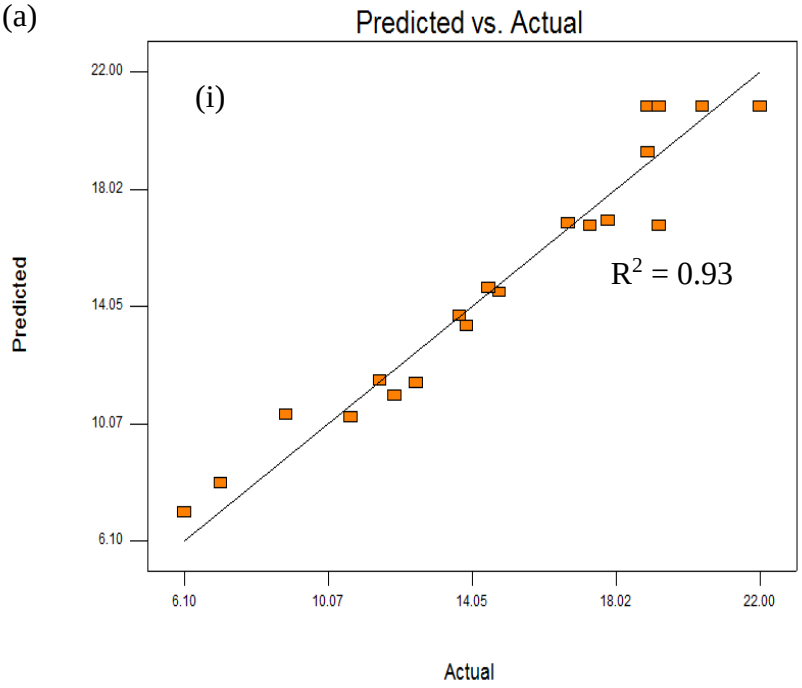
| Response | Model F-value | P | PLOF | $R^2$ | Adj. $R^2$ | Pred. $R^2$ | AP | SD | PRESS |
|---|---|---|---|---|---|---|---|---|---|
| $Y_3$ | 12.91 | < 0.0001 | 0.38 | 0.93 | 0.86 | 0.66 | 12.01 | 1.54 | 100.49 |
| $Y_4$ | 13.32 | < 0.0001 | 0.12 | 0.93 | 0.86 | 0.64 | 11.74 | 1.61 | 120.30 |

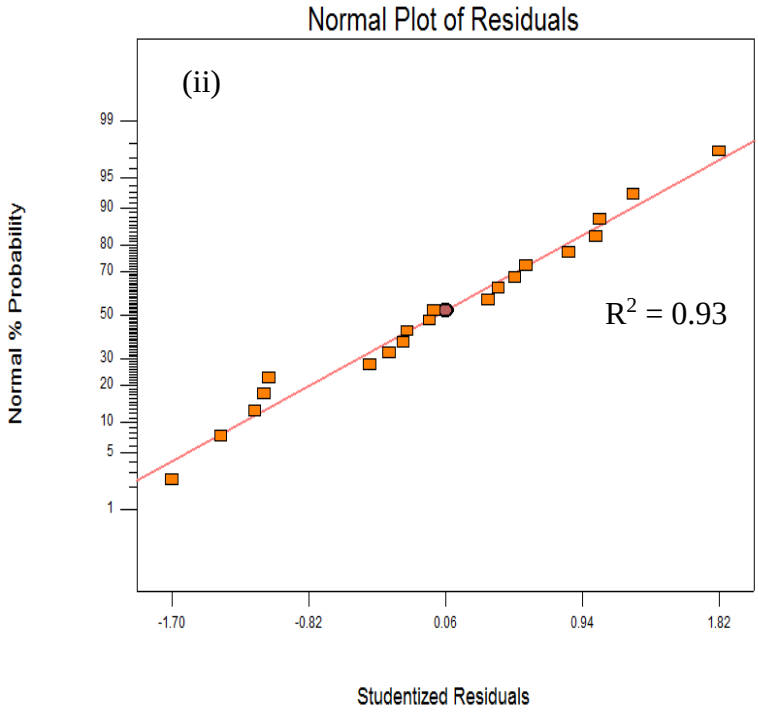
P: probability of error; PLOF: probability of lack of fit; Adj. $R^2$: adjusted $R^2$; Pred. $R^2$: predicted $R^2$; AP: adequate precision; SD: standard deviation; PRESS: predicted residual error sum of squares.

*Detailed data on the ANOVA regression model of EL yields (refer to **Appendix 5b**).

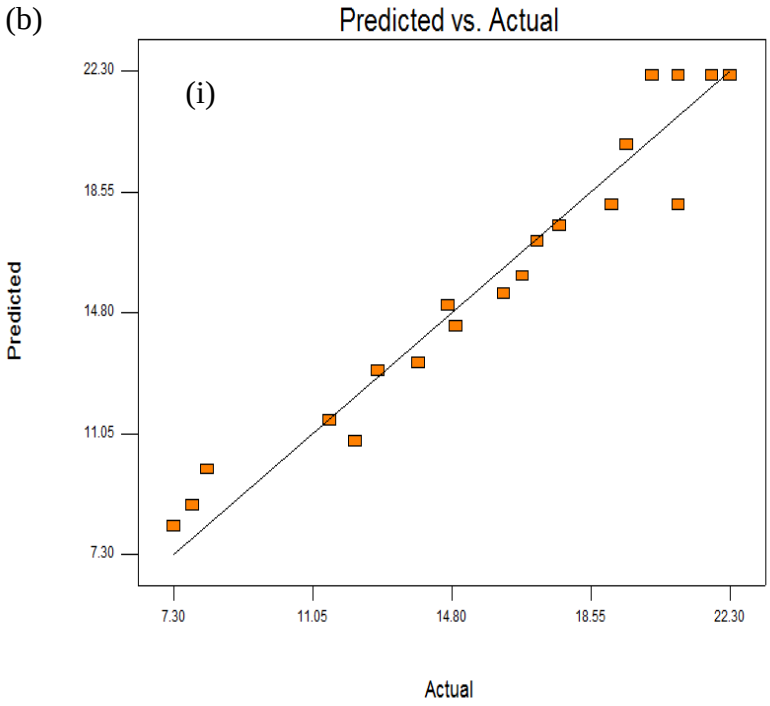
The results indicate that both models were statistically significant with <0.01% chance that the models F-values could occur due to noise. High $R^2$ of 0.93 for both $Y_3$ and $Y_4$ indicated that 93% of the total variability could be explained by the regression models. For further adequacy evaluations of the quadratic models in fitting the experimental data, various types of diagnostic plots are presented accordingly in **Figure 6.1**. The results trend was in accordance with the depolymerisation reaction, which has been discussed in **Chapter 5.3.1.1**.

(a)

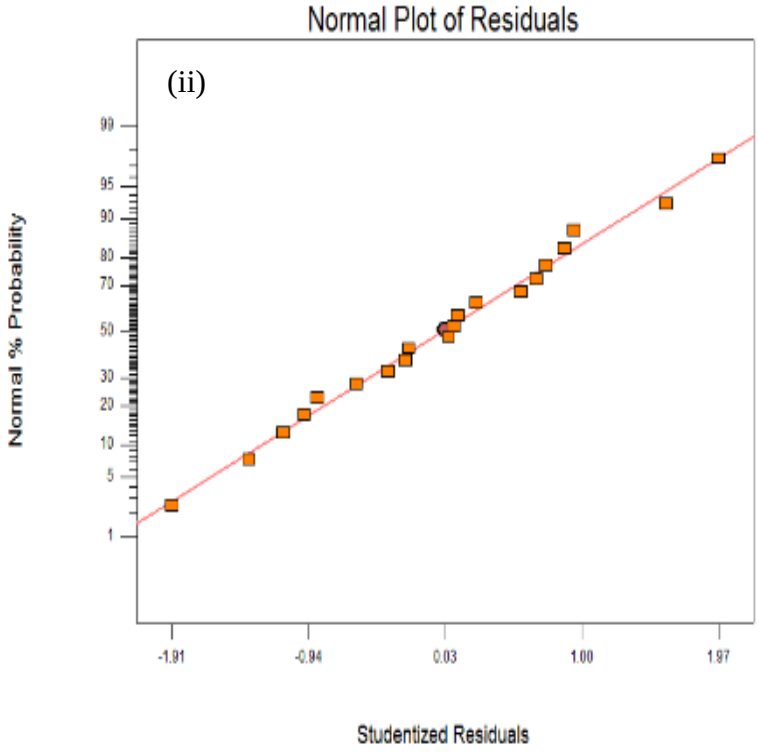

Predicted vs. Actual
(i)
$R^2$ = 0.93
Predicted
Actual
22.00
18.02
14.05
10.07
6.10
6.10
10.07
14.05
18.02
22.00


Normal Plot of Residuals
(ii)
$R^2$ = 0.93
Normal % Probability
Studentized Residuals
99
95
90
80
70
50
30
20
10
5
1
-1.70
-0.82
0.06
0.94
1.82

(b)


Predicted vs. Actual
(i)
Predicted
22.30
18.55
14.80
11.05
7.30
7.30
11.05
14.80
18.55
22.30
Actual

\


Normal Plot of Residuals
(ii)
Normal % Probability
99
95
90
80
70
50
30
20
10
5
1
-1.91
-0.94
0.03
1.00
1.97
Studentized Residuals

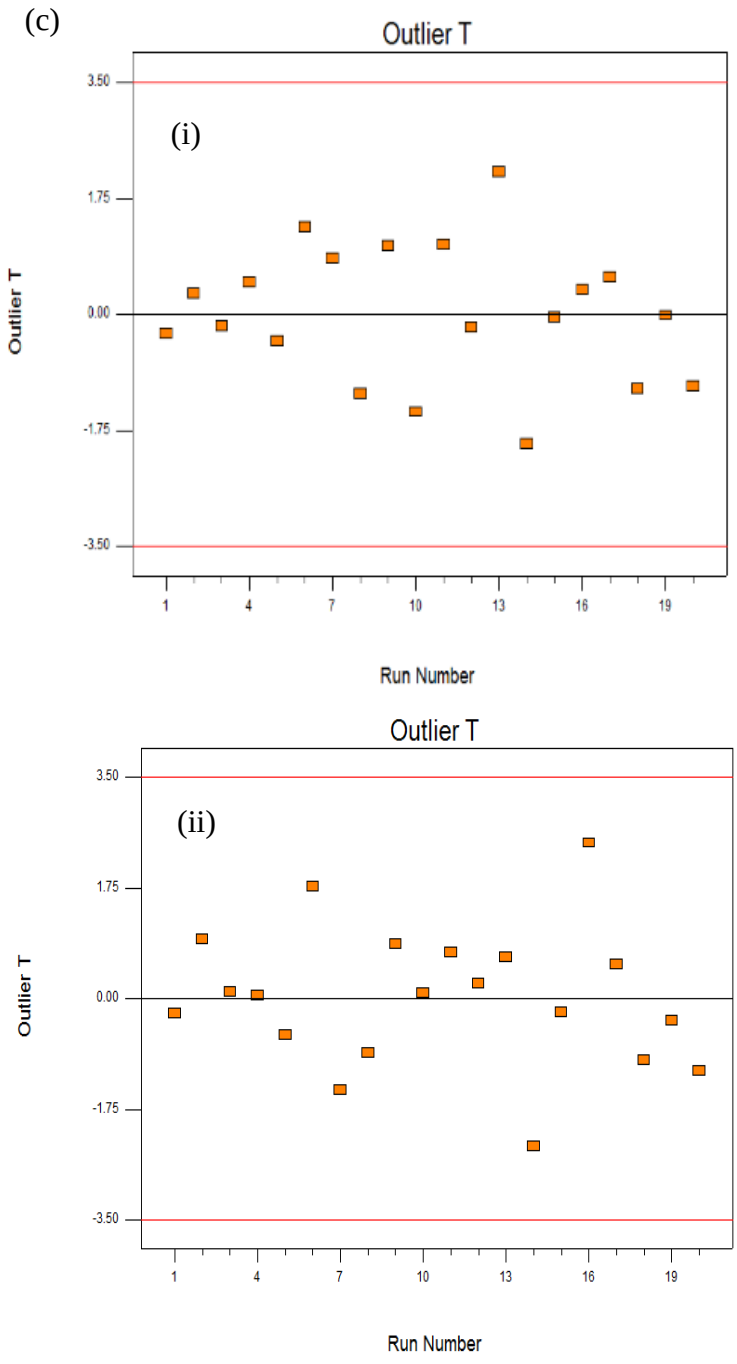



**Figure 6.1** Diagnostic of models (a) Relationship between predicted and actual values, (b) Normal % probability versus studentized residuals, and (c) Outliers T versus run number of EL yields for the conversions of (i) OPEFB ($Y_3$) and (ii) OPMF ($Y_4$).

### 6.3.1.2 Effect and interaction of variables on EL yields

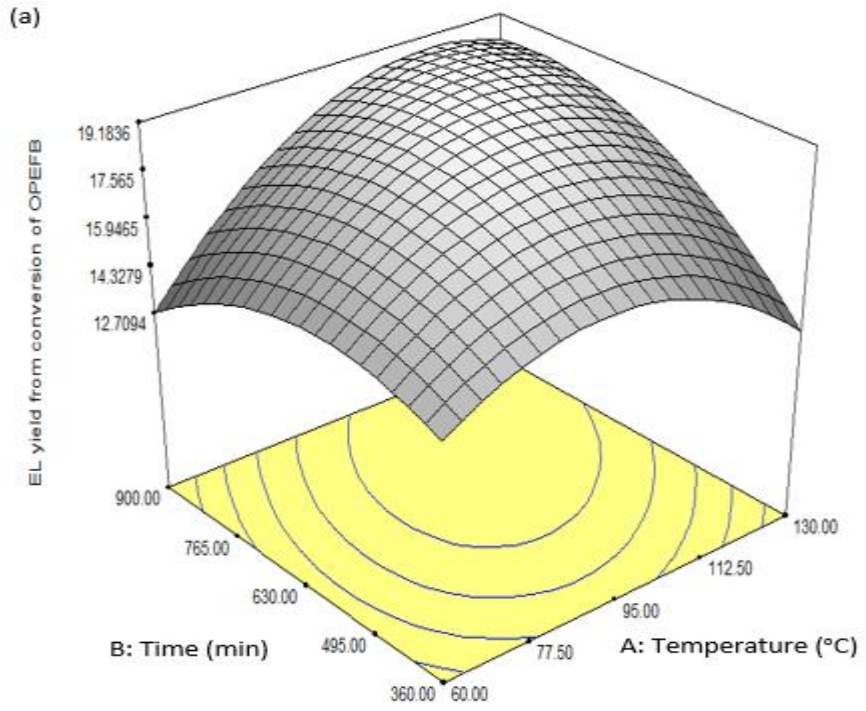
**Table 6.4** shows the variable effects of the factors and associated p-values for the two responses. For both responses, the percentage of EL yields for $Y_3$ and $Y_4$ were significantly affected by both the linear terms and quadratic terms of all variables tested, i.e. reaction temperature (E), reaction time (F) and volume of ethanol to substrate ratio (G). Noteworthy, the interaction terms of EF significantly enhanced the EL yields.

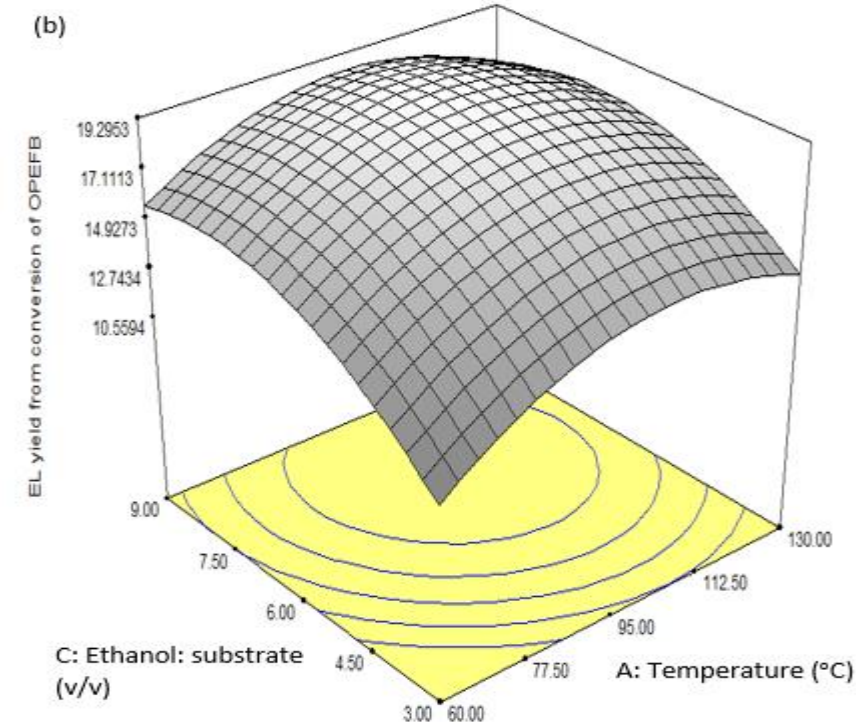
**Table 6.4** F-values and associated p-values for the responses of $Y_3$ (conversion from OPEFB) and $Y_4$ (conversion from OPMF).

| Relationship | | Factor | Responses | | | |
|---|---|---|---|---|---|---|
| | | | $Y_1$ | | $Y_2$ | |
| | | | F-value | p-value | F-value | p-value |
| Main effects | Linear | E | 6.19 | 0.0345* | 8.22 | 0.0186* |
| | | F | 4.58 | 0.0610 | 9.27 | 0.0139* |
| | | G | 22.37 | 0.0011* | 22.02 | 0.0011* |
| Interactions | Pure quadratic | $E^2$ | 36.77 | 0.0002* | 36.69 | 0.0002* |
| | | $F^2$ | 17.97 | 0.0022* | 25.13 | 0.0007* |
| | | $G^2$ | 30.72 | 0.0004* | 29.94 | 0.0004* |
| | Cross product | EF | 10.28 | 0.0107* | 1.86 | 0.0154* |
| | | EG | 0.84 | 0.3835 | 1.75 | 0.2191 |
| | | FG | 0.25 | 0.6265 | 0.16 | 0.7011 |

*Significant at 5% (p-value)

**Figure 6.2** and **6.3** show the interactions of the response surface and contour plots among the three variables on EL yields. The evaluation of these combined effects on the corresponding response has been explained in **Chapter 5.3.1.2**.



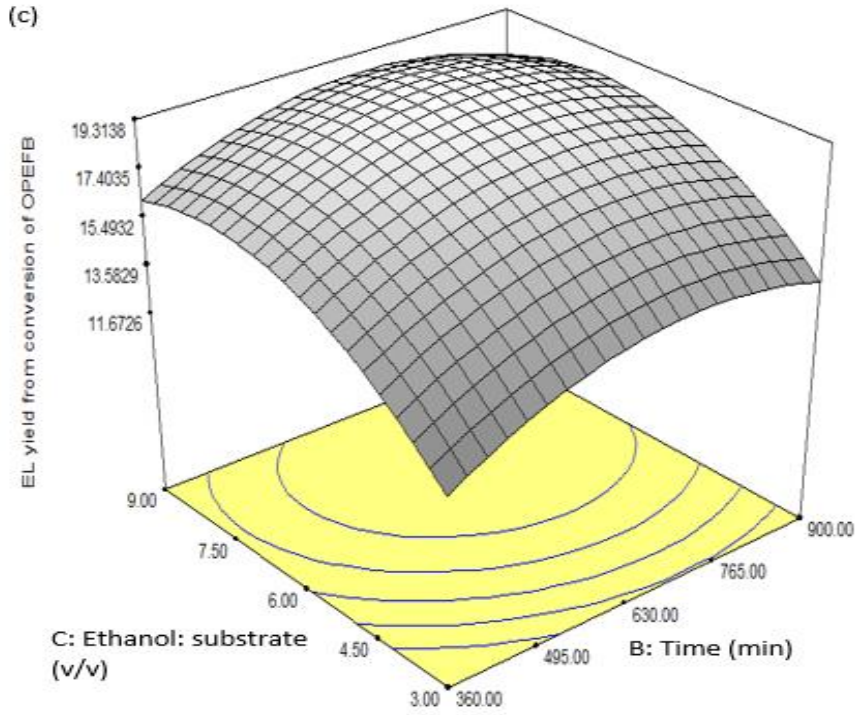
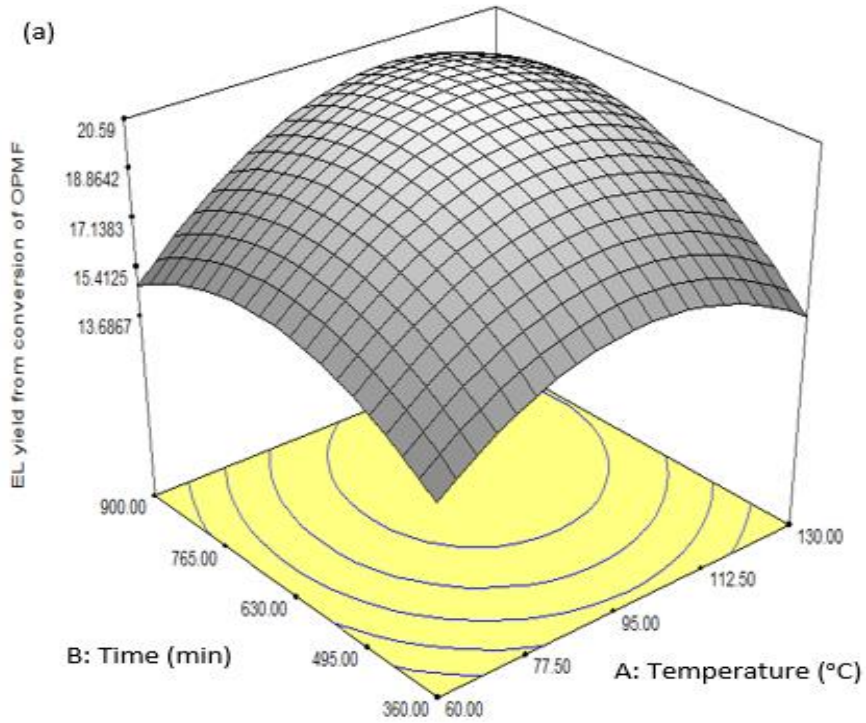



**Figure 6.2** Corresponding response surface and contour plots for EL yield from OPEFB conversion ($Y_3$), based on (a) temperature and time; (b) temperature and ethanol-to-substrate ratio; and (c) time and ethanol-to-substrate ratio.



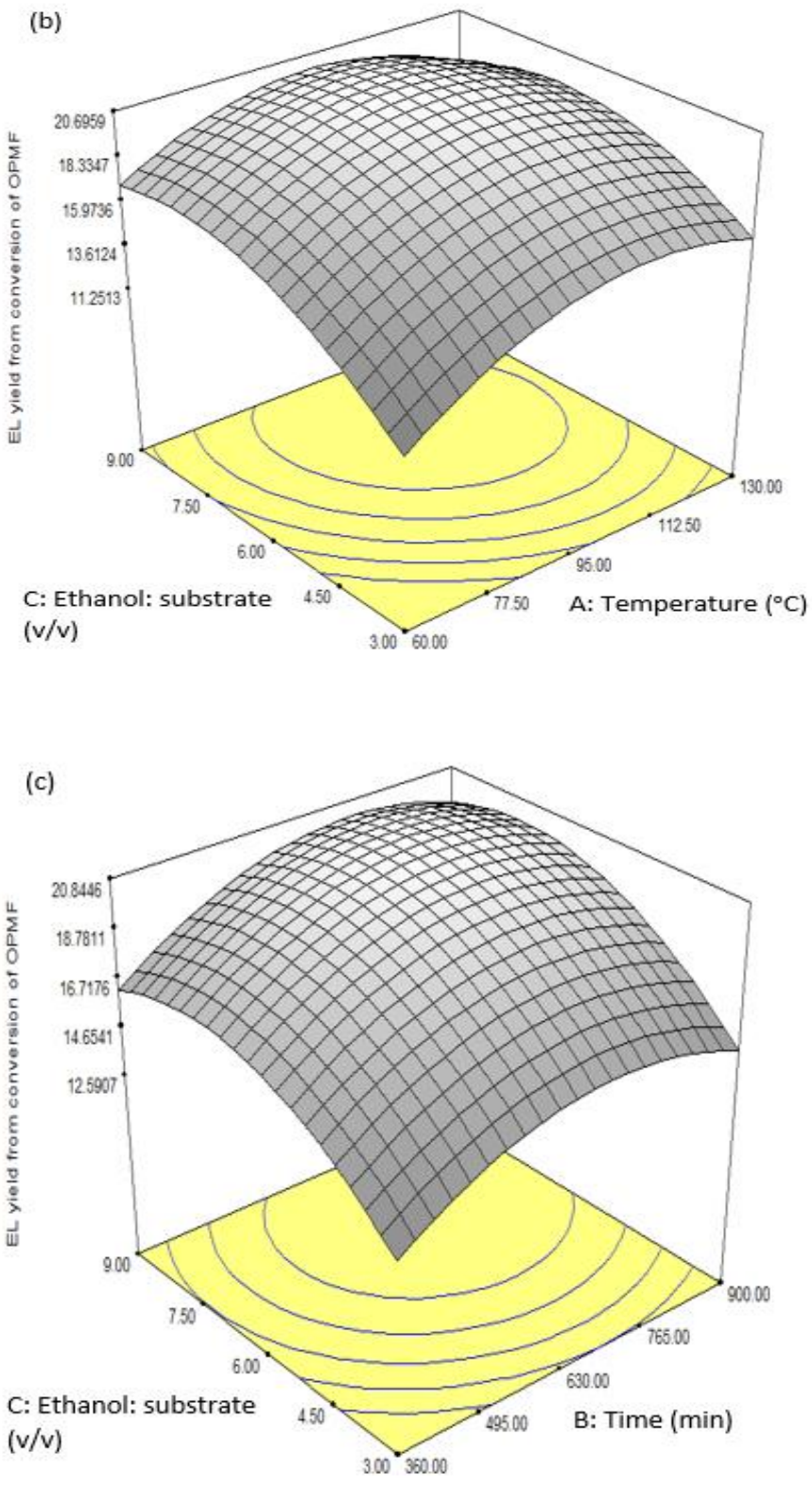



**Figure 6.3** Corresponding response surface and contour plots for EL yield from OPMF conversion ($Y_4$), based on (a) temperature and time; (b) temperature and ethanol-to-substrate ratio; and (c) time and ethanol-to-substrate ratio.

It was observed that the EL yield rapidly increased to the optimal value with increasing values of all the tested variables, i.e. reaction temperature, reaction time and volume of ethanol to substrate ratio. Specifically, the effect of reaction temperature and time was important for the reaction yield. Noteworthy, the interaction between these two variables was the most significant among all interactions terms (**Table 6.4**). As the temperature increased, the EL yield increased proportionally, but once the temperature exceeded 105°C, a reverse trend was observed and thus the yield decreased. Generally, a high EL yield could be achieved at higher temperature-shorter time, and vice versa. It has been reported that at extremely low temperatures, the EL yield grew slower as time progressed, causing an accumulation of intermediate products in the process [147], [298]. Conversely, although elevated temperature could accelerate the conversion rate, the condensation of degradation products might occur and thus increased the residue [74]. The observed trends were in accordance with ML production from biomass [299].

Furthermore, the volume of ethanol to substrate ratio was vital to achieve the highest conversion rate for EL production. At low ethanol medium, the EL yield increased moderately with increased reaction temperature and time. However, when the volume of ethanol to substrate ratio increased from 2:1 to 7:1, along with increased reaction temperature and time, the conversion of LA was enhanced as observed in the elliptical nature of the contour plots. This phenomenon depicted that the increase in reaction temperature promoted the esterification reaction rate in an appropriate reaction time [231] thereby promoting the EL product. Unfortunately, further increase in the volume of

ethanol to substrate ratio to >8:1 resulted in a reversal of the aforementioned trend. This was presumably constrained by the mass transfer rate as excess ethanol might have diluted the reactant and thus limited the conversion of LA [300]. The obtained result agreed with Su et al. [301] in which excess methanol in ML production led to side reactions such as ether formation or methyl dehydration in the presence of an acid catalyst.

#### 6.3.1.3 Optimisation and validation

A numerical optimisation method was employed to generate the optimum conditions for the esterification reaction. At the optimum conditions of 105$^{o}$C in 12.2 h, with ethanol to substrate ratio of 7.2:1 (v/v), 19.5% and 21% of EL yields were achieved for the responses of $Y_3$ (conversion from OPEFB) and $Y_4$ (conversion from OPMF), respectively. **Table 6.5** compares the predicted and experimental results. The observed experimental results were in reasonable agreement with the predicted values. The model was validated with errors less than 5%.

**Table 6.5** Optimisation and validation for EL yields.

| Experiment | Temp (°C) | Time (min) | Ethanol-to-substrate ratio (v/v) | Responses (%) | | Error[a] (%) |
|---|---|---|---|---|---|---|
| | | | | $Y_3$ | $Y_4$ | |
| CCD | 105 | 731 | 7.2:1 | 19.5 | 21.0 | $Y_1$: 4.1 |
| Validation (Trial 1) | 105 | 731 | 7.2:1 | 19.7 | 19.5 | |
| Validation (Trial 2) | 105 | 731 | 7.2:1 | 17.3 | 21.7 | |
| Validation (Trial 3) | 105 | 731 | 7.2:1 | 19.1 | 19.1 | |
| Validation[b] | 105 | 731 | 7.2:1 | 18.7 | 20.1 | $Y_2$: 4.3 |

[a]Error $= \left| \frac{\text{Validation result} - \text{CCD result}}{\text{CCD result}} \text{ x } 100\% \right|$

[b]Validation experiments were conducted thrice, and the averages of the responses are presented.

### 6.3.2 LA and EL syntheses with other by-products formation

**Figure 6.4** show the typical GC-MS chromatogram of LA syntheses from biomass conversion at the optimised reaction conditions, as reported in **Chapter 5.3.1.3**. Meanwhile, **Table 6.6** show the identification of products for the reaction mixture of LA (Refer to **Appendix 4a** for the mass spectroscopy data of the chemical compounds).

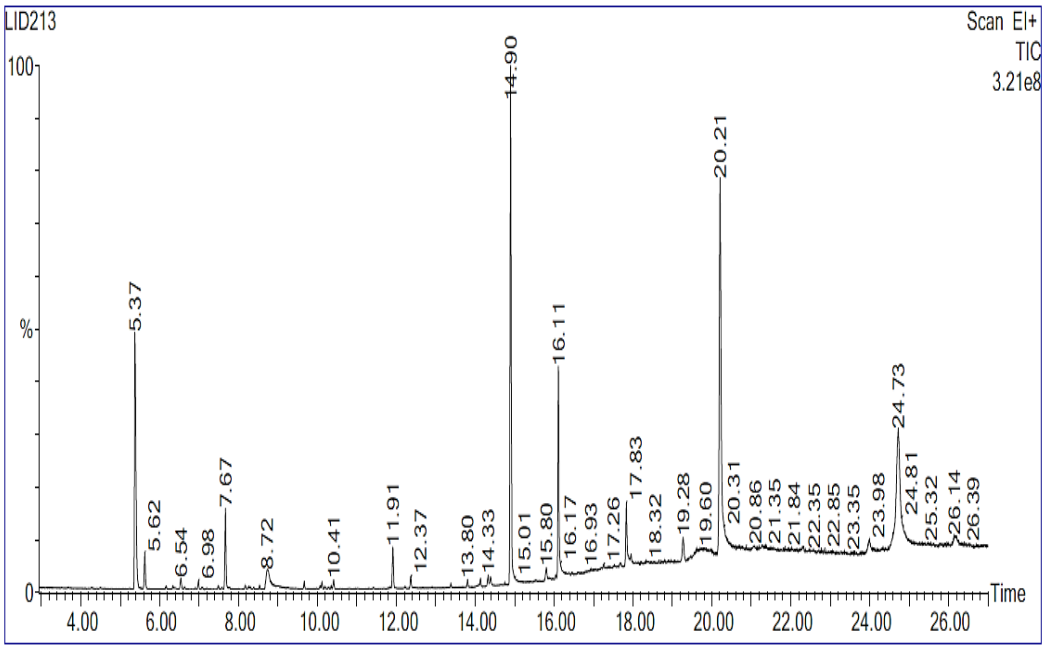



**Figure 6.4** Representative GC-MS chromatogram for the reaction mixture of LA syntheses.

**Table 6.6** Typical components identified from the GC-MS analysis for the reaction mixture of LA syntheses.

| RT (min) | Products |
|---|---|
| 5.37 | Acetic acid |
| 5.62 | Furfural |
| 7.67 | Butyric acid (Internal standard) |
| 8.74 | 1-H imidazole (ILs) |
| 14.90 | LA |
| 16.11 | Lauric acid |
| 17.83 | Myristic acid |
| 19.28 | Vanillic acid hydrazide |
| 20.21 | Palmitic acid |
| 24.73 | Stearic acid |

**Figure 6.5** shows the typical GC-MS chromatogram of EL syntheses from biomass conversion in a two-step sequential reactions (i.e. depolymerisation to LA, followed by the upgrading esterification to EL) via one-pot production at optimised reaction conditions as reported in **Chapter 5.3.1.3** (depolymerisation to LA) and **Chapter 6.3.1.3** (esterification to EL). Meanwhile, **Table 6.7** show the identification of products for the reaction mixture of EL (Refer to **Appendix 4b** for the mass spectroscopy data of the chemical compounds).

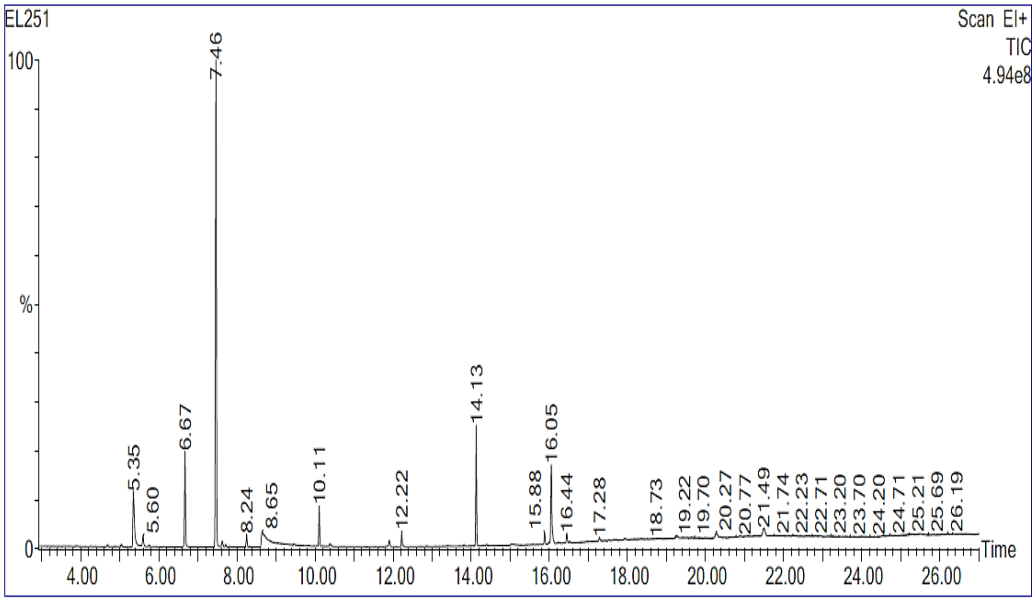



**Figure 6.5** Representative GC-MS chromatogram for the reaction mixture of EL syntheses.

**Table 6.7** Typical components identified from the GC-MS analysis for the reaction mixture of EL syntheses.

| RT (min) | Products |
|---|---|
| 5.35 | Acetic acid |
| 5.60 | Furfural |
| 6.67 | 1-Octanol (Internal standard) |
| 7.46 | EL |
| 8.24 | Ethyl succinate |
| 8.65 | 1-H imidazole (ILs) |
| 10.11 | Ethyl laurate |
| 12.22 | Ethyl myristate |
| 14.13 | Ethyl palmitate |
| 15.88 | Ethyl stearate |
| 16.05 | Ethyl oleate |
| 16.44 | Ethyl linoleate |

At the optimised reaction conditions for the biomass conversion to LA and upgrading to EL via $InCl_3$-[HMIM][$HSO_4$] catalytic system, acetic acid and furfural were consecutively produced as by-products (**Figure 6.4**, **Table 6.6**; **Figure 6.5**, **Table 6.7**). The formation of acetic acid might be due to the following two reasons: (1) wet oxidation of carbohydrates that come from the oxidation of dehydration products of aldose (glucose) [302], and (2) cleavage of acetyl group from the hemicellulose [303]. As for the furfural formation, minor furfural peak was detected in both LA and EL syntheses, instead of the LA precursor (5-HMF). Furfural formation usually take a shorter time than 5-HMF formation, mainly due to hemicellulose being more acid-labile than crystalline cellulose [287]. Specifically, both furfural formation from hemicellulose and 5-

HMF formation from cellulose consist of multiple successive steps. The steps mainly involve the hydrolysis of hemicellulose/ cellulose to xylose/ glucose, followed by the isomerisation and dehydration of the monosaccharide to furfural/ 5-HMF, and these steps can all be achieved via acid catalysts. Under certain circumstances, furfural is also formed via the loss of formaldehyde from 5-HMF [294]. Hence, this result further confirmed that LA and EL syntheses were produced mainly from the hexose (cellulose) pathway rather than the pentose (hemicellulose) pathway (refer to **Chapter 2.4**). Noteworthy, all the produced 5-HMF intermediate has been successfully converted to LA, achieving full turnover conversion efficiency of LA synthesis, foresee that there is no 5-HMF peak detected in both GC-MS chromatogram (**Figure 6.4** and **6.5**). Furthermore, slight discrepancies might have occurred due to the experimental error of incomplete isolation of ILs from the organic mixture of LA and EL syntheses.

As for the individual synthesis, i.e. LA synthesis from biomass conversion, the present results (**Figure 6.4**, **Table 6.6**) were in same agreement with Zhang et al. [287] who claimed that the condensation reactions between the intermediate products (furans and organic molecules) might generate humins, polymers and other by-products such as lauric acid, myristic acid, vanillic acid hydrazide, palmitic acid and stearic acid alongside the major LA synthesis. These by-products produced were majorly composed of organic fatty acids. Among these, palmitic acid was produced in significant amount, which could be due to it being one of the major saturated fatty acid composition in oil palm. The

finding of this work was in accordance with the acid catalysed transesterification reaction of crude palm oil [304].

As for the EL synthesis from biomass conversion (**Figure 6.5**, **Table 6.7**), the biomass could be converted into a mixture of fatty acid ethyl esters (FAEEs, commonly found in biodiesel fuel [305]), alongside the significant production of EL (main product). This result agreed with the transesterification of mainly plant-derived oils into hybrid biodiesel fuel, also known as the fatty acid-levulinate ester biodiesel fuel blends [306]. In fact, Windom et al [26] has analysed the advanced distillation curve (ADC) of this new fatty acid-levulinate ester biodiesel fuel blends (with a large amount of EL than those of any of the FAEEs) in comparison to commercial soy-based biodiesel fuel and ultra-low sulphur diesel fuel (ULSD) fuel. From the results, Windom et al [26] reported that this new fatty acid-levulinate ester biodiesel fuel blends gave a lower boiling temperature in the early distillate fractions as compared to the commercial biodiesel fuel. In addition, the enthalpies of combustion in the initial distillate fractions were also lower in this new fatty acid-levulinate ester biodiesel fuel blends than the commercial biodiesel fuel [26]. As an added benefit, the high concentration of EL in this new fatty acid-levulinate ester biodiesel fuel blends represented a possible approach to enhance the cold flow properties associated with biodiesel fuel and to reduce the associated performance and emission problems that occur at low temperatures [306]. In fact, the majority of feedstock currently used for biodiesel fuel production produces long carbon chain fatty acid esters, specifically unsaturated fatty acid esters, which are responsible for the poor cold flow properties [26]. Hence, this new fatty acid-levulinate ester

biodiesel fuel blends produced from oil palm biomass has been proposed to be a viable petroleum diesel fuel extender or replacement.

### 6.3.3 Comparative studies

As summarised in **Table 6.8**, the $InCl_3$-[HMIM][$HSO_4$] catalyst in the present study produced significantly higher LA yields than BAILs with multi-acid sites, i.e. [$C_4(MIM)_2$][$(2HSO_4)(H_2SO_4)_4$] [73] and [$C_3SO_3HMIM$][$HSO_4$] [83]. These results confirmed that the excess Bronsted acidic sites did not enhance the LA formation significantly. Instead, the Lewis acidic sites which have a stronger and more controllable acidity nature [61], were able to compensate for the weaker acidity of BAILs and thus enhanced the LA formation. Apart from that, the $InCl_3$-[HMIM][$HSO_4$] catalyst in the present study also gave higher LA yields than the hybrid catalyst, $FeCl_3$/HY zeolite coupled with [BMIM][Br] [85] and comparable yields with another hybrid catalyst, $CrCl_3$/HY zeolite coupled with [EMIM][Cl] [89] and [BMIM][$HSO_4$] [52]. The additional step of initial hydrolysis of biomass prior to conversion into LA significantly improved the LA yields [85]. Nonetheless, performing this extra step is time-consuming and would incur higher cost.

Nevertheless, the LA yields of the present study were lower than those of SFILs based BLAILs, ([SMIM][$FeCl_4$]) [7]. The synergistic effect from both Bronsted and Lewis acidic sites of [SMIM][$FeCl_4$] has resulted in better catalytic activity which was presumably due to the presence of the sulphonic acid functionalised group in the cation of ILs that gave a stronger acidity strength [7]. Nevertheless, SFILs are corrosive and not environmentally friendly [62].

Additionally, the LA yields of the present study were also much lower than those of Lewis acid $ZnCl_2$ coupled with [BMIM][Cl] [51]. $Zn^{2+}$ is among the most effective metal chlorides in cellulose degradation as observed in biochar production via pyrolysis [214]. In general, the catalytic efficiency of the metal chlorides in enhancing LA production followed the order of: $ZnCl_2 > InCl_3 \geq CrCl_3 > FeCl_3$.

In terms of EL production, the $InCl_3$-[HMIM][$HSO_4$] catalyst in the present study gave much higher EL yields than [SMIM][$FeCl_4$] [7]. Additional ILs loading improved the yield in the latter system [7], but incurred higher cost. Furthermore, the EL yields attained in the present study were also slightly higher than those of BAILs with multi-acid sites ([$HSO_3$-BMIM][$HSO_4$]) [74]. This result further suggested that the coexistence of both Bronsted and Lewis acidic sites on BLAILs resulted in better catalytic activity than sole BAILs.

Comparatively, OPMF biomass was a more feasible raw material in the conversions, giving noticeably higher LA and EL yields than OPEFB biomass, although the former contained slightly less cellulose. This was likely attributed to the OPMF biomass having a lower lignin content compared to the OPEFB biomass, as lignin is an amorphous polymer that acts as a "glue" binding hemicellulose and cellulose via ester linkages and hydrogen bonds [307]. These molecular interactions increase the recalcitrance of materials towards hydrolysis and depress the function of ILs on biomass. Overall, the proposed new environmentally friendly coupling mixed acids $InCl_3$-[HMIM][$HSO_4$] catalytic system is compatible with the biomass dissolution, and its synergistic Bronsted

and Lewis acidic catalytic sites are able to catalyse the overall conversion efficiently to both LA and EL.

**Table 6.8** Comparison of the present LA and EL productions with other studies involving different biomass and ILs.

| Feedstock | ILs | Reaction conditions | | Cellulose content of biomass (%) | Yield (%) | | Efficiency (%) | Ref. |
|---|---|---|---|---|---|---|---|---|
| | | Temp ($^oC$) | Time (h) | | Biomass | Theoretical | | |
| **(a) LA production** | | | | | | | | |
| Bamboo | $[C_4(MIM)_2][(2HSO_4)(H_2SO_4)_4]$ | 110 | 1 | 40.3 | 13.6 | 28.6 | 47.5 | [73] |
| Straw | $[C_3SO_3HMIM][HSO_4]$ | 180 | 1.5 | 34.7 | 5.3 | 24.6 | 21.6 | [83] |
| OPF[g] | [BMIM][Br] and $FeCl_3$/HY zeolite | 120 | 6 | 45.2 | 11.1 | 32.1 | 34.6 | [85] |
| OPEFB | | | | 41.1 | 9.3 | 27.1 | 34.3 | |
| OPF[a] | | 120 | 3 | 45.2 | 18.6 | 32.1 | 57.9 | |
| OPEFB[a] | | | | 41.1 | 17.6 | 27.1 | 64.9 | |
| OPEFB | [EMIM][Cl] and $CrCl_3$/HY zeolite | 177 | 2.3 | 41.1 | 20.0 | 29.2 | 68.5 | [89] |
| Kenaf | | | | 32.0 | 17.0 | 22.7 | 74.9 | |
| Bamboo shoot shell | $[BMIM][HSO_4]$ | 145 | 1.7 | 37.8 | 17.9 | 26.8 | 66.8 | [52] |

| | | | | | | | | |
|---|---|---|---|---|---|---|---|---|
| Bamboo shoot shell | [BMIM][Cl] and $ZnCl_2$ | 133 | 1.4 | 41.5 | 29.5 | 38.2 | 77.2 | [51] |
| **(b) EL production** | | | | | | | | |
| Wheat straw | $[HSO_3$-BMIM$][HSO_4]$ | 200 | 1 | N.A.[h] | 16.2 | N.A.[h] | N.A.[h] | [74] |
| **(c) LA and EL productions** | | | | | | | | |
| OPF[g] | [SMIM][$FeCl_4$] | 155[b] | 3.7[b] | 45.2 | 24.8[b] | 32.1[b] | 77.3[b] | [7] |
| | | 78[c,f] | 5[c,f] | | 20.1[c,f] | N.A.[h] | N.A.[h] | |
| | | 78[c] | 10[c] | | 12.8[c] | N.A.[h] | N.A.[h] | |
| OPEFB[d] | $InCl_3$-[HMIM][$HSO_4$] | 177[b] | 4.8[b] | 33.2[d] | 17.7[b,d] | 24.0[b,d] | 74.1[b,d] | Present |
| OPMF[e] | | 105[c] | 12.2[c] | 30.0[e] | 18.4[b,e] | 21.3[b,e] | 86.4[b,e] | study |
| | | | | | 18.7[c,d] | 29.6[c,d] | 63.2[c,d] | |
| | | | | | 20.1[c,e] | 26.7[c,e] | 75.3[c,e] | |

[a]Feedstock was hydrolysed to produce reducing sugars before subjected to LA production.
[b]Depolymerisation to LA
[c]LA esterification to EL
[d]OPEFB conversion
[e]OPMF conversion
[f]Addition of 5 g of ILs in the subsequent esterification reaction
[g]OPF - Oil palm frond
[h]N.A. - Not available

## 6.4 Concluding Remarks

The present optimisation studies reported a new environmentally friendly coupling mixed acids $InCl_3$-[HMIM][$HSO_4$] catalytic system for the subsequent upgrading esterification reaction of LA to EL, by using a RSM based on a CCD approach. A two-step sequential reaction i.e. depolymerisation to LA (**Chapter 5**), followed by the upgrading esterification to EL (**this Chapter**), via one-pot production was performed. The ANOVA results indicated that both EL models ($Y_3$ and $Y_4$) were statistically significant. The lack of fit F-value for both responses were insignificant relative to the pure error, indicating good fitting of the proposed models and thus were reliable tools for predicting EL yields. The optimum esterification was achieved at a reaction temperature of 105°C in 12.2 h with 7.2:1 (v/v) of ethanol to substrate ratio. The maximum EL yields were 18.7% and 20.1%, the corresponding EL efficiencies were 63.2% and 75.3%, for the conversions from OPEFB and OPMF biomass, respectively. Moreover, the optimised operating parameters obtained for EL, alongside the by-products (FAEEs), formed a new fatty acid-levulinate ester biodiesel fuel blend, which could be used as a viable petroleum diesel fuel extender or replacement. The present results suggested that this new environmentally friendly coupling mixed acids $InCl_3$-[HMIM][$HSO_4$] is a greener alternative catalytic system which potentially offers a better or comparable catalytic activity than other ILs catalytic system for the biomass conversion to both LA and EL. Hence, this would directly benefit subsequent pilot scale or field scale studies on the conversions from a greener and more sustainable perspective.

# Chapter 7

# Kinetic and thermodynamic studies on the biomass conversion and upgrading

## 7.1 Introduction

OPMF biomass was chosen as the feedstock for the present kinetic and thermodynamic studies, as it has been proven to be a more feasible biomass material in the conversions, giving noticeably higher LA and EL yields than OPEFB biomass in previous reaction optimisation studies (**Chapter 5** and **6**). As such, this chapter focuses on the kinetic and thermodynamic studies of OPMF cellulose conversion to LA and upgrading to EL via $InCl_3$-[HMIM][$HSO_4$] catalytic system. The biomass conversion reactions via hexose (cellulose) pathway, i.e. cellulose depolymerisation to LA, and the subsequent upgrading esterification to EL, were conducted at temperature ranges of 135-175°C and 65-105°C, respectively. The pseudo-homogeneous kinetic models were adapted to evaluate the best reaction order. Herein, the kinetic parameters, such as the reaction rate constants at various temperatures, pre-exponential factor and activation energy were determined. The thermodynamic energy was further assessed by examining the activation enthalpy, activation entropy and Gibbs free energy of activation. Finally, the results were critically compared to the literature data to assess the "greenness and energy saving" perspectives of the system. To the best of our knowledge, the kinetic and thermodynamic data for both LA and EL syntheses via ILs direct from biomass feedstock are still absent. As such, this study provides insights to the OPMF cellulose conversion to LA and EL via $InCl_3$-[HMIM][$HSO_4$] catalytic system.

## 7.2 Methodology

### 7.2.1 Materials

The preparation of OPMF biomass and chemicals involved have been reported in **Chapter 3.2.1** and **4.2.1**.

### 7.2.2 Biomass conversion reaction and products isolation

The experimental procedures of biomass conversion reactions, i.e. depolymerisation to LA, and the subsequent upgrading esterification to EL, has been reported in **Chapter 4.2.2**. The kinetic and thermodynamic studies for both depolymerisation and esterification reactions were conducted at varying reaction temperatures (135-175°C, 75-105°C) and times (60-300 min, 270-780 min). The amounts of $InCl_3$, ILs, water, and the subsequent ethanol loadings adhered to the optimised reaction conditions obtained in **Chapter 5** and **6**. The procedures for LA and EL products isolation have been reported in **Chapter 4.2.3**.

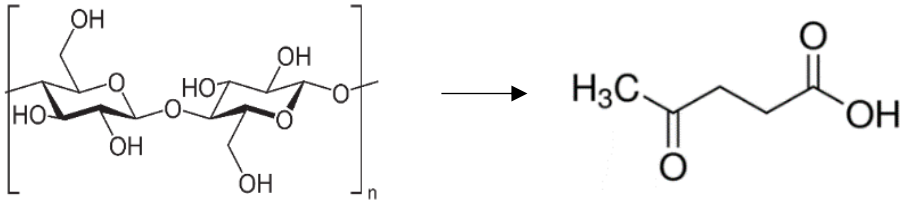
### 7.2.3 Products analysis

LA and EL contents were determined by using a GC-MS (Perkin Elmer Clarus 680, USA), as described in **Chapter 4.2.4**. The standard errors of triplicate data obtained for all yields ranged within 1.8-3.9%. The calculation formula for the efficiencies of LA and EL have been reported previously, as in **Eq. 5.3** and **Eq. 6.2**, respectively.

### 7.2.4 Determination of kinetic and thermodynamic parameters

The OPMF biomass conversion to LA and upgrading to EL primarily occurs via hexose (cellulose) route due to the rapid degradation of cellulosic carbohydrate of lignocellulosic biomass [57], [132]. As such, cellulose is hydrolysed into intermediate products and converted to LA, prior to further upgrading to EL by esterification reaction [56]. During the experimental process, the formation of intermediate products were not detected through GC-MS, and thus were considered as negligible due to their instant degradation at high temperature for the LA synthesis. This result is in agreement with a similar work reported by Zhi et al. [56]. As this conversion reaction via $InCl_3$-[HMIM][$HSO_4$] is a homogeneous catalytic system, the mass transfer diffusion effect is considered negligible.

A simplified pseudo-homogeneous model was proposed based on LA synthesis as follows:




Cellulose (C) LA

**Scheme 7.1.** A reaction scheme of depolymerisation reaction of cellulose to LA via ILs.

A few assumptions were considered to develop the kinetic model, whereby they were made based on the kinetic models reported in the literature [50], [56], [308]:

1) Cellulose depolymerisation to LA was a series of irreversible reactions.

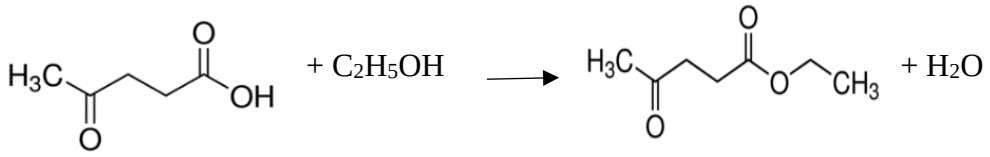
2) LA was the main product of cellulose depolymerisation reaction, while other possible by-product reactions were negligible.

Subsequently, the upgrading esterification reaction of LA to EL was further conducted via two-step sequential reactions (depolymerisation to LA, and the subsequent upgrading esterification to EL). Herein, the second kinetic model was devised for the subsequent upgrading esterification reaction to EL. Considering that excess ethanol was used to shift the equilibrium towards the product side, the reaction can be considered as an irreversible reaction [309]. To simplify the kinetic modelling, the following assumptions were made based on the kinetic models reported in the literature [233], [310], [311]:

1) Internal and external mass resistance were negligible.

2) The whole catalytic system was assumed as an ideal solution.

A simplified pseudo-homogeneous model was proposed based on EL synthesis as follow (**Scheme 7.1**, then **Scheme 7.2**):




LA ethanol EL water

**Scheme 7.2.** A reaction scheme of the upgrading esterification reaction of LA to EL via ILs.

Based on the models from **Scheme 7.1** and **7.2**, the following sets of differential equations were obtained:

$$\frac{d\,C}{dt} = -\,k\,C^{n} \qquad (7.1)$$

where *C* represents cellulose, which was expressed in the unit of percentage (%). *n* is the order of the reaction, *k* ($min^{-1}$) is the rate constant of cellulose, and *t* is the reaction time (min).

The pseudo-zero-order, pseudo-first-order and pseudo-second-order kinetic approaches were evaluated to investigate the reaction order for both LA and EL efficiencies. The above **Eq. 7.1** is then integrated to obtain the respective equations, as in **Eq. 7.2**, **7.4** and **7.6**. The integrated rate equation for zero-order ($\alpha = 0$), first-order ($\alpha = 1$) and second-order ($\alpha = 2$) kinetic reactions were further simplified, as in **Eq. 7.3**, **7.5** and **7.7**.

For a pseudo-zero-order reaction,

$$C = C_0 - k\,t \qquad (7.2)$$

After integration and rearrangement of **Eq. 7.2**,

$$X = k\,t \qquad (7.3)$$

For a pseudo-first-order reaction,

$$C = C_0\ e^{-kt} \qquad (7.4)$$

After integration and rearrangement of **Eq. 7.4**,

$$-ln\,(1-X) = k\,t \qquad (7.5)$$

For a pseudo-second-order reaction,

$$C = \frac{C_0}{1 + k\, C_0\, t} \tag{7.6}$$

After integration and rearrangement of **Eq. 7.6**,

$$X / (1- X) = k\, t \tag{7.7}$$

where $C_0$ is the initial yield of cellulose (100%). $X_{LA}$ and $X_{EL}$ refers to the LA and EL efficiencies, respectively.

The fitting of the experimental results to the kinetic models were then justified based on the correlation coefficients ($R^2$) of the good fit of the linear plots. After confirming the kinetic order of the reactions, the rate constants ($k$) at various temperatures were obtained from the linear slope of the model. The activation energy ($E_a$) and pre-exponential factor ($A$) for the reactions were determined using the following Arrhenius equation:

$$k = Ae^{-\frac{E_a}{RT}} \tag{7.8}$$

where $E_a$ is the activation energy (kJ $mol^{-1}$), $R$ is the gas constant (8.314 J $mol^{-1}$ $K^{-1}$), $T$ is the temperature (K) and $A$ is the pre-exponential factor ($min^{-1}$).

By taking the natural logarithm of **Eq. 7.8**, **Eq. 7.9** is obtained:

$$\ln k = -\frac{E_a}{R} x \frac{1}{T} + \ln A \tag{7.9}$$

where $E_a$ and $A$ were determined from the slope and intercept of a Arrhenius plot of ln $k$ versus 1/T, respectively.

Based on the transition state theory, the Eyring equation which is similar to Arrhenius equation was used to relate rate constant to temperature. Specifically, Eyring equation defines the reaction in gas, condensed and mixed-phase [312]. Hence, the Eyring equation (**Eq. 7.10**) was applied to ascertain the thermodynamic activation parameters, i.e. activation enthalpy ($\Delta H^{\ddagger}$) and activation entropy ($\Delta S^{\ddagger}$). **Eq. 7.10** gives the Erying plot of ln (*k*/T) versus 1/T for assessing both $\Delta H^{\ddagger}$ and $\Delta S^{\ddagger}$ from the slope and intercept, respectively. The Gibbs free energy of activation ($\Delta G^{\ddagger}$) was calculated from **Eq. 7.11**. From the equations, $k_B$ is the Boltzmann's constant (1.381 x $10^{-23}$ J $K^{-1}$), *h* is the Plank's constant (6.626 x $10^{-34}$ J s), and *R* is the gas constant (8.314 J $mol^{-1}$ $K^{-1}$).

$$\ln\left(\frac{k}{T}\right) = -\frac{\Delta H^{\ddagger}}{R} x \frac{1}{T} + \ln\left(\frac{k_B}{h}\right) + \frac{\Delta S^{\ddagger}}{R} \tag{7.10}$$

$$\Delta G^{\ddagger} = \Delta H^{\ddagger} - T\Delta S^{\ddagger} \tag{7.11}$$

## 7.3 Results and Discussion

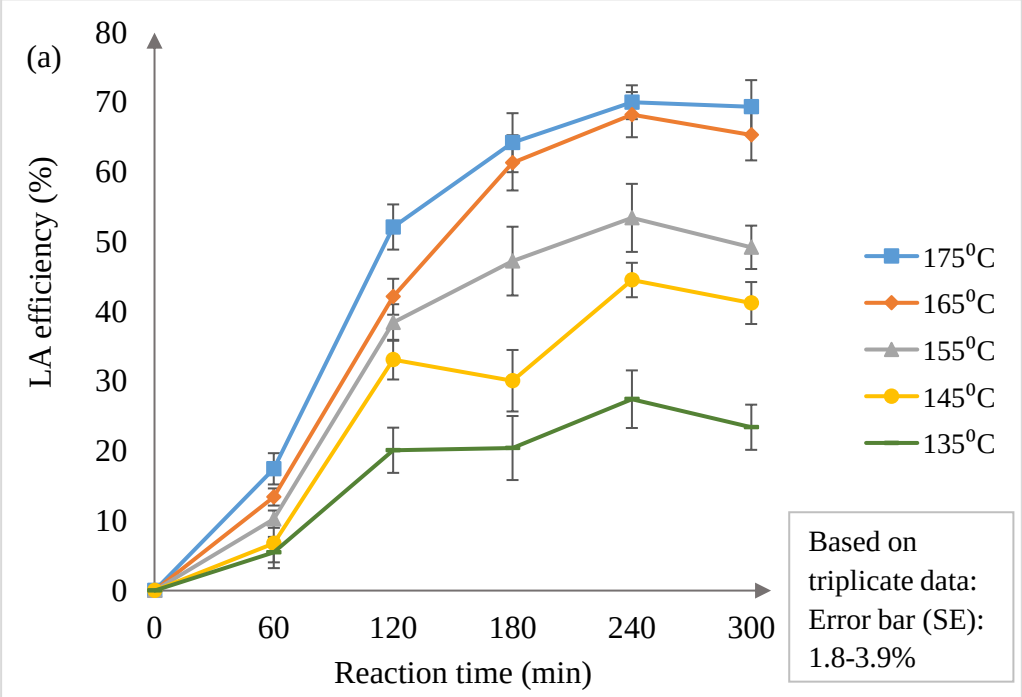
### 7.3.1 Effect of reaction temperature and time of the biomass conversion to LA and upgrading to EL

**Figure 7.1 (a)** shows that the LA efficiency varied with reaction temperature and time, in which the former played a greater role. At all reaction temperatures studied, the LA efficiency increased with time from 60-240 min, then reached a plateau at the final 240-300 min, signifying that the condition has reached the maximum reaction time at the $240^{th}$ min. Hence, a high LA efficiency of 70% was achieved at an elevated temperature of 175°C within a

shorter reaction time of 240 min. Generally, the LA efficiency could be improved by increasing the temperature or prolonging the reaction time. For instance, LA efficiency of 63% achieved at 175°C in 210 min was similar to that conducted at a lower temperature of 165°C, but with a prolonged reaction time of 300 min. Although prolonging the reaction time could promote the depolymerisation reaction towards a full turnover synthesis [313], the formation of decomposition product such as humins has been widely reported [78], [308]. As such, the production of LA at a higher temperature and with shorter reaction time is generally preferred.

Subsequently, the best performing depolymerisation conditions (105°C, 240 min) which gave the highest LA efficiency of 70.1% (**Figure 7.1a**), were applied for upgrading the reaction to EL. Herein, a similar trend was observed for EL efficiency, as shown in **Figure 7.1 (b)**, in which reaction temperature led to a significant impact on the EL synthesis. At all reaction temperatures studied, the EL efficiencies increased with time, up to 780 min. The maximum EL efficiencies of 65-70% were obtained at the highest reaction temperature studied (105°C) with prolonged reaction times of 630-780 min. Noteworthy, the EL efficiency obtained at a lower reaction temperature of 85°C with prolonged reaction times of 630-780 min (55-60%) was close to that conducted at a higher temperature of 105°C, but with a shorter reaction time of 510 min (58%). As the esterification of LA to EL is an endothermic reaction, an increase in reaction temperature would favour the forward reaction and enhance the LA conversion [314]. High temperature could also promote the kinetic energy of the reactant molecules in order to achieve the minimum amount of energy needed to

transform into products [315]. However, prolonging reaction time to >780 min (data not shown) decreased the EL efficiency at certain temperatures [78], presumably caused by the reversed reaction, i.e. hydrolysis of EL. This was similar to the transesterification reaction of crude palm oil in biodiesel synthesis [309]. A low temperature of 65°C seemed unfavourable for EL production as low EL efficiencies of <38% were obtained at all reaction times studied.



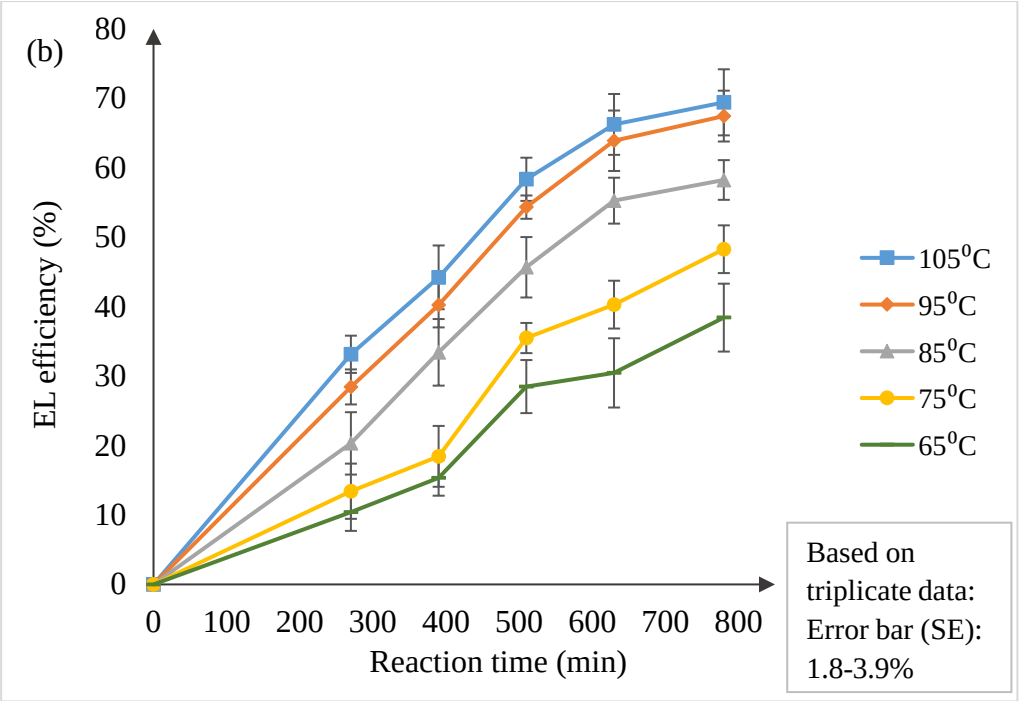
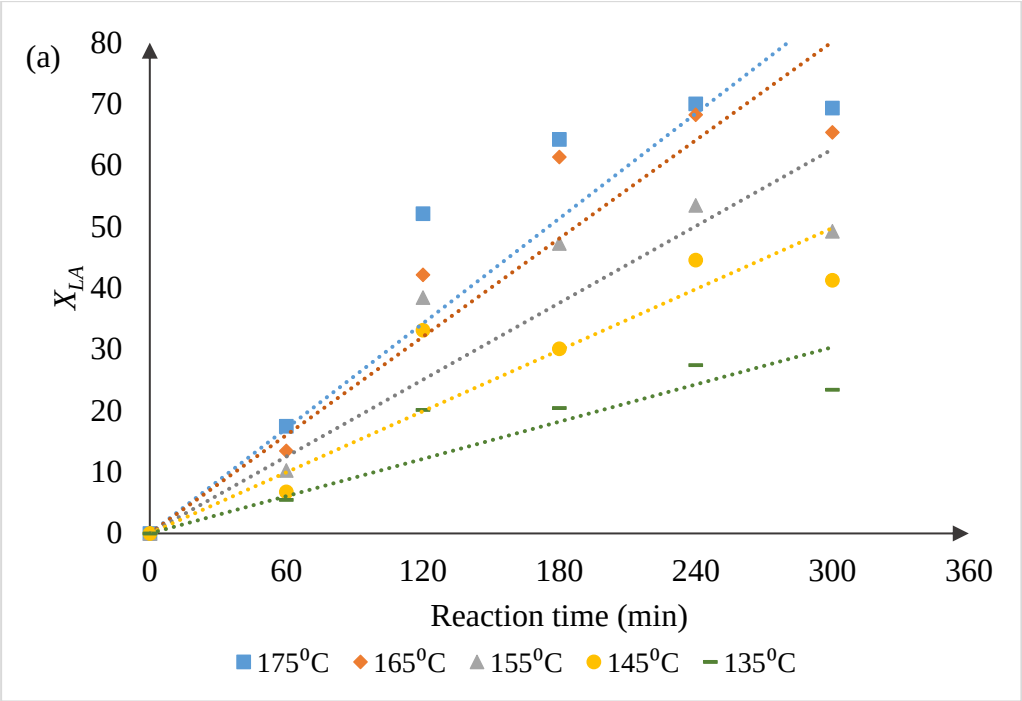
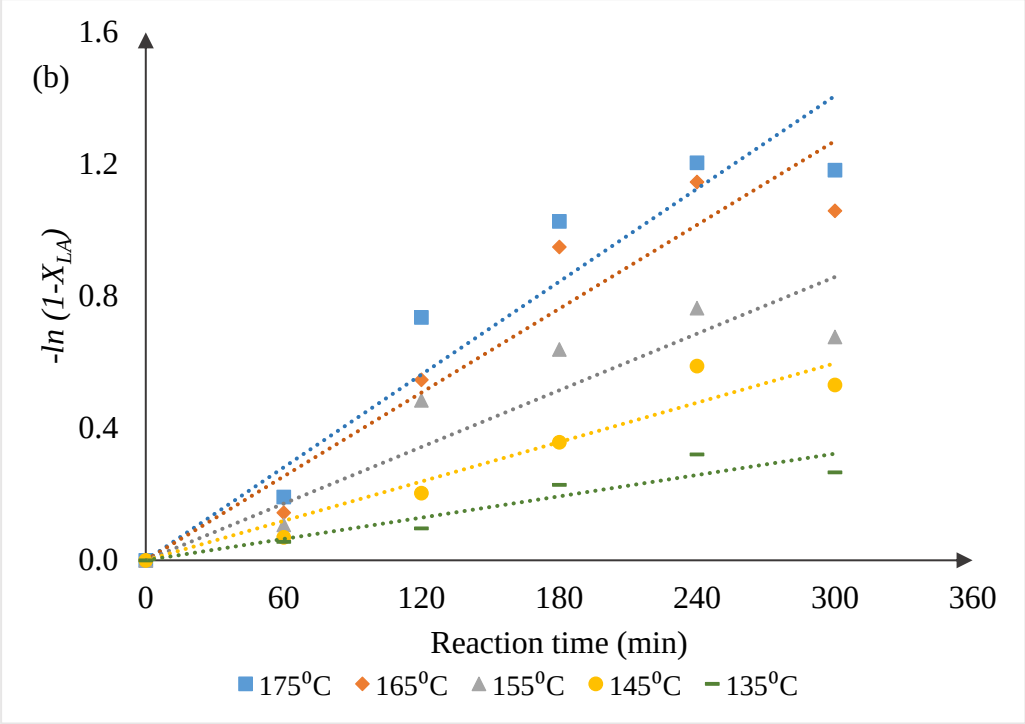



**Figure 7.1** Effect of reaction temperature and time on (a) LA efficiency and (b) EL efficiency. (ILs-to-biomass ratio of 6.6:1 (w/w) and water content of 22.7% (w/w), in excess ethanol medium for the subsequent esterification reaction)

### 7.3.2 Kinetic studies

Based on the mathematical model in **Eq. 7.2**, **7.4** and **7.6**, the pseudo-zero-order, pseudo-first-order and pseudo-second-order kinetic models are depicted in **Figure 7.2** and **7.3** (coloured graphs' trendlines), along with the respective $R^2$ in **Table 7.1**. The results of $X_{LA}$ and $X_{EL}$ were based on the data obtained in **Figure 7.1 (a)** and **(b)**, respectively.


(a)
80
70
60
50
40
30
20
10
0
$X_{LA}$
0
60
120
180
240
300
360
Reaction time (min)
175°C
165°C
155°C
145°C
135°C


(b)
1.6
1.2
0.8
0.4
0.0
-ln (1-$X_{LA}$)
0
60
120
180
240
300
360
Reaction time (min)
175°C
165°C
155°C
145°C
135°C

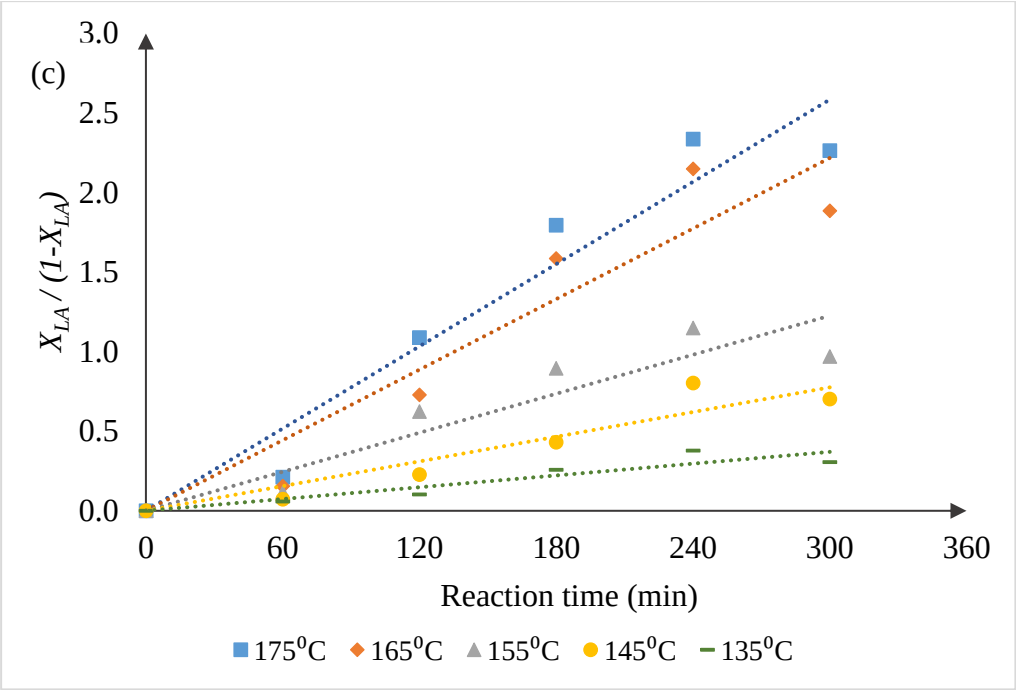
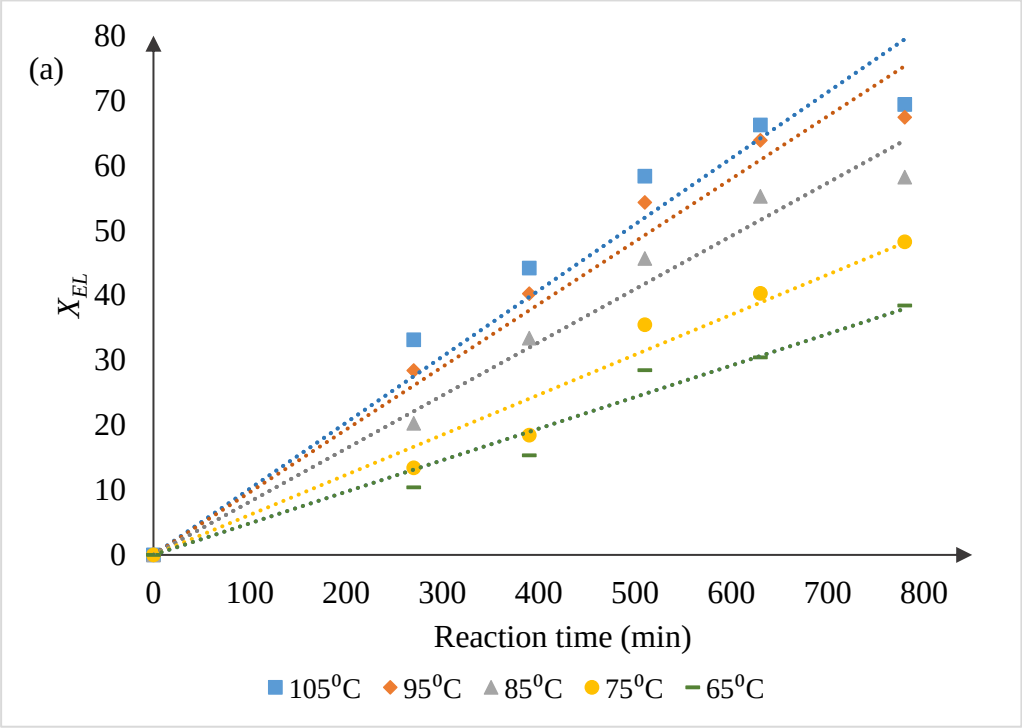
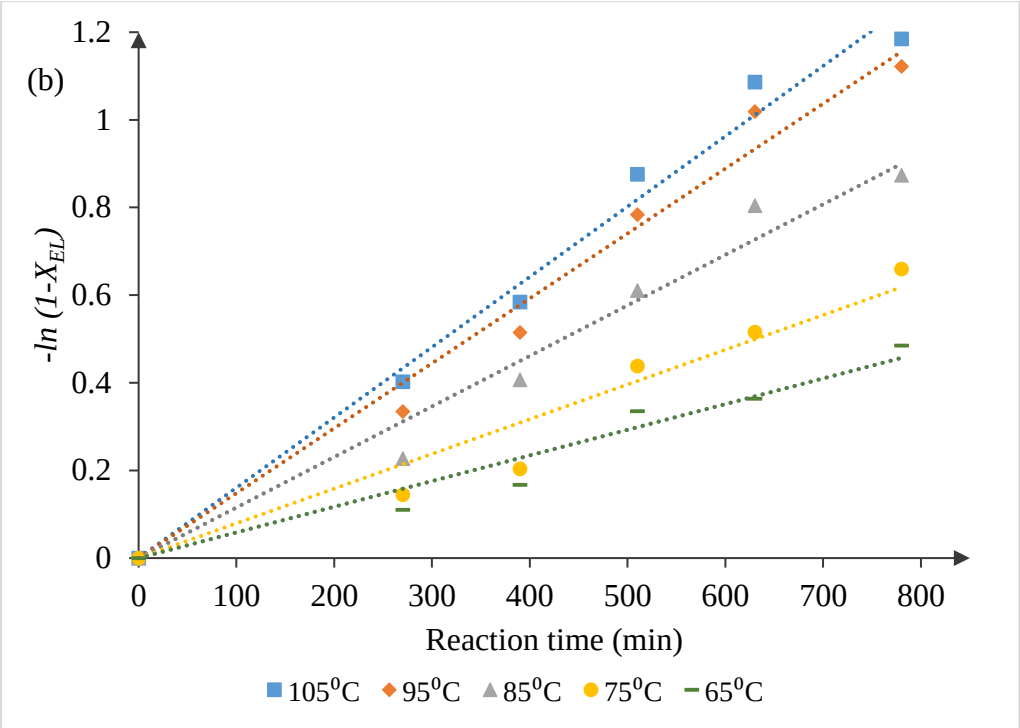



**Figure 7.2** Plot of (a) pseudo-zero-order, (b) pseudo-first-order, and (c) pseudo-second-order kinetic model of LA efficiency.





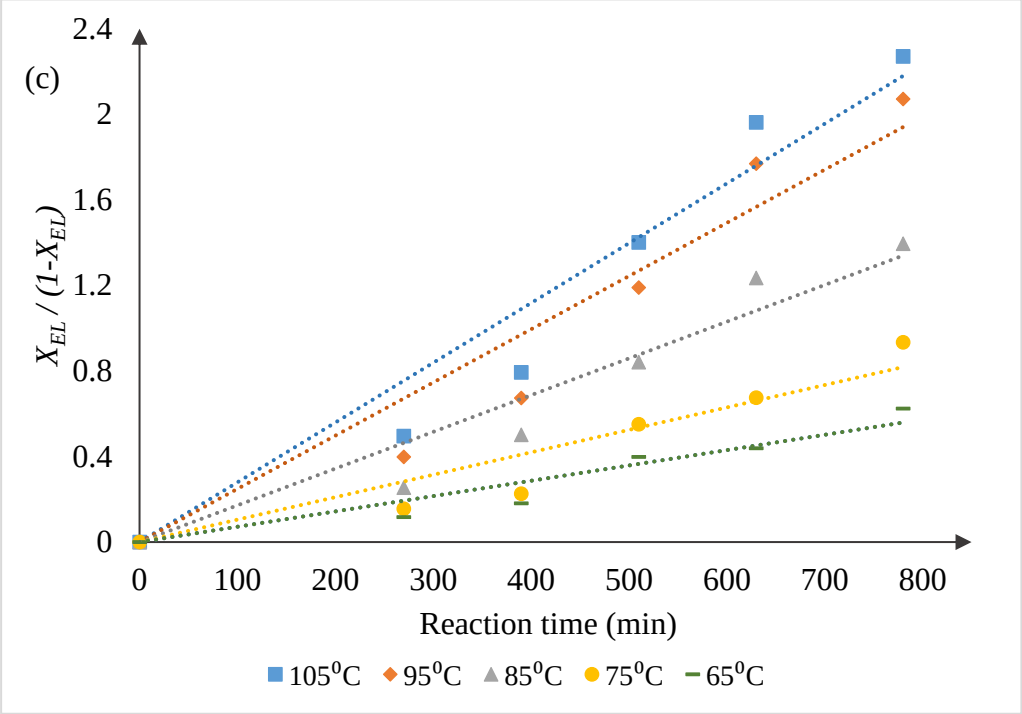




**Figure 7.3** Plot of (a) pseudo-zero-order, (b) pseudo-first-order, and (c) pseudo-second-order kinetic model of EL efficiency.

**Table 7.1** Kinetic parameters of LA and EL efficiencies.

| Temp (°C) | Pseudo-Zero Order | Pseudo-First Order | Pseudo-Second Order | Pseudo-First Order |
|---|---|---|---|---|
| | $R^2$ | $R^2$ | $R^2$ | $k$ ($min^{-1}$) |
| **(a) LA efficiency** | | | | |
| 175 | 0.8299 | 0.9041 | 0.8958 | 0.2815 |
| 165 | 0.8759 | 0.9076 | 0.8989 | 0.2541 |
| 155 | 0.8140 | 0.8455 | 0.8217 | 0.1717 |
| 145 | 0.8344 | 0.9301 | 0.9016 | 0.1194 |
| 135 | 0.7845 | 0.8862 | 0.8734 | 0.0646 |
| **(b) EL efficiency** | | | | |
| 105 | 0.9017 | 0.9736 | 0.9604 | 0.0997 |
| 95 | 0.9542 | 0.9782 | 0.9478 | 0.0921 |
| 85 | 0.9367 | 0.9713 | 0.9491 | 0.0718 |
| 75 | 0.9680 | 0.9553 | 0.9253 | 0.0494 |
| 65 | 0.9710 | 0.9633 | 0.9446 | 0.0365 |

Both LA and EL efficiencies were best fitted to the pseudo-first-order kinetic model, as indicated by the highest $R^2$ values (**Figure 7.2** and **7.3**, **Table 7.1**). However, for the esterification at lower temperatures of 65°C and 75°C, the EL efficiency was better fitted to the pseudo-zero-order (**Table 7.1b**). As the temperature increased (≥85°C), the data deviated from the linear model. Nonetheless, the data has a best fit to pseudo-first order with only up to approximately 500 mins. A similar trend was observed in the conversion of EL; at temperature ≥85°C (**Figure 7.1b**), the efficiency reduced gradually when the

time was >510 min and finally reached a plateau. These implied the transition of a pseudo-zero order reaction to a different reaction order, presumably to a pseudo-first order reaction.

**Table 7.1** shows that the reaction rate constants (*k*) of both LA and EL efficiencies via $InCl_3$-[HMIM][$HSO_4$] catalytic system were increased with increased reaction temperature. This suggested that a higher temperature was conducive for the cellulose depolymerisation to LA and the subsequent upgrading esterification to EL.

Activation parameters for both cellulose depolymerisation and the subsequent esterification were determined from the Arrhenius plots of ln *k* versus 1/T (**Figure 7.4**). The $E_a$ for cellulose depolymerisation to LA determined from the slope of the line was 56.5 kJ $mol^{-1}$ while the *A* calculated from the intercept was 1.3 x $10^6$ $min^{-1}$ (**Figure 7.4a**). As such, the Arrhenius equation for the depolymerisation reaction could be written as:

$$\ln k = 14.05 - 6.80\ T \qquad (7.12)$$

where *k* is the rate constant ($min^{-1}$) and T is the temperature (K).

Subsequently, from **Figure 7.4 (b)**, the $E_a$ for the upgrading esterification to EL determined from the slope of the line was 28.1 kJ $mol^{-1}$ while the *A* calculated from the intercept was 838.8 $min^{-1}$. As such, the Arrhenius equation for the esterification could be written as:

$$\ln k = 6.73 - 3.38\ T \qquad (7.13)$$

where *k* is the rate constant ($min^{-1}$) and T is the temperature (K).

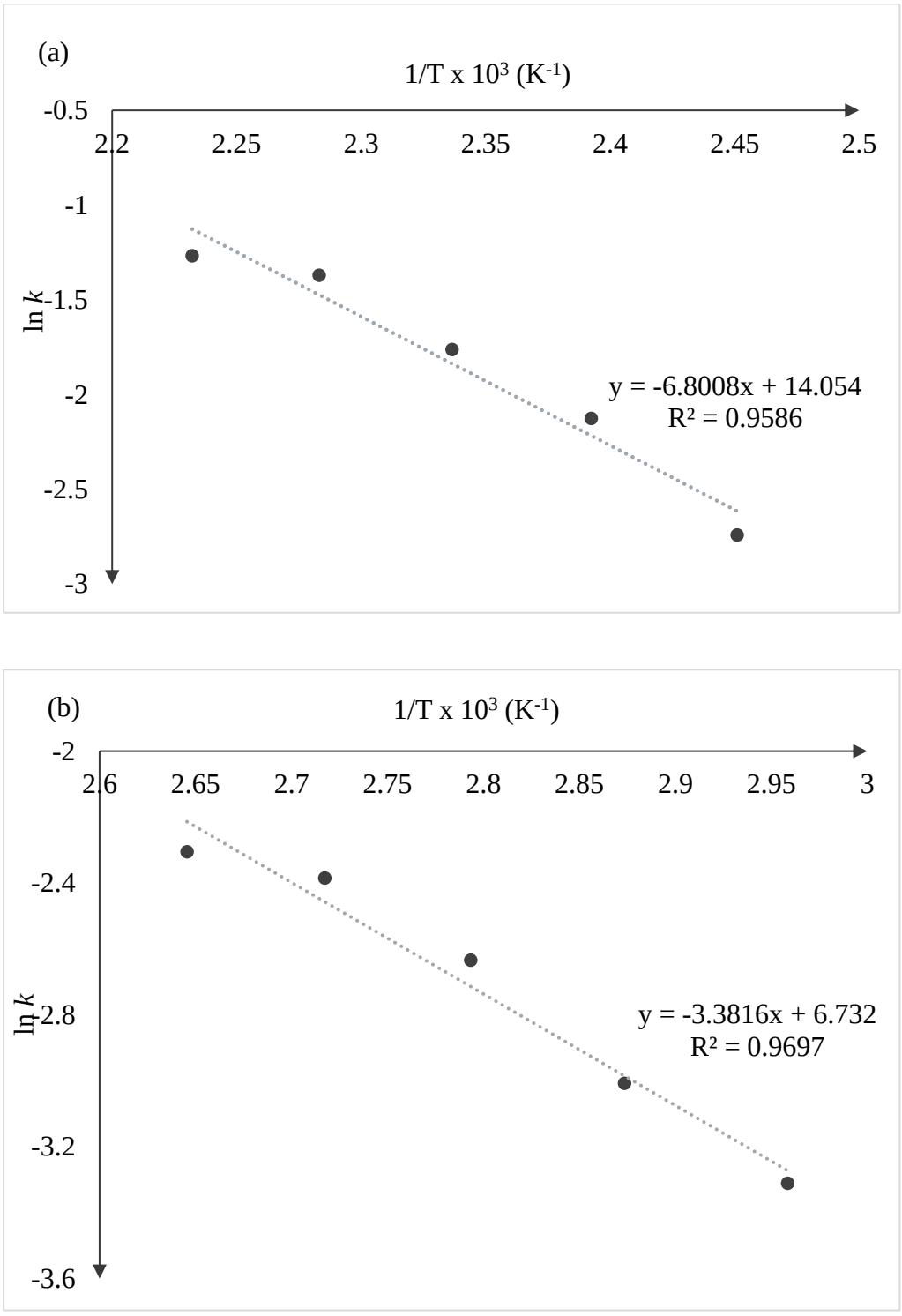



**Figure 7.4** Arrhenius plot of ln *k* versus 1/T for (a) cellulose depolymerisation to LA, and the (b) subsequent upgrading esterification to EL.

As depicted in **Table 7.2 (a)** and **(b)**, the $E_a$ value for the cellulose depolymerisation conducted via $InCl_3$-[HMIM][$HSO_4$] in the present study was lower than those of using mineral acids (HCl, $H_2SO_4$) [55], [130], [286], [308], [316]–[320], heterogeneous acid catalysts ($FeCl_3$) [56], [321], hybrid catalysts (Fe/HY zeolite) [294], mixed acid catalysts ($H_3PO_4$ and $CrCl_3$) [322] and BAILs with multi-acid sites [50], [323]. This lower $E_a$ value (56.5 kJ $mol^{-1}$) might be attributed to the adoption of mixed acid ILs catalytic system (BLAILs). Specifically, $InCl_3$ acts as a typical Lewis acid catalyst, bearing an ability to isomerise glucose into fructose [78]. Comparatively, fructose has consistently given better yields of LA and EL than glucose [59] in acid catalysed conversions of sugars. Meanwhile, the BAILs, [HMIM][$HSO_4$], having a Bronsted acidic property, is more efficient than the Lewis acid in the subsequent fructose dehydration to 5-HMF, followed by 5-HMF rehydration to LA [78]. In this context, the synergistic effect from both Bronsted and Lewis acidic sites enhances the catalytic activity and thus reduces the energy requirement [322], leading to a lower $E_a$ value. Noteworthy, the present system gave a rather similar $E_a$ value (difference of ~0.5%) to a recent work on using $SnCl_4$ for the conversion of corncobs to LA [324] (**Table 7.2a**). This infers that both Lewis acids $SnCl_4$ and $InCl_3$ contribute positive effect on the isomerisation of glucose to fructose. Furthermore, the $E_a$ value of the present system was higher than that of the direct conversion of glucose to LA via a mixed acid ILs catalytic system (BLAILs), [SMIM][$FeCl_4$] [313] (**Table 7.2b**). It was understood that the conversions from biomass feedstock generally requires harsher reaction

conditions, i.e. higher temperature and prolonged reaction time [78] due to its higher recalcitrance.

On the other hand, the subsequent upgrading for the EL synthesis reported a lower $E_a$ value (28.1 kJ $mol^{-1}$). The lower $E_a$ value indicates that the catalytic system consumes less energy and time as well as promotes the reaction rate and thus enhances the catalytic activity [325]. In comparison, the present $E_a$ value for the subsequent upgrading esterification (28.1 kJ $mol^{-1}$) was significantly lower than those reported on direct glucose conversion to EL via $H_2SO_4$ [207], [314]. The higher $E_a$ values in the $H_2SO_4$ system was perhaps caused by only a small portion of $H_2SO_4$ being involved in actual binding although a large number of collisions with the reactants occurred [326].

**Table 7.2** An overview of kinetic studies on LA synthesis.

**(a) A comparison of present study with other studies for the kinetics of LA synthesis from various biomass feedstock.**

| Feedstock | Cellulose content (%) | Catalyst | Temp. (°C) | Pre-exponential factor, A ($min^{-1}$) | Activation energy, $E_a$ ($kJ\ mol^{-1}$) | Ref. |
|---|---|---|---|---|---|---|
| *Miscanthus x giganteus*[#] | 40.7 | $H_2SO_4$ | 150-200 | Cel → Glc = $2.7 \times 10^{21}$<br>Glc → 5-HMF = $2.4 \times 10^{17}$<br>5-HMF → LA = $6.6 \times 10^{14}$ | Cel → Glc =188.9<br>Glc → 5-HMF = 155.5<br>5-HMF → LA = 121.3 | [55] |
| Sugarcane bagasse[#] | 43.3 | $H_2SO_4$ | 150-200 | Cel → Glc = $1.8 \times 10^{19}$<br>Glc → 5-HMF = $1.4 \times 10^{19}$<br>5-HMF → LA = $1.9 \times 10^{15}$ | Cel → Glc = 144.8<br>Glc → 5-HMF = 152.1<br>5-HMF → LA = 101.6 | [130] |
| Corncobs[#] | 35.4 | $H_2SO_4$ | 150-180 | Cel → Glc = $1.1 \times 10^{15}$<br>Glc → 5-HMF = $9.9 \times 10^{14}$<br>5-HMF → LA = $4.0 \times 10^{11}$ | Cel → Glc = 135.3<br>Glc → 5-HMF = 134.4<br>5-HMF → LA = 96.5 | [316] |
| Corn stalk[*] | 41.5 | $FeCl_3$ | 220-240 | Cel → LA = $7.1 \times 10^{13}$ | Cel → LA = 133.0 | [56] |

| | | | | | | |
|---|---|---|---|---|---|---|
| Corn stalk[#] | N.A. | $FeCl_3$ | 160-200 | Cel → Glc = 3.7 x $10^8$<br>Glc → 5-HMF = 1.8 x $10^{10}$<br>5-HMF → LA = 8.4 x $10^5$ | Cel → Glc = 77.6<br>Glc → 5-HMF = 93.3<br>5-HMF → LA = 42.9 | [321] |
| Wheat straw[#] | 40.4 | $H_2SO_4$ | 190-230 | Cel → Glc = 1.5 x $10^{10}$<br>Glc → 5-HMF = 1.5 x $10^5$<br>5-HMF → LA = 1.4 x $10^7$ | Cel → Glc = 78.7<br>Glc → 5-HMF = 54.5<br>5-HMF → LA = 56.5 | [286] |
| Corncobs[#] | 32.6 | $SnCl_4$ | 170-190 | Cel → Glc = 7.3 x $10^4$<br>Glc → 5-HMF = 4.2 x $10^4$<br>5-HMF → LA = 2.1 x $10^6$ | Cel → Glc = 48.2<br>Glc → 5-HMF = 46.0<br>5-HMF → LA = 57.0 | [324] |
| OPMF[*] | 30.0 | $InCl_3$-[HMIM][$HSO_4$] | 135-175 | Cel → LA = 1.3 x $10^6$ | Cel → LA = 56.5 | Present study |
| **(b) A comparison of present study with other studies for the kinetics of LA synthesis from cellulose and glucose.** | | | | | | |
| Glucose[*] | - | [$C_3SO_3$HMIM][$HSO_4$] | 160-180 | N.A. | Glc → LA = 202.0 | [50] |
| Cellulose[*] | - | [$BSO_3$HMIM][$HSO_4$] | 140-180 | N.A. | Cel → Glc = 186.8<br>Glc → LA = 114.0 | [323] |

| | | | | | | |
|---|---|---|---|---|---|---|
| Cellulose[#] | - | $H_2SO_4$ | 150-200 | N.A. | Cel → Glc = 151.5<br>Glc → 5-HMF = 152.2<br>5-HMF → LA = 110.5 | [319] |
| Glucose[#] | - | $H_2SO_4$ | 98-200 | N.A. | Glc → 5-HMF = 152.0<br>5-HMF → LA = 111.0 | [318] |
| Glucose[*] | - | $H_2SO_4$ | 98-181 | N.A. | Glc → LA = 111.0 | [308] |
| Glucose[#] | - | HCl | 90-130 | N.A. | Glc → Fructose = 77.0<br>Fructose → 5-HMF = 88.0<br>5-HMF → LA = 91.0 | [320] |
| Glucose[#] | - | $H_2SO_4$ | 170-210 | N.A. | Glc → 5-HMF = 86.0<br>5-HMF → LA = 57.0 | [317] |
| Glucose[#] | - | $H_3PO_4$ and $CrCl_3$ | 150-180 | Glc → 5-HMF = $9.2 \times 10^5$<br>5-HMF → LA = $2.9 \times 10^5$ | Glc → 5-HMF = 65.4<br>5-HMF → LA = 60.6 | [322] |
| Glucose[#] | - | Fe/HY zeolite | 120-200 | Glc → 5-HMF = $39.9 \times 10^4$<br>5-HMF → LA = $22.3 \times 10^4$ | Glc → 5-HMF = 64.0<br>5-HMF → LA = 61.0 | [294] |

| | | | | | | |
|---|---|---|---|---|---|---|
| Glucose[#] | - | [SMIM][$FeCl_4$] | 110-170 | Glc → 5-HMF = 3.72 x $10^2$<br>5-HMF → LA = 4.49 x $10^1$ | Glc → 5-HMF = 37.0<br>5-HMF → LA = 30.0 | [313] |
| **(c) A comparison of present study with other studies for the kinetics of EL synthesis from various feedstock.** | | | | | | |
| Glucose[*] | - | $H_2SO_4$ | 170-210 | 2.3 x $10^{13}$ | 123.3 | [314] |
| Glucose[*] | - | $H_2SO_4$/USY zeolite | 180-200 | 1.3 x $10^{10}$ | 79.9 | [207] |
| OPMF[*] | - | $InCl_3$-[HMIM][$HSO_4$] | Depolymerisation : 135-175<br>Esterification : 65-105 | Cel → EL = 838.8 | Cel → EL = 28.1 | Present study |

Cel – Cellulose; Glc – Glucose; 5-HMF – 5-hydroxymethylfurfural; LA – Levulinic acid; EL – Ethyl levulinate.

[*]Kinetic schemes are modelled based on one-pot production that excluded the individual reaction of other intermediates, as in the present study.

[#]Kinetic schemes are modelled based on several individual reaction schemes that involved the formation of intermediate products.

N.A. – Not available

Overall, the relatively lower $E_a$ values achieved in the present study highlights the kinetic feasibility of $InCl_3$-[HMIM][$HSO_4$] in the cellulose conversion to LA and upgrading to EL, where the reaction was conducted at a milder temperature and faster reaction rate than other studies (**Table 7.2**). Specifically, the present biomass conversion requires a higher energy transition state for the transformation of reactant into stable products. The polar active sites of the catalyst, that is, a cationic imidazolium positioned next to the oxygen of the breaking H-O bond, was proposed to stabilise the high energy transition state electrostatically relative to the bound substrate, akin to chorismate mutase catalysis [327]. In addition, the co-existence of inter- and intramolecular hydrogen bonding in the $InCl_3$-[HMIM][$HSO_4$] catalyst may also stabilise the transition state and thus lower the free energy barrier, resembling the function of sulphonate group in pyridinium-ILs [328]. The high energy transition state is also associated to the distortion of stable chair conformation, presumably facilitated by the flexibility of the glucose units in the biomass structure [329]. This change of conformation presumably stabilised by the ionic environment created allows the structure to be rearranged in order to reduce the reaction barrier, alongside the increased frequency and force of collisions between the molecules [329]. Finally, the molecules proceed through the remaining reactions to produce end products (LA and EL) favourably. The [$HSO_4$] anion of the catalyst is also believed to reduce the steric effect and enhance the reaction [326].

Furthermore, the fate of a reaction is categorised into kinetically controlled reaction with $E_a$ >14 kJ $mol^{-1}$ or diffusion limited reaction with $E_a$ <14 kJ $mol^{-1}$ [311]. The present study suggests the cellulose depolymerisation and

the subsequent upgrading esterification via $InCl_3$-[HMIM][$HSO_4$] to be categorised as kinetically controlled reactions, since high $E_a$ values of >14 kJ $mol^{-1}$ were obtained. A kinetically controlled reaction is conducted in the presence of a catalyst, where the reaction is fully catalysed to its optimum capacity to reach the highest reaction rate and full turnover synthesis of the desired chemical product, under appropriate reaction conditions [330].

### 7.3.3 Thermodynamic studies

As shown in **Figure 7.5**, the Eyring plots of ln ($k$/T) versus 1/T had good linear fits for the cellulose depolymerisation and the subsequent upgrading esterification. For both reactions, the $\Delta H^{\ddagger}$ values from the Eyring plots (**Figure 7.5**) were nearly equal, but with slightly less than the $E_a$ values from the Arrhenius plots (**Figure 7.4**). This was explained by the following relation:

$$\Delta H^{\ddagger} = E_a - RT \qquad (7.14)$$

where R is the gas constant and T is the absolute (thermodynamic) temperature.

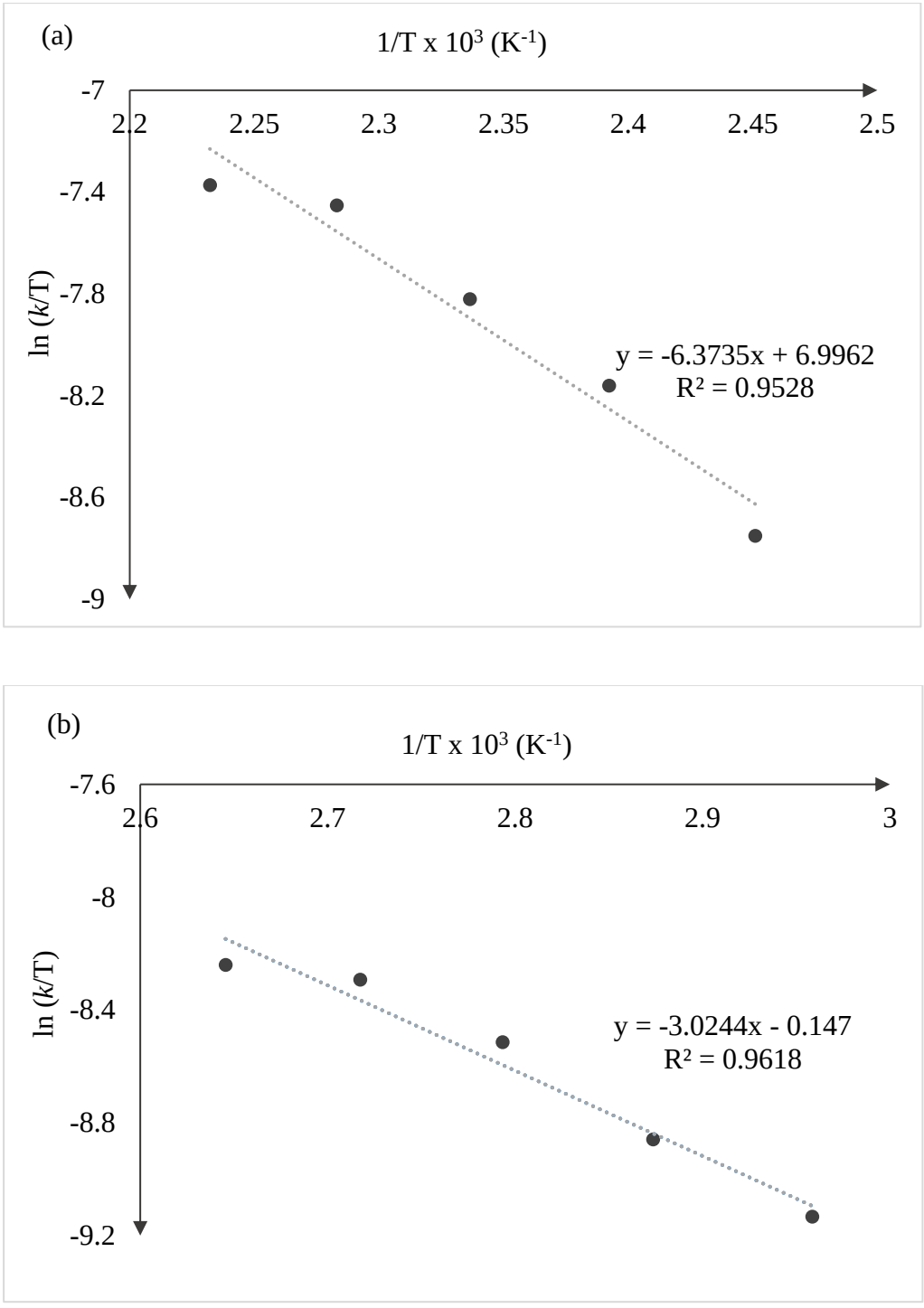



**Figure 7.5** Eyring plots of ln (*k*/T) versus 1/T for (a) cellulose depolymerisation to LA, and the (b) subsequent upgrading esterification to EL.

**Table 7.3** Thermodynamic parameters of cellulose depolymerisation and the subsequent upgrading esterification.

| Parameter | Reaction | |
|---|---|---|
| | Cellulose depolymerisation | Subsequent upgrading esterification |
| $\Delta H^{\ddagger}$ (kJ $mol^{-1}K^{-1}$) | +53.0 | +25.1 |
| $\Delta S^{\ddagger}$ (J $mol^{-1}K^{-1}$) | -139.4 | -172.4 |
| $R^2$ (Eyring plot) | 0.9528 | 0.9618 |
| $\Delta G^{\ddagger}$ (kJ $mol^{-1}$) | +115.5 (at 448 K) | +90.3 (at 378 K) |

In the present study, the value of RT was small relative to $E_a$ ($\Delta H^{\ddagger} \sim E_a$) thus an endothermic reaction was observed ($\Delta H^{\ddagger} > 0$) [331], [332]. The $\Delta H^{\ddagger}$ value refers to the events acquired to the transition state formation. Positive values of $\Delta H^{\ddagger}$ attained in both reactions (**Table 7.3**) show that heat input is necessary to bring the reactants to the transition state so as to form the products [333]. $\Delta S^{\ddagger}$ is associated with the formation of complex activated species [334]. A negative $\Delta S^{\ddagger}$ value infers the reaction between catalyst and substrate in forming the catalyst-substrate complex involves a substantial entropy loss, owing to the loss of the reactant and catalytic groups translational and rotational degrees of freedom [335]. Hence, the negative sign of $\Delta S^{\ddagger}$ obtained in both reactions (**Table 7.3**) indicated that the transition state had a more ordered structure than the reactants in the ground state [333]. Lastly, $\Delta G^{\ddagger}$ is the free energy of activation which indicates the energetic feasibility and spontaneity of a reaction [330]. Both reactions showed positive values of $\Delta G^{\ddagger}$ (**Table 7.3**), revealing that the reactions were energetically endergonic and unfavourable, and hence non-spontaneous.

The cellulose depolymerisation for the LA synthesis of the present $InCl_3$-[HMIM][$HSO_4$] catalytic system had a higher value of $\Delta H^{\ddagger}$ (+53 kJ $mol^{-1}K^{-1}$) compared to that reported by Ramli and Amin [313] for the conversion of glucose to LA via [SMIM][$FeCl_4$] (**Table 7.4**). A higher $\Delta H^{\ddagger}$ value implies a larger amount of stretching, squeezing and breaking down of the chemical bonds to reach the transition state [336], which indicates a less reactive catalytic system [334]. This scenario might due to the recalcitrance of biomass materials towards the depolymerisation reaction (refer to **Section 3.2**). In addition, a less negative $\Delta S^{\ddagger}$ value (-139.4 J $mol^{-1}K^{-1}$) was obtained in the present study, as compared to a previous work [313] (**Table 7.4**), signifying that more components are presented in the transition state, which gave a larger disorder to the system [334]. This was further explained by the fact that the ground state catalyst-substrate complex occupy a wider distribution of conformational states translated into an increased entropy of this state [337]. Finally, the $\Delta G^{\ddagger}$ value (+115.5 kJ $mol^{-1}$) attained in the present study was lower than a previous work [313] (**Table 7.4**), indicating a more energetically feasible reaction for cellulose depolymerisation to LA.

Contrastingly, the subsequent upgrading for the EL synthesis of the present $InCl_3$-[HMIM][$HSO_4$] catalytic system had a very low $\Delta H^{\ddagger}$ value (+25.1 kJ $mol^{-1}K^{-1}$) as compared to that reported by Badgujar and Bhanage [330] for the esterification reaction catalysed by enzymatic immobilised lipase (**Table 7.4**). In the present system, the conformational change to reach the transition state was presumably dominated by a decline in the number of enthalpy-driven interactions that needed to break during activation [338]. The breaking rendered

the corresponding part of catalyst more flexible for the reaction [337]. Consequently, less energy was required for the elongation and compression of chemical bonds to accomplish the transition state [336], inferring a more reactive catalytic system. A more negative $\Delta S^{\ddagger}$ value (-172.4 J $mol^{-1}K^{-1}$) was reported in the present study, as compared to a previous work [330] (**Table 7.4**), signifying a reduction in the extent of disorder, along with a more ordered environment. In this regard, the present system has a more complex rigidity and high stability, where the reaction took place easily via the formation of intermediate complex [339], leading to a more favourable way of EL synthesis. Lastly, the $\Delta G^{\ddagger}$ value (+90.3 kJ $mol^{-1}$) obtained in the present study was lower than another study [330] (**Table 7.4**), suggesting a more energetically feasible reaction for LA esterification to EL.

**Table 7.4** A comparison of present study with other studies for the thermodynamics of LA and EL syntheses.

| Feedstock | Catalyst | Temp. (°C) | $\Delta H^{\ddagger}$ (kJ $mol^{-1}K^{-1}$) | $\Delta S^{\ddagger}$ (J $mol^{-1}K^{-1}$) | $\Delta G^{\ddagger}$ (kJ $mol^{-1}$) | Ref. |
|---|---|---|---|---|---|---|
| Glc | [SMIM][$FeCl_4$] | 110-170 | Glc → 5-HMF = +33.6<br>5-HMF → LA = +22.6 | Glc → 5-HMF = -240<br>5-HMF → LA = -257.7 | Glc → 5-HMF = +128.2 (394 K)<br>5-HMF → LA = +128.4 (394 K) | [313] |
| OPMF | $InCl_3$-[HMIM][$HSO_4$] | 135-175 | Cel → LA = +53.0 | Cel → LA = -139.4 | Cel → LA = +115.5 (448 K) | Present study |
| LA | Immobilised lipase | 25-45 | +79.7 | -76.3 | +103.1 (306 K) | [330] |
| OPMF | $InCl_3$-[HMIM][$HSO_4$] | Depolymerisation : 135-175<br>Esterification : 65-105 | Cel → EL = +25.1 | Cel → EL = -172.4 | Cel → EL = +90.3<br>(Depolymerisation: 448K, then Esterification: 378 K) | Present study |

Glc – Glucose; 5-HMF – 5-hydroxymethylfurfural; LA – Levulinic acid; EL – Ethyl levulinate.

## 7.4 Concluding Remarks

This chapter investigated the kinetic and thermodynamic studies on the OPMF cellulose conversion to LA and upgrading to EL via a new environmentally friendly coupling mixed acids $InCl_3$-[HMIM][$HSO_4$] catalytic system. Both reactions fitted well to the pseudo-first-order kinetic model, with $E_a$ values of 56.5 kJ $mol^{-1}$ and 28.1 kJ $mol^{-1}$, respectively. The thermodynamic activation parameters were determined for energy assessment based on the Eyring equation. The $\Delta G^{\ddagger}$ for cellulose depolymerisation and the subsequent upgrading esterification were +115.5 kJ $mol^{-1}$ and +90.3 kJ $mol^{-1}$, respectively. Both $\Delta G^{\ddagger}$ and $E_a$ values of the present system were lower than those reported for mineral acids, heterogeneous acid catalysts and SFILs systems, indicating that the system was relatively more energetically and kinetically feasible. This study provides the fundamental information for scaled-up reactor design and process development of catalytic biomass conversion to LA and EL via $InCl_3$-[HMIM][$HSO_4$] catalytic system.

.

# Chapter 8

# Recyclability studies of $InCl_3$-[HMIM][$HSO_4$]

## 8.1 Introduction

In terms of green and sustainable chemistry, catalyst recycling is crucial for reducing the costs and environmental impacts of chemicals which could provide a more sustainable manufacturing or application of bio-based chemical products. Hence, recyclability test runs on this new environmentally friendly coupling mixed acids $InCl_3$-[HMIM][$HSO_4$] catalytic system were carried out. This study aims to maximise the production yield without sacrificing the process sustainability.

## 8.2 Methodology

### 8.2.1 Materials

The preparation of oil palm biomass (OPEFB and OPMF) and chemicals involved have been reported in **Chapter 3.2.1** and **4.2.1**.

### 8.2.2 Biomass conversion reaction, products isolation and analysis, and ILs recovery

The experimental procedures of biomass conversion reaction, i.e. depolymerisation to LA, and the subsequent upgrading esterification to EL, followed by the subsequent products isolation and analysis, have been reported previously, as in **Chapter 4.2.2**, **4.2.3** and **4.2.4**, accordingly. As for the ILs ($InCl_3$-[HMIM][$HSO_4$]) recovery, distilled water (30 ml) was added into the

aqueous layer and the biomass residue was filtered. The used ILs was recovered by drying the aqueous solution overnight at 105°C, followed by vacuum drying at 60°C for 24 h to completely remove water. The recovered ILs was used directly in the repeated runs to check the reusability. All experiments were conducted in triplicate, to test on its reproducibility. The fresh and reused ILs were characterised by viscosity, $^{1}$H NMR, and FTIR/ATR analyses. The viscosity was measured using a Brookfield AMETEK viscometer (LVDVE230, USA) at temperatures ranging from 293 to 353 K at 1 atm. For $^{1}$H NMR analysis, 30 mg of ILs was dissolved in 600 µl of $D_2O$ in the NMR tube at 25°C using a Bruker/Advance III HD 400 MHz NMR spectrometer. For FTIR/ATR analysis, the spectra were acquired using a PerkinElmer® Frontier FT Mid-IR spectrometers operating with a Golden Gate TM diamond ATR accessory.

### 8.2.3 Products analysis

The EL content was determined by using a GC-MS (Perkin Elmer Clarus 680), as described in **Chapter 4.2.4**. The standard errors of triplicate data obtained for all yields ranged within 0.5-1.6%. The calculation formulas for both the LA and EL yields have been reported previously, as in **Eq. 5.1** and **Eq. 4.1,** respectively.

## 8.3 Results and Discussion

### 8.3.1 Recyclability test runs on the efficiency of EL production

**Figure 8.1** shows that the recycled $InCl_3$-[HMIM][$HSO_4$] managed to retain 76-80% of the efficiencies in terms of EL yields for the first three consecutive runs, signifying the potential reusability of the catalyst. In the

subsequent cycles, the efficiencies declined to 45-69%. In the final test run, only <25% efficiencies were retained for both biomass conversions.

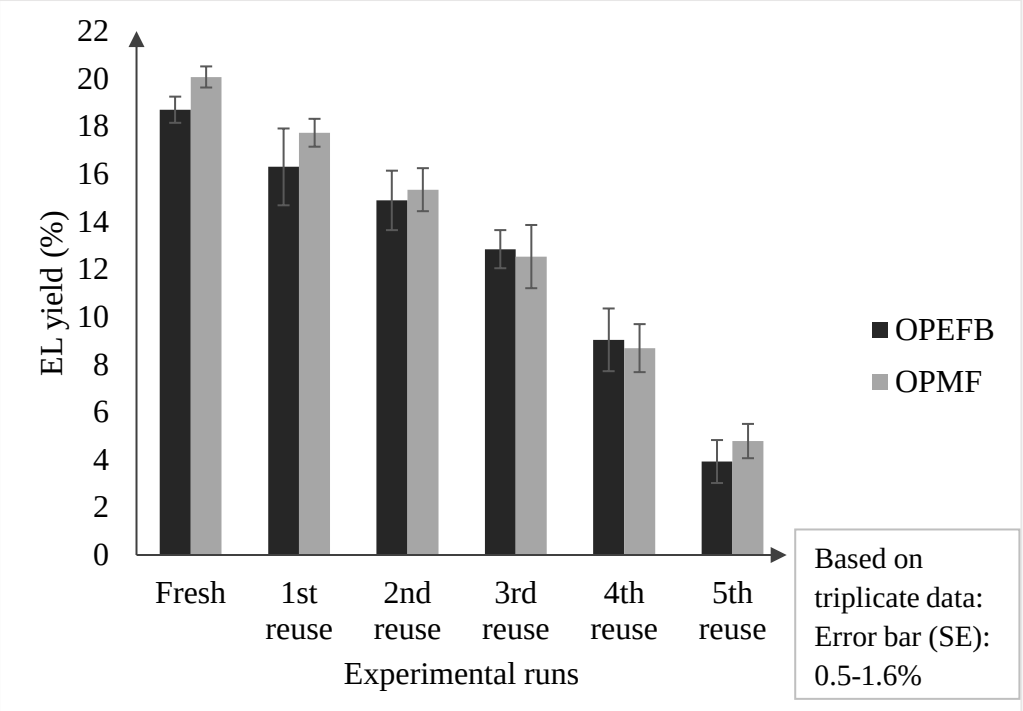



**Figure 8.1** The performance of recycled $InCl_3$-[HMIM][$HSO_4$] on the EL yields from the conversions of OPEFB and OPMF biomass compared to the fresh ILs. (Depolymerisation: ILs-to-biomass ratio of 6.6:1 (w/w), 0.15 mmol $InCl_3$, 177°C, 4.8h and 22.7% (w/w) water; Esterification: 105°C, 12.2 h and ethanol to substrate ratio of 7.2:1 (v/v)).

The colour of ILs was significantly changed from the initial light yellow to dark brown at the fifth cycle (**Figure 8.2**), which was likely contaminated by degradation products of ILs and lignocelluloses, as well as added chemicals, solvents, and water [340]. Along the cycles, the number of available active sites of ILs were reasonably reduced due to repeated filtration and washing after each recovery [138].

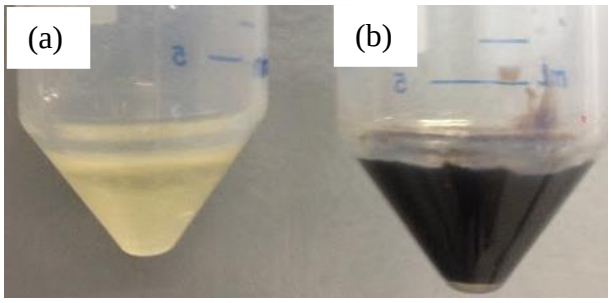



**Figure 8.2** The colour change between the (a) fresh ILs (light yellow) and (b) reused ILs for the fifth cycle (dark brown).

The viscosity of the recycled ILs was significantly increased along the cycles (**Figure 8.3**), which was likely caused by the presence of the ILs soluble humins precursors [276]. These unreacted feedstock or organic molecules (humins and polymers) might also give unfavourable effects that reduce the functionality of the ILs.

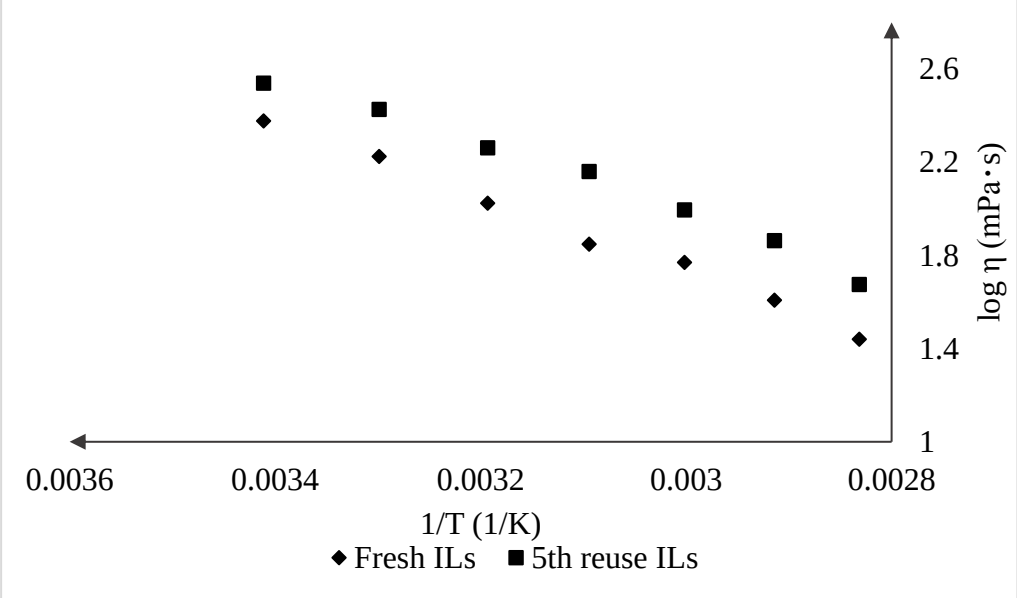
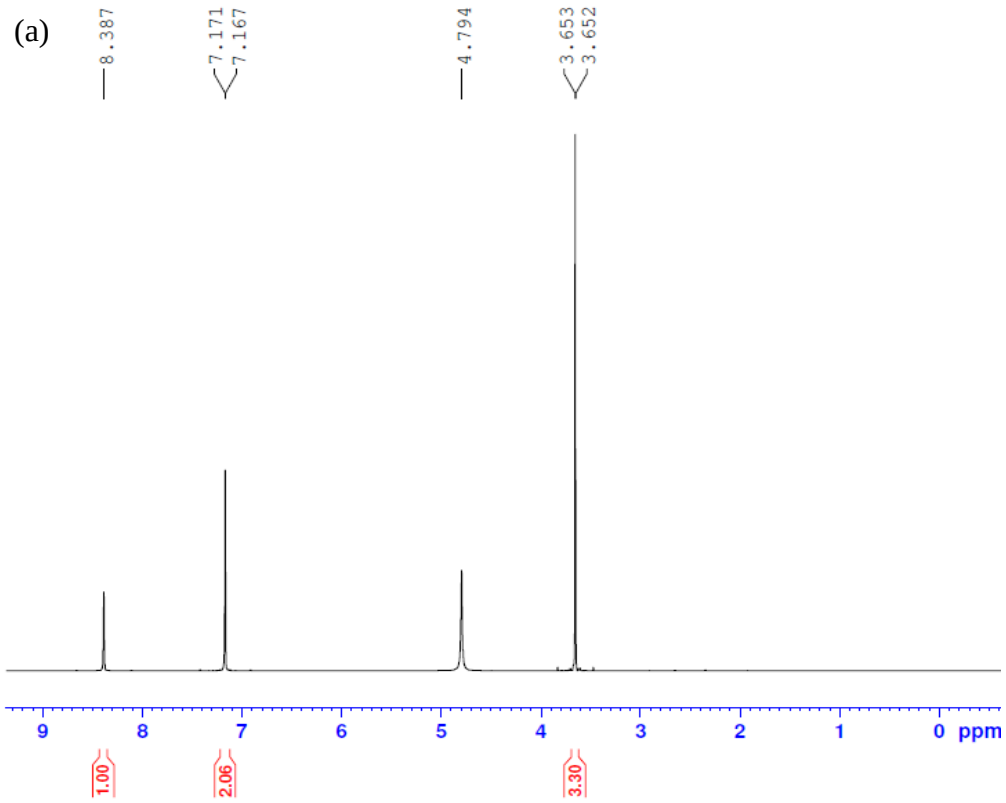



**Figure 8.3** Temperature effect on the viscosities of fresh ILs and reuse ILs for the fifth cycle.

Even so, the $^{1}$H NMR spectra of the fifth-cycled ILs was still featured by four proton signals the same as the fresh IL (**Figure 8.4**) with no additional peaks observed, suggesting that the ILs did not decompose significantly. Noteworthy, all four proton signals showed slightly broader peaks (**Figure 8.4b**), signifying the recycled ILs contains some impurities, mostly from the recovery process. The broadening of peaks (**Figure 8.4b**) is specifically due to the slow exchange of protons from the ILs. This is owing to the weakening of the ILs acidity (the presence of the hydrogen atom attached to carbon flanked between two nitrogen atoms) along the consecutive recycling process. This observation was in accordance with Matsagar and Dhepe [278]. However, the appearance of all the peaks in the $^{1}$H NMR spectra of recycled ILs that correspond to those of fresh ILs suggested that the ILs are stable under the reaction conditions.

(a)


8.387
7.171
7.167
4.794
3.653
3.652
9
8
7
6
5
4
3
2
1
0 ppm
1.00
2.06
3.30

(b)

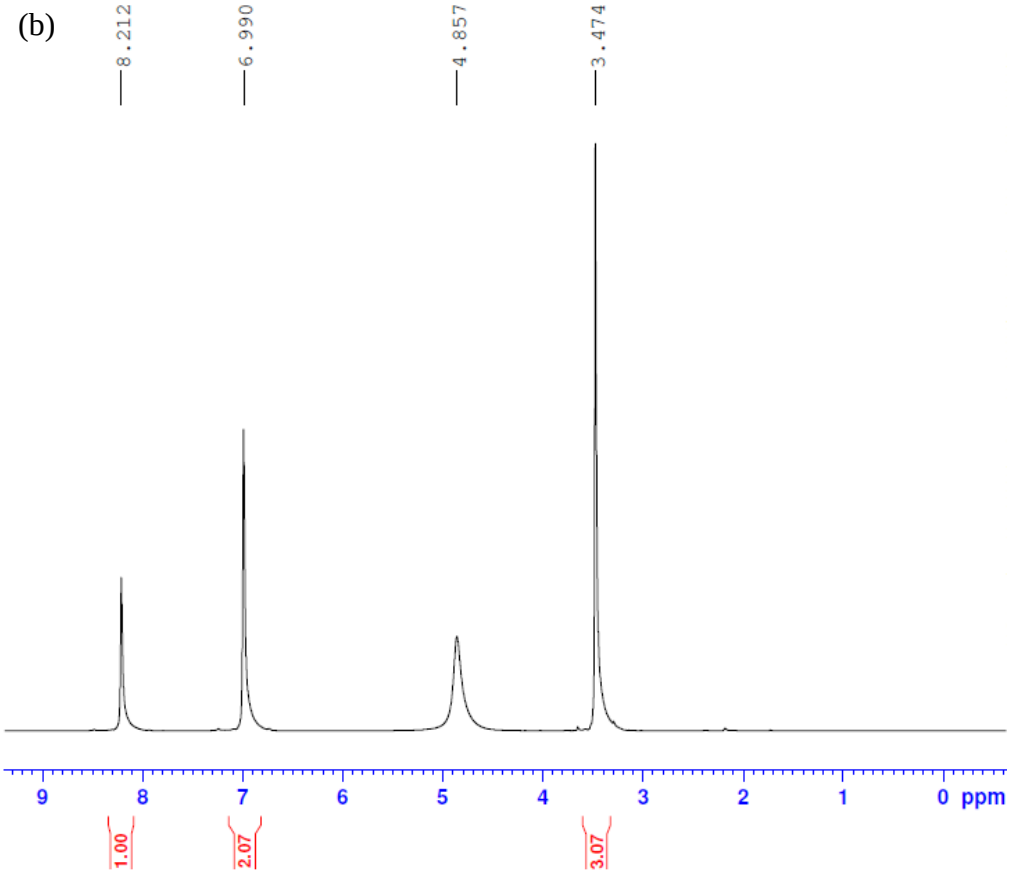

8.212
6.990
4.857
3.474
9
8
7
6
5
4
3
2
1
0 ppm
1.00
2.07
3.07

**Figure 8.4** $^{1}H$ NMR spectra of $InCl_3$-[HMIM][$HSO_4$] in $D_2O$ (a) fresh ILs and (b) reuse ILs for the fifth cycle.

The absorption bands of the fifth-cycled ILs were slightly shifted in FTIR/ATR analysis, but not to a great extent (**Figure 8.5**), further confirming that the ILs were stable in which the original chemical structure was maintained. The corresponding absorption FTIR spectra peaks was depicted in **Table 8.1**. In comparison, at absorption band of 2900 $cm^{-1}$ and 2700 $cm^{-1}$, the peaks of the fifth-cycled ILs become less significant, signifying the relative absorption intensity decreased upon ILs-catalysed biomass conversion to EL. Nonetheless, two new absorption peaks were detected at 1740 $cm^{-1}$ and 1695 $cm^{-1}$ for the fifth-cycled ILs. This results revealed that the recycled ILs could have degraded to decomposition products, regards to the presence of new functional groups (saturated aldehyde and primary amide) [185], thus causing a loss in efficiency. Noteworthy, at low absorption bands (1000-500 $cm^{-1}$), the fifth-cycled ILs shifted as compared to the fresh ILs, signifying the chemical structure of the recycled ILs has transformed and thus is not as pure as the fresh ones. In this regard, this could have been the solid reason for the efficiency loss of <25% efficiencies at the fifth-cycled ILs for the biomass conversion to EL.

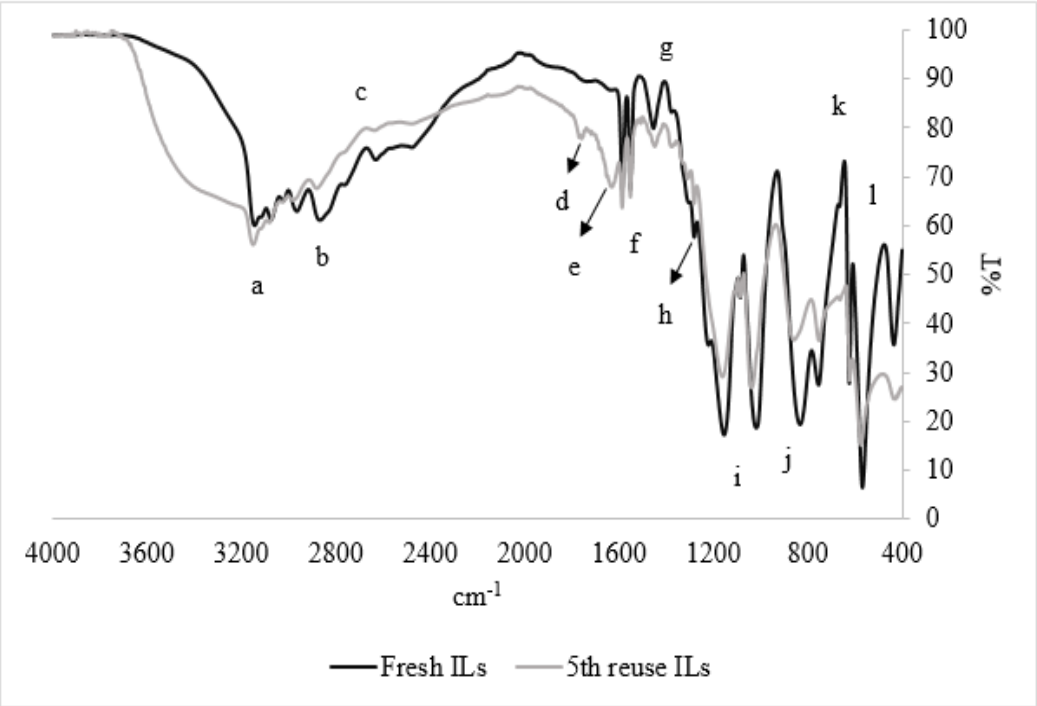



**Figure 8.5** FTIR/ATR spectroscopy for fresh ILs and reused ILs for the fifth cycle.

**Table 8.1** Infrared spectra and band assignments for fresh ILs and reused ILs for the fifth cycle.

| Label | Infrared band ($cm^{-1}$) | Band assignments* |
|---|---|---|
| a | 3200 | O-H (alcohol) |
| b | 2900 | C-H (alkane) |
| c | 2700 | C-H (aldehyde) |
| d | 1740 | C=O (saturated aldehyde) |
| e | 1695 | C=O, C=C (primary amide) |
| f | 1600-1550 | N-O (nitro compound) |
| g | 1500-1400 | C-H (methyl alkane) |
| h | 1300 | C-O (aromatic ester) |
| i | 1200-1085 | C-O (aliphatic ester) |

| | | |
|---|---|---|
| j | 1000-800 | C=C (alkene) |
| k | 730-665 | C=C (alkene) |
| l | 600-500 | C-Cl (halo compound) |

*The band assignments for the functional groups was based on Adel et al. [258] and Muhammad et al. [185].

Aside from that, according to Keil et al. [341], the decomposition of alkylimidazolium cation of the ILs occurs via three mechanisms, as shown in **Figure 8.6**. First, a reverse reaction of the quaternization occurs, causing the formation of at least two equivalents of volatiles (**Reaction 8.1**, **Figure 8.6**). Second, the previous dealkylated cation is realkylated with an anion. The resulted cations may carry the same type of alkyl chain, or two cations may exchange their alkyl chains (**Reaction 8.2**, **Figure 8.6**). Lastly, the C2-atom of the fused ring of imidazolium-derived cations is protonised by strong nucleophiles causing decomposition (**Reaction 8.3**, **Figure 8.6**). These scenarios activate the resulting carbenes and hence they react with dissolved decomposition products in the liquid phase and reduce the efficiencies of LA and EL productions. Nonetheless, these contaminants from decomposition products cannot be spotted through solely NMR or FTIR analysis. For specifying the contaminants produced, a combination of a few techniques are required. Specifically, a compound is identified by matching its proton and/or carbon NMR spectra to NIH PubChem molecular structures. The matching process involves analysing 1D proton, 1D carbon, Distortionless Enhancement by Polarization Transfer (DEPT), and/or Heteronuclear single quantum coherence

spectroscopy (HSQC) spectra, as well as comparing the number of NMR resonances, detected proton and carbon shifts.

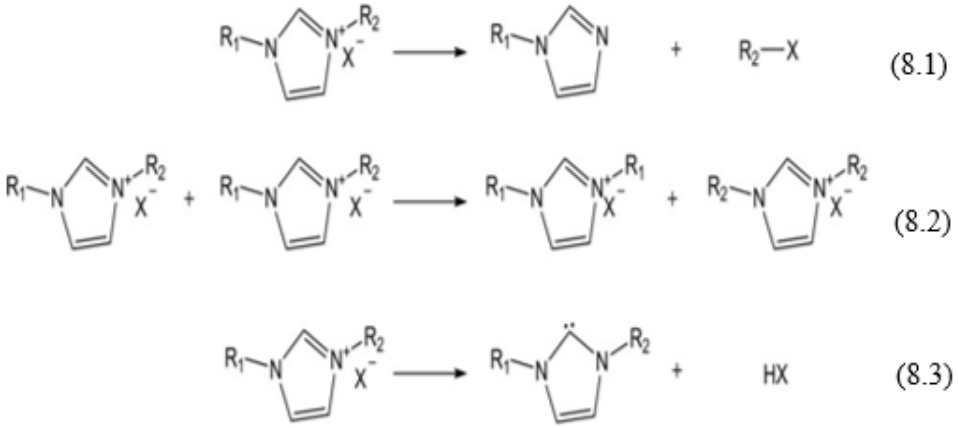



**Figure 8.6** Decomposition mechanisms of dialkylimidazolium cations.

## 8.4 Concluding Remarks

A new environmentally friendly coupling mixed acids $InCl_3$-[HMIM][$HSO_4$] catalytic system managed to retain >76% of efficiencies for both OPEFB and OPMF biomass conversions to EL for the first three consecutive runs, signifying the potential reusability of the catalyst. There was approximate 25% loss of its capability owing to several possibilities: (1) contamination from the degradation products of $InCl_3$-[HMIM][$HSO_4$], lignocelluloses, added chemicals, solvents, and water, (2) number of available active sites of $InCl_3$-[HMIM][$HSO_4$] were reduced due to repeated filtration and washing steps after each recovery, and (3) the recycled $InCl_3$-[HMIM][$HSO_4$] became more viscous owing to the presence of the soluble humins precursors. As for the characterisation studies on the structural changes between the fresh

and fifth reused $InCl_3$-[HMIM][$HSO_4$], both the $^1H$ NMR and FTIR/ATR analyses did not show great changes. This further suggested that the structure of the fifth reused $InCl_3$-[HMIM][$HSO_4$] did not degrade significantly and thus was still considered stable by means of its original chemical structure.

# Chapter 9

# Conclusions and Recommendations

## 9.1 Conclusions

This study has reported on a new environmentally friendly coupling mixed acids BLAILs catalytic system, i.e. $InCl_3$-[HMIM][$HSO_4$], for the catalytic conversions of OPEFB and OPMF biomass to LA and upgrading to EL. This newly developed BLAILs was made up of a noncorrosive sole acidic [$HSO_4$] anion mono-alkylated BAILs ([HMIM][$HSO_4$]) and an eco-friendly Lewis acid $InCl_3$.

At the beginning of this study, the thermal degradation TGA analysis, followed by cellulose and hemicellulose characterisation studies, revealed that OPEFB and OPMF contains 4.3-4.4% moisture, 16.3-18.5% lignin, 18.9-23.1% ash, 30-33.2% cellulose and 25-26.3% hemicellulose. As for the ILs physical properties studies, the mono-alkylated ILs, [HMIM][$HSO_4$] showed higher density and thermal stability, as well as stronger acidity and lesser viscosity.

In the screening and selection for the best catalytic activity of ILs, [HMIM][$HSO_4$] exhibited better catalytic activity of EL yields (+9.5-11.2%) than the longer chain alkylated BAILs, [BMIM][$HSO_4$]. In contrast, the neutral based ILs, [BMIM][Cl], was incapable of producing EL. Therefore, [HMIM][$HSO_4$] was selected for further studies, i.e. statistical analysis, reaction optimisation, kinetic, thermodynamic as well as its recyclability test runs on the catalytic conversion activity.

The statistical analysis and reaction optimisation studies reported on the $InCl_3$-[HMIM][$HSO_4$] catalytic system for the conversions of OPEFB and OPMF biomass to LA and upgrading to EL, by using a RSM based on a CCD method. The ANOVA results indicated that all LA and EL models were statistically significant. The lack of fit F-value for all responses (LA and EL) were insignificant relative to the pure error, indicating good fitting of the proposed models, and thus were reliable tools for predicting LA and EL yields. The optimum conditions for the depolymerisation was achieved at 177°C in 4.8 h, with 0.15 mmol of $InCl_3$, 6.6:1 (w/w) of ILs-to-biomass ratio and 22.7% (w/w) of water content. The maximum LA yields were 17.7% and 18.4%, with the corresponding LA efficiencies of 74.1% and 86.4%, for the conversions from OPEFB and OPMF biomass, respectively. Whilst, the subsequent esterification reaction was achieved at 105°C in 12.2 h with 7.2:1 (v/v) of ethanol to substrate ratio. The maximum EL yields were 18.7% and 20.1%, the corresponding EL efficiencies were 63.2% and 75.3%, for the conversions from OPEFB and OPMF biomass, respectively. The results suggested that $InCl_3$-[HMIM][$HSO_4$] offers a better or comparable catalytic activity to other various ILs catalytic system in various biomass conversions to LA and EL [7], [73], [74], [83], [85], [89]. Noteworthy, the recycled feedstock cannot be further improved the yield, as the remained feedstock are significantly less and in dark charcoal colour, thus would be considered as ash.

Additionally, this work also investigated the kinetic and thermodynamic parameters on the conversion of OPMF cellulose to LA and upgrading to EL via $InCl_3$-[HMIM][$HSO_4$] catalytic system. The kinetic results showed that both

reactions of cellulose depolymerisation and the subsequent upgrading esterification were pseudo-homogenous first-order, with $E_a$ values of 56.5 kJ $mol^{-1}$ and 28.1 kJ $mol^{-1}$, respectively. As for the thermodynamic study, the $\Delta G^{\ddagger}$ for cellulose depolymerisation and the subsequent upgrading esterification were +115.5 kJ $mol^{-1}$ and +90.3 kJ $mol^{-1}$, respectively. Both $\Delta G^{\ddagger}$ and $E_a$ values of the present system were lower than those reported for mineral acids, heterogeneous acid catalysts and SFILs systems, indicating that the present $InCl_3$-[HMIM][$HSO_4$] catalytic system was relatively more energetically and kinetically feasible.

Finally, $InCl_3$-[HMIM][$HSO_4$] catalyst managed to be recycled up to three consecutive runs with a minimal loss of <25% of EL yield, signifying the potential reusability of the catalyst. To sum up, $InCl_3$-[HMIM][$HSO_4$] catalytic system have facilitated the steps of biomass pretreatment, hydrolysis, isomerisation, dehydration and rehydration reactions to LA, then esterification reaction to EL, via one-pot production. The results revealed the potential and feasibility of this new environmentally friendly coupling $InCl_3$-[HMIM][$HSO_4$] catalytic system for biorefinery processing of OPEFB and OPMF biomass in a greener and more sustainable approach for the production of LA and EL under adequate process conditions.

## 9.2 Recommendations

As $InCl_3$-[HMIM][$HSO_4$] offers new environmentally friendly coupling mixed acids BLAILs catalytic system for the productions of LA and EL, there

are several possibilities for further exploration by using this novel coupling catalytic system. As such, the recommendations for future works are as follows:

**1) Alcohol effect and the related detailed catalytic mechanism studies.**

- Studies on the mechanism of the different branched chain alcohol effect could contribute an influence on the formation of intermediates and their further transformation via the hydrogen bonds formed with $InCl_3$-[HMIM][$HSO_4$], based on a study reported on fructose dehydration to 5-HMF in [EMIM][Cl]/ alcohol catalytic system [342]. This is owing to the difference in polarity and the existence of steric hindrance from different branched chain alcohols could lead to variations in forming the hydrogen bonds with $InCl_3$-[HMIM][$HSO_4$]. Furthermore, a detailed catalytic mechanism which involves all the key intermediates in the pathway could be identified by studying FTIR, $^{1}$H NMR, $^{13}$C NMR, 2D NMR and HR-ESI-MS spectra of $InCl_3$-[HMIM][$HSO_4$] catalysed transformations of C-1 and C-2 $^{13}$C labelled D-glucose (as the model of biomass) under the optimised reaction conditions obtained in the present study.

**2) A comprehensive techno-economic analysis.**

- A conceptual process integration and techno-economic analysis of plausible biorefinery schemes of biomass conversion to LA and EL via $InCl_3$-[HMIM][$HSO_4$] catalytic system can be conducted. This study involves the biorefinery process design and simulation

framework, yield models of processes in $InCl_3$-[HMIM][$HSO_4$]-biorefinery catalytic system. It includes the investigation of the design and modelling of the integrated processes of biomass conversion by evaluating the process yields and economic profit criteria. The analysis involves process simulation and a hybrid optimization framework which includes a two layer optimization strategy composed of strategic and operational level decisions. The results could reveal the identification of major parameters that determine techno-economic feasibility and independence for successful commercialisation.

**3) A theoretical elucidation study.**

- A density functional theory (DFT) aims to understand the fundamental reaction chemistry of the $InCl_3$-[HMIM][$HSO_4$]-promoted conversion. The theoretical results would provide a clear elementary-step mechanism profile (e.g. reactants, intermediates, transition states, and products) of the biomass conversion to LA and EL via $InCl_3$-[HMIM][$HSO_4$] catalytic system.

## References


[1] L. Hu, L. Lin, Z. Wu, S. Zhou, and S. Liu, "Recent advances in catalytic transformation of biomass-derived 5-hydroxymethylfurfural into the innovative fuels and chemicals," *Renew. Sustain. Energy Rev.*, vol. 74, pp. 230–257, 2017.

[2] A. Mukherjee, M.-J. Dumont, and V. Raghavan, "Review: Sustainable production of hydroxymethylfurfural and levulinic acid: Challenges and opportunities," *Biomass and Bioenergy*, vol. 72, pp. 143–183, 2015.

[3] R. A. Sheldon, "Green chemistry, catalysis and valorization of waste biomass," *J. Mol. Catal. A Chem.*, vol. 422, pp. 3–12, 2016.

[4] A. Corma, S. Iborra, and A. Velty, "Chemical routes for the transformation of biomass into chemicals," *Chem. Rev.*, vol. 107, no. 6, pp. 2411–2502, 2007.

[5] M. Tripathi, J. N. Sahu, and P. Ganesan, "Effect of process parameters on production of biochar from biomass waste through pyrolysis: A review," *Renew. Sustain. Energy Rev.*, vol. 55, pp. 467–481, 2016.

[6] C. Chatterjee, F. Pong, and A. Sen, "Chemical conversion pathways for carbohydrates," *Green Chem.*, vol. 17, pp. 40–71, 2015.

[7] N. A. S. Ramli and N. A. S. Amin, "Optimization of biomass conversion to levulinic acid in acidic ionic liquid and upgrading of levulinic acid to ethyl levulinate," *BioEnergy Res.*, vol. 10, no. 1, pp. 50–63, 2016.

[8] C. Chang, G. Xu, and X. Jiang, "Production of ethyl levulinate by direct conversion of wheat straw in ethanol media," *Bioresour. Technol.*, vol. 121, pp. 93–99, 2012.

[9] J. Feng *et al.*, "Preparation of methyl levulinate from fractionation of direct liquefied bamboo biomass," *Appl. Energy*, vol. 154, pp. 520–527, 2015.

[10] R. Le Van Mao, Q. Zhao, G. Dima, and D. Petraccone, "New process for the acid-catalyzed conversion of cellulosic biomass (AC3B) into alkyl levulinates and other esters using a unique one-pot system of reaction and product extraction," *Catal. Letters*, vol. 141, no. 2, pp. 271–276, 2011.

[11] E. Koivisto, N. Ladommatos, and M. Gold, "Compression ignition and exhaust gas emissions of fuel molecules which can be produced from lignocellulosic biomass: Levulinates, valeric esters, and ketones," *Energy & Fuels*, vol. 29, pp. 5875–5884, 2015.

[12] H. Mahmood, M. Moniruzzaman, S. Yusup, and H. M. Akil, "Pretreatment of oil palm biomass with ionic liquids: a new approach for fabrication of green composite board," *J. Clean. Prod.*, vol. 126, pp. 677–685, 2016.

[13] T. Lei *et al.*, "Performance and emission characteristics of a diesel engine running on optimized ethyl levulinate–biodiesel–diesel blends," *Energy*, vol. 95, pp. 29–40, 2016.

[14] J. J. Bozell and G. R. Petersen, "Technology development for the production of biobased products from biorefinery carbohydrates—the US Department of Energy's 'Top 10' revisited," *Green Chem.*, vol. 12, no. 4, pp. 539–554, 2010.

[15] A. Démolis, N. Essayem, and F. Rataboul, "Synthesis and applications of alkyl levulinates," *ACS Sustain. Chem. Eng.*, vol. 2, pp. 1338–1352, 2014.

[16] M. Kang, S. W. Kim, J.-W. Kim, T. H. Kim, and J. S. Kim, "Optimization of levulinic acid production from Gelidium amansii," *Renew. Energy*, vol. 54, pp. 173–179, Jun. 2013.

[17] D. W. Rackemann and W. O. Doherty, "The conversion of lignocellulosics to levulinic acid," *Biofuels, Bioprod. Biorefining*, vol. 5, no. 2, pp. 198–214, 2011.

[18] A. Morone, M. Apte, and R. A. Pandey, "Levulinic acid production from renewable waste resources: Bottlenecks, potential remedies, advancements and applications," *Renew. Sustain. Energy Rev.*, vol. 51, pp. 548–565, 2015.

[19] D. R. Fernandes, a. S. Rocha, E. F. Mai, C. J. a Mota, and V. Teixeira Da Silva, "Levulinic acid esterification with ethanol to ethyl levulinate production over solid acid catalysts," *Appl. Catal. A Gen.*, vol. 425–426, pp. 199–204, 2012.

[20] A. Phanopoulos, A. J. P. White, N. J. Long, and P. W. Miller, "Catalytic Transformation of Levulinic Acid to 2-Methyltetrahydrofuran Using Ruthenium - N-Triphos Complexes," *ACS Catal.*, vol. 5, no. 4, pp. 2500–2512, 2015.

[21] S. G. Wettstein, D. M. Alonso, Y. Chong, and J. a. Dumesic, "Production of levulinic acid and gamma-valerolactone (GVL) from cellulose using GVL as a solvent in biphasic systems," *Energy Environ. Sci.*, vol. 5, no. 8, pp. 8199–8203, 2012.

[22] K. Kon, W. Onodera, and K. Shimizu, "Selective hydrogenation of levulinic acid to valeric acid and valeric biofuels by a Pt/HMFI catalyst.," *Catal. Sci. Technol.*, vol. 4, no. 9, pp. 3227–3234, 2014.

[23] J. P. Lange *et al.*, "Valeric biofuels: A platform of cellulosic transportation fuels," *Angew. Chemie - Int. Ed.*, vol. 49, no. 26, pp. 4479–4483, 2010.

[24] M. Mascal, S. Dutta, and I. Gandarias, "Hydrodeoxygenation of the angelica lactone dimer, a cellulose-based feedstock: Simple, high-yield synthesis of branched C7-C10 gasoline-like hydrocarbons," *Angew. Chemie - Int. Ed.*, vol. 53, no. 7, pp. 1854–1857, 2014.

[25] Z. W. Wang, T. Z. Lei, L. Liu, J. L. Zhu, X. F. He, and Z. F. Li, "Performance investigations of a diesel engine using ethyl levulinate-diesel blends," *BioResources*, vol. 7, no. 4, pp. 5972–5982, 2012.

[26] B. C. Windom, T. M. Lovestead, M. Mascal, E. B. Nikitin, and T. J. Bruno, "Advanced distillation curve analysis on ethyl levulinate as a diesel fuel oxygenate and a hybrid biodiesel fuel," *Energy & Fuels*, vol. 25, no. 4, pp. 1878–1890, 2011.

[27] E. Christensen, A. Williams, S. Paul, S. Burton, and R. L. McCormick, "Properties and performance of levulinate esters as diesel blend components," *Energy and Fuels*, vol. 25, no. 11, pp. 5422–5428, 2011.

[28] X. Tang, Y. Sun, X. Zeng, W. Hao, L. Lin, and S. Liu, "Novel process for the extraction of ethyl levulinate by toluene with less humins from the ethanolysis products of carbohydrates," *Energy & Fuels*, vol. 28, pp. 4251–4255, 2014.

[29] H. Li, L. Peng, L. Lin, K. Chen, and H. Zhang, "Synthesis, isolation and characterization of methyl levulinate from cellulose catalyzed by extremely low concentration acid," *J. Energy Chem.*, vol. 22, no. 6, pp. 895–901, Nov. 2013.

[30] Y. Kuwahara, W. Kaburagi, K. Nemoto, and T. Fujitani, "Esterification of levulinic acid with ethanol over sulfated Si-doped $ZrO_2$ solid acid catalyst: Study of the structure–activity relationships," *Appl. Catal. A Gen.*, vol. 476, pp. 186–196, Apr. 2014.

[31] Y. Qu, Q. Wei, H. Li, P. Oleskowicz-Popiel, C. Huang, and J. Xu, "Microwave-assisted conversion of microcrystalline cellulose to 5-hydroxymethylfurfural catalyzed by ionic liquids," *Bioresour. Technol.*, vol. 162, pp. 358–364, 2014.

[32] K. C. Badgujar and B. M. Bhanage, "Factors governing dissolution process of lignocellulosic biomass in ionic liquid: Current status, overview and challenges," *Bioresour. Technol.*, vol. 178, pp. 2–18, 2015.

[33] C.-Z. Liu, F. Wang, A. R. Stiles, and C. Guo, "Ionic liquids for biofuel production: Opportunities and challenges," *Appl. Energy*, vol. 92, pp. 406–414, 2012.

[34] M. Petkovic, K. R. Seddon, L. P. N. Rebelo, and C. Silva Pereira, "Ionic liquids: a pathway to environmental acceptability.," *Chem. Soc. Rev.*, vol. 40, no. 3, pp. 1383–1403, 2011.

[35] A. Chinnappan, C. Baskar, and H. Kim, "Biomass into chemicals: green chemical conversion of carbohydrates into 5-hydroxymethylfurfural in ionic liquids," *RSC Adv.*, vol. 6, no. 68, pp. 63991–64002, 2016.

[36] C. Li, Q. Wang, and Z. K. Zhao, "Acid in ionic liquid: An efficient system for hydrolysis of lignocellulose," *Green Chem.*, vol. 10, no. 2, pp. 177–182, 2008.

[37] F. Xu *et al.*, "Transforming biomass conversion with ionic liquids: process intensification and the development of a high-gravity, one-pot process for the production of cellulosic ethanol," *Energy Environ. Sci.*, vol. 9, pp. 1042–1049, 2016.

[38] P. Halder, S. Kundu, S. Patel, A. Setiawan, and R. Atkin, "Progress on the pre-treatment of lignocellulosic biomass employing ionic liquids," *Renew. Sustain. Energy Rev.*, vol. 105, pp. 268–292, 2019.

[39] K. C. Badgujar, L. D. Wilson, and B. M. Bhanage, "Recent advances for sustainable production of levulinic acid in ionic liquids from biomass: Current scenario, opportunities and challenges," *Renew. Sustain. Energy Rev.*, vol. 102, pp. 266–284, 2019.

[40] G. G. Eshetu, M. Armand, H. Ohno, B. Scrosati, and S. Passerini, "Ionic liquids as tailored media for the synthesis and processing of energy conversion materials," *Energy Environ. Sci.*, vol. 9, pp. 49–61, 2016.

[41] J. Li *et al.*, "Biodiesel production from Camptotheca acuminata seed oil catalyzed by novel Brönsted-Lewis acidic ionic liquid," *Appl. Energy*, vol. 115, pp. 438–444, 2014.

[42] A. R. Hajipour, M. Karimzadeh, and H. Tavallaei, "Fast synthesis of pyrano[2,3-c]pyrazoles: Strong effect of Bronsted and Lewis acidic ionic liquids," *J. Iran. Chem. Soc.*, vol. 12, no. 6, pp. 987–991, 2015.

[43] P. Gogoi, A. K. Dutta, P. Sarma, and R. Borah, "Development of Bronsted-Lewis acidic solid catalytic system of 3-methyl-1-sulfonic acid imidazolium transition metal chlorides for the preparation of bis(indolyl)methanes," *Appl. Catal. A Gen.*, vol. 492, no. 1, pp. 133–139, 2015.

[44] C. Antonetti, D. Licursi, S. Fulignati, G. Valentini, and A. Raspolli Galletti, "New frontiers in the catalytic synthesis of levulinic acid: from sugars to raw and waste biomass as starting feedstock," *Catalysts*, vol. 6, no. 12, p. 196, 2016.

[45] Y. Fukaya, Y. Iizuka, K. Sekikawa, and H. Ohno, "Bio ionic liquids: room temperature ionic liquids composed wholly of biomaterials," *Green Chem.*, vol. 9, no. 11, pp. 1155–1157, 2007.

[46] J. D. Holbrey *et al.*, "Efficient, halide free synthesis of new, low cost ionic liquids: 1,3-dialkylimidazolium salts containing methyl- and ethyl-sulfate anions," *Green Chem.*, vol. 4, no. 5, pp. 407–413, 2002.

[47] A. S. Amarasekara and B. Wiredu, "Acidic ionic liquid catalyzed one-pot conversion of cellulose to ethyl levulinate and levulinic acid in ethanol-water solvent system," *BioEnergy Res.*, vol. 7, pp. 1237–1243, 2014.

[48] H. Ma, J.-X. Long, F.-R. Wang, L.-F. Wang, and X.-H. Le, "Conversion of cellulose to butyl levulinate in bio-butanol medium catalyzed by acidic ionic liquids," *Acta Phys.-Chim.Sin.*, vol. 31, no. 5, pp. 973–979, 2015.

[49] B. Wiredu, J. N. Dominguez, and A. S. Amarasekara, “The co-catalyst effect of zeolites on acidic ionic liquid cata- lyzed one-pot conversion of cellulose to ethyl levulinate and levulinic acid in aqueous ethanol,” *Curr. Catal.*, vol. 4, no. 2, pp. 1–9, 2015.

[50] H. Ren, B. Girisuta, Y. Zhou, and L. Liu, “Selective and recyclable depolymerization of cellulose to levulinic acid catalyzed by acidic ionic liquid,” *Carbohydr. Polym.*, vol. 117, pp. 569–576, 2015.

[51] C. Zhou *et al.*, “The preparation of levulinic acid by acid-catalyzed hydrolysis of bamboo shoot shell in the presence of acidic ionic liquid using the Box-Behnken design.,” *Energy Sources A Recover. Util. Environ. Eff.*, vol. 35, no. 19, pp. 1852–1862, 2013.

[52] C. Zhou, X. Yu, H. Ma, R. He, and S. Vittayapadung, “Optimization on the conversion of bamboo shoot shell to levulinic acid with environmentally benign acidic ionic liquid and response surface analysis,” *Chinese J. Chem. Eng.*, vol. 21, no. 5, pp. 544–550, 2013.

[53] A. S. Amarasekara, “Acidic ionic liquids,” *Chem. Rev.*, vol. 116, no. 10, pp. 6133–6183, 2016.

[54] C. Chang, P. Cen, and X. Ma, “Levulinic acid production from wheat straw,” *Bioresour. Technol.*, vol. 98, no. 7, pp. 1448–1453, 2007.

[55] K. Dussan, B. Girisuta, D. Haverty, J. J. Leahy, and M. H. B. Hayes, “Kinetics of levulinic acid and furfural production from Miscanthus x giganteus,” *Bioresour. Technol.*, vol. 149, pp. 216–224, 2013.

[56] Z. Zhi, N. Li, Y. Qiao, X. Zheng, H. Wang, and X. Lu, “Kinetic study of levulinic acid production from corn stalk at relatively high temperature using $FeCl_3$ as catalyst : A simplified model evaluated,” *Ind. Crop. Prod.*, vol. 76, pp. 672–680, 2015.

[57] Y. W. Tiong, C. L. Yap, S. Gan, and W. S. P. Yap, “Conversion of biomass and its derivatives to levulinic acid and levulinate esters via ionic liquids,” *Ind. Eng. Chem. Res.*, vol. 57, no. 14, pp. 4749–4766, 2018.

[58] S. Saravanamurugan, O. N. Van Buu, and A. Riisager, “Conversion of mono- and disaccharides to ethyl levulinate and ethyl pyranoside with sulfonic acid-functionalized ionic liquids,” *ChemSusChem*, vol. 4, pp. 723–726, 2011.

[59] X. Hu *et al.*, “Acid-catalyzed conversion of mono- and poly-sugars into platform chemicals: Effects of molecular structure of sugar substrate,” *Bioresour. Technol.*, vol. 133, pp. 469–474, 2013.

[60] T. Wang, J. A. Glasper, and B. H. Shanks, “Kinetics of glucose dehydration catalyzed by homogeneous Lewis acidic metal salts in water,” *Appl. Catal. A Gen.*, vol. 498, pp. 214–221, 2015.

[61] C. Yue, D. Fang, L. Liu, and T. F. Yi, “Synthesis and application of task-

specific ionic liquids used as catalysts and/or solvents in organic unit reactions," *J. Mol. Liq.*, vol. 163, no. 3, pp. 99–121, 2011.

[62] D. J. Tao, X. M. Lu, J. F. Lu, K. Huang, Z. Zhou, and Y. T. Wu, "Noncorrosive ionic liquids composed of [$HSO_4$] as esterification catalysts," *Chem. Eng. J.*, vol. 171, pp. 1333–1339, 2011.

[63] L. Chen, M. Sharifzadeh, N. Mac Dowell, T. Welton, N. Shah, and J. P. Hallett, "Inexpensive ionic liquids: [$HSO_4$]$^-$-based solvent production at bulk scale," *Green Chem.*, vol. 16, pp. 3098–3106, 2014.

[64] Y. Shen, J. K. Sun, Y. X. Yi, B. Wang, F. Xu, and R. C. Sun, "One-pot synthesis of levulinic acid from cellulose in ionic liquids," *Bioresour. Technol.*, vol. 192, pp. 812–816, 2015.

[65] F. Liu *et al.*, "Conversion of wheat straw to furfural and levulinic acid in a concentrated aqueous solution of betaine hydrochloride," *RSC Adv.*, vol. 4, pp. 28836–28841, 2014.

[66] L. Peng, L. Lin, J. Zhang, J. Zhuang, B. Zhang, and Y. Gong, "Catalytic conversion of cellulose to levulinic acid by metal chlorides," *Molecules*, vol. 15, pp. 5258–5272, 2010.

[67] Z. Yuan, C. Xu, S. Cheng, and M. Leitch, "Catalytic conversion of glucose to 5-hydroxymethyl furfural using inexpensive co-catalysts and solvents," *Carbohydr. Res.*, vol. 346, no. 13, pp. 2019–2023, 2011.

[68] M. Tan, L. Zhao, and Y. Zhang, "Production of 5-hydroxymethyl furfural from cellulose in $CrCl_2$/Zeolite/BMIMCl system," *Biomass and Bioenergy*, vol. 35, pp. 1367–1370, 2011.

[69] L. Hu, Y. Sun, and L. Lin, "Efficient conversion of glucose into 5-hydroxymethylfurfural by chromium(III) chloride in inexpensive ionic liquid," *Ind. Eng. Chem. Res.*, vol. 51, no. 3, pp. 1099–1104, 2012.

[70] A. George *et al.*, "Design of low-cost ionic liquids for lignocellulosic biomass pretreatment," *Green Chem.*, vol. 17, no. 2, pp. 1728–1734, 2015.

[71] R. Q. Xie, X. Y. Li, and Y. F. Zhang, "Cellulose pretreatment with 1-methyl-3-methylimidazolium dimethylphosphate for enzymatic hydrolysis," *Cellul. Chem. Technol.*, vol. 46, no. 5–6, pp. 349–356, 2012.

[72] A. S. Khan *et al.*, "Dicationic ionic liquids as sustainable approach for direct conversion of cellulose to levulinic acid," *J. Clean. Prod.*, vol. 170, pp. 591–600, 2018.

[73] A. S. Khan *et al.*, "Efficient conversion of lignocellulosic biomass to levulinic acid using acidic ionic liquids," *Carbohydr. Polym.*, vol. 181, pp. 208–214, 2018.

[74] Q. Guan *et al.*, "Preparation of ethyl levulinate from wheat straw catalysed by sulfonate ionic liquid," *Ind. Crop. Prod.*, vol. 113, pp. 150–

156, 2018.

[75] J. Fraga-dubreuil, K. Bourahla, M. Rahmouni, J. Pierre, and J. Hamelin, "Catalysed esterifications in room temperature ionic liquids with acidic counteranion as recyclable reaction media," *Catal. Commun.*, vol. 3, pp. 185–190, 2002.

[76] C. Chiappe, S. Rajamani, and F. D'Andrea, "A dramatic effect of the ionic liquid structure in esterification reactions in protic ionic media," *Green Chem.*, vol. 15, pp. 137–143, 2012.

[77] H. Li *et al.*, "InCl3-ionic liquid catalytic system for efficient and selective conversion of cellulose into 5-hydroxymethylfurfural," *RSC Adv.*, vol. 3, no. 11, pp. 3648–3654, 2013.

[78] Y. W. Tiong, C. L. Yap, S. Gan, and W. S. P. Yap, "One-pot conversion of oil palm empty fruit bunch and mesocarp fiber biomass to levulinic acid and upgrading to ethyl levulinate via indium trichloride-ionic liquids," *J. Clean. Prod.*, vol. 168, pp. 1251–1261, 2017.

[79] Y. Shen, Y. Xu, J. Sun, B. Wang, F. Xu, and R. Sun, "Efficient conversion of monosaccharides into 5-hydroxymethylfurfural and levulinic acid in $InCl_3$-$H_2O$ medium," *Catal. Commun.*, vol. 50, pp. 17–20, 2014.

[80] Y. Shen *et al.*, "$InCl_3$-catalyzed conversion of carbohydrates into 5-hydroxymethylfurfural in biphasic system," *Bioresour. Technol.*, vol. 172, pp. 457–460, 2014.

[81] N. Muhammad *et al.*, "An overview of the role of ionic liquids in biodiesel reactions," *J. Ind. Eng. Chem.*, vol. 21, pp. 1–10, 2015.

[82] S. Peleteiro, S. Rivas, J. L. Alonso, V. Santos, and J. C. Parajó, "Furfural production using ionic liquids: A review," *Bioresour. Technol.*, vol. 202, pp. 181–191, 2016.

[83] L. Liu, Z. Li, W. Hou, and H. Shen, "Direct conversion of lignocellulose to levulinic acid catalyzed by ionic liquid," *Carbohydr. Polym.*, vol. 181, pp. 778–784, 2018.

[84] Y. Teramoto, S.-H. Lee, and T. Endo, "Cost reduction and feedstock diversity for sulfuric acid-free ethanol cooking of lignocellulosic biomass as a pretreatment to enzymatic saccharification.," *Bioresour. Technol.*, vol. 100, no. 20, pp. 4783–9, 2009.

[85] N. A. S. Ramli and N. A. S. Amin, "Catalytic hydrolysis of cellulose and oil palm biomass in ionic liquid to reducing sugar for levulinic acid production," *Fuel Process. Technol.*, vol. 128, pp. 490–498, 2014.

[86] N. Ya'aini, N. A. S. Amin, and M. Asmadi, "Optimization of levulinic acid from lignocellulosic biomass using a new hybrid catalyst," *Bioresour. Technol.*, vol. 116, pp. 58–65, 2012.

[87] N. A. S. Ramli and N. A. S. Amin, "Optimization of Oil Palm Fronds Conversion to Levulinic Acid using Fe/HY Zeolite Catalyst," *Sains Malaysiana*, vol. 44, no. 6, pp. 883–890, 2015.

[88] N. A. S. Ramli, N. A. S. Amin, and I. Ware, "Optimization of oil palm fronds pretreatment using ionic liquid for levulinic acid production," *J. Teknol.*, vol. 1, pp. 33–41, 2014.

[89] N. Ya'aini and N. A. S. Amin, "Catalytic Conversion of Lignocellulosic Biomass to Levulinic Acid in Ionic Liquid," *Bioresources.com*, vol. 8, pp. 5761–5772, 2013.

[90] N. A. S. Ramli, N. Ya'aini, and N. A. S. Amin, "Comparison of response surface methodology and artificial neural network for optimum levulinic acid production from glucose, empty fruit bunch and kenaf," *Int. J. Nano Biomater.*, vol. 5, no. 1, pp. 59–74, 2014.

[91] M. F. Awalludin, O. Sulaiman, R. Hashim, and W. N. A. W. Nadhari, "An overview of the oil palm industry in Malaysia and its waste utilization through thermochemical conversion, specifically via liquefaction," *Renew. Sustain. Energy Rev.*, vol. 50, pp. 1469–1484, 2015.

[92] S. H. Shuit, K. T. Tan, K. T. Lee, and A. H. Kamaruddin, "Oil palm biomass as a sustainable energy source: A Malaysian case study," *Energy*, vol. 34, no. 9, pp. 1225–1235, 2009.

[93] H. B. Aditiya, W. T. Chong, T. M. I. Mahlia, A. H. Sebayang, M. A. Berawi, and H. Nur, "Second generation bioethanol potential from selected Malaysia's biodiversity biomasses: A review," *Waste Manag.*, vol. 47, pp. 46–61, 2015.

[94] A. A. Bazmi, G. Zahedi, and H. Hashim, "Progress and challenges in utilization of palm oil biomass as fuel for decentralized electricity generation," *Renew. Sustain. Energy Rev.*, vol. 15, no. 1, pp. 574–583, 2011.

[95] S. N. H. Abu Bakar *et al.*, "A review of moving-bed biofilm reactor technology for palm oil mill effluent treatment," *J. Clean. Prod.*, vol. 171, pp. 1532–1545, 2018.

[96] S. Sumathi, S. P. Chai, and a. R. Mohamed, "Utilization of oil palm as a source of renewable energy in Malaysia," *Renew. Sustain. Energy Rev.*, vol. 12, no. 9, pp. 2404–2421, 2008.

[97] W. P. Q. Ng, H. L. Lam, F. Y. Ng, M. Kamal, and J. H. E. Lim, "Waste-to-wealth: green potential from palm biomass in Malaysia," *J. Clean. Prod.*, vol. 34, no. September 2011, 2012.

[98] A. Johari *et al.*, "The challenges and prospects of palm oil based biodiesel in Malaysia," *Energy*, vol. 81, pp. 255–261, 2015.

[99] J. D. Bala, J. Lalung, and N. Ismail, "Studies on the reduction of organic

load from palm oil mill effluent (POME) by bacterial strains," *Int. J. Recycl. Org. Waste Agric.*, vol. 4, no. 1, pp. 1–10, 2015.

[100] T. L. Chew and S. Bhatia, "Catalytic processes towards the production of biofuels in a palm oil and oil palm biomass-based biorefinery," *Bioresour. Technol.*, vol. 99, no. 17, pp. 7911–7922, 2008.

[101] N. A. Samiran, M. N. Mohd Jaafar, C. T. Chong, and N. Jo-Han, "A review of palm oil biomass as a feedstock for syngas fuel technology," *J. Teknol.*, vol. 72, no. 5, pp. 13–18, 2015.

[102] I. Mukherjee and B. K. Sovacool, "Palm oil-based biofuels and sustainability in southeast Asia: A review of Indonesia, Malaysia, and Thailand," *Renew. Sustain. Energy Rev.*, vol. 37, pp. 1–12, 2014.

[103] N. Mohammad, M. Z. Alam, N. a. Kabbashi, and A. Ahsan, "Effective composting of oil palm industrial waste by filamentous fungi: A review," *Resour. Conserv. Recycl.*, vol. 58, pp. 69–78, 2012.

[104] A. Shariff, N. Syairah, M. Aziz, and N. Abdullah, "Slow pyrolysis of oil palm empty fruit bunches for biochar production and characterisation," *J. Phys. Sci.*, vol. 25, no. 2, pp. 97–112, 2014.

[105] H. Febriansyah, A. A. Setiawan, K. Suryopratomo, and A. Setiawan, "Gama stove: Biomass stove for palm kernel shells in Indonesia," *Energy Procedia*, vol. 47, pp. 123–132, 2014.

[106] P. Singh, O. Sulaiman, R. Hashim, L. C. Peng, and R. P. Singh, "Using biomass residues from oil palm industry as a raw material for pulp and paper industry: Potential benefits and threat to the environment," *Environ. Dev. Sustain.*, vol. 15, no. 2, pp. 367–383, 2013.

[107] D. M. Alonso, J. Q. Bond, and J. A. Dumesic, "Catalytic conversion of biomass to biofuels," *Green Chem.*, vol. 12, pp. 1493–1513, 2010.

[108] J. Jae *et al.*, "Depolymerization of lignocellulosic biomass to fuel precursors : maximizing carbon efficiency by combining hydrolysis with pyrolysis," *Energy Environ. Sci.*, vol. 3, pp. 358–365, 2010.

[109] H. Wang, G. Gurau, and R. D. Rogers, "Ionic liquid processing of cellulose," *Chem. Soc. Rev.*, vol. 41, no. 4, p. 1519, 2012.

[110] A. Victor, I. N. Pulidindi, and A. Gedanken, "Levulinic acid production from Cicer arietinum, cotton, Pinus radiata and sugarcane bagasse," *RSC Adv.*, vol. 4, pp. 44706–44711, 2014.

[111] J. Song, H. Fan, J. Ma, and B. Han, "Conversion of glucose and cellulose into value-added products in water and ionic liquids," *Green Chem.*, vol. 15, pp. 2619–2635, 2013.

[112] S. Devi, H. Bhaskar, K. Kundu, and V. R. Dahake, "Production of ethyl levulinate ( an additive to biodiesel ) using paper waste," *Int. J. Curr. Eng.*

*Technol.*, vol. 3, no. 2, pp. 672–676, 2013.

[113] I. Delidovich, K. Leonhard, and R. Palkovits, "Cellulose and hemicellulose valorisation: an integrated challenge of catalysis and reaction engineering," *Energy Environ. Sci.*, vol. 7, no. 9, pp. 2803–2830, 2014.

[114] M. J. Climent, A. Corma, and S. Iborra, "Conversion of biomass platform molecules into fuel additives and liquid hydrocarbon fuels," *Green Chem.*, vol. 16, no. 2, pp. 516–547, 2014.

[115] W. Deng, Q. Zhang, and Y. Wang, "Catalytic transformations of cellulose and cellulose-derived carbohydrates into organic acids," *Catal. Today*, vol. 234, no. 1, pp. 31–41, 2014.

[116] A. Bohre, S. Dutta, B. Saha, and M. M. Abu-Omar, "Upgrading furfurals to drop-in biofuels: An overview," *ACS Sustain. Chem. Eng.*, vol. 3, no. 7, pp. 1263–1277, 2015.

[117] R. Weingarten, W. C. Conner, and G. W. Huber, "Production of levulinic acid from cellulose by hydrothermal decomposition combined with aqueous phase dehydration with a solid acid catalyst," *Energy Environ. Sci.*, vol. 5, no. 6, pp. 7559–7574, 2012.

[118] A. M. Hengne, S. B. Kamble, and C. V. Rode, "Single pot conversion of furfuryl alcohol to levulinic esters and γ-valerolactone in the presence of sulfonic acid functionalized ILs and metal catalysts," *Green Chem.*, vol. 15, no. 9, pp. 2540–2547, 2013.

[119] T. Werpy and G. Peterson, "Top Value Added Chemicals from Biomass Volume I — Results of Screening for Potential Candidates from Sugars and Synthesis Gas Top Value Added Chemicals From Biomass Volume I : Results of Screening for Potential Candidates," *U.S. Dep. Energy*, vol. 1, 2004.

[120] R. Mariscal López, P. Maireles-Torres, M. Ojeda, I. Sadaba, and M. López Granados, "Furfural: a renewable and versatile platform molecule for the synthesis of chemicals and fuels," *Energy Environ. Sci.*, vol. 9, no. 4, pp. 1144–1189, 2016.

[121] F. D. Pileidis, M. Tabassum, S. Coutts, and M.-M. Ttitirici, "Esterification of levulinic acid into ethyl levulinate catalysed by sulfonated hydrothermal carbons," *Chinese J. Catal.*, vol. 35, no. 6, pp. 929–936, 2014.

[122] K. Yan, G. Wu, J. Wen, and A. Chen, "One-step synthesis of mesoporous $H_4SiW_{12}O_{40}$-$SiO_2$ catalysts for the production of methyl and ethyl levulinate biodiesel," *Catal. Commun.*, vol. 34, pp. 58–63, 2013.

[123] F. G. Cirujano, a. Corma, and F. X. Llabrés i Xamena, "Conversion of levulinic acid into chemicals: Synthesis of biomass derived levulinate esters over Zr-containing MOFs," *Chem. Eng. Sci.*, vol. 124, pp. 52–60,

2015.

[124] H. Joshi, B. R. Moser, J. Toler, W. F. Smith, and T. Walker, “Ethyl levulinate: A potential bio-based diluent for biodiesel which improves cold flow properties,” *Biomass and Bioenergy*, vol. 35, no. 7, pp. 3262–3266, 2011.

[125] Z. Ting and C. Chun, “Study on the production of ethyl levulinate from biomass in the ethanol system,” *IEEE Xplore*, 2013.

[126] G. Xu, C. Chang, S. Fang, and X. Ma, “Cellulose reactivity in ethanol at elevate temperature and the kinetics of one-pot preparation of ethyl levulinate from cellulose,” *Renew. Energy*, vol. 78, pp. 583–589, Jun. 2015.

[127] X. Hu, S. Wang, L. Wu, D. Dong, M. Mahmudul Hasan, and C. Z. Li, “Acid-treatment of C5 and C6 sugar monomers/oligomers: Insight into their interactions,” *Fuel Process. Technol.*, vol. 126, pp. 315–323, 2014.

[128] X. Hu *et al.*, “Acid-catalyzed conversion of C6 sugar monomer/oligomers to levulinic acid in water, tetrahydrofuran and toluene: Importance of the solvent polarity,” *Fuel*, vol. 141, pp. 56–63, 2015.

[129] S. Kang and J. Yu, “An intensified reaction technology for high levulinic acid concentration from lignocellulosic biomass,” *Biomass and Bioenergy*, vol. 95, pp. 214–220, 2016.

[130] B. Girisuta, K. Dussan, D. Haverty, J. J. Leahy, and M. H. B. Hayes, “A kinetic study of acid catalysed hydrolysis of sugar cane bagasse to levulinic acid,” *Chem. Eng. J.*, vol. 217, pp. 61–70, 2013.

[131] S. G. Wettstein, D. Martin Alonso, E. I. Gürbüz, and J. a. Dumesic, “A roadmap for conversion of lignocellulosic biomass to chemicals and fuels,” *Curr. Opin. Chem. Eng.*, vol. 1, no. 3, pp. 218–224, 2012.

[132] P. Wang, H. Yu, S. Zhan, and S. Wang, “Catalytic hydrolysis of lignocellulosic biomass into 5-hydroxymethylfurfural in ionic liquid,” *Bioresour. Technol.*, vol. 102, no. 5, pp. 4179–4183, 2011.

[133] X. Hu, Y. Song, L. Wu, M. Gholizadeh, and C. Z. Li, “One-pot synthesis of levulinic acid/ester from C5 carbohydrates in a methanol medium,” *ACS Sustain. Chem. Eng.*, vol. 1, no. 12, pp. 1593–1599, 2013.

[134] P. Neves, S. Lima, M. Pillinger, S. M. Rocha, J. Rocha, and A. a. Valente, “Conversion of furfuryl alcohol to ethyl levulinate using porous aluminosilicate acid catalysts,” *Catal. Today*, vol. 218–219, pp. 76–84, 2013.

[135] R. Skoda-Földes, “The use of supported acidic ionic liquids in organic synthesis,” *Molecules*, vol. 19, no. 7, pp. 8840–8884, 2014.

[136] G. Singh and A. Kumar, “Ionic liquids : Physico-chemical, solvent

properties and their applications in chemical processes," *Indian J. Chem.*, vol. 47, pp. 495–503, 2008.

[137] G. Gonfa and M. a Bustam, "Unique structure and solute–solvent interaction in imidazolium based ionic liquids: A review," *Asian Trans. Eng.*, vol. 1, no. 5, pp. 24–34, 2011.

[138] O. A. El Seoud, A. Koschella, L. C. Fidale, S. Dorn, and T. Heinze, "Applications of ionic liquids in carbohydrate chemistry: A window of opportunities," *Biomacromolecules*, vol. 8, no. 9, pp. 2629–2647, 2007.

[139] A. D. Sawant, D. G. Raut, N. B. Darvatkar, and M. M. Salunkhe, "Recent developments of task-specific ionic liquids in organic synthesis," *Green Chem. Lett. Rev.*, vol. 4, no. 1, pp. 41–54, 2011.

[140] Y. Gu, a Karam, F. Jerome, and J. Barrault, "Selectivity enhancement of silica-supported sulfonic acid catalysts in water by ionic liquid coating," *Org. Lett.*, vol. 9, no. 2, pp. 3145–3148, 2007.

[141] H. Olivier-Bourbigou, L. Magna, and D. Morvan, "Ionic liquids and catalysis: Recent progress from knowledge to applications," *Appl. Catal. A Gen.*, vol. 373, pp. 1–56, 2010.

[142] A. Arfan and J. P. Bazureau, "Efficient combination of recyclable task specific ionic liquid and microwave dielectric heating for the synthesis of lipophilic esters," *Org. Process Res. Dev.*, vol. 9, no. 6, pp. 743–748, 2005.

[143] M. Vafaeezadeh and H. Alinezhad, "Bronsted acidic ionic liquids: Green catalysts for essential organic reactions," *J. Mol. Liq.*, vol. 218, pp. 95–105, 2016.

[144] R. Ratti, "Ionic Liquids : Synthesis and applications in catalysis," *Adv. Chem.*, 2014.

[145] S. Lee, "Functionalized imidazolium salts for task-specific ionic liquids and their applications.," *Chem. Commun.*, no. 10, pp. 1049–1063, 2006.

[146] J. Zhang, S. Bao, and J. G. Yang, "Synthesis of a novel multi-$SO_3H$ functionalized strong Bronsted acidic ionic liquid and its catalytic activities for acetalization," *Chinese Sci. Bull.*, vol. 54, no. 21, pp. 3958–3964, 2009.

[147] L. Peng, X. Gao, and K. Chen, "Catalytic upgrading of renewable furfuryl alcohol to alkyl levulinates using $AlCl_3$ as a facile, efficient, and reusable catalyst," *Fuel*, vol. 160, pp. 123–131, 2015.

[148] H. Ren, Y. Zhou, and L. Liu, "Selective conversion of cellulose to levulinic acid via microwave-assisted synthesis in ionic liquids," *Bioresour. Technol.*, vol. 129, pp. 616–619, 2013.

[149] N. Ya'Aini, N. A. S. Amin, and S. Endud, "Characterization and performance of hybrid catalysts for levulinic acid production from

glucose," *Microporous Mesoporous Mater.*, vol. 171, pp. 14–23, 2013.

[150] A. C. Cole *et al.*, "Novel Bronsted acidic ionic liquids and their use as dual solvent-catalysts novel brønsted acidic ionic liquids and their use as dual solvent-catalysts," *J. Am. Chem. Soc.*, pp. 5962–5963, 2002.

[151] D. A. B. Sidik, N. Ngadi, and N. A. S. Amin, "Optimization of lignin production from empty fruit bunch via liquefaction with ionic liquid," *Bioresour. Technol.*, vol. 135, pp. 690–696, 2013.

[152] K. Ninomiya *et al.*, "Saccharification and ethanol fermentation from cholinium ionic liquid-pretreated bagasse with a different number of post-pretreatment washings," *Bioresour. Technol.*, vol. 189, pp. 203–209, 2015.

[153] S. K. Bardhan, S. Gupta, M. E. Gorman, and M. A. Haider, "Biorenewable chemicals: Feedstocks, technologies and the conflict with food production," *Renew. Sustain. Energy Rev.*, vol. 51, pp. 506–520, 2015.

[154] A. Brandt, M. J. Rat, T. Q. To, D. J. Leak, R. J. Murphy, and T. Welton, "Ionic liquid pretreatment of lignocellulosic biomass with ionic liquid-water mixtures," *Green Chem.*, vol. 13, pp. 2489–2499, 2011.

[155] A. Limayem and S. C. Ricke, "Lignocellulosic biomass for bioethanol production: Current perspectives, potential issues and future prospects," *Prog. Energy Combust. Sci.*, vol. 38, no. 4, pp. 449–467, Aug. 2012.

[156] L. W. Lai and A. Idris, "Disruption of oil palm trunks and fronds by microwave-alkali pretreatment," *BioResources*, vol. 8, no. 2, pp. 2792–2804, 2013.

[157] Q. Fang and M. A. Hanna, "Experimental studies for levulinic acid production from whole kernel grain sorghum," *Bioresour. Technol.*, vol. 81, no. 3, pp. 187–192, 2002.

[158] H. Tadesse and R. Luque, "Advances on biomass pretreatment using ionic liquids: An overview," *Energy Environ. Sci.*, vol. 4, no. 10, pp. 3913–3929, 2011.

[159] R. M. Wahlstrom and A. Suurnakki, "Enzymatic hydrolysis of lignocellulosic polysaccharides in the presence of ionic liquids," *Green Chem.*, vol. 17, no. 2, pp. 694–714, 2015.

[160] A. Xu, J. Wang, and H. Wang, "Effects of anionic structure and lithium salts addition on the dissolution of cellulose in 1-butyl-3-methylimidazolium-based ionic liquid solvent systems," *Green Chem.*, vol. 12, no. 2, pp. 268–275, 2010.

[161] M. Mora-Pale, L. Meli, T. V. Doherty, R. J. Linhardt, and J. S. Dordick, "Room temperature ionic liquids as emerging solvents for the pretreatment of lignocellulosic biomass," *Biotechnol. Bioeng.*, vol. 108, no. 6, pp. 1229–1245, 2011.

[162] T. Erdmenger, C. Haensch, R. Hoogenboom, and U. S. Schubert, "Homogeneous tritylation of cellulose in 1-butyl-3-methylimidazolium chloride," *Macromol. Biosci.*, vol. 7, no. 4, pp. 440–445, 2007.

[163] S. Zhang, J. Sun, X. Zhang, J. Xin, Q. Miao, and J. Wang, "Ionic liquid-based green processes for energy production," *Chem. Soc. Rev.*, vol. 43, no. 22, pp. 7838–7869, 2014.

[164] R. C. Remsing, R. P. Swatloski, R. D. Rogers, and G. Moyna, "Mechanism of cellulose dissolution in the ionic liquid 1-n-butyl-3-methylimidazolium chloride: a 13C and 35/37Cl NMR relaxation study on model systems.," *Chem. Commun.*, no. 12, pp. 1271–1273, 2006.

[165] J. X. Long, X. H. Li, L. F. Wang, and N. Zhang, "Ionic liquids: Efficient solvent and medium for the transformation of renewable lignocellulose," *Sci. China Chem.*, vol. 55, no. 8, pp. 1500–1508, 2012.

[166] T. Vancov, A. S. Alston, T. Brown, and S. McIntosh, "Use of ionic liquids in converting lignocellulosic material to biofuels," *Renew. Energy*, vol. 45, pp. 1–6, 2012.

[167] Y. Cao, R. Zhang, T. Cheng, J. Guo, M. Xian, and H. Liu, "Imidazolium-based ionic liquids for cellulose pretreatment: Recent progresses and future perspectives," *Appl. Microbiol. Biotechnol.*, vol. 101, no. 2, pp. 521–532, 2017.

[168] I. Kilpelainen, H. Xie, A. King, M. Granstrom, S. Heikkinen, and D. S. Argyropoulos, "Dissolution of Wood in Ionic Liquids," *J. Agric. Food Chem.*, vol. 55, pp. 9142–9148, 2007.

[169] A. A. Aziz, M. Basri, and a B. U. B. Salleh, "Swelling and Dissolution of Oil Palm Biomass in Ionic Liquids Swelling and Dissolution of Oil Palm Biomass in Ionic Liquids," *J. Oil Palm Res.*, vol. 24, pp. 1267–1276, 2012.

[170] H. T. Tan, K. T. Lee, and A. R. Mohamed, "Pretreatment of lignocellulosic palm biomass using a solvent-ionic liquid [BMIM]Cl for glucose recovery: An optimisation study using response surface methodology," *Carbohydr. Polym.*, vol. 83, pp. 1862–1868, 2011.

[171] H. T. Tan and K. T. Lee, "Understanding the impact of ionic liquid pretreatment on biomass and enzymatic hydrolysis," *Chem. Eng. J.*, vol. 183, pp. 448–458, 2012.

[172] M. Misson, R. Haron, M. F. A. Kamaroddin, and N. A. S. Amin, "Pretreatment of empty palm fruit bunch for production of chemicals via catalytic pyrolysis," *Bioresour. Technol.*, vol. 100, no. 11, pp. 2867–2873, 2009.

[173] A. S. Amarasekara and P. Shanbhag, "Degradation of untreated switchgrass biomass into reducing sugars in 1-(alkylsulfonic)-3-methylimidazolium bronsted acidic ionic liquid medium under mild

conditions," *Bioenergy Res.*, vol. 6, pp. 719–724, 2013.

[174] R. Arora *et al.*, "Monitoring and analyzing process streams towards understanding ionic liquid pretreatment of switchgrass (*Panicum virgatum L.*)," *Bioenergy Res.*, vol. 3, no. 2, pp. 134–145, 2010.

[175] C. Li *et al.*, "Comparison of dilute acid and ionic liquid pretreatment of switchgrass: Biomass recalcitrance, delignification and enzymatic saccharification," *Bioresour. Technol.*, vol. 101, no. 13, pp. 4900–4906, 2010.

[176] L. W. Yoon, T. N. Ang, G. C. Ngoh, and A. S. M. Chua, "Regression analysis on ionic liquid pretreatment of sugarcane bagasse and assessment of structural changes," *Biomass and Bioenergy*, vol. 36, pp. 160–169, 2012.

[177] L. W. Yoon, G. C. Ngoh, A. S. May Chua, and M. A. Hashim, "Comparison of ionic liquid, acid and alkali pretreatments for sugarcane bagasse enzymatic saccharification," *J. Chem. Technol. Biotechnol.*, vol. 86, no. 10, pp. 1342–1348, 2011.

[178] Z. Zhang, I. M. O'Hara, and W. O. S. Doherty, "Pretreatment of sugarcane bagasse by acid-catalysed process in aqueous ionic liquid solutions," *Bioresour. Technol.*, vol. 120, pp. 149–156, 2012.

[179] Z. Zhu, M. Zhu, and Z. Wu, "Pretreatment of sugarcane bagasse with NH4OH-H2O2 and ionic liquid for efficient hydrolysis and bioethanol production," *Bioresour. Technol.*, vol. 119, pp. 199–207, 2012.

[180] T. V Doherty, M. Mora-pale, S. E. Foley, J. Linhardt, and J. S. Dordick, "Ionic liquid solvent properties as predictors of lignocellulose pretreatment efficacy," *Green Chem.*, no. 11, pp. 1967–1975, 2010.

[181] S. S. Y. Tan *et al.*, "Extraction of lignin from lignocellulose at atmospheric pressure using alkylbenzenesulfonate ionic liquid," *Green Chem.*, vol. 11, no. 4, pp. 339–345, 2009.

[182] N. Sun, M. Rahman, Y. Qin, M. L. Maxim, H. Rodríguez, and R. D. Rogers, "Complete dissolution and partial delignification of wood in the ionic liquid 1-ethyl-3-methylimidazolium acetate," *Green Chem.*, vol. 11, no. 5, p. 646, 2009.

[183] C. Froschauer, M. Hummel, M. Iakovlev, A. Roselli, H. Schottenberger, and H. Sixta, "Separation of hemicellulose and cellulose from wood pulp by means of ionic liquid/cosolvent systems," *Biomacromolecules*, vol. 14, no. 6, pp. 1741–1750, 2013.

[184] H. Ren, M. H. Zong, H. Wu, and N. Li, "Efficient pretreatment of wheat straw using novel renewable cholinium ionic liquids to improve enzymatic saccharification," *Ind. Eng. Chem. Res.*, vol. 55, no. 6, pp. 1788–1795, 2016.

[185] N. Muhammad, Z. Man, M. A. Bustam, M. I. A. Mutalib, C. D. Wilfred, and S. Rafiq, "Dissolution and delignification of bamboo biomass using amino acid-based ionic liquid," *Appl. Biochem. Biotechnol.*, vol. 165, no. 3–4, pp. 998–1009, 2011.

[186] K. Okushita, E. Chikayama, and J. Kikuchi, "Solubilization mechanism and characterization of the structural change of bacterial cellulose in regenerated states through ionic liquid treatment," *Biomacromolecules*, vol. 13, no. 5, pp. 1323–1330, 2012.

[187] Y.-X. An, M.-H. Zong, H. Wu, and N. Li, "Pretreatment of lignocellulosic biomass with renewable cholinium ionic liquids: Biomass fractionation, enzymatic digestion and ionic liquid reuse," *Bioresour. Technol.*, vol. 192, pp. 165–171, 2015.

[188] K. Ninomiya, A. Ohta, S. Omote, C. Ogino, K. Takahashi, and N. Shimizu, "Combined use of completely bio-derived cholinium ionic liquids and ultrasound irradiation for the pretreatment of lignocellulosic material to enhance enzymatic saccharification," *Chem. Eng. J.*, vol. 215–216, pp. 811–818, 2013.

[189] A. M. Socha *et al.*, "Efficient biomass pretreatment using ionic liquids derived from lignin and hemicellulose," *Proc. Natl. Acad. Sci.*, vol. 111, no. 35, pp. E3587–E3595, 2014.

[190] J. P. Hallett and T. Welton, "Room-temperature ionic liquids: Solvents for synthesis and catalysis. 2," *Chem. Rev.*, vol. 111, pp. 3508–3576, 2011.

[191] B. Girisuta, B. Danon, R. Manurung, L. P. B. M. Janssen, and H. J. Heeres, "Experimental and kinetic modelling studies on the acid-catalysed hydrolysis of the water hyacinth plant to levulinic acid," *Bioresour. Technol.*, vol. 99, no. 17, pp. 8367–8375, 2008.

[192] L. Yan, N. Yang, H. Pang, and B. Liao, "Production of levulinic acid from bagasse and paddy straw by liquefaction in the presence of hydrochloride acid," *Clean*, vol. 36, no. 2, pp. 158–163, 2008.

[193] D. B. Bevilaqua, M. K. D. Rambo, T. M. Rizzetti, A. L. Cardoso, and A. F. Martins, "Cleaner production: Levulinic acid from rice husks," *J. Clean. Prod.*, vol. 47, pp. 96–101, 2013.

[194] H. Chen, B. Yu, and S. Jin, "Production of levulinic acid from steam exploded rice straw via solid superacid, $S_2O_8(^{2-})/ZrO_2$-$SiO_2$-$Sm_2O_3$.," *Bioresour. Technol.*, vol. 102, no. 3, pp. 3568–70, 2011.

[195] N. A. S. Ramli and N. A. S. Amin, "A new functionalized ionic liquid for efficient glucose conversion to 5-hydroxymethyl furfural and levulinic acid," *J. Mol. Catal. A Chem.*, vol. 407, pp. 113–121, 2015.

[196] K. Kumar, F. Parveen, T. Patra, and S. Upadhyayula, "Hydrothermal conversion of glucose to levulinic acid using multifunctional ionic liquids: effects of metal ion co-catalysts on the product yield," *New J. Chem.*, vol.

42, pp. 228–236, 2018.

[197] J. Chen, G. Zhao, and L. Chen, “Efficient production of 5-hydroxymethylfurfural and alkyl levulinate from biomass carbohydrate using ionic liquid-based polyoxometalate salts,” *RSC Adv.*, vol. 4, no. 8, pp. 4194–4202, 2014.

[198] I. Thapa, B. Mullen, A. Saleem, C. Leibig, R. T. Baker, and J. B. Giorgi, “Efficient green catalysis for the conversion of fructose to levulinic acid,” *Appl. Catal. A Gen.*, vol. 539, pp. 70–79, 2017.

[199] Y. Shen, J. Sun, Y. Yi, B. Wang, F. Xu, and R. Sun, “5-Hydroxymethylfurfural and levulinic acid derived from monosaccharides dehydration promoted by $InCl_3$ in aqueous medium,” *J. Mol. Catal. A Chem.*, vol. 394, pp. 114–120, 2014.

[200] S. Alipour and H. Omidvarborna, “Enzymatic and catalytic hybrid method for levulinic acid synthesis from biomass sugars,” *J. Clean. Prod.*, vol. 143, pp. 490–496, 2017.

[201] Y. Sun, Q. Zhang, P. Zhang, D. Song, and Y. Guo, “Nitrogen-doped carbon-based acidic ionic liquid hollow nanospheres for efficient and selective conversion of fructose to 5-ethoxymethylfurfural and ethyl levulinate,” *ACS Sustain. Chem. Eng.*, vol. 6, no. 5, pp. 6771–6782, 2018.

[202] Y. Leng, J. Wang, D. Zhu, X. Ren, H. Ge, and L. Shen, “Heteropolyanion-based ionic liquids: Reaction-induced self-separation catalysts for esterification,” *Angew. Chemie - Int. Ed.*, vol. 48, no. 1, pp. 168–171, 2009.

[203] R. Liu, J. Chen, X. Huang, L. Chen, L. Ma, and X. Li, “Conversion of fructose into 5-hydroxymethylfurfural and alkyl levulinates catalyzed by sulfonic acid-functionalized carbon materials,” *Green Chem.*, vol. 15, no. 10, pp. 2895–2903, 2013.

[204] Z. Sun *et al.*, “One-pot depolymerization of cellulose into glucose and levulinic acid by heteropolyacid ionic liquid catalysis,” *RSC Adv.*, vol. 2, no. 24, pp. 9058–9065, 2012.

[205] M. C. C. Ribeiro, “High viscosity of imidazolium ionic liquids with the hydrogen sulfate anion: A Raman spectroscopy study,” *J. Phys. Chem. B*, vol. 116, pp. 7281–7290, 2012.

[206] Q. Wu, H. Chen, M. Han, D. Wang, and J. Wang, “Transesterification of cottonseed oil catalyzed by bronsted acidic ionic liquids,” *Ind. Eng. Chem. Res.*, vol. 46, no. 24, pp. 7955–7960, 2007.

[207] G.-Z. Xu, C. Chang, W.-N. Zhu, B. Li, X.-J. Ma, and F.-G. Du, “A comparative study on direct production of ethyl levulinate from glucose in ethanol media catalysed by different acid catalysts,” *Chem. Pap.*, vol. 67, no. 11, pp. 1355–1363, 2013.

[208] C. D. Tran, S. H. De Paoli Lacerda, and D. Oliveira, "Absorption of water by room-temperature ionic liquids: Effect of anions on concentration and state of water," *Appl. Spectrosc.*, vol. 57, no. 2, pp. 152–157, 2003.

[209] L. Hu, Z. Wu, J. Xu, Y. Sun, L. Lin, and S. Liu, "Zeolite-promoted transformation of glucose into 5-hydroxymethylfurfural in ionic liquid," *Chem. Eng. J.*, vol. 244, pp. 137–144, 2014.

[210] C. C. Hines, D. B. Cordes, S. T. Griffin, S. I. Watts, V. A. Cocaliay, and R. D. Rogers, "Flexible coordination environments of lanthanide complexes grown from chloride-based ionic liquids," *New J. Chem.*, vol. 32, pp. 872–877, 2008.

[211] P. K. Rout, A. D. Nannaware, O. Prakash, A. Kalra, and R. Rajasekharan, "Synthesis of hydroxymethylfurfural from cellulose using green processes: A promising biochemical and biofuel feedstock," *Chem. Eng. Sci.*, vol. 142, pp. 318–346, 2016.

[212] L. Filiciotto, A. M. Balu, J. C. Van der Waal, and R. Luque, "Catalytic insights into the production of biomass-derived side products methyl levulinate, furfural and humins," *Catal. Today*, vol. 302, pp. 2–15, 2018.

[213] A. S. Amarasekara and C. C. Ebede, "Zinc chloride mediated degradation of cellulose at 200ºC and identification of the products," *Bioresour. Technol.*, vol. 100, no. 21, pp. 5301–5304, 2009.

[214] P. T. Williams and P. A. Horne, "The Role of Metal Salts in the Pyrolysis of Biomass," *Renew. Energy*, vol. 4, no. 1, pp. 1–13, 1994.

[215] L. Zhou *et al.*, "Conversion of carbohydrate biomass to methyl levulinate with $Al_2(SO_4)_3$ as a simple, cheap and efficient catalyst," *Catal. Commun.*, vol. 50, pp. 13–16, 2014.

[216] N. A. S. Ramli and N. A. S. Amin, "Fe / HY zeolite as an effective catalyst for levulinic acid production from glucose: Characterization and catalytic performance," *Appl. Catal. B Environ.*, vol. 163, pp. 487–498, 2015.

[217] H. Li *et al.*, "Immobilizing Cr3+ with SO3H-functionalized solid polymeric ionic liquids as efficient and reusable catalysts for selective transformation of carbohydrates into 5-hydroxymethylfurfural.," *Bioresour. Technol.*, vol. 144, pp. 21–7, Sep. 2013.

[218] A. Chinnappan, A. H. Jadhav, W.-J. Chung, and H. Kim, "Conversion of sugars (sucrose and glucose) into 5-hydroxymethylfurfural in pyridinium based dicationic ionic liquid ($[C10(EPy)_2]2Br^-$) with chromium chloride as a catalyst," *Ind. Crops Prod.*, vol. 76, pp. 12–17, 2015.

[219] N. A. S. Ramli and N. A. S. Amin, "Optimization of renewable levulinic acid production from glucose conversion catalyzed by Fe/HY zeolite catalyst in aqueous medium," *Energy Convers. Manag.*, vol. 95, pp. 10–19, 2015.

[220] N. F. Adnan, N. A. Mohamad Nordin, N. Hamzah, and M. A. Yarmo, "Lewis acidic ionic liquids as new addition catalyst for oleic acid to monoestolide synthesis," *J. Sci. Technol.*, vol. 2, no. 2, pp. 25–33, 2011.

[221] S. Sunitha, S. Kanjilal, P. S. Reddy, and R. B. N. Prasad, "Liquid-liquid biphasic synthesis of long chain wax esters using the Lewis acidic ionic liquid choline chloride2$ZnCl_2$," *Tetrahedron Lett.*, vol. 48, no. 39, pp. 6962–6965, 2007.

[222] R. J. Van Putten, J. C. Van Der Waal, E. De Jong, C. B. Rasrendra, H. J. Heeres, and J. G. De Vries, "Hydroxymethylfurfural, a versatile platform chemical made from renewable resources," *Chem. Rev.*, vol. 113, no. 3, pp. 1499–1597, 2013.

[223] A. Pinkert, K. N. Marsh, and S. Pang, "Reflections on the solubility of cellulose," *Ind. Eng. Chem. Res.*, vol. 49, no. 22, pp. 11121–11130, 2010.

[224] B. Kosan, C. Michels, and F. Meister, "Dissolution and forming of cellulose with ionic liquids," *Cellulose*, vol. 15, no. 1, pp. 59–66, 2008.

[225] J. Vitz, T. Erdmenger, C. Haensch, and U. S. Schubert, "Extended dissolution studies of cellulose in imidazolium based ionic liquids," *Green Chem.*, vol. 11, no. 3, pp. 417–424, 2009.

[226] A. Pinkert, K. N. Marsh, S. Pang, and M. P. Staiger, "Ionic liquids and their interaction with cellulose," *Chem. Rev.*, vol. 109, no. 12, pp. 6712–6728, 2009.

[227] G. Wang, Z. Zhang, and L. Song, "Efficient and selective alcoholysis of furfuryl alcohol to alkyl levulinates catalyzed by double $SO_3H$-functionalized ionic liquids," *Green Chem.*, vol. 16, no. 3, pp. 1436–1443, 2014.

[228] J. Zhang, X. Yu, F. Zou, Y. Zhong, N. Du, and X. Huang, "Room-temperature ionic liquid system converting fructose into 5-hydroxymethylfurfural in high efficiency," *ACS Sustain. Chem. Eng.*, vol. 3, no. 12, pp. 3338–3345, 2015.

[229] H. Zhang, F. Xu, X. Zhou, G. Zhang, and C. Wang, "A Bronsted acidic ionic liquid as an efficient and reusable catalyst system for esterification," *Green Chem.*, vol. 9, pp. 1208–1211, 2007.

[230] X.-F. Liu *et al.*, "Efficient conversion of furfuryl alcohol to ethyl levulinate with sulfonic acid-functionalized MIL-101(Cr)," *RSC Adv.*, vol. 6, no. 93, pp. 90232–90238, 2016.

[231] K. Y. Nandiwale, S. K. Yadava, and V. V. Bokade, "Production of octyl levulinate biolubricant over modified H-ZSM-5: Optimization by response surface methodology," *J. Energy Chem.*, vol. 23, no. 4, pp. 535–541, 2014.

[232] J. A. Melero, G. Morales, J. Iglesias, M. Paniagua, B. Hernández, and S.

Penedo, “Efficient conversion of levulinic acid into alkyl levulinates catalyzed by sulfonic mesostructured silicas,” *Appl. Catal. A Gen.*, vol. 466, pp. 116–122, Sep. 2013.

[233] K. Y. Nandiwale *et al.*, “Catalytic upgrading of renewable levulinic acid to ethyl levulinate biodiesel using dodecatungstophosphoric acid supported on desilicated H-ZSM-5 as catalyst,” *Appl. Catal. A Gen.*, vol. 460–461, pp. 90–98, 2013.

[234] Y. Deng, Y. Deng, F. Shi, F. Shi, K. Qiao, and K. Qiao, “Ionic liquid as a green catalytic reaction medium for esterifications,” *J. Mol. Catal.*, vol. 165, pp. 33–36, 2001.

[235] B. Aghabarari, N. Dorostkar, M. Ghiaci, S. G. Amini, E. Rahimi, and M. V. Martinez-Huerta, “Esterification of fatty acids by new ionic liquids as acid catalysts,” *J. Taiwan Inst. Chem. Eng.*, vol. 45, no. 2, pp. 431–435, 2014.

[236] D. Naydenov, H. Hasse, G. Maurer, and H.-J. Bart, “Esterifications in Ionic Liquids with 1-Alkyl-3-Methylimidazolium Cation and Hydrogen Sulfate Anion: Conversion and Phase Equilibrium,” *Open Chem. Eng. J.*, vol. 3, pp. 17–26, 2009.

[237] J. Gui, X. Cong, D. Liu, X. Zhang, Z. Hu, and Z. Sun, “Novel Bronsted acidic ionic liquid as efficient and reusable catalyst system for esterification,” *Catal. Commun.*, vol. 5, no. 9, pp. 473–477, 2004.

[238] H.-P. Zhu, F. Yang, J. Tang, and M.-Y. He, “Brønsted acidic ionic liquid 1-methylimidazolium tetrafluoroborate: a green catalyst and recyclable medium for esterification,” *Green Chem.*, vol. 5, no. 1, p. 38, 2003.

[239] D. J. Tao, Y. T. Wu, Z. Zhou, J. Geng, X. B. Hu, and Z. B. Zhang, “Kinetics for the esterification reaction of n -butanol with acetic acid catalyzed by noncorrosive bronsted acidic ionic liquids,” *Ind. Eng. Chem. Res.*, vol. 50, no. 4, pp. 1989–1996, 2011.

[240] D. J. Tao, X. L. Zhang, N. Hu, Z. M. Li, and X. S. Chen, “Kinetics study of the esterification of acetic acid with methanol using low-corrosive Bronsted acidic ionic liquids as catalysts,” *Int. J. Chem. React. Eng.*, vol. 10, no. 1, 2012.

[241] Y. W. Tiong, C. L. Yap, S. Gan, and W. S. P. Yap, “Conversion of oil palm biomass to ethyl levulinate via ionic liquids,” *Chem. Eng. Trans.*, vol. 56, pp. 1021–1026, 2017.

[242] K. W. Omari, J. E. Besaw, and F. M. Kerton, “Hydrolysis of chitosan to yield levulinic acid and 5-hydroxymethylfurfural in water under microwave irradiation,” *Green Chem.*, vol. 14, no. 5, p. 1480, 2012.

[243] J. Jae *et al.*, “Investigation into the shape selectivity of zeolite catalysts for biomass conversion,” *J. Catal.*, vol. 279, no. 2, pp. 257–268, 2011.

[244] N. M. Xavier, S. D. Lucas, and A. P. Rauter, "Zeolites as efficient catalysts for key transformations in carbohydrate chemistry," *J. Mol. Catal. A Chem.*, vol. 305, no. 1–2, pp. 84–89, 2009.

[245] M. Zavrel, D. Bross, M. Funke, J. Büchs, and A. C. Spiess, "High-throughput screening for ionic liquids dissolving (ligno-)cellulose," *Bioresour. Technol.*, vol. 100, no. 9, pp. 2580–2587, 2009.

[246] M. E. Zakrzewska, E. Bogel-łukasik, and R. Bogel-łukasik, "Ionic Liquid-Mediated Formation of 5-Hydroxymethylfurfural - A Promising Biomass-Derived Building Block," *Chem. Rev.*, vol. 2, pp. 397–417, 2011.

[247] N. Muhammad *et al.*, "Synthesis and physical properties of choline carboxylate ionic liquids," *J. Chem. Eng. Data*, vol. 57, no. 8, pp. 2191–2196, 2012.

[248] A. Stark, "Ionic liquids in the biorefinery: a critical assessment of their potential," *Energy Environ. Sci.*, vol. 4, no. 1, pp. 19–32, 2011.

[249] Z. Zhang, B. Du, Z.-J. Quan, Y.-X. Da, and X.-C. Wang, "Dehydration of biomass to furfural catalyzed by reusable polymer bound sulfonic acid (PEG-$OSO_3H$) in ionic liquid," *Catal. Sci. Technol.*, vol. 4, no. 3, pp. 633–638, 2014.

[250] X. Hu *et al.*, "Production of value-added chemicals from bio-oil via acid catalysis coupled with liquid–liquid extraction," *RSC Adv.*, vol. 2, no. 25, pp. 9366–9370, 2012.

[251] P. N. Reddy, P. Padmaja, B. V. Subba Reddy, and G. Rambabu, "Ionic liquid/water mixture promoted organic transformations," *RSC Adv.*, vol. 5, pp. 51035–51054, 2015.

[252] M. Mascal and E. B. Nikitin, "High-yield conversion of plant biomass into the key value-added feedstocks 5-(hydroxymethyl)furfural, levulinic acid, and levulinic esters via 5-(chloromethyl)furfural," *Green Chem.*, vol. 12, no. 3, pp. 370–373, 2010.

[253] X.-X. Han *et al.*, "Syntheses of novel halogen-free Bronsted–Lewis acidic ionic liquid catalysts and their applications for synthesis of methyl caprylate," *Green Chem.*, vol. 17, pp. 499–508, 2015.

[254] M. El-Harbawi, "Toxicity measurement of imidazolium ionic liquids using acute toxicity test," *Procedia Chem.*, vol. 9, pp. 40–52, 2014.

[255] X. Wu, Z.-H. Tong, L.-L. Li, and H.-Q. Yu, "Toxic effects of imidazolium-based ionic liquids on Caenorhabditis elegans: the role of reactive oxygen species.," *Chemosphere*, vol. 93, no. 10, pp. 2399–404, 2013.

[256] S. Aparicio, M. Atilhan, M. Khraisheh, and R. Alcalde, "Study on hydroxylammonium-based ionic liquids . I . Characterization," *J. Phys. Chem. B*, pp. 12473–12486, 2011.

[257] J. Liu, Z. Li, J. Chen, and C. Xia, “Synthesis, properties and catalysis of novel methyl- or ethyl- sulfate-anion-based acidic ionic liquids,” *Catal. Commun.*, vol. 10, no. 6, pp. 799–802, Feb. 2009.

[258] A. M. Adel, Z. H. A. El-Wahab, A. a. Ibrahim, and M. T. Al-Shemy, “Characterization of microcrystalline cellulose prepared from lignocellulosic materials. Part I. Acid catalyzed hydrolysis,” *Bioresour. Technol.*, vol. 101, no. 12, pp. 4446–4455, 2010.

[259] J. Lunagariya, A. Dhar, and R. L. Vekariya, “Efficient esterification of n-butanol with acetic acid catalyzed by the Bronsted acidic ionic liquids: influence of acidity,” *RSC Adv.*, vol. 7, no. 9, pp. 5412–5420, 2017.

[260] E. Ahmad, M. I. Alam, K. K. Pant, and M. A. Haider, “Catalytic and mechanistic insights into the production of ethyl levulinate from biorenewable feedstocks,” *Green Chem.*, vol. 18, pp. 4804–4823, 2016.

[261] K. M. Sabil, M. a. Aziz, B. Lal, and Y. Uemura, “Effects of torrefaction on the physiochemical properties of oil palm empty fruit bunches, mesocarp fiber and kernel shell,” *Biomass and Bioenergy*, vol. 56, pp. 351–360, 2013.

[262] N. I. Iberahim, J. M. Jahim, S. Harun, M. T. M. Nor, and O. Hassan, “Sodium hydroxide pretreatment and enzymatic hydrolysis of oil palm mesocarp fiber,” *Int. J. Chem. Eng. Appl.*, vol. 4, no. 3, pp. 101–105, 2013.

[263] S. De Santis *et al.*, “Cholinium-amino acid based ionic liquids: a new method of synthesis and physico-chemical characterization,” *Phys. Chem. Chem. Phys.*, vol. 17, no. 32, pp. 20687–20698, 2015.

[264] K. C. Lethesh, S. N. Shah, and M. I. Abdul Mutalib, “Synthesis, characterization, and thermophysical properties of 1,8-diazobicyclo[5.4.0]undec-7-ene based thiocyanate ionic liquids,” *J. Chem. Eng. Data*, vol. 59, pp. 1788–1795, 2014.

[265] B. González, E. Gómez, A. Domínguez, M. Vilas, and E. Tojo, “Physicochemical Characterization of New Sulfate Ionic Liquids,” *J. Chem. Eng. Data*, vol. 56, pp. 14–20, 2011.

[266] M. Tariq, P. A. S. Forte, M. F. C. Gomes, J. N. C. Lopes, and L. P. N. Rebelo, “Densities and refractive indices of imidazolium- and phosphonium-based ionic liquids: Effect of temperature, alkyl chain length, and anion,” *J. Chem. Thermodyn.*, vol. 41, no. 6, pp. 790–798, 2009.

[267] A. S. Khan *et al.*, “Dicationic imidazolium based ionic liquids: Synthesis and properties,” *J. Mol. Liq.*, vol. 227, pp. 98–105, 2017.

[268] C. Fareeda, H. J. You, K. Muthukumar, and T. Murugesan, “Effect of L-arginine on the physical properties of choline chloride and glycerol bases DES,” *J. Mol. Liq.*, vol. 212, pp. 605–611, 2015.

[269] D. Zhao, Z. Fei, R. Scopelliti, and P. J. Dyson, "Synthesis and Characterization of Ionic Liquids Incorporating the Nitrile Functionality," *Inorg. Chem.*, vol. 43, no. 6, pp. 2197–2205, 2004.

[270] Z. Ullah, M. A. Bustam, Z. Man, S. N. Shah, A. S. Khan, and N. Muhammad, "Synthesis, characterization and physicochemical properties of dual-functional acidic ionic liquids," *J. Mol. Liq.*, vol. 223, pp. 81–88, 2016.

[271] A. P. Fröba, H. Kremer, and A. Leipertz, "Density, Refractive index, interfacial tension, and viscosity of ionic liquids [EMIM][$EtSO_4$], [EMIM][$NTf_2$], [EMIM][$N(CN)_2$], and [OMA][$NTf_2$] in dependence on temperature at atmospheric pressure," *J. Phys. Chem. B*, vol. 112, no. 39, pp. 12420–12430, 2008.

[272] C. P. Fredlake, J. M. Crosthwaite, D. G. Hert, S. N. V. K. Aki, and J. F. Brennecke, "Thermophysical properties of imidazolium-based ionic liquids," *J. Chem. Eng. Data*, vol. 49, no. 4, pp. 954–964, 2004.

[273] N. Muhammad, Z. Man, M. Bustam, A. Mutalib, C. Wilfred, and S. Rafiq, "Synthesis and thermophysical properties of low viscosity amino acid-based ionic liquids," *J. Chem. Eng. Data*, vol. 56, no. 7, pp. 3157–3162, 2011.

[274] L. G. Sánchez, J. R. Espel, F. Onink, G. W. Meindersma, and A. B. de Haan, "Density, viscosity, and surface tension of synthesis grade imidazolium, pyridinium, and pyrrolidinium based room temperature ionic liquids," *J. Chem. Eng. Data*, vol. 54, no. 10, pp. 2803–2812, 2009.

[275] J. M. Crosthwaite, M. J. Muldoon, J. K. Dixon, J. L. Anderson, and J. F. Brennecke, "Phase transition and decomposition temperatures, heat capacities and viscosities of pyridinium ionic liquids," *J. Chem. Thermodyn.*, vol. 37, no. 6, pp. 559–568, 2005.

[276] H. Guo, X. Qi, Y. Hiraga, T. M. Aida, R. Lee, and S. Jr, "Efficient conversion of fructose into 5-ethoxymethylfurfural with hydrogen sulfate ionic liquids as co-solvent and catalyst," *Chem. Eng. J.*, vol. 314, pp. 508–514, 2017.

[277] H. L. Ngo, K. LeCompte, L. Hargens, and A. B. McEwen, "Thermal properties of imidazolium ionic liquids," *Thermochim. Acta*, vol. 357–358, pp. 97–102, 2000.

[278] B. M. Matsagar and P. L. Dhepe, "Brönsted acidic ionic liquid-catalyzed conversion of hemicellulose into sugars," *Catal. Sci. Technol.*, vol. 5, no. 1, pp. 531–539, 2015.

[279] P. Lu, Z. P. Zhao, X. Y. Wang, G. J. Lan, and X. L. Wang, "Understanding effect of molecular structure of imidazole-based ionic liquids on catalytic performance for biomass inulin hydrolysis," *Mol. Catal.*, vol. 435, pp. 24–32, 2017.

[280] X. Qi, M. Watanabe, T. M. Aida, and R. L. Smith Jr., "Efficient one-pot production of 5-hydroxymethylfurfural from inulin in ionic liquids," *Green Chem.*, vol. 12, no. 10, p. 1855, 2010.

[281] J. Wang, H. Wang, S. Zhang, H. Zhang, and Y. Zhao, "Conductivities, volumes, fluorescence, and aggregation behavior of ionic liquids [C4mim][$BF_4$] and [$C_n$mim] Br (n= 4, 6, 8, 10, 12) in aqueous solutions," *J. Phys. Chem. B*, vol. 111, no. 22, pp. 6181–6188, 2007.

[282] C. Shi *et al.*, "Effects of cations and anions of ionic liquids on the production of 5-hydroxymethylfurfural from fructose," *Chem. Commun.*, vol. 48, no. 34, p. 4103, 2012.

[283] C.-H. Zhou, X. Xia, C.-X. Lin, D.-S. Tong, and J. Beltramini, "Catalytic conversion of lignocellulosic biomass to fine chemicals and fuels.," *Chem. Soc. Rev.*, vol. 40, no. 11, pp. 5588–617, 2011.

[284] F. Jiang, Q. Zhu, D. Ma, X. Liu, and X. Han, "Direct conversion and NMR observation of cellulose to glucose and 5-hydroxymethylfurfural (HMF) catalyzed by the acidic ionic liquids," *J. Mol. Catal. A Chem.*, vol. 334, no. 1–2, pp. 8–12, 2011.

[285] Y. Liu, E. Lotero, and J. G. G. Jr, "Effect of carbon chain length on esterification of carboxylic acids with methanol using acid catalysis," *J. Catal.*, vol. 243, pp. 221–228, 2006.

[286] C. Chang, X. Ma, and P. Cen, "Kinetic Studies on Wheat Straw Hydrolysis to Levulinic Acid," *Chinese J. Chem. Eng.*, vol. 17, no. 5, pp. 835–839, Oct. 2009.

[287] L. Zhang, G. Xi, J. Zhang, H. Yu, and X. Wang, "Efficient catalytic system for the direct transformation of lignocellulosic biomass to furfural and 5-hydroxymethylfurfural," *Bioresour. Technol.*, vol. 224, pp. 656–661, 2017.

[288] W. Zhao, Y. Li, C. Song, S. Liu, X. Li, and J. Long, "Intensified levulinic acid/ester production from cassava by one-pot cascade prehydrolysis and delignification," *Appl. Energy*, vol. 204, pp. 1094–1100, 2017.

[289] A. Herbst and C. Janiak, "Selective glucose conversion to 5-hydroxymethylfurfural (5-HMF) instead of levulinic acid with MIL-101Cr MOF-derivatives," *New J. Chem.*, vol. 40, pp. 7958–7967, 2016.

[290] J. . Cha and M. . Hanna, "Levulinic acid production based on extrusion and pressurized batch reaction," *Ind. Crops Prod.*, vol. 16, no. 2, pp. 109–118, 2002.

[291] B. M. Matsagar, M. K. Munshi, A. A. Kelkar, and P. L. Dhepe, "Conversion of concentrated sugar solutions into 5-hydroxymethyl furfural and furfural using Bronsted acidic ionic liquids," *Catal. Sci. Technol.*, vol. 5, no. 12, pp. 5086–5090, 2015.

[292] S. X. Chin, C. H. Chia, S. Zakaria, Z. Fang, and S. Ahmad, "Ball milling pretreatment and diluted acid hydrolysis of oil palm empty fruit bunch (EFB) fibres for the production of levulinic acid," *J. Taiwan Inst. Chem. Eng.*, vol. 52, pp. 85–92, 2015.

[293] H. Guo, X. Qi, L. Li, and R. L. Smith, "Hydrolysis of cellulose over functionalized glucose-derived carbon catalyst in ionic liquid," *Bioresour. Technol.*, vol. 116, pp. 355–359, 2012.

[294] N. A. S. Ramli and N. A. S. Amin, "Kinetic study of glucose conversion to levulinic acid over Fe/HY zeolite catalyst," *Chem. Eng. J.*, vol. 283, pp. 150–159, 2016.

[295] B. Saha and M. M. Abu-omar, "Advances in 5-hydroxymethylfurfural production from biomass in biphasic solvents," *Green Chem.*, pp. 24–38, 2014.

[296] A. Ghorbani-Choghamarani and M. Norouzi, "Synthesis and characterization of ionic liquid immobilized on magnetic nanoparticles: A recyclable heterogeneous organocatalyst for the acetylation of alcohols," *J. Magn. Magn. Mater.*, vol. 401, pp. 832–840, 2016.

[297] R. Aggarwal, S. Singh, and G. Hundal, "Synthesis, characterization, and evaluation of surface properties of cyclohexanoxycarbonylmethylpyridinium and cyclohexanoxycarbonylmethylimidazolium ionic liquids," *Ind. Eng. Chem. Res.*, vol. 52, no. 3, pp. 1179–1189, 2013.

[298] S. Quereshi, E. Ahmad, K. K. Pant, and S. Dutta, "Insights into the metal salt catalyzed ethyl levulinate synthesis from biorenewable feedstocks," *Catal. Today*, vol. 291, pp. 187–194, 2017.

[299] H. Li, Z. Fang, J. Luo, and S. Yang, "Direct conversion of biomass components to the biofuel methyl levulinate catalyzed by acid-base bifunctional zirconia-zeolites," *Appl. Catal. B Environ.*, vol. 200, pp. 182–191, 2017.

[300] S. Ghosh, P. Bhanja, N. Salam, R. Khatun, A. Bhaumik, and S. M. Islam, "Porous iron-phosphonate nanomaterial as an efficient catalyst for the CO 2 fixation at atmospheric pressure and esterification of biomass-derived levulinic acid," *Catal. Today*, vol. 309, pp. 253–262, 2018.

[301] F. Su, L. Ma, D. Song, X. Zhang, and Y. Guo, "Design of a highly ordered mesoporous $H_3PW_{12}O_{40}/ZrO_2$–Si(Ph)Si hybrid catalyst for methyl levulinate synthesis," *Green Chem.*, vol. 15, no. 4, p. 885, 2013.

[302] F. Jin, Z. Zhou, T. Moriya, H. Kishida, H. Higashijima, and H. Enomoto, "Controlling hydrothermal reaction pathways to improve acetic acid production from carbohydrate biomass," *Environ. Sci. Technol.*, vol. 39, no. 6, pp. 1893–1902, 2005.

[303] G. Gozaydin and A. Yuksel, "Valorization of hazelnut shell waste in hot

compressed water," *Fuel Process. Technol.*, vol. 166, pp. 96–106, 2017.

[304] M. Bahadi Awadh, A. Japir wali, N. Salih, and J. Salimon, "Free Fatty Acids Separation From Malaysian High Free Fatty Acid Crude Palm Oil Using Molecular Distillation," *Malaysian J. Anal. Sci.*, vol. 20, no. 5, pp. 1042–1051, 2016.

[305] M. Benziane, K. Khimeche, I. Mokbel, T. Sawaya, A. Dahmani, and J. Jose, "Experimental vapor pressures of five saturated fatty acid ethyl ester (FAEE) components of biodiesel," *J. Chem. Eng. Data*, vol. 56, no. 12, pp. 4736–4740, 2011.

[306] M. Mascal and E. B. Nikitin, "Co-processing of carbohydrates and lipids in oil crops to produce a hybrid biodiesel," *Energy and Fuels*, vol. 24, no. 3, pp. 2170–2171, 2010.

[307] A. M. da Costa Lopes, K. G. João, A. R. C. Morais, E. Bogel-Łukasik, and R. Bogel-Łukasik, "Ionic liquids as a tool for lignocellulosic biomass fractionation," *Sustain. Chem. Process.*, vol. 1, pp. 1–31, 2013.

[308] B. Girisuta, L. P. B. M. Janssen, and H. J. Heeres, "A kinetic study on the decomposition of 5-hydroxymethylfurfural into levulinic acid," *Green Chem.*, vol. 8, no. 8, pp. 701–709, 2006.

[309] W. W. S. Ho, H. K. Ng, S. Gan, and S. H. Tan, "Evaluation of palm oil mill fly ash supported calcium oxide as a heterogeneous base catalyst in biodiesel synthesis from crude palm oil," *Energy Convers. Manag.*, vol. 88, pp. 1167–1178, 2014.

[310] D. Unlu, O. Ilgen, and N. D. Hilmioglu, "Biodiesel additive ethyl levulinate synthesis by catalytic membrane: $SO_4^{2-}/ZrO_2$ loaded hydroxyethyl cellulose," *Chem. Eng. J.*, vol. 302, pp. 260–268, 2016.

[311] K. Y. Nandiwale, P. S. Niphadkar, S. S. Deshpande, and V. V. Bokade, "Esterification of renewable levulinic acid to ethyl levulinate biodiesel catalyzed by highly active and reusable desilicated H-ZSM-5," *J. Chem. Technol. Biotechnol.*, vol. 89, pp. 1507–1515, 2013.

[312] M. M. Zainol, N. Aishah, S. Amin, and M. Asmadi, "Kinetics and thermodynamic analysis of levulinic acid esterification using lignin-furfural carbon cryogel catalyst," *Renew. Energy*, vol. 130, pp. 547–557, 2019.

[313] N. A. S. Ramli and N. A. S. Amin, "Thermo-kinetic assessment of glucose decomposition to 5-hydroxymethyl furfural and levulinic acid over acidic functionalized ionic liquid," *Chem. Eng. J.*, vol. 335, pp. 221–230, 2018.

[314] L. Peng, L. Lin, and H. Li, "Extremely low sulfuric acid catalyst system for synthesis of methyl levulinate from glucose," *Ind. Crops Prod.*, vol. 40, no. 1, pp. 136–144, 2012.

[315] S. Y. Chin, M. A. A. Ahmad, M. R. Kamaruzaman, and C. K. Cheng,

"Kinetic studies of the esterification of pure and dilute acrylic acid with 2-ethyl hexanol catalysed by Amberlyst 15," *Chem. Eng. Sci.*, vol. 129, pp. 116–125, 2015.

[316] C. Liang, Y. Hu, L. Guo, L. Wu, and W. Zhang, "Kinetic study of acid hydrolysis of corncobs to levulinic acid," *BioResources*, vol. 12, no. 2, pp. 4049–4061, 2017.

[317] C. Chang, X. Ma, and P. Cen, "Kinetics of levulinic acid formation from glucose decomposition at high temperature," *Chinese J. Chem. Eng.*, vol. 14, no. 5, pp. 708–712, 2006.

[318] B. Girisuta, L. P. B. M. Janssen, and H. J. Heeres, "Green chemicals: A kinetic study on the conversion of glucose to levulinic acid," *Chem. Eng. Res. Des.*, vol. 84, no. 5, pp. 339–349, May 2006.

[319] B. Girisuta *et al.*, "Kinetic Study on the Acid-Catalysed Hydrolysis of Cellulose to Levulinic Acid," *Ind. Eng. Chem. Res.*, vol. 46, pp. 1696–1708, 2007.

[320] D. Garcés, E. Díaz, and S. Ordóñez, "Aqueous phase conversion of hexoses into 5-hydroxymethylfurfural and levulinic acid in the presence of hydrochloric acid: mechanism and kinetics," *Ind. Eng. Chem. Res.*, vol. 56, no. 18, pp. 5221–5230, 2017.

[321] X. Zheng, Z. Zhi, X. Gu, X. Li, R. Zhang, and X. Lu, "Kinetic study of levulinic acid production from corn stalk at mild temperature using $FeCl_3$ as catalyst," *Fuel*, vol. 187, pp. 261–267, 2017.

[322] W. Weiqi and W. Shubin, "Experimental and kinetic study of glucose conversion to levulinic acid catalyzed by synergy of Lewis and Bronsted acids," *Chem. Eng. J.*, vol. 307, pp. 389–398, 2017.

[323] J. Fu, X. Xu, X. Lu, and X. Lu, "Hydrothermal decomposition of carbohydrates to levulinic acid with catalysis by ionic liquids," *Ind. Eng. Chem. Res.*, vol. 55, no. 42, pp. 11044–11051, 2016.

[324] Q. Qing, Q. Guo, P. Wang, H. Qian, X. Gao, and Y. Zhang, "Kinetics study of levulinic acid production from corncobs by tin tetrachloride as catalyst," *Bioresour. Technol.*, vol. 260, no. March, pp. 150–156, 2018.

[325] S. H. Jadhav and P. R. Gogate, "Intensification in the Activity of Lipase Enzyme Using Ultrasonic Irradiation and Stability Studies," *Ind. Eng. Chem. Res.*, vol. 53, no. 4, pp. 1377–1385, 2014.

[326] B. E. Gurkan, T. R. Gohndrone, M. J. McCready, and J. F. Brennecke, "Reaction kinetics of $CO_2$ absorption in to phosphonium based anion-functionalized ionic liquids," *Phys. Chem. Chem. Phys.*, vol. 15, no. 20, pp. 7796–7811, 2013.

[327] D. Burschowsky *et al.*, "Electrostatic transition state stabilization rather than reactant destabilization provides the chemical basis for efficient

chorismate mutase catalysis," *Proc. Natl. Acad. Sci.*, vol. 111, no. 49, pp. 17516–17521, 2014.

[328] K. Li *et al.*, "Mechanistic and kinetic studies on biodiesel production catalyzed by an efficient pyridinium based ionic liquid," *Green Chem.*, vol. 17, no. 8, pp. 4271–4280, 2015.

[329] A. J. Kunov-Kruse, A. Riisager, S. Saravanamurugan, R. W. Berg, S. B. Kristensen, and R. Fehrmann, "Revisiting the Bronsted acid catalysed hydrolysis kinetics of polymeric carbohydrates in ionic liquids by in situ ATR-FTIR spectroscopy," *Green Chem.*, vol. 15, no. 10, pp. 2843–2848, 2013.

[330] K. C. Badgujar and B. M. Bhanage, "Thermo-chemical energy assessment for production of energy-rich fuel additive compounds by using levulinic acid and immobilized lipase," *Fuel Process. Technol.*, vol. 138, pp. 139–146, 2015.

[331] A. M. Gumel, M. S. M. Annuar, T. Heidelberg, and Y. Chisti, "Thermo-kinetics of lipase-catalyzed synthesis of 6-O-glucosyldecanoate," *Bioresour. Technol.*, vol. 102, no. 19, pp. 8727–8732, 2011.

[332]C.M.Lai and M.A.Tabatabai, "Kinetic parameters of immobilized urease," *Soil Biol. Biochem.*, vol. 24, no. 3, pp. 225–228, 1992.

[333] P. Nautiyal, K. A. Subramanian, and M. G. Dastidar, "Kinetic and thermodynamic studies on biodiesel production from Spirulina platensis algae biomass using single stage extraction – transesterification process," *Fuel*, vol. 135, pp. 228–234, 2014.

[334] K. R. Spacino, D. Borsato, G. M. Buosi, and L. T. Chendynski, "Determination of kinetic and thermodynamic parameters of the B100 biodiesel oxidation process in mixtures with natural antioxidants," *Fuel Process. Technol.*, vol. 137, pp. 366–370, 2015.

[335] M. Graber, M.-P. Bousquet-Dubouch, N. Sousa, S. Lamare, and M.-D. Legoy, "Water plays a different role on activation thermodynamic parameter alcoholysis reaction catalyzed by lipase in gaseous and organic media," *Biochim. Biophys. Acta*, vol. 1645, pp. 56–62, 2003.

[336] J. Yan, G. Pan, C. Ding, and G. Quan, "Kinetic and thermodynamic parameters of β-glucosidase immobilized on various colloidal particles from a paddy soil," *Colloids Surfaces B Biointerfaces*, vol. 79, no. 1, pp. 298–303, 2010.

[337] T. Lonhienne, C. Gerday, and G. Feller, "Psychrophilic enzymes: Revisiting the thermodynamic parameters of activation may explain local flexibility," *Biochim. Biophys. Acta*, vol. 1543, no. 1, pp. 1–10, 2000.

[338] C. Gerday *et al.*, "Psychrophilic enzymes: A thermodynamic challenge," *Biochim. Biophys. Acta*, vol. 1342, pp. 119–131, 1997.

[339] E. A. Abu-Gharib, R. M. EL-Khatib, L. A. E. Nassr, and A. M. Abu-Dief, "Kinetics, reactivity, initial-transition state analysis and thermodynamic parameters of base-catalyzed hydrolysis of coumalic acid in solvents with different polarities," *Arab. J. Chem.*, vol. 10, pp. S988–S995, 2017.

[340] S. S. Mohtar, T. N. Z. Tengku Malim Busu, A. M. Md Noor, N. Shaari, and H. Mat, "An ionic liquid treatment and fractionation of cellulose, hemicellulose and lignin from oil palm empty fruit bunch," *Carbohydr. Polym.*, vol. 166, pp. 291–299, 2017.

[341] P. Keil, M. Kick, and A. König, "Long-term stability, regeneration and recycling of imidazolium-based ionic liquids," *Chemie-Ingenieur-Technik*, vol. 84, no. 6, pp. 859–866, 2012.

[342] J. Zhang, Y. Xiao, Y. Zhong, N. Du, and X. Huang, "Alcohol Effect and the Related Mechanism on Fructose Dehydration into 5-Hydroxymethylfurfural in the Deep Eutectic Solvent of [Emim]Cl/Alcohol," *ACS Sustain. Chem. Eng.*, vol. 4, no. 7, pp. 3995–4002, 2016.

# Appendices

## Appendix 1

Holocellulose (sum of hemicellulose and cellulose) was analysed according to the method reported by Teramoto et al. [84]**,** as follow:

The biomass sample was treated with deionised water containing acetic acid and $NaClO_2$ for 1 h at 75°C. Then, 0.04 ml of acetic acid and 0.2 g of $NaClO_2$ were added to the mixture every 1 h for 3 h. The residue was filtered, washed, and then dried overnight to a constant weight. The holocellulose content was then determined from the solid residues obtained. The cellulose content was determined by shaking 0.2 g of previously obtained holocellulose in a flask with 5 ml of 17.5% NaOH aqueous solution at 30°C for 40 min in a water bath shaker. Next, 5 ml of deionised water was added to the mixture with continued shaking for 5 min before the mixture was filtered. The remaining residue was then washed with 8 ml of 10% acetic acid and boiling water. Finally, the cellulose residue was dried overnight and weighed. The hemicellulose content was calculated as the difference between holocellulose and cellulose contents.

## Appendix 2

A preliminary parametric study on using $InCl_3$-[HMIM][$HSO_4$] for the conversion of OPEFB and OPMF biomass to LA and upgrading to EL was first conducted in order to obtain the desired parametric ranges for the statistical analysis and reaction optimisation studies. Full details are reported in the following journal article:

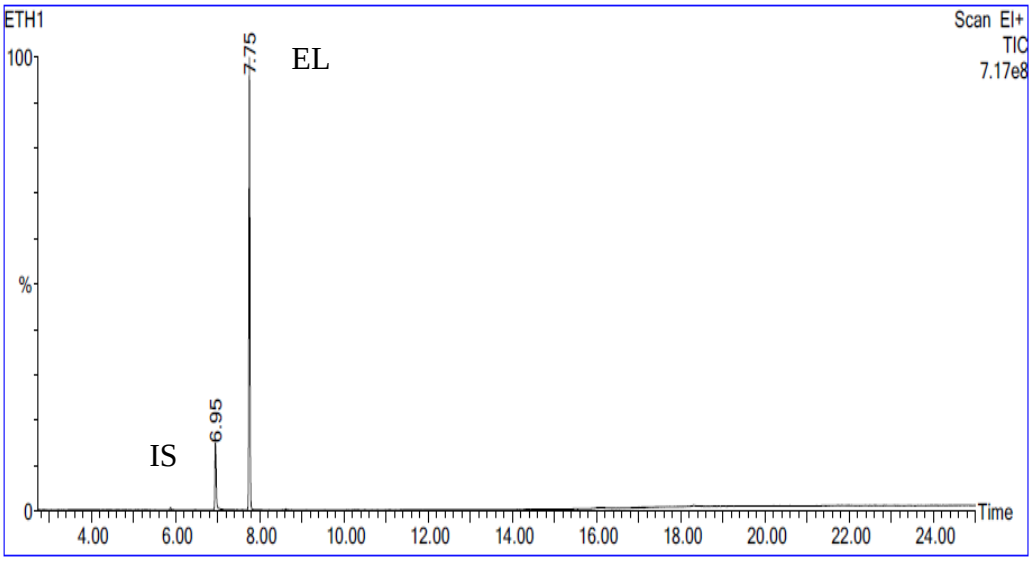
- **Tiong, Y.W.**, Yap, C.L., Gan, S., Yap, W.S.P. 2017. One-pot conversion of oil palm empty fruit bunch and mesocarp fiber biomass to levulinic acid and upgrading to ethyl levulinate via indium trichloride-ionic liquids. *Journal of Cleaner Production*, 168, 1251-1261. DOI: 10.1016/j.jclepro.2017.09.050

## Appendix 3

a) Calibration for EL using GC-MS analysis.

(IS – 1-octanol)

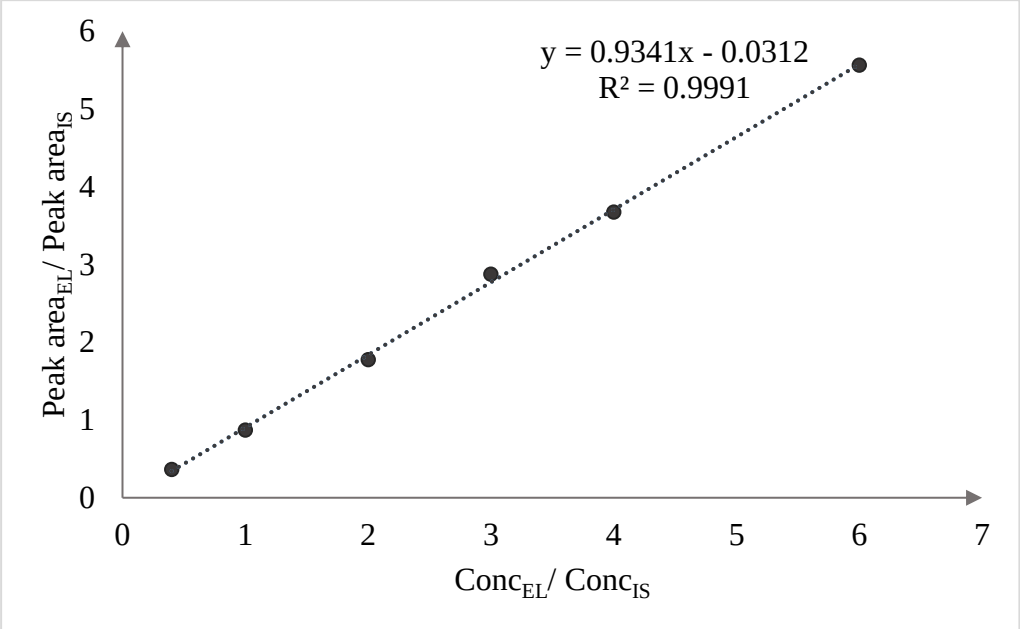
Representative GC-MS chromatogram of EL at RT 7.75 (1500 ppm), and IS at RT 6.95 (250 ppm)




A total of six different concentrations of EL have been analysed for the calibration curve.

| Conc for EL (ppm) | Conc for IS (ppm) | Area for IS | Area for IS (%) | Area for EL | Area for EL (%) |
|---|---|---|---|---|---|
| 1500 | 250 | 4008277 | 12.2 | 16870306 | 80.1 |
| 1000 | 250 | 4545191 | 17.7 | 12430539 | 74.9 |
| 750 | 250 | 4644920 | 20.5 | 10090096 | 69.7 |
| 500 | 250 | 5279585 | 26.4 | 7414630 | 60.1 |
| 250 | 250 | 5827165 | 39.3 | 4048745 | 45.6 |
| 100 | 250 | 6146463 | 47.5 | 1753490 | 28.3 |

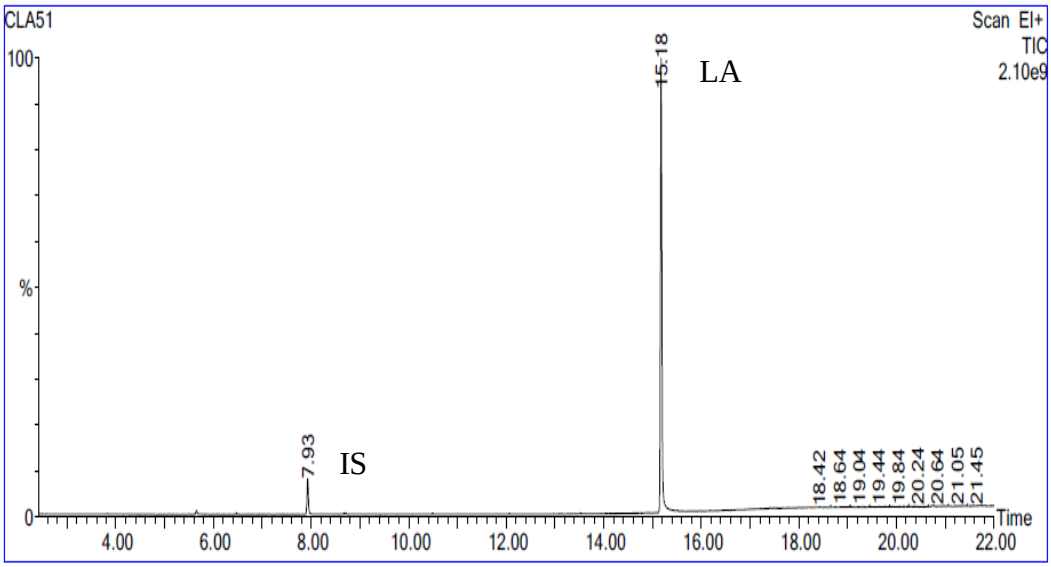
Calibration curve of EL




**b)** Calibration for LA using GC-MS analysis.

(IS – butyric acid)

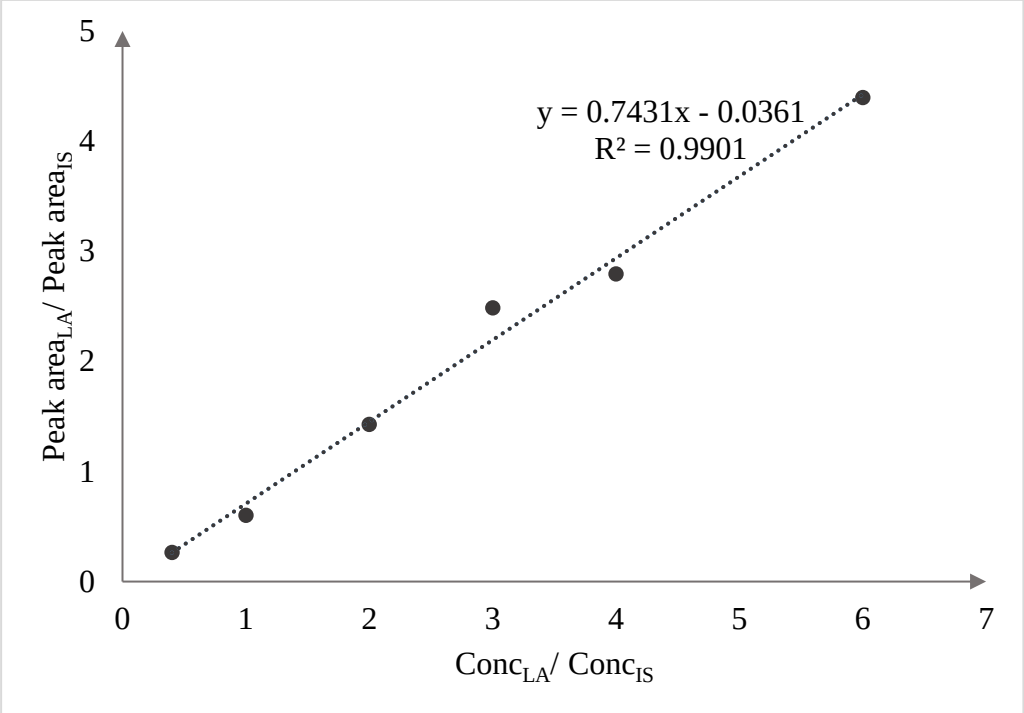
Representative GC-MS chromatogram of LA at RT 15.18 (1500 ppm), and IS at RT 7.93 (250 ppm)



A total of six different concentrations of LA have been analysed for the calibration curve.

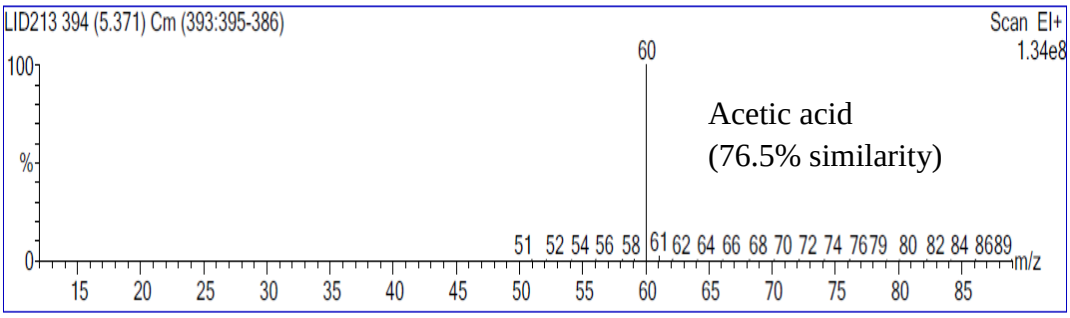
| Conc for LA (ppm) | Conc for IS (ppm) | Area for IS | Area for IS (%) | Area for LA | Area for LA (%) |
|---|---|---|---|---|---|
| 1500 | 250 | 8181916 | 5.6 | 35969932 | 83.7 |
| 1000 | 250 | 8461019 | 9.8 | 23641456 | 77.9 |
| 750 | 250 | 7939657 | 15.3 | 19726324 | 70.6 |
| 500 | 250 | 9827341 | 23.0 | 14038853 | 64.5 |
| 250 | 250 | 9902382 | 38.9 | 5964581 | 45.3 |
| 100 | 250 | 10463970 | 42.7 | 2771907 | 30.0 |

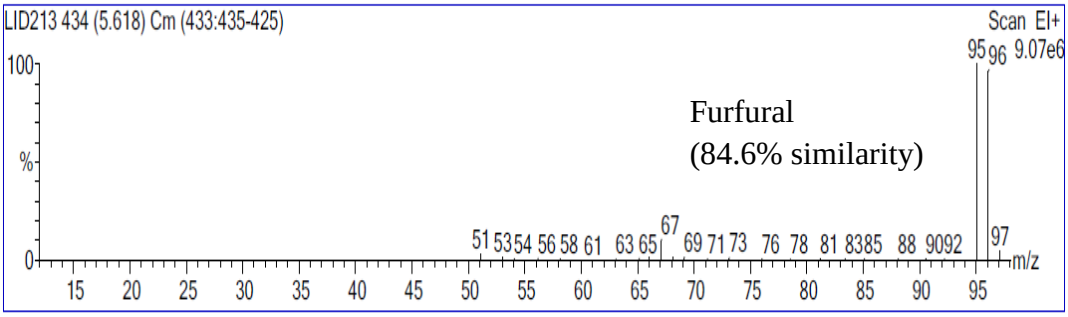
Calibration curve of LA

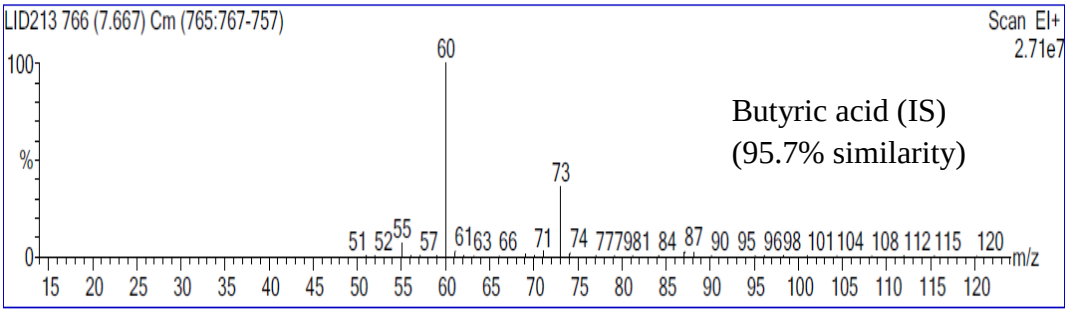


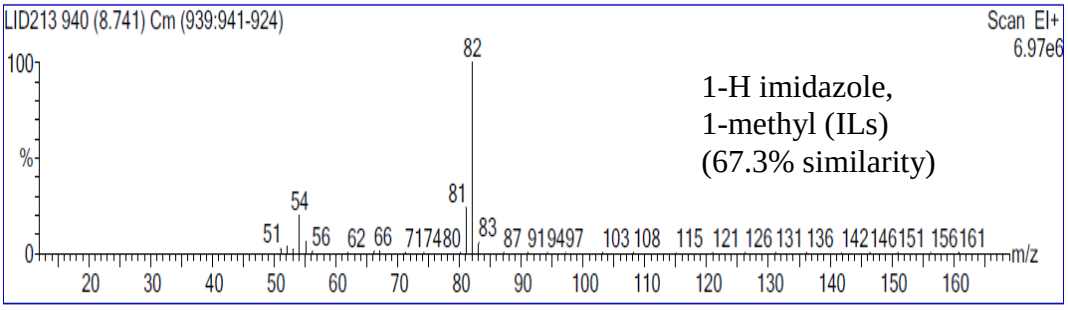
## Appendix 4

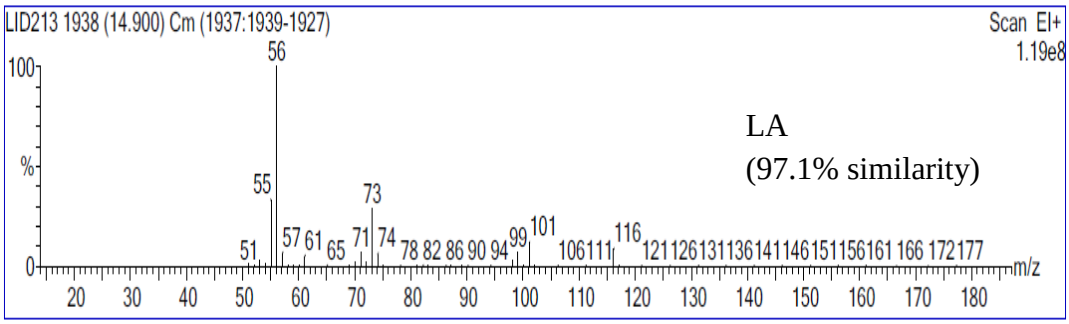
**a)** LA synthesis with other by-products formation

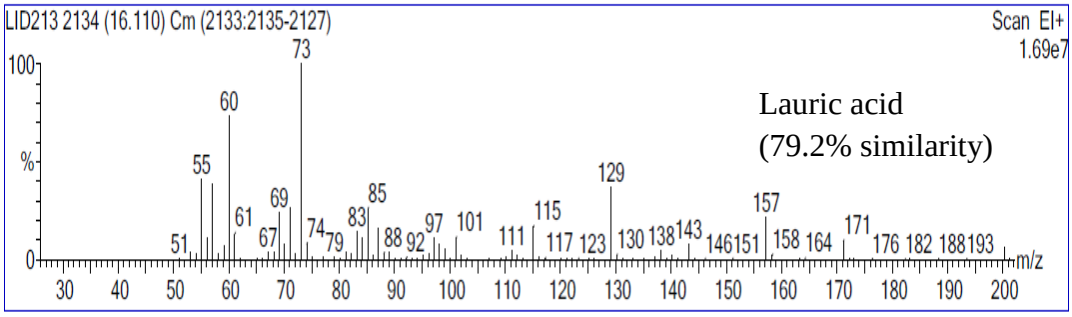


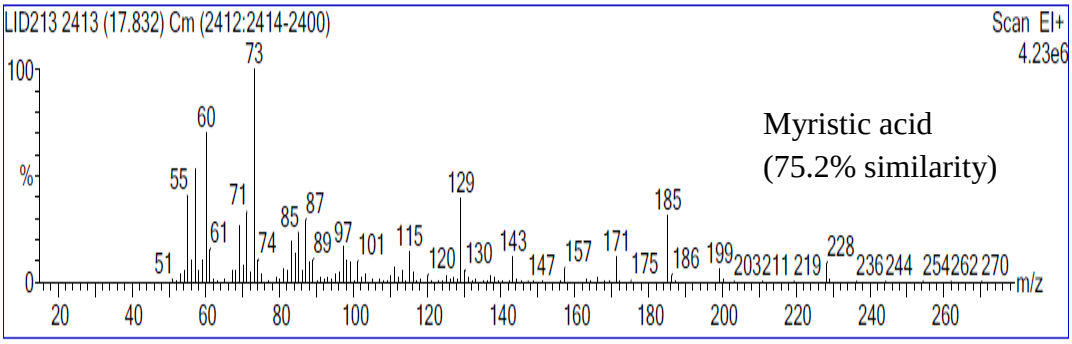



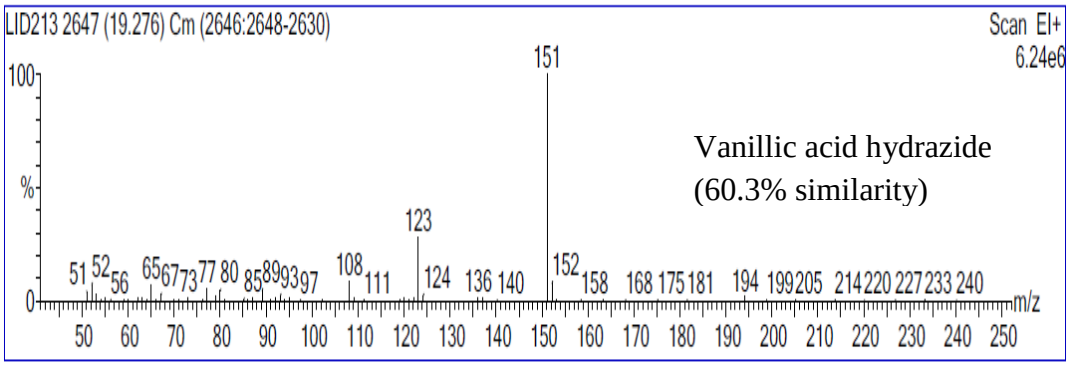



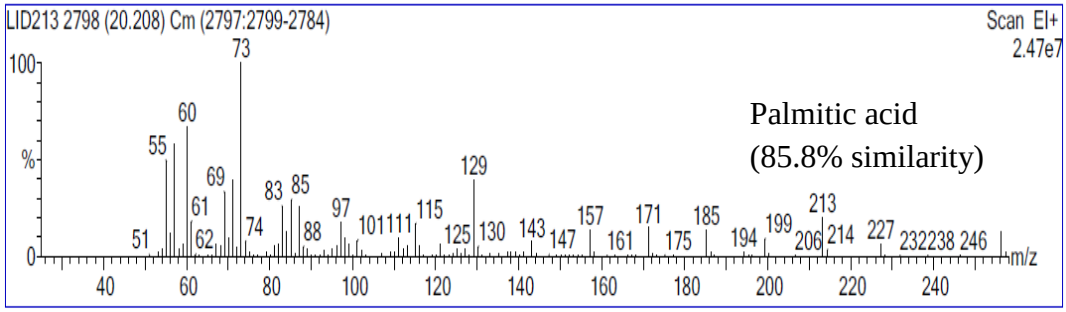



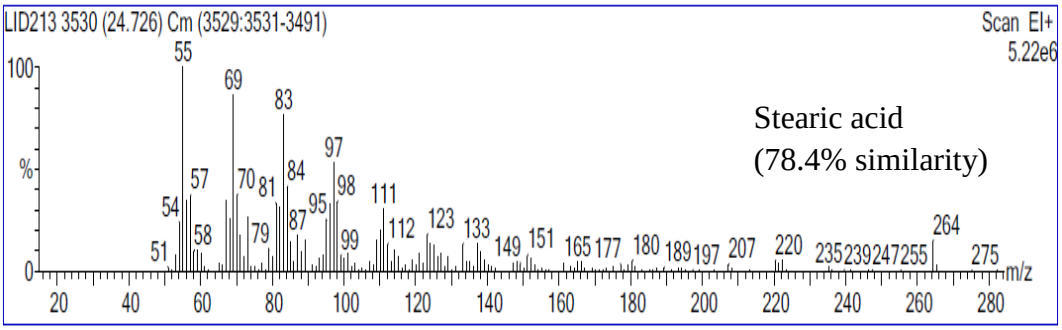

LID213 1938 (14.900) Cm (1937:1939-1927)
Scan EI+
1.19e8
LA
(97.1% similarity)


LID213 2134 (16.110) Cm (2133:2135-2127)
Scan EI+
1.69e7
Lauric acid
(79.2% similarity)

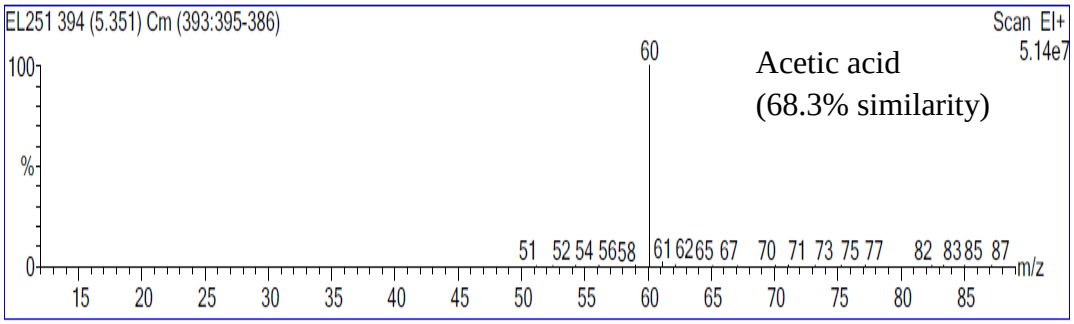

LID213 2413 (17.832) Cm (2412:2414-2400)
Scan EI+
4.23e6
Myristic acid
(75.2% similarity)

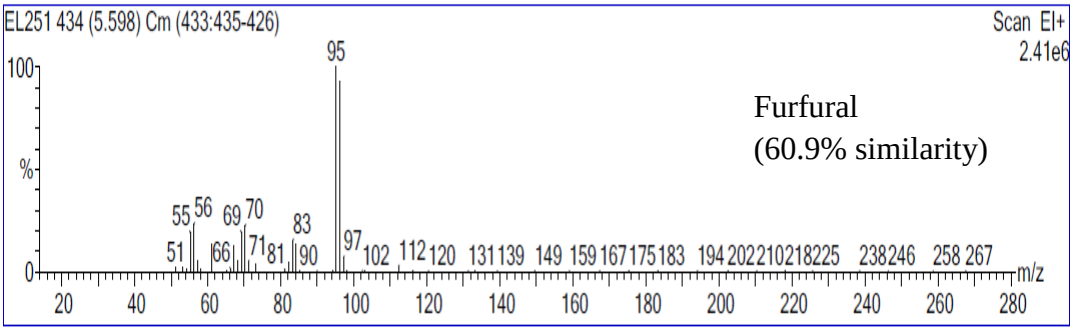

LID213 2647 (19.276) Cm (2646:2648-2630)
Scan EI+
6.24e6
Vanillic acid hydrazide
(60.3% similarity)

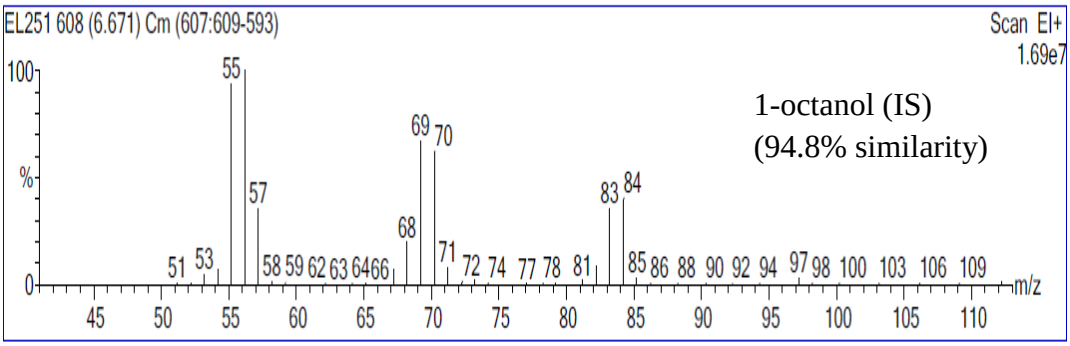

LID213 2798 (20.208) Cm (2797:2799-2784)
Scan EI+
2.47e7
Palmitic acid
(85.8% similarity)

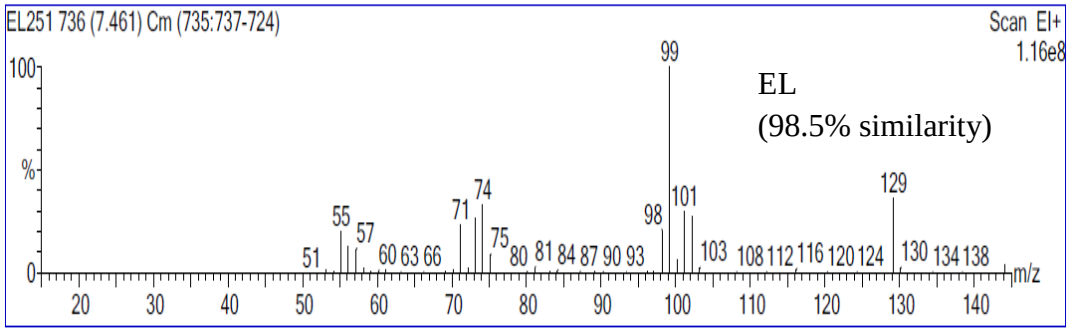


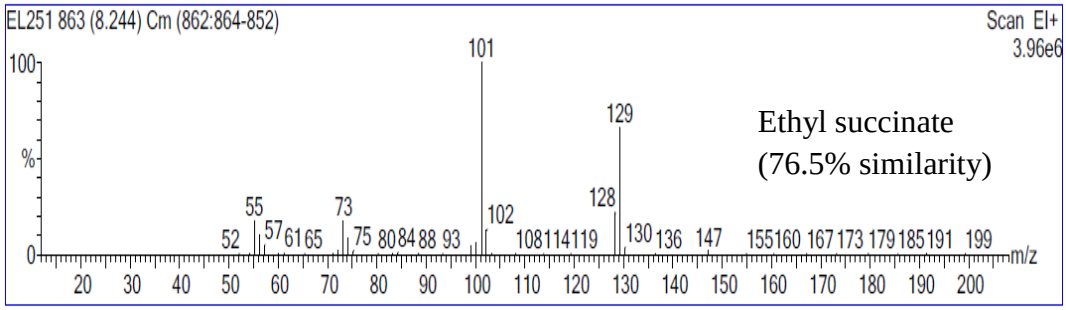

**b)** EL synthesis with other by-products formation

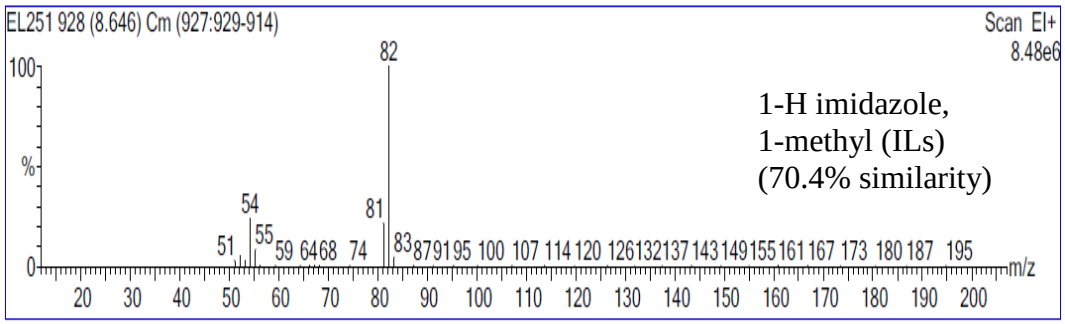


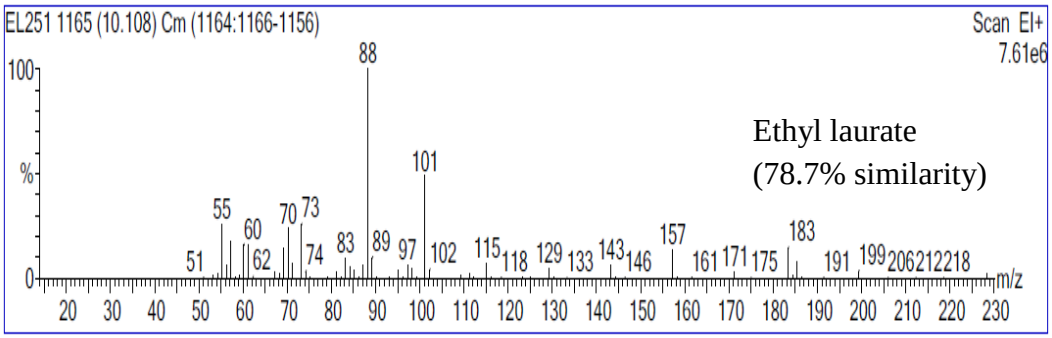



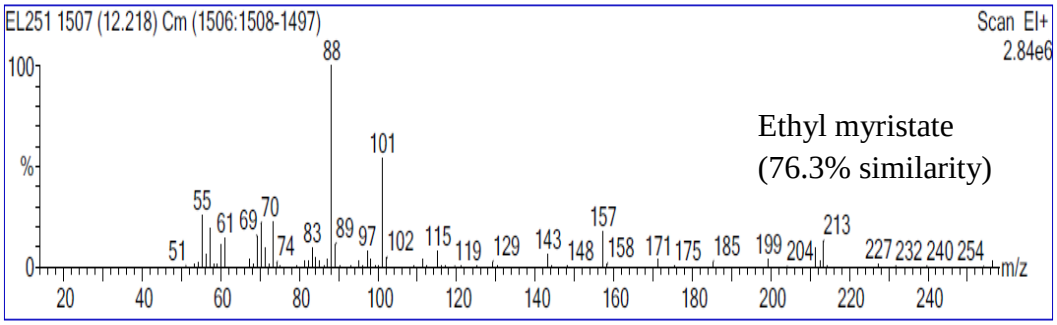



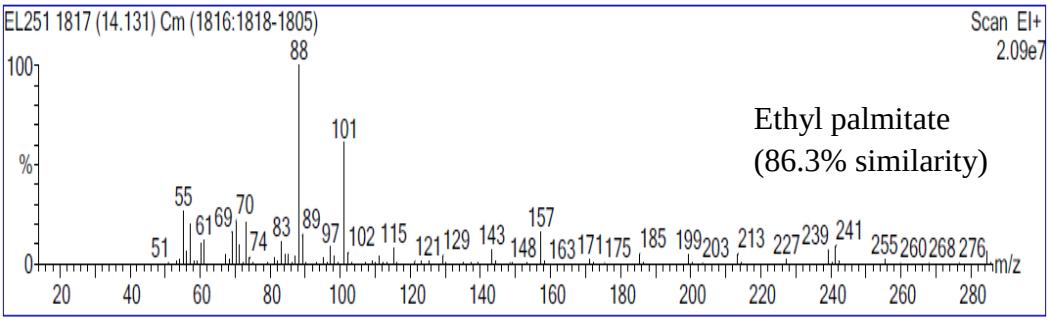

EL251 736 (7.461) Cm (735:737-724)
Scan EI+
1.16e8
EL
(98.5% similarity)

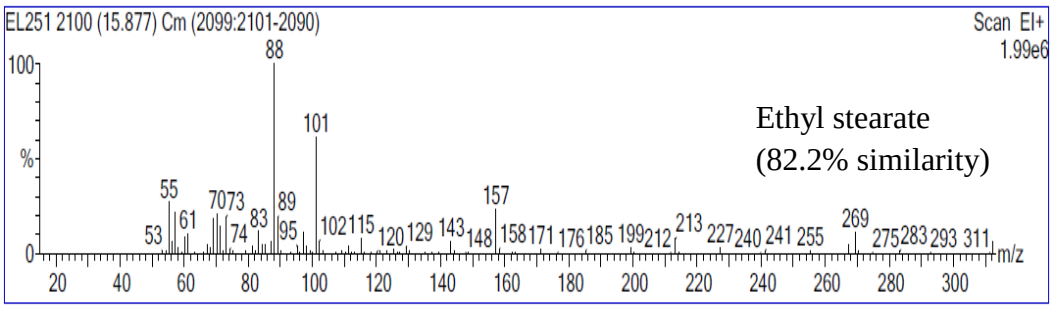

EL251 863 (8.244) Cm (862:864-852)
Scan EI+
3.96e6
Ethyl succinate
(76.5% similarity)

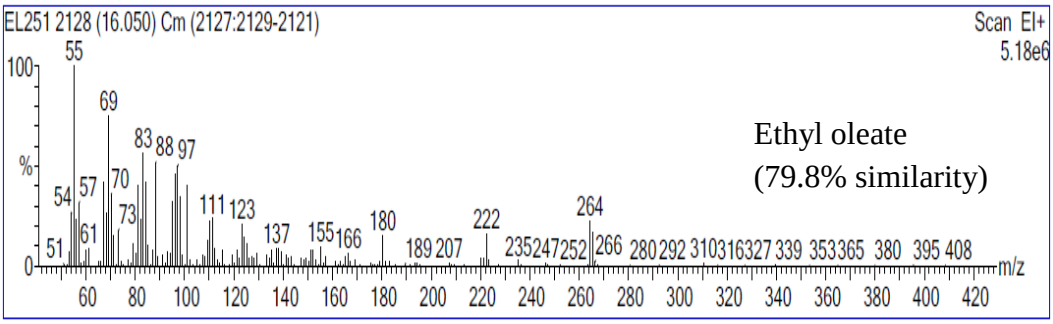

EL251 928 (8.646) Cm (927:929-914)
Scan EI+
8.48e6
1-H imidazole,
1-methyl (ILs)
(70.4% similarity)

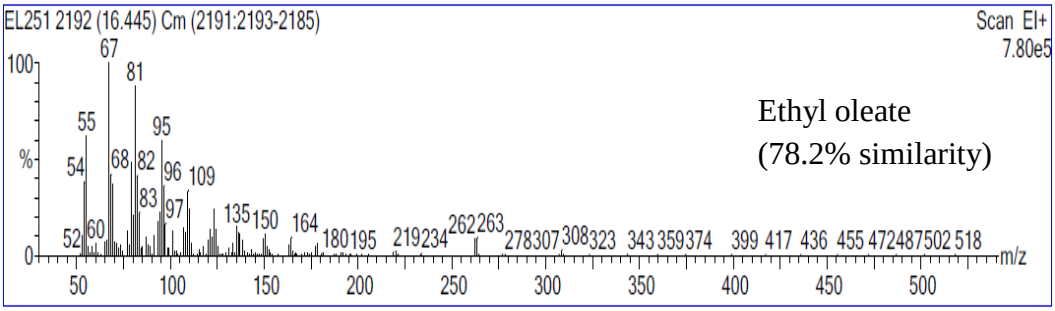

EL251 1165 (10.108) Cm (1164:1166-1156)
Scan EI+
7.61e6
Ethyl laurate
(78.7% similarity)


EL251 1507 (12.218) Cm (1506:1508-1497)
Scan EI+
2.84e6
Ethyl myristate
(76.3% similarity)


EL251 1817 (14.131) Cm (1816:1818-1805)
Scan EI+
2.09e7
Ethyl palmitate
(86.3% similarity)
m/z


EL251 2100 (15.877) Cm (2099:2101-2090)
Scan EI+
1.99e6
Ethyl stearate
(82.2% similarity)
m/z


EL251 2128 (16.050) Cm (2127:2129-2121)
Scan EI+
5.18e6
Ethyl oleate
(79.8% similarity)
m/z


EL251 2192 (16.445) Cm (2191:2193-2185)
Scan EI+
7.80e5
Ethyl oleate
(78.2% similarity)
m/z

## Appendix 5

**a) (i)** Detailed data on the ANOVA regression model of LA yields from OPEFB conversion ($Y_1$).

| Source | Sum of squares | Degree of freedom | Mean of square | F value | Prob > F | Remarks |
|---|---|---|---|---|---|---|
| Model | 351.08 | 14 | 25.08 | 17.97 | < 0.0001 | Significant |
| A | 40.48 | 1 | 40.48 | 29.01 | < 0.0001 | |
| B | 12.20 | 1 | 12.20 | 8.74 | 0.0104 | |
| C | 45.95 | 1 | 45.95 | 32.93 | < 0.0001 | |
| D | 9.26 | 1 | 9.26 | 6.64 | 0.0220 | |
| $A^2$ | 68.90 | 1 | 68.90 | 49.37 | < 0.0001 | |
| $B^2$ | 100.31 | 1 | 100.31 | 71.88 | < 0.0001 | |
| $C^2$ | 67.60 | 1 | 67.60 | 48.44 | < 0.0001 | |
| $D^2$ | 87.26 | 1 | 87.26 | 62.53 | < 0.0001 | |
| AB | 0.011 | 1 | 0.011 | 7.529E-0.03 | 0.9321 | |
| AC | 11.89 | 1 | 11.89 | 8.52 | 0.0112 | |
| AD | 0.22 | 1 | 0.22 | 0.16 | 0.6952 | |
| BC | 0.48 | 1 | 0.48 | 0.34 | 0.5671 | |
| BD | 0.82 | 1 | 0.82 | 0.59 | 0.4551 | |
| CD | 1.87 | 1 | 1.87 | 1.34 | 0.2664 | |
| Residual | 19.54 | 14 | 1.40 | | | |
| Lack of Fit | 15.69 | 10 | 1.57 | 1.63 | 0.3369 | Not significant |
| Pure Error | 3.85 | 4 | 0.96 | | | |
| Cor Total | 370.63 | 29 | | | | |

**a) (ii)** Detailed data on the ANOVA regression model of LA yields from OPMF conversion ($Y_2$).

| Source | Sum of squares | Degree of freedom | Mean of square | F value | Prob > F | Remarks |
|---|---|---|---|---|---|---|
| Model | 422.27 | 14 | 30.16 | 15.46 | < 0.0001 | Significant |
| A | 81.40 | 1 | 81.40 | 41.71 | < 0.0001 | |
| B | 14.92 | 1 | 14.92 | 7.64 | 0.0152 | |
| C | 71.28 | 1 | 71.28 | 36.53 | < 0.0001 | |
| D | 13.68 | 1 | 13.68 | 7.01 | 0.0191 | |
| $A^2$ | 50.48 | 1 | 50.48 | 25.87 | 0.0002 | |
| $B^2$ | 106.63 | 1 | 106.63 | 54.64 | < 0.0001 | |
| $C^2$ | 48.82 | 1 | 48.82 | 25.02 | 0.0002 | |
| $D^2$ | 94.68 | 1 | 94.68 | 48.52 | < 0.0001 | |
| AB | 1.81 | 1 | 1.81 | 0.93 | 0.3520 | |
| AC | 15.33 | 1 | 15.33 | 7.85 | 0.0141 | |
| AD | 1.04 | 1 | 1.04 | 0.53 | 0.4773 | |
| BC | 5.64 | 1 | 5.64 | 2.89 | 0.1112 | |
| BD | 1.28 | 1 | 1.28 | 0.65 | 0.4321 | |
| CD | 1.23 | 1 | 1.23 | 0.63 | 0.4401 | |
| Residual | 27.32 | 14 | 1.95 | | | |
| Lack of Fit | 18.92 | 10 | 1.89 | 0.90 | 0.5957 | Not significant |
| Pure Error | 8.40 | 4 | 2.10 | | | |
| Cor Total | 449.90 | 29 | | | | |

**b) (i)** Detailed data on the ANOVA regression model of EL yields from OPEFB conversion ($Y_3$).

| Source | Sum of squares | Degree of freedom | Mean of square | F value | Prob > F | Remarks |
|---|---|---|---|---|---|---|
| Model | 276.98 | 9 | 30.78 | 12.91 | 0.0004 | Significant |
| A | 14.76 | 1 | 14.76 | 6.19 | 0.0345 | |
| B | 10.91 | 1 | 10.91 | 4.58 | 0.0610 | |
| C | 53.31 | 1 | 53.31 | 22.37 | 0.0011 | |
| $A^2$ | 87.63 | 1 | 87.63 | 36.77 | 0.0002 | |
| $B^2$ | 42.82 | 1 | 42.82 | 17.97 | 0.0022 | |
| $C^2$ | 73.21 | 1 | 73.21 | 30.72 | 0.0004 | |
| AB | 24.50 | 1 | 24.50 | 10.28 | 0.0107 | |
| AC | 2.00 | 1 | 2.00 | 0.84 | 0.3835 | |
| BC | 0.61 | 1 | 0.61 | 0.25 | 0.6265 | |
| Residual | 21.45 | 9 | 2.38 | | | |
| Lack of Fit | 13.70 | 5 | 2.74 | 1.41 | 0.3797 | Not significant |
| Pure Error | 7.75 | 4 | 1.94 | | | |
| Cor Total | 387.70 | 19 | | | | |

**b) (ii)** Detailed data on the ANOVA regression model of EL yields from OPMF conversion ($Y_4$).

| Source | Sum of squares | Degree of freedom | Mean of square | F value | Prob > F | Remarks |
|---|---|---|---|---|---|---|
| Model | 309.12 | 9 | 34.35 | 13.32 | 0.0003 | Significant |
| A | 21.18 | 1 | 21.18 | 8.22 | 0.0186 | |
| B | 23.90 | 1 | 23.90 | 9.27 | 0.0139 | |
| C | 56.77 | 1 | 56.77 | 22.02 | 0.0011 | |
| $A^2$ | 94.60 | 1 | 94.60 | 36.69 | 0.0002 | |
| $B^2$ | 64.79 | 1 | 64.79 | 25.13 | 0.0007 | |
| $C^2$ | 77.21 | 1 | 77.21 | 29.94 | 0.0004 | |
| AB | 4.81 | 1 | 4.81 | 1.86 | 0.2054 | |
| AC | 4.50 | 1 | 4.50 | 1.75 | 0.2191 | |
| BC | 0.41 | 1 | 0.41 | 0.16 | 0.7011 | |
| Residual | 23.21 | 9 | 2.58 | | | |
| Lack of Fit | 18.97 | 5 | 3.79 | 3.58 | 0.1203 | Not significant |
| Pure Error | 4.24 | 4 | 1.06 | | | |
| Cor Total | 420.57 | 19 | | | | |